

Mitochondrial structure and distribution in *Saccharomyces cerevisiae*

DISSERTATION

zur Erlangung des akademischen Grades

eines Doktors der Naturwissenschaften

- Dr. rer. nat.-

an der Bayreuther Graduiertenschule für Mathematik und

Naturwissenschaften (BayNAT) der Universität Bayreuth

vorgelegt von

Till Klecker

aus Johannesburg (RSA)

Bayreuth, 2014

Die vorliegende Arbeit wurde in der Zeit von Oktober 2009 bis Februar 2014 in Bayreuth am Institut für Zellbiologie unter Betreuung von Herrn Professor Dr. Benedikt Westermann angefertigt.

Vollständiger Abdruck der von der Bayreuther Graduiertenschule für Mathematik und Naturwissenschaften (BayNAT) der Universität Bayreuth genehmigten Dissertation zur Erlangung des akademischen Grades eines Doktors der Naturwissenschaften (Dr. rer. nat.).

Dissertation eingereicht am: 19.02.2014

Zulassung durch das Leitungsgremium: 07.03.2014

Wissenschaftliches Kolloquium: 23.06.2014

Amtierender Direktor: Herr Prof. Dr. Franz Xaver Schmid

Prüfungsausschuss:

Prof. Dr. Benedikt Westermann	(Erstgutachter)
Prof. Dr. Stephan Clemens	(Zweitgutachter)
PD. Dr. Stefan Heidmann	(Vorsitz)
Prof. Dr. Matthias Weiss	

Drittgutachter: Prof. Dr. Andreas Reichert

Table of contents

Table of contents.....	III
Abbreviations	VI
Gene descriptions.....	VII
Summary	X
Zusammenfassung.....	XI
Introduction.....	1
Mitochondrial fusion and division.....	2
Mitochondrial division.....	3
Mitochondrial inner membrane division.....	4
Num1 and Mdm36	5
Mitochondrial fusion	6
Mitochondrial movement and partitioning	7
Mitochondria-ER contact sites	9
Mitochondrial phospholipid biosynthesis.....	10
Biosynthesis of phosphatidylethanolamine	11
Biosynthesis of cardiolipin.....	11
Associated factors	11
Prohibitins	12
Aims and scope of this thesis	14
Synopsis.....	15
Num1 anchors mitochondria at the mother cell cortex.....	15
Mitochondria form contacts with plasma membrane invaginations.....	17
Link between mitochondrial division and mitochondrial anchorage.....	17
Role of Mdm36 in mitochondrial tethering	19
Two models for mitochondrial tethering by Num1.....	19
Role of Dnm1 in mitochondrial cell cortex attachment.....	20
Molecular function of Mdm33	22
<i>MDM33</i> interacts with genes involved in phospholipid homeostasis	22
Mapping of the interactome of <i>MDM33</i>	23
Mdm33 acts in mitochondrial biosynthesis of phosphatidylethanolamine.....	24
Role of Mdm33 in mitochondrial fission	25
Ups1 catalyzes intramitochondrial transport of phosphatidic acid	27
Ups1 acts early during CL synthesis.....	27

Ups1 is a novel lipid transfer protein	29
References.....	31
The yeast cell cortical protein Num1 integrates mitochondrial dynamics into cellular architecture...	45
Summary	46
Introduction.....	46
Results	46
Antagonistic roles of Num1 and Mmr1 in mitochondrial distribution.....	46
Retention of mitochondria in mother cells by Num1.....	48
Mitochondrial tips colocalize with Num1 in mother cells.....	48
Mitochondria form direct contacts with the plasma membrane in the retention zone.....	48
A chimeric plasma membrane tether rescues mitochondrial morphology defects in $\Delta num1$ and $\Delta mdm36$ mutants.....	49
Discussion.....	49
Materials and methods	51
Plasmids and cloning procedures.....	51
Yeast strain constructions	51
Microscopy	51
Acknowledgments	51
Author contributions.....	51
Funding.....	51
References.....	51
Supplementary material.....	53
Mdm33 links phospholipid homeostasis to mitochondrial division.....	57
Abstract	58
Introduction.....	58
Results	59
<i>MDM33</i> interacts with genes involved in phospholipid metabolism and mitochondrial membrane homeostasis.....	59
Suppression of <i>MDM33</i> overexpression-dependent growth arrest	60
<i>MDM33</i> is part of a genetic network regulating mitochondrial phospholipid biosynthesis.....	61
Mdm33 physically interacts with Phb1, Phb2, and Atp20	62
Mdm33 controls phospholipid homeostasis in mitochondria	62
Mdm33 contributes to mitochondrial division	63
Mdm33 foci are present at sites of mitochondrial division	64
Discussion.....	64

Materials and Methods	66
Plasmids and cloning procedures	66
Yeast strain constructions	66
Microscopy	67
Microarray design and hybridization	67
Genetic interaction network	68
Immunoprecipitation and LC MS/MS analysis	68
Lipid profiling by mass spectrometry and in vitro Psd1 activity assay	69
Online supplemental material.....	70
Acknowledgments	70
Abbreviations list.....	70
References.....	71
Figure Legends.....	76
Tables	78
Supplemental materials	78
Figures	80
Intramitochondrial Transport of Phosphatidic Acid in Yeast by a Lipid Transfer Protein.....	89
References and Notes	93
Acknowledgments	93
Supplementary Materials.....	94
Materials and Methods	95
Figures	99
Tables.....	115
References and Notes	117
Acknowledgments.....	120
Appendix.....	121
List of publications.....	121
CD-ROM.....	121
Copyright and Permissions.....	122
Erklärung	123

Abbreviations

BAR	BIN/Amphiphysin/Rvs
CDP-DAG	cytidine d iphosphate- d iacylglycerol
cER	cortical e ndoplasmic r eticulum
CL	cardiolipin
DIC	d ifferential i nterference c ontrast
ERMES	ER mitochondria e ncounter s tructure
IMS	inter m embrane s pace
MECA	m itochondria- ER -cortex a nchor
MIM	m itochondrial i nnner m embrane
MLCL	m onolysocardiolipin
MOM	m itochondrial o uter m embrane
mtDNA	m itochondrial DNA
PA	p hosphatidic a cid
PC	p hosphatidyl ch oline
PE	p hosphatidylethanolamine
PG	p hosphatidyl g lycerol
PGP	p hosphatidyl g lycerol p hosphate
PM	p lasma m embrane
PS	p hosphatidyl s erine

Gene descriptions

Gene	Name	Encoded protein: short description
<i>ARP2</i> <i>ARP3</i>	Actin related protein	Highly conserved actin nucleation mediator. Required for the motility and integrity of actin patches.
<i>ATP20</i>	ATP synthase	Subunit g of the mitochondrial F ₁ F ₀ ATP synthase. Required for dimerization of the ATP synthase complex.
<i>ATP23</i>	ATPase	Metalloprotease of the mitochondrial inner membrane.
<i>CAF4</i>	CCR4 associated factor	Molecular adaptor that connects Fis1 and Dnm1. High structural similarity to Mdv1.
<i>CAN1</i>	canavanine resistance	Plasma membrane arginine permease.
<i>CDS1</i>	CDP-diacylglycerol synthase	CDP-Diacylglycerol synthase of the ER.
<i>CHO1</i>	Choline requiring	Phosphatidylserine synthase of the ER. Involved in the biosynthesis of phosphatidylethanolamine.
<i>CHPPR</i>	Chondrocyte protein with a poly-proline region	Mitochondrial inner membrane protein that likely plays a role in mitochondrial division. Not present in yeast.
<i>CLD1</i>	Cardiolipin-specific deacylase	Mitochondrial cardiolipin-specific phospholipase; generates monolysocardiolipin. Involved in the remodeling of cardiolipin.
<i>CRD1</i>	Cardiolipin synthase	Cardiolipin synthase. Produces cardiolipin.
<i>DNM1</i>	Dynammin-related	GTPase that forms spirals around mitochondrial tubules and mechanochemically severs them.
<i>DRP1</i>	Dynammin-related protein	Mammalian homolog of Dnm1.
<i>DRP-1</i>	Dynammin-related protein	<i>C. elegans</i> homolog of Dnm1.
<i>FIS1</i>	Mitochondrial fission	Mitochondrial receptor for the fission machinery.
<i>FMP30</i>	Found in mitochondrial proteome	Protein required for the biosynthesis of cardiolipin in the absence of Psd1.
<i>FtsZ</i>	Filamenting temperature-sensitive mutant Z	Protein involved in prokaryotic cell division. Assembles as a ring at the mid-point of the cell, forming a functional analog of the contractile ring used in cytokinesis of many eukaryotic cells.
<i>FZO1</i>	Fuzzy onions homolog	GTPase that mediates mitochondrial outer membrane fusion.
<i>GEM1</i>	GTPase EF-hand protein of mitochondria	Regulatory subunit of the mitochondria-ER encounter structure. Gem1 is a cytosolic protein and solves the interaction between the mitochondria-ER encounter structure and Dnm1 upon mitochondrial division.
<i>GEP4</i>	Genetic interactors of prohibitins	Mitochondrial phosphatidylglycerol-phosphatase. Involved in the biosynthetic pathway of cardiolipin.
<i>MCP1</i> <i>MCP2</i>	Mdm10 complementing protein	Proteins of unknown function. Overexpression rescues the phenotype of yeast cells lacking ER-mitochondrial contacts.
<i>MDM10</i> <i>MDM12</i> <i>MDM34</i>	Mitochondrial distribution and morphology	Components of the mitochondria-ER encounter structure that tethers the mitochondria to the ER. 10 and 34 are mitochondrial proteins. 12 is a cytosolic protein.
<i>MDM30</i>	Mitochondrial distribution and morphology	F-box component of an SCF complex; required for Fzo1 ubiquitination and for mitochondrial fusion.
<i>MDM31</i>	Mitochondrial distribution and morphology	Mitochondrial inner membrane protein with similarity to Mdm32; required for normal mitochondrial morphology, distribution, and nucleoid organization. Overexpression rescues the phenotype of yeast cells lacking ER-mitochondrial contacts.

Gene	Name	Encoded protein: short description
<i>MDM32</i>	Mitochondrial distribution and morphology	Mitochondrial inner membrane protein with similarity to Mdm31; required for normal mitochondrial morphology, distribution, and nucleoid organization.
<i>MDM33</i>	Mitochondrial distribution and morphology	Mitochondrial inner membrane protein that possibly plays a role in mitochondrial division. Overexpression causes a growth defect and mitochondrial fragmentation.
<i>MDM35</i>	Mitochondrial distribution and morphology	Required for import of Ups1 and Ups2 in the intermembrane space. Protects them against proteolytic degradation.
<i>MDM36</i>	Mitochondrial distribution and morphology	Mitochondrial fission promoting protein. Required for interaction between Num1 and Dnm1. The deletion mutant mitochondrial phenotype is indistinguishable from that of $\Delta num1$ stains.
<i>MDV1</i>	Mitochondrial division	Molecular adaptor that connects Fis1 and Dnm1.
<i>Mfn1</i> <i>Mfn2</i>	Mitofusin	Human homologs of Fzo1.
<i>MGM1</i>	Mitochondrial genome maintenance	GTPase that mediates mitochondrial inner membrane fusion. Also required for cristae formation.
<i>MGM101</i>	Mitochondrial genome maintenance	Mitochondrial nucleoid protein required for mitochondrial DNA recombination.
<i>MIP1</i>	Mitochondrial DNA polymerase	DNA polymerase that mediates the replication of the mitochondrial DNA.
<i>MMM1</i>	Maintenance of mitochondrial morphology	ER component of the mitochondria-ER encounter structure that tethers mitochondria to the ER.
<i>MMR1</i>	Mitochondrial Myo2 receptor-related	Anchors mitochondria to the cortical ER in small buds. Candidate for the mitochondrial Myo2 receptor.
<i>MTGM</i>	Mitochondrial targeting GxxxG motif	Mitochondrial inner membrane protein that likely plays a role in mitochondrial division. Not present in yeast.
<i>MTP18</i>	Mitochondrial protein	Mitochondrial inner membrane protein that likely plays a role in mitochondrial division. Not present in yeast.
<i>MYO2</i>	Myosin	Class V myosin that transports mitochondria.
<i>NUM1</i>	Nuclear migration	High copy suppressor of a mutant Dnm1 allele. Required for orientation of the mitotic spindle and for maintenance of mitochondrial morphology. Likely involved in mitochondrial fission. Interacts with Dnm1.
<i>OPA1</i>	Optic atrophy	Mammalian homolog of Mgm1.
<i>OPY1</i>	Overproduction-induced pheromone-resistant yeast	Sensor and modulator of the phosphatidylinositol 4,5-bisphosphate synthesis.
<i>PAM17</i>	Presequence translocase-associated motor	Component of the mitochondrial protein import motor.
<i>PCP1</i>	Processing of cytochrome c peroxidase	Mitochondrial rhomboid intramembrane peptidase required for the processing of various mitochondrial proteins.
<i>PGS1</i>	PGP synthase	Protein of the mitochondrial cardiolipin biosynthetic pathway.
<i>PHB1</i> <i>PHB2</i>	Prohibitin	Subunits of the ring-shaped inner mitochondrial membrane prohibitin complex influencing mitochondrial protein stability.
<i>PMA1</i>	plasma membrane ATPase	Plasma membrane H ⁺ -ATPase that pumps protons out of the cell.
<i>PMI</i>	Pantagruelian Mitochondrion I	Mitochondrial inner membrane protein that likely plays a role in mitochondrial division. Not present in yeast.
<i>PSD1</i>	Phosphatidylserine decarboxylase	Phosphatidylserine decarboxylase of the mitochondrial inner membrane; converts phosphatidylserine to phosphatidylethanolamine.
<i>PSD2</i>	Phosphatidylserine decarboxylase	Phosphatidylserine decarboxylase of the golgi/vacuole; converts phosphatidylserine to phosphatidylethanolamine.
<i>RTN1</i> <i>RTN2</i>	Reticulon-like	Reticulon proteins; involved in formation of tubular ER by stabilizing membrane curvature.

Gene	Name	Encoded protein: short description
<i>shibire</i>	Japanese for paralyzed	Encodes Dynamin. Pinches-off endocytic vesicles.
<i>TAM41</i>	T ranslocator a ssembly and m aintenance	CDP-Diacylglycerol synthase of the mitochondria. Involved in the biosynthetic pathway of cardiolipin.
<i>TAZ1</i>	T afazzin	Monolysocardiolipin acyltransferase. Involved in the remodeling of cardiolipin.
<i>TOM20</i>	T ranslocase of the o uter m itochondrial m embrane	Component of the mitochondrial protein import machinery. Attached to the outer membrane via its N-terminal transmembrane domain.
<i>UGO1</i>	Japanese for fusion	Mitochondrial fusion factor that orchestrates Mgm1 and Fzo1 activity. Plays a role in Fzo1 dimer formation.
<i>UPS1</i>	U nprocessed	Involved in cardiolipin biosynthesis and in topogenesis of Mgm1.
<i>UPS2</i>	U nprocessed	Antagonizes Ups1. Involved in phosphatidylethanolamine stability and cristae biogenesis.
<i>VAC17</i>	V acuole related	Vacuole-specific receptor for Myo2.
<i>YME1</i>	Y east m itochondrial e scape	Catalytic subunit of the mitochondrial inner membrane i-AAA protease complex.
<i>YOP1</i>	Y IP O ne P artner	Membrane protein required to maintain ER morphology.
<i>YTA10</i> <i>YTA12</i>	Y east t at-binding a nalog	Components of the mitochondrial inner membrane m-AAA protease complex.

Summary

Mitochondria play diverse roles in the physiology and metabolism of eukaryotic cells. Like most membrane bounded organelles, they cannot be synthesized de novo but grow and split into distinct organelles and must be inherited to daughter cells upon cell division. The structure of the highly dynamic mitochondrial network is adjusted to fit cellular needs by orchestrating mitochondrial movement, fusion, and fission. All three processes are important for the maintenance of functional mitochondria. The core components of the transport, fusion, and division machineries have been identified in baker's yeast. However, the mechanisms controlling mitochondrial dynamics remain poorly understood.

The synoptic aim of this work was to characterize the molecular function of three genes that are involved in maintaining structural integrity of mitochondria: *NUM1*, *MDM33*, and *UPS1*. Yeast cells lacking *NUM1* or *MDM33* show defects in mitochondrial fission, whereas *UPS1* has been reported to be involved in mitochondrial fusion and the biosynthesis of the mitochondrial signature lipid cardiolipin. This work assigns a specific process to each of the three genes and provides evidence how these processes influence mitochondrial behavior. In summary, this study elucidates how various processes influence the fusion and fission of a double membrane bounded organelle.

First, Num1 was identified as key component of a tethering complex that anchors mitochondria at the mother cell cortex. The tethering complex serves to counteract bud-directed mitochondrial movement and assures that a part of the mitochondria remains in the mother cell upon cell division. It acts antagonistically to a known mitochondrial anchor containing Mmr1 at the tip of the daughter cell. Thus, Num1 in the mother and Mmr1 in the bud form two separate cortical tethers to ensure proper distribution of mitochondria by generating opposing forces at spatially distinct and exclusive locations. Strikingly, the tethering of mitochondria at the mother cell cortex was identified as a prerequisite for efficient mitochondrial division.

Second, it was shown that Mdm33 orchestrates mitochondrial fission and phospholipid biosynthesis. Genetic analysis revealed a tight association of *MDM33* and genes affecting mitochondrial phospholipid metabolism. Consistently, Mdm33 overexpression alters mitochondrial lipid composition and directly influences mitochondrial phospholipid biosynthesis. Mutants lacking Mdm33 show reduced mitochondrial fission activity, indicating that Mdm33 promotes mitochondrial division but is no essential component of the fission machinery. Furthermore, Mdm33 was found to act upstream of mitochondrial fission and fusion and to be required to keep mitochondria in a fission competent shape. The results suggest an intriguing connection between mitochondrial fission and phospholipid homeostasis.

Third, it was investigated by electron microscopy whether cells lacking Ups1 or other cardiolipin biosynthesis factors show aberrant mitochondrial ultrastructure. Intriguingly, reduction of cardiolipin levels only affected the shape of the mitochondrial inner membrane when it was accompanied by an increase in mitochondrial cytidine diphosphate-diacylglycerol. A genetic epistasis analysis with focus on mitochondrial ultrastructure revealed that Ups1 acts prior to the first enzymatic reaction of the cardiolipin biosynthesis. This pointed to a role of Ups1 in supplying the CL biosynthesis machinery with precursor lipids. Thus, Ups1 mainly functions in cardiolipin biosynthesis and it is conceivable that reduced cardiolipin levels in $\Delta ups1$ mutants cause mitochondrial fragmentation.

Zusammenfassung

Mitochondrien sind von essentieller Bedeutung für die Physiologie und den Metabolismus eukaryontischer Zellen. Als membranöse Organellen können sie nicht *de novo* erschaffen werden, sondern müssen bei der Zellteilung an die Tochterzelle weitergegeben werden. Die Struktur des mitochondrialen Netzwerkes ist sehr dynamisch und wird durch koordinierte Teilung, Fusion und Bewegung an die Bedürfnisse der Zelle angepasst. Die Hauptkomponenten, die den Transport, die Teilung und die Fusion von Mitochondrien ermöglichen, wurden in der Bäckerhefe identifiziert. Die Mechanismen, die diese Prozesse regulieren, sind jedoch kaum verstanden.

Das synoptische Ziel dieser Arbeit war die Charakterisierung von drei Genen, die an dem Erhalt der strukturellen Integrität des mitochondrialen Netzwerkes beteiligt sind: *NUM1*, *MDM33* und *UPS1*. Zellen ohne Num1 oder Mdm33 weisen Defekte in der Teilung der Mitochondrien auf, wohingegen Ups1 für die Fusion von Mitochondrien und die Biosynthese von Cardiolipin benötigt wird. In dieser Arbeit wird die molekulare Funktion jedes dieser drei Gene untersucht und es wird aufgezeigt, wie diese Funktion das Verhalten sowie die Fusion und die Teilung des mitochondrialen Netzwerkes beeinflusst.

Zuerst wurde Num1 als Bestandteil eines Komplexes identifiziert, der die Mitochondrien an der Plasmamembran der Mutterzelle verankert. Diese Verankerung wirkt dem Transport der Mitochondrien in die Knospe entgegen und stellt sicher, dass ein Teil des mitochondrialen Netzwerkes in der Mutterzelle verbleibt. Num1 wirkt somit antagonistisch zu Mmr1, der Hauptkomponente eines ähnlichen Verankerungskomplexes an der Knospenspitze. Es ist daher anzunehmen, dass die Vererbung von Mitochondrien durch die Koordination von Transport und Verankerung in der Mutter und der Knospe sichergestellt wird. Erstaunlicherweise ist eben diese Verankerung zwingend für die effiziente Teilung von Mitochondrien erforderlich.

Als nächstes wurde herausgefunden, dass Mdm33 mitochondriale Teilung und Phospholipid-Biosynthese miteinander verknüpft. Genetische Analysen zeigten eine enge Assoziation zwischen *MDM33* und Genen der mitochondrialen Phospholipid-Biosynthese auf. Tatsächlich beeinflusst die Überexpression von *MDM33* die Lipidzusammensetzung der Mitochondrien und beeinträchtigt die mitochondriale Phospholipid-Biosynthese. Zellen ohne Mdm33 weisen Defekte in der Teilung von Mitochondrien auf. Mdm33 ist für die Teilung der Mitochondrien jedoch nicht essentiell und übt eine Funktion aus, die der Teilung und Fusion von Mitochondrien übergeordnet ist. Dennoch wird Mdm33 auch benötigt, um eine teilungsfähige Form der Mitochondrien aufrechtzuerhalten. Dies deutet auf eine interessante Verbindung zwischen mitochondrialer Teilung und Phospholipid-Homöostase hin.

Schließlich wurde der Effekt von Defekten der Cardiolipin-Biosynthese auf die Ultrastruktur der Mitochondrien untersucht. Interessanterweise wurde beobachtet, dass reduzierte Cardiolipin Level nur die Ultrastruktur verändern, wenn simultan der Gehalt an Cytidindiphosphat-Diacylglycerin ansteigt. Im Zuge einer genetischen Epistase Analyse wurde festgestellt, dass Ups1 im Hinblick auf die Ultrastruktur der Mitochondrien anderen Genen der Cardiolipin Biosynthese übergeordnet ist. Dies deutet darauf hin, dass Ups1 vor der enzymatischen Kaskade agiert, die die Synthese von Cardiolipin katalysiert. Letztendlich wurde geschlussfolgert, dass der Fusionsdefekt in Abwesenheit von Ups1 sekundär durch die defekte Cardiolipin-Biosynthese begründet ist.

Introduction

Mitochondria are essential organelles of almost all eukaryotic cells. They generate energy in the form of ATP by oxidative phosphorylation, participate in intracellular signaling and apoptosis, are the site of many catabolic and anabolic pathways including the citric acid cycle, the assembly of iron-sulfur clusters, and are involved in the biosynthesis of heme, certain phospholipids as well as fatty acids (Scheffler, 2001; Osellame et al., 2012). This multitude of different functions is reflected in their complex structure. They are double membrane bounded organelles and the smooth outer membrane (MOM) surrounds the highly folded inner membrane (MIM), which in turn enwraps a dense, protein rich matrix. Both membranes enclose an aqueous compartment, the intermembrane space (IMS). The MIM can be subdivided into the inner boundary membrane that faces the MOM and infoldings – termed cristae – that protrude into the matrix (Mannella, 2006). Textbooks often depict mitochondria as small isolated organelles, as seen in electron micrographs (Keyhani, 1980), but in most cell types they form large interconnected networks (Fig. 1A, B). Mitochondria are highly dynamic: They move along the cytoskeleton, undergo frequent division, and fuse with other mitochondria (Fig. 1C; Bereiter-Hahn and Voth, 1994). The shape of the cristae and mitochondrial network is highly variable, depending on cell type and physiological state of the cell (Griparic and van der Bliek, 2001). Mitochondria contain their own genome and protein biosynthesis machinery but the vast majority of all mitochondrial proteins is encoded in the nucleus and imported into the mitochondria post-translationally. In baker's yeast, mitochondria contain more than 750 different proteins (Sickmann et al., 2003), of which only 8 are encoded in the mitochondrial genome (Lipinski et al., 2010). The number of genes that remain encoded on the mitochondrial DNA (mtDNA) varies among species (Gray et al., 1999) but in all cases the essential contribution of the mitochondrial genome to the oxidative phosphorylation demands that mtDNA is faithfully maintained and inherited (Chen and Butow, 2005). This contributes to the semi-autonomous nature of mitochondria: Mitochondrial growth requires the import of nuclear-encoded proteins from the cytosol, the synthesis of polypeptides encoded by the mitochondrial genome, the incorporation of lipids produced mostly in the endoplasmic reticulum (ER), and the replication of mtDNA.

As this work was performed in *Saccharomyces cerevisiae*, the focus will from now on be on mitochondrial biology in baker's yeast. In addition to its obvious amenability to genetic analysis, *S. cerevisiae* is particularly suitable to study mitochondrial behavior because it can generate the required energy solely by fermentation (Altmann et al., 2007). Therefore, genes that are required for oxidative phosphorylation are dispensable for yeast cells growing on fermentable carbon sources. Respiratory-deficient mutants are referred to as *petite* due to their small colony phenotype on media with limited amount of fermentable carbon sources (Ephrussi et al., 1949). Since most complexes of the respiratory chain are composed of mitochondrial and nuclear encoded subunits, the *petite* phenotype can be caused by mutations in the nuclear (nuclear *petite*) or mitochondrial genome (cytoplasmic *petite*; Ephrussi and Slonimski, 1955). Cytoplasmic petite mutants are characterized by the absence of functional [*rho*⁺] mtDNA, either through a complete loss [*rho*⁰], or extensive deletions [*rho*⁻] (Lipinski et al., 2010).

In budding yeast, mitochondria form a branched reticulum below the cell cortex (Koning et al., 1993). The intracellular position, number, size, and morphology of the mitochondria are tightly orchestrated to the cellular needs. For example, if yeast cells enter stationary phase or late meiosis, the branched network rapidly splits into smaller organelles (Miyakawa et al., 1984; Yaffe, 2003). Furthermore, the

network reversibly gets far more extended and branched when the cells are grown on non-fermentable carbon sources (Egner et al., 2002; Jakobs et al., 2003). Two genome wide screens identified the genes that are required to maintain mitochondrial morphology in yeast (Dimmer et al., 2002; Altmann and Westermann, 2005). In the past decade most of the novel mediators have been assigned to a specific process or function that is required to maintain mitochondrial morphology.

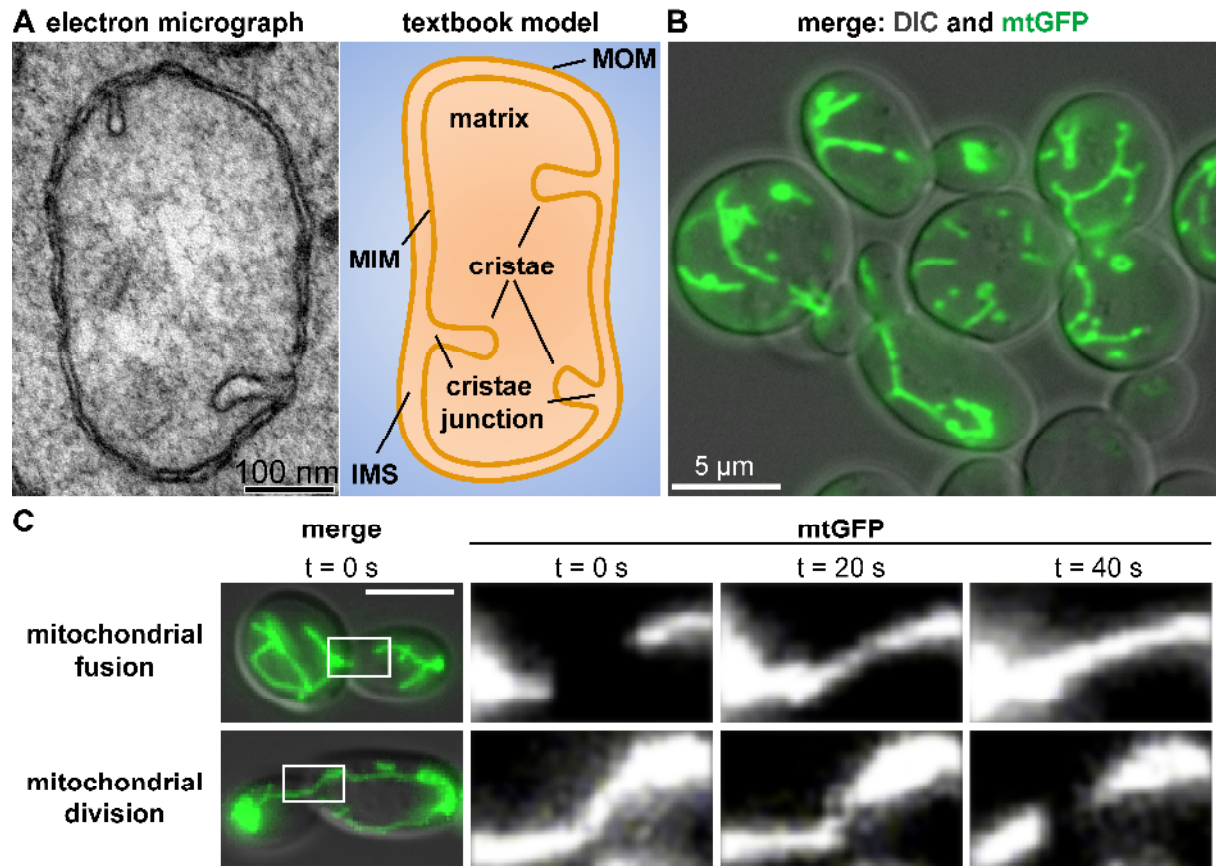


Figure 1 | Mitochondrial ultrastructure and dynamics in *S. cerevisiae*. **A**. Electron micrograph and cartoon depicting mitochondrial ultrastructure. MOM = mitochondrial outer membrane. MIM = mitochondrial inner membrane. IMS = intermembrane space. **B**. Mitochondria of exponentially growing yeast cells visualized with matrix targeted GFP. Shown is a merge of GFP fluorescence and DIC. **C**. 4d-microscopy of exponentially growing yeast cells. Mitochondria are visualized with matrix targeted GFP. Images on the left are merges of a 2d-projection of 10 z-stacks of GFP fluorescence and the corresponding DIC image. On the right, time courses of 2d-projections of 10 z-stacks of GFP fluorescence are shown. All images are unpublished.

Mitochondrial fusion and division

Mitochondria frequently fuse and divide. Mitochondrial fusion serves to unify the mitochondrial compartment thereby counteracting mitochondrial dysfunction caused by mutations of the mtDNA (Westermann, 2002). Furthermore, extended mitochondrial networks generated by fusion activity are electrically united systems and help to distribute energy within the cell (Amchenkova et al., 1988; Skulachev, 2001). As yeast mutants lacking the mitochondrial fusion machinery rapidly lose their mtDNA, fusion of mitochondria obviously acts in the maintenance of the mitochondrial genome (Jones and Fangman, 1992; Hermann et al., 1998). In contrast, the generation of smaller organelles by mitochondrial division plays an important role in the removal of damaged organelles by autophagy (Mao et al., 2013), regulation of developmental processes, and in proper mitochondrial

distribution (Lackner and Nunnari, 2009). In yeast between 0.5 and 2.5 events of mitochondrial fusion and fission occur per minute. The exact number depends on the growth phase and on the carbon source (Nunnari et al., 1997; Jakobs et al., 2003). If mitochondrial fusion is unopposed by fission, mitochondria turn into a highly interconnected single organelle (Bleazard et al., 1999; Santel and Fuller, 2001; Smirnova et al., 2001). Likewise, a lack of mitochondrial fusion leads to fragmentation of the organelle (Hermann et al., 1998; Chen et al., 2003). The mitochondrial morphology is maintained by balancing these two antagonizing processes. Hence, if fusion and fission are blocked simultaneously, tubular mitochondrial morphology is restored (Bleazard et al., 1999; Sesaki and Jensen, 1999; Fekkes et al., 2000).

Mitochondrial division

Mitochondrial division is mediated by the proteins Dnm1 (**d**ynam**i**n-related) in yeast and DRP1 (**d**ynam**i**n related **p**rotein) in mammals that are large self-assembling GTPases belonging to the family of dynamin related proteins (Lackner and Nunnari, 2009). Members of the dynamin superfamily are well known to be involved in the scission of a wide range of vesicles and organelles (Praefcke and McMahon, 2004). The role of dynamins in membrane scission was first discovered in paralyzed *Drosophila melanogaster* mutants (Grigliatti et al., 1973). The mutants were immobile due to an accumulation of endocytic profiles caused by a temperature sensitive allele of the dynamin *shibire* (van der Bliek and Meyerowitz, 1991). Classical dynamins form spirals around membranes and they mechanochemically sever these driven by oligomerization-stimulated GTPase activity (Praefcke and McMahon, 2004).

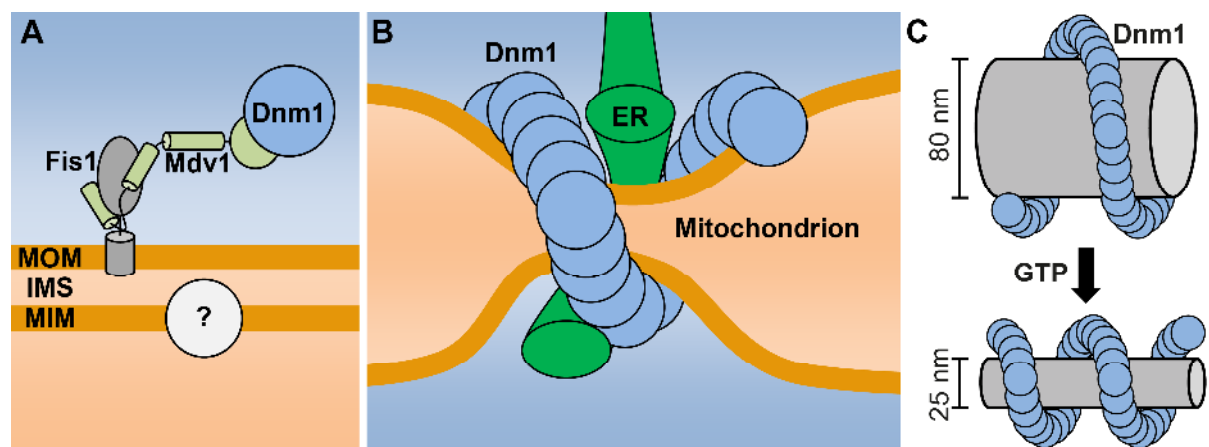


Figure 2 | Model of mitochondrial division in *S. cerevisiae*. **A.** Cartoon depicting the mitochondrial division machinery. MOM = mitochondrial outer membrane. MIM = mitochondrial inner membrane. IMS = intermembrane space. **B.** Model for ER-mediated mitochondrial constriction and Dnm1 assembly. **C.** Dnm1 assembles as a helix and the inner lumen of Dnm1 spirals decreases from ~80 nm to ~25 nm upon addition of GTP. All images are unpublished. See text for details.

In yeast, the soluble protein Dnm1 assembles on mitochondria into punctate structures (Otsuga et al., 1998; Sesaki and Jensen, 1999). These assemblies are either laterally associated with mitochondria and most likely involved in anchoring the mitochondria at the cell cortex or they completely surround the mitochondrial tubules and drive mitochondrial division (Legesse-Miller et al., 2003; Schauss et al., 2006). The recruitment of Dnm1 from the cytosol is mediated by two cooperating proteins, Fis1 (mitochondrial **f**ission) and Mdv1 (**m**itochondrial **d**ivision; Fig. 2A). Fis1 is an integral protein of the MOM with a C-terminal transmembrane domain and an N-terminal

tetratricopeptide repeat domain facing the cytosol (Mozdy et al., 2000). Mdv1 acts as a molecular bridge between Fis1 and Dnm1 (Karren et al., 2005). The N-terminal extension domain interacts directly with the cytosolic part of Fis1 (Tieu et al., 2002) whilst the C-terminal WD-40 repeat domain interacts with Dnm1 (Fig. 2A; Cervený and Jensen, 2003). Mdv1 furthermore assembles into punctate structures that colocalize with Dnm1 assemblies. This assembly depends on Dnm1 (Tieu et al., 2002) and succeeds the formation of Dnm1 punctae (Naylor et al., 2006), indicating that Mdv1 also acts after targeting Dnm1 to the mitochondria. Consistent with this idea, *in vitro* data show that Mdv1 promotes GTP-bound Dnm1 oligomerization and could co-assemble with Dnm1 in a stoichiometric manner (Lackner et al., 2009). Therefore, Mdv1 might act simultaneously as a nucleator for Dnm1 assembly and later on as a scaffold to stabilize Dnm1 assemblies.

Interestingly, GTP-bound Dnm1 assembled on liposomes forms spirals that have a diameter of 100 nm which would be insufficient to surround a mitochondrion with a mean diameter of 300 nm (Ingerman et al., 2005). Therefore, mitochondrial constriction has to precede the assembly of mitochondria-surrounding Dnm1 spirals. Indeed, the constriction of the mitochondrial matrix and MOM was found to be independent of Fis1 or Dnm1, respectively (Jakobs et al., 2003; Legesse-Miller et al., 2003). Recent electron microscopical studies showed that the ER wraps around mitochondria at sites of future division (Fig. 2B). This causes a constriction of the mitochondria to a diameter of approximately 100 nm, perfectly fitting the diameter of assembled Dnm1 spirals (Friedman et al., 2011). Thus, mitochondrial division is spatially linked to ER-mitochondria contact sites (Murley et al., 2013). Taken together, the current model for mitochondrial division is that Fis1 and Mdv1 cooperatively recruit GTP-bound Dnm1 to ER-mediated mitochondrial constriction sites. There Dnm1 co-oligomerizes with Mdv1 to form large spirals that completely surround the mitochondrion. Subsequently, the Dnm1 spirals undergo self-assembly stimulated GTP-hydrolysis what leads to a conformational change causing a constriction of the spiral (Fig. 2C; Mears et al., 2011). Dnm1 thereby mechanochemically severs the mitochondrion by a mechanism that is strikingly similar to the action of classical dynamins in endocytosis.

Mitochondrial inner membrane division

It is unclear whether the activity of Dnm1 is sufficient to simultaneously sever both mitochondrial membranes or whether an independent machinery divides the MIM (Westermann, 2008). However, there is evidence that separate machineries for MOM and MIM division exist. First, mitochondrial matrix constriction can be observed in absence of Dnm1 or Fis1. This could be explained by the ER constricting the mitochondria, but in some cases the matrix constriction occurs independently of the MOM (Jakobs et al., 2003; Legesse-Miller et al., 2003). Second, it was shown in *C. elegans* that in cells lacking the Dnm1 homolog DRP-1 the matrix is divided into bleb-like structures whereas the MOM stays connected by thin tubules devoid of matrix content (Labrousse et al., 1999). Third, isolated rat liver mitochondria change the amount of cristae junctions per cristae according to the environmental conditions (Mannella et al., 2001). Generation of additional cristae junctions requires membrane remodeling, topologically identical to MIM division (Mannella, 2006). And fourth, plastids, the plant-specific double membrane bounded organelles that share an endosymbiotic origin with mitochondria, are known to be divided by cooperation of a dynamin-like protein that acts from the outside and a homolog of the prokaryotic fission protein FtsZ (**f**ilamenting **t**emperature-sensitive mutant **Z**) that acts from the inside (Yoshida et al., 2012).

There are few known MIM proteins likely involved in mitochondrial fission and therefore candidates for MIM division: Mdm33 (**m**itochondrial **d**istribution and **m**orphology) in yeast, PMI (**P**antagruelian **M**itochondrion **I**) in flies, CHPPR (**C**hondrocyte Protein With a **P**oly-**P**roline **R**egion) in chicken, and MTGM (**m**itochondrial **t**argeting **G**xxx**G** **m**otif) and MTP18 (**m**itochondrial **p**rotein) in humans (Messerschmitt et al., 2003; Tonachini et al., 2004; Tondera et al., 2004; Tondera et al., 2005; Zhao et al., 2009; Rival et al., 2011; Macchi et al., 2013). Most of these proteins are conserved among mouse, fly, and human, except of Mdm33 that has no homolog in higher eukaryotes. Interestingly, none of the mammalian factors has a homolog in yeast. Overexpression of most of these proteins is associated with mitochondrial fragmentation whilst deletion or knockdown results in fewer but larger mitochondria (Tab. 1). This suggests a role of each of these proteins in mitochondrial fission.

Table 1 | Candidate proteins for mitochondrial inner membrane (MIM) division. See text for more details.

Name	organism	localization	overexpression	deletion / knockdown	reference
CHPPR	chicken, conserved	MIM	fragmented mitochondria	not determined	Tonachini et al., 2004
Mdm33	yeast	MIM - integral	fragmented mitochondria	mitochondrial swelling	Messerschmitt et al., 2003
MTGM	human, conserved	MIM - integral	fragmented mitochondria	mitochondrial elongation	Zhao et al., 2009
MTP18	human, conserved	MIM - integral	fragmented mitochondria	mitochondrial aggregation	Tondera et al., 2004; Tondera et al., 2005
PMI	fly, conserved	MIM - integral	not determined	mitochondrial swelling	Rival et al., 2011; Macchi et al., 2013

Mdm33 is a 54 kDa protein of the MIM that forms homo-oligomeric complexes. It has two C-terminal transmembrane domains that are connected by a small IMS linker. The N-terminal part of the protein faces the matrix. Deletion of *MDM33* causes the formation of giant ring-like mitochondria which are composed of very long stretches of both mitochondrial membranes enclosing a very narrow matrix space. Typically, these structures are swollen at some parts which are tightly packed with cristae. In striking contrast, *MDM33* overexpression causes a growth arrest, rapid mitochondrial fragmentation, and the formation of MIM septa (Messerschmitt et al., 2003). It is persuasive that Mdm33 promotes mitochondrial division: The extremely extended structures in the deletion mutant can form only in the absence of frequent division. Furthermore, overexpression causes a shift of the balance between mitochondrial fusion and fission towards fission.

Num1 and Mdm36

There are two additional cytosolic factors that contribute to mitochondrial division and distribution in baker's yeast, namely Num1 (**n**uclear **m**igration) and Mdm36. Num1 is a large cell-cortical protein that is required for proper orientation of the mitotic spindle (Heil-Chapdelaine et al., 2000) and was found to be a high copy suppressor of a dominant negative Dnm1 allele (Cervený et al., 2007). *NUM1* and *MDM36* were identified in a genome wide screen for mutants with altered mitochondrial morphology (Dimmer et al., 2002). Cells lacking either of both display severely altered mitochondria with interconnected aggregated nets located in the middle of the cell. They are no essential components of the mitochondrial division machinery as $\Delta num1$ and $\Delta mdm36$ mutant mitochondria

retain fission ability and double mutants with $\Delta fzo1$ contain fragmented mitochondria. Num1 physically interacts with Dnm1 and a colocalization of Mdv1-free Dnm1 spots and Num1 can be observed in fluorescence micrographs (Cervený et al., 2007; Hammermeister et al., 2010). These Dnm1 spots are spatially oriented towards the cell cortex and have been described to be formed independently of Mdv1 (Schauss et al., 2006). Intriguingly, the colocalization of Num1 and Dnm1 depends on Mdm36 (Hammermeister et al., 2010). The cortical localization of Num1 together with the absence of peripheral mitochondria and an increase in mitochondrial motility in both $\Delta num1$ and $\Delta mdm36$ mutants suggested that the proteins might be involved in anchoring the mitochondria to the cell cortex (Cervený et al., 2007; Hammermeister et al., 2010). Yet, it remained unknown how this may contribute to mitochondrial fission (Schauss and McBride, 2007).

Mitochondrial fusion

Although dynamins usually act in membrane scission, mitochondrial fusion is mediated by distantly related members of the dynamin superfamily: Fzo1 (**f**uzzy **o**nions homolog) acting in MOM fusion and Mgm1 (**m**itochondrial **g**enome **m**aintenance) acting in MIM fusion. Fzo1 is conserved from yeast to humans and was first identified in sterile male flies that failed to rearrange their mitochondria during spermatogenesis. Normally, in *D. melanogaster* the mitochondria aggregate next to the spermatid nuclei to form a structure called *Nebenkern*. The *Nebenkern* consists of two giant mitochondria that are wrapped around each other and have the shape of a sliced onion in electron micrographs (Tokuyasu, 1975). In the fuzzy onions mutant the mitochondria failed to fuse during *Nebenkern* formation, giving the structure a fuzzy appearance (Hales and Fuller, 1997). Yeast Fzo1 (**m**itofusins Mfn1 and Mfn2 in humans) is a large GTPase with two MOM spanning transmembrane domains. Only a small loop connects the transmembrane domains and resides in the IMS whilst the rest of the protein faces the cytosol (Fig. 3A; Hermann et al., 1998; Fritz et al., 2001).

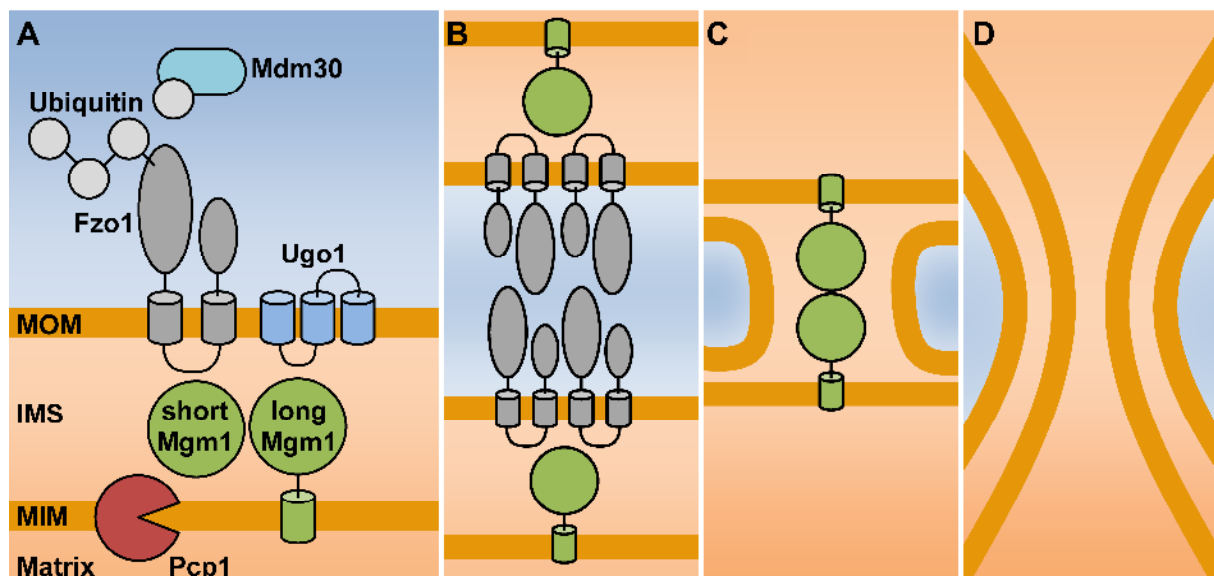


Figure 3 | Model of mitochondrial fusion in *S. cerevisiae*. **A.** Cartoon depicting the mitochondrial fusion machinery. MOM = mitochondrial outer membrane. MIM = mitochondrial inner membrane. IMS = intermembrane space. **B.** Tethering of two mitochondria by Fzo1 *cis*- and *trans*-dimer formation. **C.** Mgm1 *trans*-dimer formation directly after MOM-fusion. **D.** Fused mitochondria with unified matrix. The proteins in **B** and **C** are depicted according to **A**. See text for details. All images are unpublished.

Mgm1 (**o**ptic **a**trophy 1 or OPA1 in humans) is a large evolutionary conserved GTPase that exists in two isoforms. The large isoform contains an N-terminal transmembrane domain that anchors the protein in the MIM with the major part of the protein facing the IMS (Wong et al., 2000; Herlan et al., 2003). Upon processing by the rhomboid protease Pcp1 (**p**rocessing of **c**ytochrome **c** **p**eroxidase) a small isoform is generated that lacks the transmembrane domain but still contains the GTPase domain (Fig. 3A) and is a soluble protein of the IMS (Herlan et al., 2003; McQuibban et al., 2003). Apparently, both isoforms are required for mitochondrial fusion (Herlan et al., 2003; McQuibban et al., 2003). Fzo1 and Mgm1 are essential components of the mitochondrial division machinery as $\Delta fzo1$ and $\Delta mgm1$ mutants show fragmented mitochondria (Guan et al., 1993; Hermann et al., 1998; Rapaport et al., 1998), no mitochondrial fusion upon mating (Hermann et al., 1998; Wong et al., 2000), and mitochondria isolated from these mutants fail to fuse their matrices in vitro (Meeusen et al., 2004; Meeusen et al., 2006). Both proteins share typical features with known fusion proteins: First, they have GTPase domains that could be used to overcome the energy barrier of membrane fusion (Martens and McMahan, 2008). Second, Fzo1 and Mgm1 form homotypic *trans*-complexes that are required to tether the fusion partners together (DeVay et al., 2009; Anton et al., 2011). Third, Mgm1 and most likely also Fzo1 undergo a conformational change upon GTP hydrolysis, pulling the opposing membranes together (Anton et al., 2011; Abutbul-Ionita et al., 2012). Since MOM fusion is abolished in $\Delta fzo1$ but not in $\Delta mgm1$ mutants (Meeusen et al., 2004; Meeusen et al., 2006), Fzo1 most likely catalyzes the fusion of the MOM whilst Mgm1 catalyzes the fusion of the MIM. Interestingly, cells lacking Mgm1 show decreased cristae abundance (Meeusen et al., 2006) and an alteration in cristae structure (Sesaki et al., 2003). Since yeast cells with severe defects in oxidative phosphorylation show similar phenotypes (Sauvanet et al., 2012), the cristae alterations in $\Delta mgm1$ strains could well be a secondary effect caused by the loss of the mtDNA.

In yeast, two additional proteins have been identified that are required for MOM fusion, Ugo1 (which is Japanese for fusion) and Mdm30 (Fig. 3A). Since mitochondria are surrounded by two membranes, fusion of both membranes has to be orchestrated. In yeast, the MOM protein Ugo1 might fulfill this role as it physically links Fzo1 and Mgm1 (Wong et al., 2003; Sesaki and Jensen, 2004). Furthermore, Ugo1 promotes Fzo1 *cis*-dimerization (Anton et al., 2011) and seems to exhibit an essential function after membrane tethering in later steps of both MIM and MOM fusion (Hoppins et al., 2009). Mdm30 is a mitochondria-associated F-box protein required for mitochondrial fusion (Fritz et al., 2003). It regulates mitochondrial fusion by mediating Fzo1-ubiquitylation and degradation in a proteasome-dependent manner (Dürr et al., 2006; Cohen et al., 2008). This is not required for Fzo1-mediated membrane tethering but for membrane fusion (Cohen et al., 2011). The current model for mitochondrial fusion is that Ugo1 and GTP binding promote Fzo1 *cis*-dimer formation and these *cis*-dimers then form *trans*-complexes with Fzo1 dimers of opposing mitochondrial membranes. GTP hydrolysis leads to a conformational change in Fzo1, what allows Mdm30 dependent ubiquitylation and degradation of Fzo1 and finally leads to MOM fusion (Fig. 3A, B). Afterwards *trans*-complexes between Mgm1 of the two opposing MIMs are formed and the MIMs are fused by a GTP-hydrolysis driven conformational change in Mgm1 (Fig. 3C, D).

Mitochondrial movement and partitioning

Most membrane bounded organelles cannot be generated de novo and therefore have to be inherited from the mother to the daughter cell. In budding yeast the cell division is asymmetrical, producing a smaller daughter cell, called bud. Hence, the process is termed budding. At the

beginning of the cell cycle a site for bud emergence is selected and the whole cytoskeleton is polarized towards the newly formed bud what establishes an axis of polarity and an intrinsic cellular asymmetry. All organelles, mRNAs and even the mitotic spindle are transported along the actin cytoskeleton. After a bud site is selected the growth of the yeast cell is limited to the bud and the organelles are duplicated and segregated into the bud (Pruyne et al., 2004).

There are two conflicting models for mitochondrial transport in budding yeast. The first states that mitochondrial movement is driven by Arp2/3 (actin-related protein) mediated actin polymerization (Vevea et al., 2013), similar to the movement of the intracellular pathogen *Listeria monocytogenes* (Tilney and Portnoy, 1989; Tilney et al., 1990). In this model, the Arp2/3 complex is directly targeted to the mitochondria by a structure called mitochore, consisting of the proteins Mmm1 (maintenance of mitochondrial morphology), Mdm10 (mitochondrial distribution and morphology), and Mdm12 (Boldogh et al., 2001; Boldogh et al., 2003). Since Mmm1 was mislocalized to the mitochondria upon its first description (Burgess et al., 1994; Kondo-Okamoto et al., 2003) but actually resides in the ER and serves in ER-mitochondria tethering (Kornmann et al., 2009), the model is rather unlikely. The alternative and more reasonable model postulates that the class V myosin motor protein Myo2 is bound on the mitochondria by an unknown receptor and actively transports them along existing actin cables (Förtsch et al., 2011). This model is mainly supported by the findings that (I) actin-binding of isolated mitochondria is ATP-dependent (Lazzarino et al., 1994), (II) isolated mitochondria show motor activity in cell-free actin gliding assays (Simon et al., 1995), (III) *myo2* mutants fail to efficiently segregate mitochondria into the bud (Itoh et al., 2002), (IV) this can be rescued by an artificial mitochondria-anchored version of Myo2 when the mutations are in the Myo2 cargo-binding domain (Förtsch et al., 2011), (V) mitochondria isolated from strains lacking functional Myo2 lose their ability to interact with actin filaments in vitro (Altmann et al., 2008), and (VI) Myo2 is found on isolated mitochondria by immuno-electron microscopy (Förtsch et al., 2011). Usually, Myo2 is recruited to the cargo organelles by specific receptors in the organellar membranes. The best mitochondrial Myo2 receptor candidate is the bud-localized peripheral MOM protein Mmr1 (Itoh et al., 2004). Overexpression of *MMR1* results in accumulation of mitochondria in the bud and rescues mitochondrial distribution defects of *myo2* mutants. Mmr1 physically interacts with the cargo binding domain of Myo2 (Itoh et al., 2004) and the binding site partially overlaps with the binding site of the vacuolar receptor Vac17 (Ishikawa et al., 2003; Eves et al., 2012). This is consistent with the idea that vacuoles and mitochondria compete for Myo2 binding and that this is required for coordination of the inheritance of both cargoes (Eves et al., 2012). However, the mitochondrial inheritance defect of Δ *mmr1* mutants is unexpectedly mild (Itoh et al., 2004; Frederick et al., 2008) and Myo2 cargo-binding domain mutants are not synthetic sick with but epistatic to the deletion of Mmr1 (Förtsch et al., 2011), suggesting that Mmr1 is not the mitochondrial Myo2 receptor.

After cell division, mother and daughter cells both should contain a complete set of organelles. Therefore, a mechanism in addition to the bud-directed transport of organelles must exist and ensure proper segregation. Recent studies indicate that Mmr1 does not act as mitochondrial Myo2 receptor but instead localizes to bud tips and physically links mitochondria to the cortical ER (Swayne et al., 2011). Thereby mitochondria are anchored and retained at the bud tip what is of particular importance directly before cell division when the actin cytoskeleton of the mother cell and the bud reorganizes and is no longer oriented towards the bud tip but towards the mother bud neck (Moseley and Goode, 2006). It was shown that mitochondria are also immobilized in the mother cell distal to the bud. This anchorage of mitochondria in the so-called 'retention zone' most likely ensures

that some mitochondria remain in the mother cell (Yang et al., 1999). The molecular mechanism underlying the establishment of the retention zone remained unknown.

Mitochondria-ER contact sites

Interorganellar membrane contact sites play important roles in lipid transfer, signal transduction, and Ca^{2+} -trafficking (Rowland and Voeltz, 2012). Most known contact sites are formed between the ER and other organelles, including the mitochondria, vacuole, Golgi, peroxisomes, as well as the plasma membrane (Elbaz and Schuldiner, 2011; Toulmay and Prinz, 2011). In yeast, the contacts between the mitochondria and the ER are formed by a proteinaceous structure called ER mitochondria encounter structure (ERMES). The ERMES consists of four core subunits (Fig. 4): Mdm34 (**m**itochondrial **d**istribution and **m**orphology) and Mdm10 in the MOM, Mdm12 in the cytosol, and the integral ER protein Mmm1 (**m**aintenance of **m**itochondrial **m**orphology; Kornmann et al., 2009). Disruption of any of the subunits causes a complete disassembly of the complex leading to swollen mitochondria, the loss of mtDNA, and a severe growth defect (Burgess et al., 1994; Sogo and Yaffe, 1994; Berger et al., 1997; Youngman et al., 2004).

The loss of the mitochondrial genome in ERMES mutants could be explained by the fact that the ERMES colocalizes with actively replicating nucleoids. The 'replisome' consists of mtDNA, the **m**itochondrial **g**enome **m**aintenance factor Mgm101, and the **m**itochondrial DNA polymerase Mip1 (Fig. 4). Interestingly, the ERMES subunit Mmm1 colocalizes with Mgm101 even in the absence of mtDNA what indicates a three membrane spanning protein complex (Meeusen and Nunnari, 2003). This complex might also contain the MIM proteins Mdm31 and Mdm32 as in either deletion mutant the colocalization between Mmm1 and the nucleoids is abolished (Dimmer et al., 2005). The ERMES contains an additional regulatory subunit, the MOM GTPase Gem1 (**G**TPase **E**F-hand protein of **m**itochondria; Kornmann et al., 2011; Stroud et al., 2011). Since mitochondrial division occurs at sites of mitochondria-ER contacts (see above), the ERMES complex colocalizes with assembled Dnm1 on mitochondria. Directly after division, this interaction has to be dismantled what is done by Gem1. Interestingly, the connection between ERMES and mtDNA probably also serves to link mitochondrial division and nucleoid segregation because mitochondrial nucleoids are associated with over 80% of mitochondrial division events (Murley et al., 2013).

As the contacts between ER and mitochondria are important for lipid exchange (Achleitner et al., 1999) and phosphatidylethanolamine (PE) biosynthesis (see below), the ERMES mutants display a lipid phenotype (Kornmann et al., 2009; Osman et al., 2009a). Intriguingly, most of ERMES mutant phenotypes including the alterations in lipid composition can be alleviated by overexpression of the

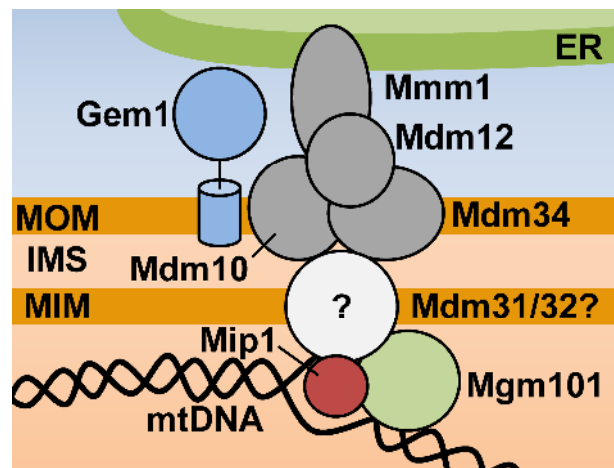


Figure 4 | Cartoon depicting the ER mitochondria encounter structure in *S. cerevisiae*. MOM = mitochondrial outer membrane. MIM = mitochondrial inner membrane. IMS = intermembrane space. mtDNA = mitochondrial DNA. Unpublished. See text for details.

poorly characterized genes *MCP1* or *MCP2* (Mdm10 complementing protein). This implies that there might be an ERMES independent lipid transport between ER and mitochondria (Tan et al., 2013).

Mitochondrial phospholipid biosynthesis

Phospholipids play many essential roles in the biology of the cell that extend beyond lipid metabolism and membrane integrity. They are of vital importance for vesicular and non-vesicular transport (Balla, 2013), membrane identity (Nakatsu et al., 2012), folding and import of membrane proteins (Joshi et al., 2009), and many more cellular processes (Henry et al., 2012). Mitochondria contain a specific set of phospholipids that is required to maintain their morphology and functionality. In yeast, all glycerolipids are derived from the precursor lipid phosphatidic acid (PA) via sequential modifications by multiple phospholipid-synthetic enzymes located in various cellular compartments. Whilst mitochondria contribute to the synthesis of few cellular fatty acids and phospholipids, most are produced in the ER. The ER synthesizes the majority of PA, phosphatidylinositol, phosphatidylserine (PS), and phosphatidylcholine (PC), whereas mitochondria produce PE and cardiolipin (CL; Fig. 5; Henry et al., 2012).

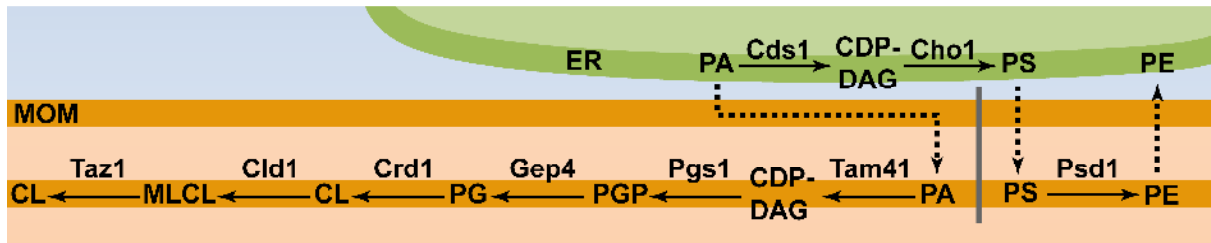


Figure 5 | Mitochondrial phospholipid biosynthesis in *S. cerevisiae*. MOM = mitochondrial outer membrane. CL = cardiolipin. MLCL = monolysocardiolipin. PG = phosphatidylglycerol. PGP = phosphatidylglycerol phosphate. CDP-DAG = cytidine diphosphate-diacylglycerol. PA = phosphatidic acid. PS = phosphatidylserine. PE = phosphatidylethanolamine. Dashed lines indicate transport processes. Unpublished. See text for details.

Although most membrane phospholipids, such as PC, form stable lipid bilayers at physiological temperatures, some cellular lipids intrinsically destabilize bilayers. When they are purified, they do not assemble bilayer phases at physiological conditions. This is mainly caused by a small headgroup or bulky sidechains resulting in a cone-like shape. Whereas bilayers are mainly formed by cylindrical lipids, conical lipids prefer the formation of structures with a high intrinsic curvature such as liposomes or micelles. The presence of non-bilayer lipids is important to disorder membranes and thereby keep them in a fluid state. However, the overall lipid mixture of cellular membranes is always balanced to form metastable lipid bilayers (Frolov et al., 2011). The phospholipids CL and PE which are produced in mitochondria both have a small headgroup compared to the size of the sidechains and therefore are non-bilayer forming. They are fusogenic, play crucial roles in maintaining mitochondrial morphology, and can confer negative curvature to mitochondrial membranes (Joshi et al., 2009; Tamura et al., 2009; Potting et al., 2010; Kuroda et al., 2011). Interestingly, the combined deletion of genes that are involved in production of CL and PE are synthetically lethal in yeast, indicating that CL and PE are partially redundant and that a sufficient level of either of them is required for life (Gohil et al., 2005). This overlap of function can also be seen in their role in mitochondrial fusion. When both lipids are depleted simultaneously, the mutants exhibit fragmented mitochondria, reduced membrane potential, and loss of mtDNA, characteristic of fusion mutants (Joshi et al., 2012). When only PE or CL is depleted, the phenotype is similar but considerably less

severe (Chen et al., 2010; Chan and McQuibban, 2012). How the non-bilayer lipids contribute to mitochondrial fusion is not completely understood.

Biosynthesis of phosphatidylethanolamine

In yeast, PE is synthesized by two alternative pathways: The Kennedy pathway and the cytidine diphosphate-diacylglycerol (CDP-DAG) pathway. In the CDP-DAG pathway, CDP-DAG is processed into PS in the ER by the PS-synthase Cho1 (**ch**oline requiring; Atkinson et al., 1980; Letts et al., 1983). PS is then either transported into the mitochondria and decarboxylated by the **PS** decarboxylase Psd1 (Clancey et al., 1993; Trotter et al., 1993) or transported into the golgi/vacuole where the decarboxylation is performed by Psd2 (Trotter and Voelker, 1995). The product of this reaction, PE, is subsequently transported back into the ER and further processed into PC (Fig. 5). In the Kennedy pathway, PE and PC are directly synthesized from ethanolamine and choline, bypassing PS as an intermediate (Kennedy and Weiss, 1956). The CDP-DAG pathway is the major route for PE biosynthesis and more than 75% of the cellular PE is synthesized by Psd1 (Clancey et al., 1993; Trotter et al., 1993). Interestingly, both pathways are used by wildtype cells, regardless of whether or not ethanolamine and choline are present in the growth medium (Henry et al., 2012).

Biosynthesis of cardiolipin

CL has a characteristic dimeric structure with two phosphatidyl moieties that are linked by a glycerol. It is well known as the mitochondrial signature lipid and plays a critical role in mitochondrial function and biogenesis (Joshi et al., 2009). The first step of the CL biosynthesis is the conversion of PA to CDP-DAG but unlike the PE biosynthesis pathway, all of the enzymes for de novo synthesis of CL are present in the mitochondria (Fig. 5; Henry et al., 2012). For long time, only the ER residing **CDP-DAG** synthase Cds1 was known. Since isolated mitochondria showed CDP-DAG synthase activity it was a matter of debate whether Cds1 might be as well imported into the mitochondria (Kuchler et al., 1986; Shen et al., 1996). Recently, the debate was put to an end by identification of an additional mitochondrial CDP-DAG synthase, Tam41 (**trans**locator **as**sembly and **ma**intenance; Tamura et al., 2013). The CDP-DAG produced by Tam41 serves as a substrate for the **PGP** synthase Pgs1 and is converted to phosphatidylglycerol phosphate (PGP; Chang et al., 1998). Gep4 (**gen**etic **i**nteractors of **pro**hibitins) subsequently forms phosphatidylglycerol (PG) via dephosphorylation of PGP (Kelly and Greenberg, 1990; Osman et al., 2010). The **cardiolipin** synthase Crd1 afterwards catalyzes an irreversible condensation reaction to couple PG and CDP-DAG and form CL (Tuller et al., 1998). CL then undergoes remodeling — deacylation by Cld1 (**cardiolipin**-specific **de**acylase) leads to the formation of monolysocardiolipin (MLCL) and Taz1 (**ta**fazzin) then removes an acyl chain from another phospholipid and adds it to MLCL, consequently regenerating CL with a different sidechain (Gu et al., 2004; Beranek et al., 2009). Astonishingly, CL biosynthesis and remodeling by Cld1p are associated with the matrix-facing leaflet of the MIM (Schlame and Haldar, 1993; Baile et al., 2013) whilst Taz1 is sorted into the IMS with two segments inserting it into the MIM and the MOM (Claypool et al., 2006; Herndon et al., 2013). Hence, MLCL must be transported to the IMS-facing MIM leaflet in order to gain access to Taz1.

Associated factors

Mitochondrial phospholipid biosynthesis does not only depend on the proteins directly involved in the biosynthetic pathway but as well on other associated factors. Since mitochondrial phospholipid

biosynthesis requires the import of precursors from the ER it is not surprising that ERMES mutants show reduced levels of CL and PE (Osman et al., 2009a; Tan et al., 2013). A specific reduction of CL levels can be observed in cells lacking the IMS protein Ups1 (**un**processed; Osman et al., 2009a; Tamura et al., 2009). Yeast cells grown on glucose and lacking *UPS1* show a growth defect, reduced mitochondrial protein import, defects in assembly of the ATP/ADP carrier, impaired processing of Mgm1, and reduced mitochondrial membrane potential (Sesaki et al., 2006; Osman et al., 2009a; Tamura et al., 2009). Since $\Delta ups1$ mutants also harbor fragmented mitochondria it was assumed that Ups1 might play a role in mitochondrial fusion. Ups1 has a closely related homologue – Ups2 – that is an IMS protein and belongs to the same protein family as Ups1. Loss of Ups2 causes defects in mitochondrial PE stability as well as reduced cristae biogenesis. Strikingly, additional loss of *UPS2* rescues all phenotypes apart from the mitochondrial morphology defects in $\Delta ups1$ mutants (Osman et al., 2009a; Tamura et al., 2009). This suggests antagonizing functions of Ups1 and Ups2. Consistently, overexpression of Ups2 causes defects similar to that of $\Delta ups1$ mutants as it reduces CL levels. However, overexpression of Ups1 causes no reduction in PE stability (Osman et al., 2009a). Both, Ups1 and Ups2, depend on the small twin CX₂C protein family member Mdm35 which ensures efficient import into the IMS and protects both proteins against proteolytic degradation by the MIM i-AAA protease Yme1 (**y**east **m**itochondrial **e**scape) and the MIM metalloprotease Atp23 (**A**T**P**ase; Potting et al., 2010). How Ups1 and Ups2 regulate mitochondrial morphology and mitochondrial phospholipid metabolism is still unknown.

Another protein that is required for the biosynthesis of CL is the integral MIM protein Fmp30 (found in **m**itochondrial **p**roteome). Fmp30 shows strong similarity to mammalian N-acyl-PE-specific phospholipase D which is a member of a superfamily including a wide variety of hydrolases, the metallo-b-lactamase family. Functional analysis renders it likely that Fmp30 has hydrolase activity, and that this activity is essential for the function of the protein. Though, the molecular function of Fmp30 is unknown. Intriguingly, Fmp30 is only required for the formation of CL in the absence of Psd1 (Kuroda et al., 2011). Thus, the double mutant $\Delta fmp30 \Delta psd1$ is inviable as cells cannot tolerate simultaneous reduction of CL and PE levels (Gohil et al., 2005).

Prohibitins

Members of the conserved **prohibitin** membrane protein family have been identified in organisms of all phylogenetic kingdoms with two closely related proteins – Phb1 and Phb2 – being present in each case. Though the localization of the prohibitins is controversial, recent studies indicate that they mainly act in the MIM (Osman et al., 2009b). They are named prohibitins because the injection of *PHB1* mRNA into human dermal fibroblasts inhibits the initiation of DNA synthesis (McClung et al., 1989). This was later assigned to the 3' untranslated region of the *PHB1* mRNA (Jupe et al., 1996). Single particle electron microscopy and crosslinking studies suggest that yeast Phb1 and Phb2 form a large ring-like complex in the MIM that is built up of multiple Phb1 and Phb2 subunits alternating with each other (Back et al., 2002; Tatsuta et al., 2005). When the complex formation is inhibited by deletion of one subunit, the presence of the other subunit can no longer be detected (Berger and Yaffe, 1998). Intriguingly, deletion of the prohibitins shortens replicative lifespan in yeast cells (Coates et al., 1997; Piper and Bringloe, 2002; Kirchman et al., 2003). This seems to be caused by mitochondrial dysfunction in aged prohibitin mutants as they show alterations in mitochondrial morphology and inheritance (Piper et al., 2002). The molecular function of the prohibitins is only poorly understood. They form a large supercomplex with the mitochondrial m-AAA protease in the

MIM and the observation that protein stability is decreased in the prohibitin mutants suggests that they negatively regulate the m-AAA protease activity (Steglich et al., 1999). The prohibitin complex is furthermore able to stabilize newly synthesized mitochondrial translation products through direct interaction (Nijtmans et al., 2000), pointing to a potential role as membrane-bound chaperones. Consistently, a constitutive mitochondrial unfolded protein response can be observed in cells lacking Phb1 and Phb2 (Schleit et al., 2013). Interestingly, although the prohibitin deletion mutants grow well under normal conditions, prohibitins become essential for cell survival when cells are deficient for CL or PE. Therefore, they show strong negative genetic interactions with genes involved in mitochondrial morphology maintenance and with genes involved in the mitochondrial phospholipid biosynthesis (Berger and Yaffe, 1998; Osman et al., 2009a). In addition to this, prohibitin mutants cannot tolerate a loss of their mtDNA or defects in mitochondrial proteolysis (Dunn et al., 2006; Osman et al., 2007; Osman et al., 2009a). The diversity of different processes that the prohibitins are involved in implies a role of the prohibitins as major MIM organizing factors.

Aims and scope of this thesis

Many genes and processes are involved in the maintenance of the tubular mitochondrial network in yeast, some of which are only poorly characterized. The best analyzed processes are undoubtedly mitochondrial fusion and fission (Westermann, 2010) and although the principle of mitochondrial division was established almost 40 years ago (Kolb-Bachofen and Vogell, 1975), many questions about the regulation and exact mechanism of mitochondrial fission remain unsolved. Especially the interplay of the various processes that regulate mitochondrial morphology is poorly understood. The main scope of this thesis was to characterize the molecular function of three proteins that have been reported to participate in mitochondrial fusion and fission: Mdm33, Num1, and Ups1. In all three cases the mitochondrial phenotypes of the deletion mutants differ from that of known division and fusion mutants. This suggests that the proteins might only be indirectly involved in the fusion or fission of mitochondria. To unravel the molecular function of these proteins within the processes of mitochondrial dynamics was the synoptic goal of this work.

Num1 is known to play a role in mitochondrial division though the mitochondrial division machinery retains residual activity in the absence of Num1 (Cervený et al., 2007). Previous research has illustrated that Num1 functions as a cortical anchor for dynein motor proteins, facilitating transport of the nucleus along astral microtubules from the mother cell to the emerging bud (Bloom, 2001). The aggregation of mitochondria in the middle of the cell in $\Delta num1$ mutants suggests that Num1 may play a similar role in anchoring mitochondria to the cell cortex (Schauss and McBride, 2007). Thus, mitochondrial fission and segregation appear somehow connected. It was one major goal of this thesis to study the connection between the two processes by further analyzing mitochondrial behavior of $\Delta num1$ mutants.

Next, Mdm33 is the best candidate for MIM division, though functional data is missing (Messerschmitt et al., 2003). It was speculated that fission of the MIM might trigger MOM constriction thereby promoting the assembly of Dnm1 (Westermann, 2008). Hence, it was a major interest to investigate the assembly and activity of Dnm1 in the absence of Mdm33. Membrane scission is an energy requiring process but Mdm33 lacks energy providing domains. Thus, if Mdm33 is a key player of MIM division, other proteins must be assisting it. Interestingly, overexpression of *MDM33* is associated with a growth arrest and mitochondrial fragmentation (Espinete et al., 1995; Messerschmitt et al., 2003). It is tempting to speculate that other proteins act in close cooperation with Mdm33 and that absence of either of these proteins might have an alleviating effect on the overexpression of *MDM33*. To address this, a microarray based genome wide suppressor screen was designed to identify those deletion strains that render the overexpression of *MDM33* less toxic.

Finally, it is well established that sufficient CL and PE levels are required for mitochondrial fusion (Chan and McQuibban, 2012; Joshi et al., 2012). How the lipids contribute to the fusion process is unknown. Cells lacking Ups1 show reduced CL levels and fragmented mitochondria, but it remained unclear whether Ups1 acts mainly in mitochondrial fusion or CL metabolism (Sesaki et al., 2006; Tamura et al., 2009). Thus, elucidating the main molecular function of Ups1 and the impact of this function on mitochondrial morphology and ultrastructure was the third major scope of this thesis.

Synopsis

Num1 anchors mitochondria at the mother cell cortex

In his doctoral studies, Johannes König (University of Bayreuth, Westermann group) developed an assay to study the relative mitochondrial content of mother cells and buds by 3d-fluorescence microscopy. This enabled him to systematically test known morphology component mutants for defects in mitochondrial distribution. Upon analysis of cells lacking the mitochondrial protein Mmr1 and comparing them to wildtype cells, he observed that $\Delta mmr1$ mutants retained more mitochondria in the mother cell and less were present in the bud (Klecker *et al.*, 2013). This was in agreement with previous reports (Itoh *et al.*, 2004). It is assumed that this phenotype is caused by Mmr1 anchoring the mitochondria at the bud tip and counteracting retrograde mitochondrial transport into the mother cell (Swayne *et al.*, 2011). Strikingly, it was reported that additional deletion of *NUM1* has an alleviating effect on the growth of $\Delta mmr1$ mutants (Hoppins *et al.*, 2011). Thus, we decided to further investigate the mitochondrial distribution defects of $\Delta num1$ and $\Delta num1 \Delta mmr1$ mutants. Former studies had already shown that mitochondrial distribution is defective in $\Delta num1$ mutants (Dimmer *et al.*, 2002; Cerveny *et al.*, 2007). In our analysis, cells lacking Num1 showed the opposite phenotype of the $\Delta mmr1$ mutants as the mitochondrial distribution was heavily shifted towards the mother cell. Intriguingly, $\Delta num1 \Delta mmr1$ double mutants showed $\Delta num1$ -like mitochondrial morphology but a more wildtype-like distribution than either single mutant (Klecker *et al.*, 2013). This suggested that Num1 acts antagonistically to Mmr1 and counteracts anterograde movement of mitochondria into the bud. Num1 is known to attach dynein motor proteins to the cell cortex (Bloom, 2001) and the mitochondrial phenotype of $\Delta num1$ mutants pointed to a possible role of Num1 as mitochondrial cell cortex anchor (Schauss and McBride, 2007). In cells with small buds Num1 exclusively localizes to the cortex of the mother cell (Heil-Chapdelaine *et al.*, 2000) whilst Mmr1 is mainly found at the bud tip (Itoh *et al.*, 2004; Swayne *et al.*, 2011). Thus, Num1 and Mmr1 could execute similar functions but at distinct parts of the cell. We therefore adapted our working hypothesis to a model in that Num1 mainly functions as mitochondrial anchor in the mother cell.

Yeast mitochondria are highly dynamic and continuously move back and forth along the actin cytoskeleton (Fehrenbacher *et al.*, 2004). The attachment of mitochondria to the cell cortex most likely serves to ensure partitioning of mitochondria between the mother cell and the bud. Fixing the mitochondria at the opposite pole of the mother cell counteracts bud-directed mitochondrial transport (Simon *et al.*, 1997; Yang *et al.*, 1999). We reasoned that retention of mitochondria in the mother cell should therefore become essential when the transport is heavily shifted towards the bud (Fig. 6). To address this, we took advantage of the fact that in cells expressing a mitochondrial anchored version of the motor protein Myo2 the mitochondrial transport is heavily shifted towards the anterograde direction. Förtsch *et al.* (2011) replaced the cargo binding domain of Myo2 by the transmembrane domain of the MOM protein Fis1 (Myo2-Fis1) in order to attach the motor to mitochondria. Expression of Myo2-Fis1 causes an accumulation of mitochondria in small buds but the mitochondria remain anchored at the mother cell cortex (Förtsch *et al.*, 2011). Indeed, we found Myo2-Fis1 to be toxic in cells lacking Num1 (Klecker *et al.*, 2013). In wildtype cells one or two mitochondria tubules were still anchored at the retention zone when we expressed Myo2-Fis1 but this could not be observed in $\Delta num1$ cells. Instead, we found the mitochondria to be completely transported into the bud, implicative of a lack of mitochondrial anchors in the mother cell. To rule

out the possibility that this effect is caused by the mitochondrial division defect of $\Delta num1$ cells, we also tested growth and mitochondrial distribution of cells lacking the essential mitochondrial division component Dnm1 and expressing Myo2-Fis1. These cells did not show any defects in growth or mitochondrial distribution (Klecker *et al.*, 2013). Taken together, our results indicate that mitochondrial retention in the mother cell is defective in cells lacking Num1, but not in cells lacking Dnm1. Our results imply that defective mitochondrial division alone is not sufficient to impair mitochondrial retention and highlight a specific role of Num1 in this process.

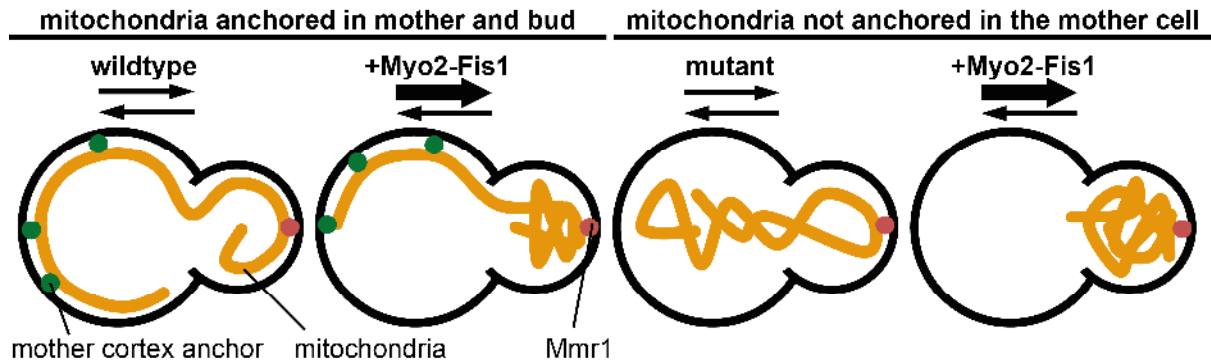


Figure 6 | Model of mitochondrial distribution in mutant strains. Arrows indicate mitochondrial transport. Unpublished. In wildtype strains mitochondrial movements in anterograde and retrograde direction are balanced. When the mitochondrial motor, Myo2, is covalently linked to the MOM by fusion to the transmembrane domain of Fis1 (Myo2-Fis1), the movement is heavily shifted to the anterograde direction (Förtsch *et al.*, 2011). If the mitochondrial cortex anchor in the mother cell is missing, expression of Myo2-Fis1 results in transport of the whole mitochondrial content into the bud.

Num1 could either regulate the retention of mitochondria in the mother cell or be an integral part of the mitochondrial cell cortex tether. If the latter was true, Num1 should colocalize with the cell cortex and the mitochondria at the retention zone. We addressed this possibility by fluorescence microscopy. In wildtype cells, Num1 was preferentially found at the sites where mitochondria were in close proximity to the cell cortex, consistent with Num1 being an integral part of the tethering complex. In cells expressing Myo2-Fis1 Num1 colocalized in a statistically significant manner with the terminal parts of mitochondrial tubules that protrude into the mother cell (Klecker *et al.*, 2013). Since these sites represent the retention zone and $\Delta num1$ mutants lack mitochondrial retention, Num1 fulfills all requirements to be an essential component of the mitochondrial anchor in mother cells.

Mdm36 is a mitochondria-associated protein and the phenotype of $\Delta num1$ and $\Delta mdm36$ strains is strikingly similar. In both mutants mitochondria form highly interconnected collapsed networks that are positioned in the center of the cell (Hammermeister *et al.*, 2010). One explanation for the phenotypical similarity could be the defect in mitochondrial fission that is common for both mutants. However, the phenotype is obviously different from that of other mitochondrial division mutants (Cerveny *et al.*, 2007; Hammermeister *et al.*, 2010). Thus, Mdm36 is likely also involved in cortical tethering of mitochondria. We decided to examine whether the main defect of both mutants is the absence of mitochondrial cell cortex attachment. To test this, we generated chimeric proteins that artificially tether the mitochondria to the plasma membrane (PM) and investigated the effect of these constructs on mitochondrial morphology in $\Delta num1$ and $\Delta mdm36$ strains. To assure stable association of the tether with the mitochondria, we first fused the transmembrane domain of the MOM protein Tom20 to GFP. Since the transmembrane domain of Tom20 carries the localization signal (Waizenegger *et al.*, 2003), this protein is faithfully inserted into the MOM with the GFP

domain facing the cytosol. This construct was then fused to a cortex binding domain (Fig. 7). We chose two different pleckstrin homology domains and according to Yu et al. (2004) both have a high affinity of binding to the cell cortex. The domain was either taken directly from Num1 or from the completely unrelated phosphatidylinositol 4,5-bisphosphate synthesis factor Opy1 (Ling et al., 2012). The tethers were expressed in wildtype cells and we observed the formation of GFP punctae at the contact sites between the mitochondria and the cell cortex, indicating that the constructs worked as intended. Intriguingly, the expression efficiently rescued mitochondrial morphology defects of $\Delta num1$ and $\Delta mdm36$ cells, demonstrating that Num1 and Mdm36 mainly influence mitochondrial structure and inheritance via cortical tethering. Consistently, the constructs did not influence the mitochondrial morphology of cells lacking the essential fission component Dnm1 (Klecker et al., 2013).

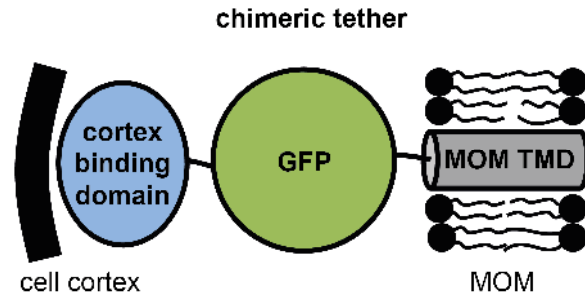


Figure 7 | Chimeric cortex tethers rescue the mitochondrial morphology and distribution phenotype of cortex anchor mutants. Shown is a cartoon depicting the structure of the constructed chimeric tethering proteins. MOM = mitochondrial outer membrane. MOM TMD = transmembrane domain of a MOM protein. Unpublished.

Mitochondria form contacts with plasma membrane invaginations

To get an idea of the structural composition of the mitochondrial cell cortex tether, Dirk Scholz (University of Bayreuth, Westermann group) searched for and imaged the retention zone by electron tomography. He found the mitochondria to be frequently localized in close contact to PM invaginations. In some cases he could observe direct contact between these invaginations and mitochondria (Klecker et al., 2013). Interestingly, the N-terminal domain of Num1 exhibits structural and functional similarities to BIN/Amphiphysin/Rvs (BAR) domains (Tang et al., 2012). BAR domains are known to bind membranes and sense or induce membrane curvatures upon recruitment to the membrane surface (Qualmann et al., 2011). Thus, it is tempting to speculate that Num1 binds to PM microdomains with high curvature by its BAR-like domain. Consistently, Tang et al. (2012) reported that mutations in its BAR-like domain disrupt the assembly of Num1 into cortical patches.

Link between mitochondrial division and mitochondrial anchorage

Our results indicated that the main mitochondrial defect of $\Delta num1$ mutants is the loss of cortical tethering in the mother cell. The mitochondrial fission defect of cells lacking Num1 could be a secondary effect, if mitochondrial cell cortex tethering was an essential prerequisite for mitochondrial division. Even though the chimeric cortex anchors rescued the mitochondrial morphology of $\Delta num1$ and $\Delta mdm36$ strains, it was not clear whether they also restored mitochondrial division activity. We therefore decided to address this by shifting the balance between mitochondrial fusion and fission towards fission and examine the effect of the chimeric cortex anchors under these conditions. An increase of mitochondrial fission can be achieved by treating the cells with sodium azide. Sodium azide efficiently depletes the cells of ATP by inhibition of the respiratory chain due to irreversible binding of the heme in the cytochrome c oxidase (Seligman et al., 1968; Wilson et al., 1972). This causes several cellular defects and rapid mitochondrial fragmentation. Since the mitochondrial fragmentation depends on the division machinery it is a

suitable assay to test for fission activity (Fekkes et al., 2000). Treatment of wildtype cells with sodium azide led to rapid fragmentation of the mitochondria what could not be observed in cells lacking Num1, Mdm36 or Dnm1. When we additionally expressed the chimeric cortex tethers, fission activity was restored in $\Delta num1$ and $\Delta mdm36$ strains, but not in cells lacking Dnm1 (Klecker et al., 2013). This demonstrates that the primary defect of cells lacking Num1 or Mdm36 is the impaired anchorage of the mitochondria to the mother cell cortex. This lack of mitochondrial anchoring then causes a secondary defect in mitochondrial division.

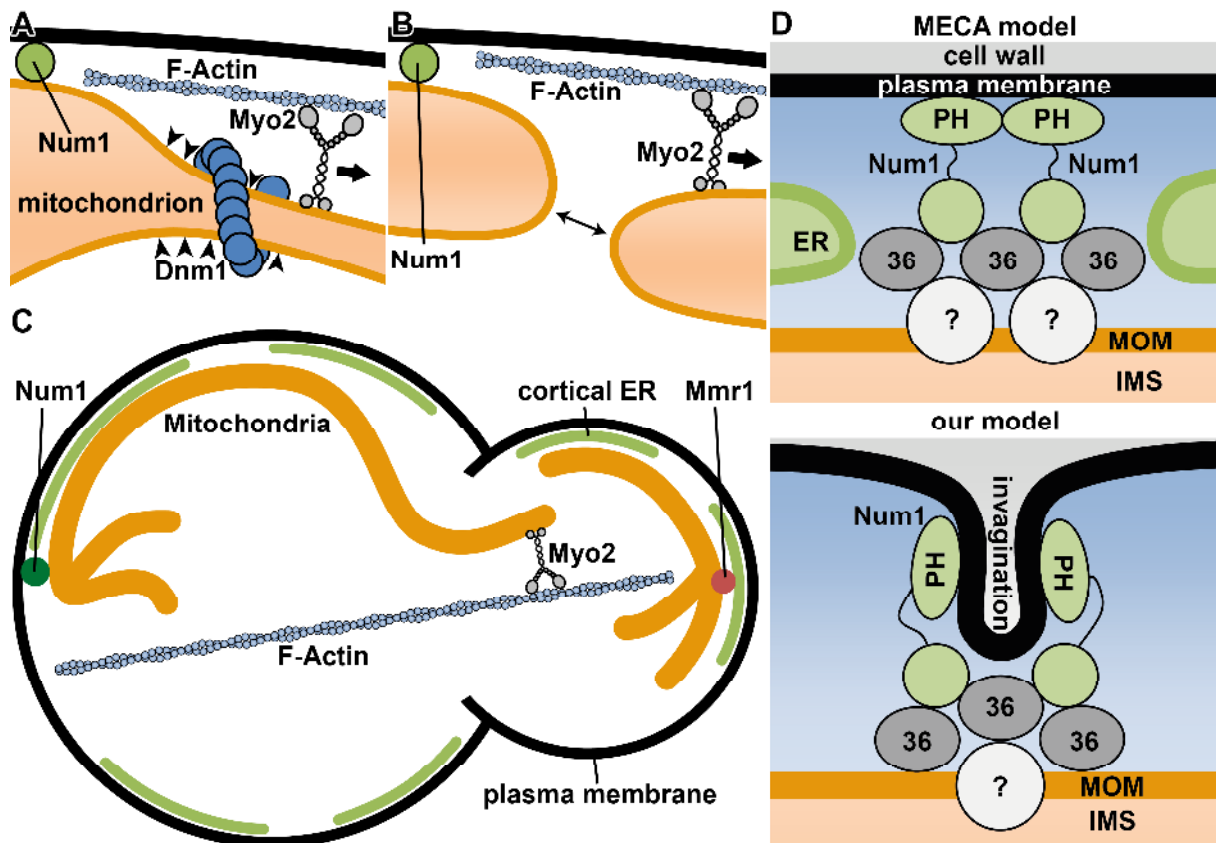


Figure 8 | Mechanisms ensuring proper mitochondrial distribution in budding yeast. **A** and **B**. Two nonexclusive models of how mitochondrial anchorage and mitochondrial division could be linked. Arrows indicate mitochondrial transport, arrowheads represent tension forces and double-headed arrows depict fusion tendency. **C**. Model for mitochondrial inheritance in yeast. Mitochondria are transported into the bud by Myo2. Anchorage of the mitochondria at the cell cortex of the mother and daughter cell by Num1 and Mmr1, respectively, ensures equal partitioning. **D**. Two models for the mitochondrial mother cell cortex anchor are shown. In both models the anchor consists of Num1, Mdm36, and an unknown mitochondrial factor. The MECA (mitochondria-ER-cortex anchor) model additionally contains ER whilst our model includes binding to invaginations of the plasma membrane. PH = pleckstrin homology domain. MOM = mitochondrial outer membrane. IMS = intermembrane space. 36 = Mdm36. All images are unpublished. See text for more details.

Though we were able to show that mitochondrial cortex anchoring indeed is an essential prerequisite for mitochondrial division, the exact mechanism remains unknown. One possible explanation would be that the stable anchoring of mitochondria at the cell cortex applies tension forces to the mitochondria when Myo2 is moving them along actin cables. This tension could either result in mitochondrial constriction or directly aid the process of membrane scission (Fig. 8A). Furthermore, it is convincing that mitochondrial tips must be separated after a fission event to prevent direct re-fusion. If mitochondrial division was spatially linked to the anchoring sites, one tubule would remain

stationary while the other would rapidly depart due to Myo2 driven mitochondrial movement (Fig. 8B). Both explanations do not exclude each other. Astonishingly, overexpression of a shortened version of Num1 rescued mitochondrial division defects in cells expressing Dnm1 and a dominant negative, cytosolic version of Dnm1 (Cervený et al., 2007). This implied that Num1 directly promotes mitochondrial division what is contradicted by our findings. This could be explained by the shortened Num1 version binding the dominant negative version of Dnm1. By sequestration of the mutant Dnm1 the inhibitory effect could be relieved what would restore fission activity.

One of the main goals of the project was to define the activity of Num1 in molecular detail. Taken together, our results show that yeast cells have two separate cortical tethers – Num1 in the mother and Mmr1 in the bud – that ensure the proper distribution of mitochondria by generating opposing forces at spatially distinct locations (Fig. 8C). Mmr1 attaches newly inherited mitochondria to the bud tip while Num1 facilitates retention of mitochondria in the mother cell. It appears that the combination of anterograde and retrograde movements together with attachments of mitochondria to the cell cortex ensures equal partitioning of mitochondria during cell division. The main function of Num1 is to tether the mitochondria at the mother cell cortex. Loss of this cell cortex anchor then causes a secondary defect in mitochondrial fission by a yet unknown mechanism.

Role of Mdm36 in mitochondrial tethering

We propose that Mdm36 is a primary constituent of the mitochondrial tethering complex, based on the similarity of the mitochondrial phenotypes of $\Delta mdm36$ and $\Delta num1$ mutants. This hypothesis is further strengthened by Lackner et al. (2013) observing a direct interaction between Num1 and Mdm36. Furthermore, mitochondrial morphology and mitochondrial fission defects of $\Delta mdm36$ mutants can be rescued by synthetic mitochondria-PM tethers (Klecker et al., 2013). Interestingly, Mdm36 associates with mitochondria due to binding of an unknown mitochondrial interaction partner (Hammermeister et al., 2010). This together with the direct interaction between Num1 and Mdm36 suggests that Mdm36 might act as a receptor mediating binding of Num1 to mitochondria. Indeed, Mdm36 forms foci associated with the cortical side of mitochondrial tubules. These foci are adjacent to but only partially overlap with Num1 clusters and are located between Num1 and mitochondria (Lackner et al., 2013), indicative of Num1 binding to mitochondria via interaction with Mdm36.

Two models for mitochondrial tethering by Num1

While our manuscript was in revision, Lackner et al. (2013) published that they identified Num1 as a key component of the mitochondrial cell cortex anchor in mother cells by a completely different approach. They systematically screened for genes that influence the fitness of a yeast strain lacking MOM fusion and fission (absence of *FZO1* and *DNM1*). In their screen the presence of *NUM1* was essential for cell viability in $\Delta fzo1 \Delta dnm1$ double mutants. Lackner and coworkers observed the localization of the entire mitochondrial network in daughter buds at non permissive temperatures in $\Delta dnm1 \Delta num1$ double mutants harboring a temperature sensitive allele of *fzo1*. This further supports our hypothesis that Num1 acts as a mitochondrial retention factor in mother cells.

The yeast PM is subdivided in at least two different non-overlapping compartments that were named according to the first described residing protein: the membrane compartment occupied by the plasma membrane ATPase Pma1 and the membrane compartment containing the arginine permease

Can1 (**can**avanine resistance; Malinska et al., 2003; Opekarova et al., 2010). The Can1-positive compartment consists of evenly distributed isolated patches that were later described as eisosomes (Walther et al., 2006) – organelles with a controversial role in endocytosis (Stradalova et al., 2012). Strikingly, eisosomal proteins are almost exclusively found at PM invaginations (Stradalova et al., 2009). Lackner et al. (2013) reported three major components of the eisosomes to co-immunoprecipitate with Mdm36, offering the intriguing possibility that mitochondria might be anchored at eisosomal PM invaginations. However, a role of eisosomes in the cortex anchoring of mitochondria lacks experimental proof.

Lackner et al. (2013) postulate the presence of a tethering complex consisting of at least Num1, Mdm36, and ER and they termed it mitochondria-ER-cortex anchor (MECA). In their model, Num1 functions as the core component of the MECA by mediating interactions with the PM, the ER, and Mdm36 (Fig. 8D). The model is based on high resolution fluorescence microscopy experiments that revealed close proximity between ER and sites where Num1 or Mdm36 colocalize with the mitochondria. Furthermore, to show that Num1 binds cortical ER (cER) Lackner and coworkers deleted the ER tubule-shaping proteins Rtn1/2 (**reticulon-like**) and Yop1 (**YIP one partner**). In the triple mutant the cER displays expanded sheet-like structures (Voeltz et al., 2006) and they observed a re-distribution of Num1 to sites of the cell where misshaped cER is present (Lackner et al., 2013). These results are contrary to our electron microscopy which showed that the ER was absent from the sites where the mitochondria encountered the PM (Klecker et al., 2013). We postulate that Num1 and Mdm36 cooperatively tether the mitochondria to PM invaginations without involvement of the ER (Fig. 8D).

Based on the experimental results it is hard to decide which model is correct. The cER is well known to anchor peroxisomes (Knoblach et al., 2013) that are also transported by Myo2 (Fagarasanu et al., 2006). Furthermore, it is assumed that mitochondria are anchored at the cER in bud tips by Mmr1 (Swayne et al., 2011). It is persuasive that a similar mechanism might also be used in mother cells. Though, in the MECA model the ER is only one component of the tethering complex and the mitochondria are not directly tethered to the ER. The observed colocalization of Num1 and the cER could well happen by chance as the cER underlies about 40-50 % of the cell surface (Manford et al., 2012; Wolf et al., 2012). Thus, the role of the cER in mitochondrial anchoring in the mother cell remains ambiguous. An obvious approach to test for both hypotheses would be the investigation of the localization of Num1 by immuno-electron microscopy.

Role of Dnm1 in mitochondrial cell cortex attachment

It is still unknown how Dnm1 contributes to the anchoring of mitochondria. Already in the very first description of Dnm1 it was hypothesized that the protein might be required to “spread out and anchor portions of the mitochondrial network at the cell periphery” (Otsuga et al., 1998). This was based on the observation that mitochondria accumulate at one side of the cell in $\Delta dnm1$ mutants. Since we were not able to rescue this phenotype by expression of our tethering proteins, it is most likely a secondary consequence of the mitochondrial fission defect in cells lacking Dnm1. Though, Dnm1 forms stable foci at the cell cortex and these foci colocalize with the mitochondria and with Num1 (Otsuga et al., 1998; Schauss et al., 2006; Cervený et al., 2007). This subset of Dnm1 puncta depends on a close relative to Mdv1, the CCR4-NOT complex associated factor Caf4 that has an identical domain structure but seems to play only a minor role in mitochondrial division (Griffin et al., 2005). When either Caf4 or Mdm36 are missing, Num1 does not colocalize with Dnm1 (Schauss et al.,

2006; Hammermeister et al., 2010; Lackner et al., 2013). Since $\Delta caf4$ mutants show no defect in mitochondrial division or mitochondrial distribution (Griffin et al., 2005), the function of the cortical Dnm1 puncta remains elusive. It is clear that they do not act in mitochondrial division, as they are devoid of Mdv1 (Cervený et al., 2007) and lack fission activity (Schauss et al., 2006; Lackner et al., 2013). Intriguingly, double mutants of Dnm1 and Num1 have a severely reduced fitness and produce mother cells devoid of mitochondria when grown on higher temperatures (Cervený et al., 2007). This could be explained by Num1 and Dnm1 cooperating on mitochondrial retention with residual activity in the single mutants. The double mutants would then completely lack the activity what could be causative for the synthetic effect. But this does not match the observation that impaired mitochondrial fusion worsens the phenotype of the double mutants (Lackner et al., 2013). Thus, the function of the cortical Dnm1 assemblies, the meaning of the interaction between Num1 and Dnm1, and the role of Dnm1 in mitochondrial anchoring has to be further investigated.

Molecular function of Mdm33

Strains lacking Mdm33 display large ring-like mitochondria that can obviously not be generated in the presence of frequent mitochondrial fission. Furthermore, overexpression of *MDM33* is associated with rapid fragmentation of the mitochondrial network. The localization of Mdm33 in the MIM and the formation of MIM septa upon overexpression of *MDM33* pointed to an involvement in MIM division (Messerschmitt et al., 2003), but the molecular function of Mdm33 remained elusive. Therefore, we decided to examine the function of Mdm33 in more detail.

***MDM33* interacts with genes involved in phospholipid homeostasis**

In the past decade several groups systematically analyzed on a genome-wide level which genes act in similar pathways (Costanzo et al., 2010; Hoppins et al., 2011; Frost et al., 2012). To achieve this, the so called functional genomic research approach uses the phenomenon of genetic interactions that has been identified more than 100 years ago (Bateson et al., 1905). In a general sense a genetic interaction occurs when the combination of two mutations results in a surprising phenotype that cannot be explained simply by combination of the independent effects observed for each mutation alone. Thus, a genetic interaction highlights that the functions of two genes are somehow connected. Most of the functional genomics studies take cell growth as a measurable phenotype. A genetic interaction is annotated when the double mutant growth significantly differs from the combination of the growth rates of each single mutant. The interaction can be positive or negative if the growth of the double mutant is better or worse than expected, respectively (Dixon et al., 2009). In 2011 a functional genomic study was published that measured 616,270 distinct pairwise genetic interactions of a total of 1,482 genes that are involved in processes related to mitochondrial functions (Hoppins et al., 2011). We took advantage of this so-called MITO-MAP and determined the genetic interactome of *MDM33*. Strikingly, *MDM33* showed no significant genetic interactions with genes involved in fusion or fission of mitochondria. Instead, we found strong interactions with genes encoding mitochondrial phospholipid biosynthesis factors or subunits of the F_1F_0 ATP synthase. Furthermore, *MDM33* showed strong positive genetic interactions with both subunits of the inner membrane prohibitin complex which modulates mitochondrial phospholipid homeostasis (Klecker et al., in preparation).

All of the genetic interactions that are reported in the MITO-MAP are based on growth of the double mutants. Since a genetic interaction can be observed for all different types of measurable phenotypes, we asked whether the reported genetic interactions also have an impact on mitochondrial morphology. We systematically generated strains lacking *MDM33* and one respective interaction partner that is involved in mitochondrial function, structure or dynamics and examined mitochondrial morphology. The phenotype of the $\Delta mdm33$ strain was not affected by deletion of most interaction partners, indicating a central role of *MDM33* in mitochondrial morphogenesis. However, deletion of *PHB1/2*, *FMP30*, *MDM31*, all subunits of the ERMES complex, or *GEM1* altered the mitochondrial morphology of $\Delta mdm33$ mutants (Klecker et al., in preparation). Intriguingly, all of these genes have been implicated to play an important role in mitochondrial lipid metabolism: (I) Lipid production in the mitochondria requires import of precursor lipids from the ER at mitochondria-ER contact sites that are formed by the ERMES (Kornmann et al., 2009). The formation of these contact sites is regulated by Gem1 (Kornmann et al., 2011; Stroud et al., 2011). (II) Fmp30 and prohibitins show strong genetic interactions with genes involved in mitochondrial CL and PE

biosynthesis and Fmp30 is required for the maintenance of a sufficient CL level in the absence of mitochondrial PE synthesis (Birner et al., 2003; Osman et al., 2009a; Kuroda et al., 2011). (III) Mdm31 is known to play an important role in CL biosynthesis in mitochondria and overexpression of *MDM31* can partially compensate for the loss of ERMES (Tamura et al., 2012). The genetic interaction profile of *MDM33* and the requirement of mitochondrial phospholipid biosynthesis factors for the formation of the Δ *mdm33* mitochondrial morphology phenotype pointed to a role of Mdm33 in mitochondrial phospholipid homeostasis.

Mapping of the interactome of *MDM33*

To further investigate the cellular process which Mdm33 participates in, we decided to take advantage of the fact that overexpression of *MDM33* causes a growth defect (Espinet et al., 1995). We assumed that Mdm33 acts in close cooperation with other mitochondrial proteins and that the presence of these proteins is required for the overexpression of *MDM33* to become toxic. Therefore, the deletion of a gene encoding a protein that acts in close cooperation with Mdm33 should rescue the growth defect. We expressed *MDM33* from the galactose-inducible *GAL1/10* promoter in a pooled library of 4,987 viable haploid deletion strains and found some strains to be able to grow under inductive conditions. Each of the deletion strains carries a start- to stop-codon deletion of a single gene and one or two unique identifier sequences termed 'barcodes' (Winzeler et al., 1999; Giaever et al., 2002). Thus, each strain can be identified by its barcode sequence (Shoemaker et al., 1996; Winzeler et al., 1999). To be able to identify the strains that are able to cope with high Mdm33 levels, Alfons Weig (DNA Analytics, University of Bayreuth) designed a spot array that carries probes that are complementary to each barcode present in the deletion library. Hence, each strain that is present in a pool of strains can be identified simultaneously by PCR-based labelling of all barcode sequences and hybridizing them to the array. Using this method, the screen revealed several 100 deletion strains that suppress the *MDM33* overexpression conferred growth defect (Klecker et al., *in preparation*). Similar numbers of suppressing gene deletions have been reported for genome wide suppressor screens to identify Cdc42 recycling factors (Das et al., 2012), telomere capping factors (Downey et al., 2006; Addinall et al., 2008) or genes that ameliorate the toxicity of the huntingtin protein (Mason et al., 2013).

We reasoned that close interaction partners should genetically interact with *MDM33* upon both, overexpression and deletion, and therefore we merged the results from the MITO-MAP and the suppressor screen. We found that six genes show genetic interactions with *MDM33* in the MITO-MAP and suppress the overexpression coupled growth defect and consider these as very close interaction partners. Among them was *ELP3*, which encodes a subunit of the elongator complex, which is a major component of the RNA polymerase II holoenzyme and responsible for transcriptional elongation (Wittschieben et al., 1999). The gene shows a very high number of genetic interactions and we assume that the suppression of the growth defect is caused by inefficient expression of *MDM33*. We therefore excluded *ELP3* from further analyses. Each of the remaining five genes encodes a mitochondrial protein: We found both subunits of the MIM organizing prohibitin complex, *PHB1* and *PHB2* (Osman et al., 2009b); the subunit g of the F_1F_0 ATP synthase, *ATP20* (Boyle et al., 1999); a regulatory subunit of the mitochondrial protein import motor complex, *PAM17* (presequence translocase-associated motor; Popov-Celeketic et al., 2008); and a CL biosynthesis factor, *FMP30* (Kuroda et al., 2011). Importantly, the suppression of the overexpression induced toxicity by Δ *phb1* could be complemented by expression of the deleted protein. We also checked for reduced

promoter activity or protein biosynthesis in the prohibitin mutants by expressing other toxic genes from the same promoter, but the suppression was limited to the expression of *MDM33* (Kleckner *et al.*, *in preparation*). Thus, our genetic analysis suggests that Mdm33, Phb1, Phb2, Pam17, Fmp30, and Atp20 act in closely related cellular pathways.

In an independent approach to identify Mdm33 interaction partners, Megan Wemmer and Jodi Nunnari (UC Davis) performed a mass spectrometry-based proteomic analysis of Mdm33 immunoprecipitations to identify interacting proteins. Strikingly, among the most robust interacting proteins were Phb1 and Phb2 and the alpha and beta subunits of the F₁F₀ ATP synthase (Kleckner *et al.*, *in preparation*). The observed genetic and direct interactions suggest close functional and spatial proximity between Mdm33, the prohibitin complex, and maybe also the ATP synthase.

We asked whether the close Mdm33 interaction partners share anything in common besides their mitochondrial localization. We integrated the MITO-MAP interactions of all five genes into a genetic interaction network and observed a highly interconnected genetic cluster consisting of *MDM33*, *PHB1*, *PHB2*, *PAM17*, *FMP30*, *ATP20*, *PSD1*, *CRD1*, *GEM1*, and the subunits of the ERMES complex (Kleckner *et al.*, *in preparation*). All genes that we found to be associated with *MDM33* and its five close interaction partners are involved in mitochondrial phospholipid biosynthesis: (I) Psd1 decarboxylates PS to PE within mitochondria (Fig. 5; Clancey *et al.*, 1993; Trotter *et al.*, 1993); (II) Crd1 synthesizes CL by coupling PG and CDP-DAG (Fig. 5; Tuller *et al.*, 1998); and (III) the ERMES complex and its regulatory subunit Gem1 link the ER to mitochondria what is important for the import of precursor lipids from the ER into the mitochondria where they are further processed (Kornmann *et al.*, 2009; Kornmann *et al.*, 2011; Stroud *et al.*, 2011). Based on our physical and genetic interaction data we therefore postulate that Mdm33 acts in mitochondrial phospholipid metabolism.

Mdm33 acts in mitochondrial biosynthesis of phosphatidylethanolamine

To address the potential role of Mdm33 in mitochondrial phospholipid metabolism, we determined by mass spectrometry the mitochondrial phospholipidome of wildtype cells and cells overexpressing *MDM33* (in cooperation with Mathias Haag and Thomas Langer; University of Cologne). Intriguingly, we found mitochondrial PE and CL levels to be reduced upon *MDM33* overexpression (Kleckner *et al.*, *in preparation*). This was of particular interest as both CL and PE are synthesized in the mitochondria and the enzymes catalyzing the formation of PE and CL, Psd1 and Crd1, were found to show strong genetic interactions with *MDM33* and its five close interaction partners, respectively. As described above, the combined deletion of genes required for production of PE and CL is synthetic lethal in yeast (Gohil *et al.*, 2005). Thus, the simultaneous reduction of mitochondrial PE and CL upon overexpression of *MDM33* might be causative for the observed growth defect. Furthermore, it is known from different organisms that changes in mitochondrial lipid composition can cause misshaping of mitochondrial membranes (Claypool *et al.*, 2008; Mileykovskaya and Dowhan, 2009; Pineau *et al.*, 2013; Tasseva *et al.*, 2013). Therefore, we consider it likely that changes of mitochondrial ultrastructure observed upon overexpression of *MDM33* are a consequence of alterations of mitochondrial PE and CL levels. Consistently, we found MIM remodeling and growth arrest upon *MDM33* overexpression to be independent of the outer membrane fission machinery. However, we did not observe mitochondrial fragmentation but swelling of the mitochondrial network in cells overexpressing *MDM33* in the absence of the essential MOM fission factor Dnm1 (Kleckner *et al.*, *in preparation*).

The biosynthesis of PE and CL within mitochondria requires import of precursor lipids from the ER. Kornmann et al. (2009) suggested that the ERMES complex is essential for the formation of mitochondria-ER contacts that are required for phospholipid exchange between both organelles. Intriguingly, we found the formation of the ERMES complex to be unaffected by the overexpression of *MDM33*. We then directly measured PE biosynthesis activity by addition of liposomes containing fluorescently labeled PS to isolated mitochondria and observed a reduced PS to PE conversion rate upon overexpression of *MDM33* (Klecker et al., in preparation). Taken together, our results indicate that Mdm33 directly influences mitochondrial phospholipid biosynthesis.

Role of Mdm33 in mitochondrial fission

Mdm33 plays an important role in the maintenance of mitochondrial morphology and $\Delta mdm33$ mutants exhibit gigantic ring-shaped mitochondria that can obviously only be maintained in the absence of frequent mitochondrial division. Furthermore, overexpression of *MDM33* leads to rapid fragmentation of the mitochondrial network. These observations are suggestive of a role of Mdm33 in mitochondrial fission (Messerschmitt et al., 2003). We decided to address the potential role of Mdm33 in mitochondrial division by shifting the balance between mitochondrial fusion and fission towards fission in strains lacking *MDM33*. After a short treatment with azide, we observed rapid fragmentation of the mitochondria in wildtype cells whereas those of cells lacking Dnm1 remained connected. In $\Delta mdm33$ strains mitochondrial fragmentation was delayed but observable, indicative of Mdm33 not being essential for but promoting mitochondrial division (Klecker et al., in preparation). Since assembled Dnm1 spirals are too tight to even wrap around normal mitochondrial tubules, it is convincing that the giant mitochondria in $\Delta mdm33$ mutants might be too big to be divided by Dnm1. We decided to test this by imaging the residual division events in $\Delta mdm33$ mutants by time-resolved live-cell fluorescence microscopy. In agreement with our hypothesis, we found mitochondrial division to be exclusively limited to mostly tubular parts of the mitochondria in the mutant cells (Fig. 9A). The time course of Dnm1 assembly and mitochondrial division was not significantly altered in mutant cells (Klecker et al., in preparation). We conclude that Mdm33 contributes to efficient mitochondrial division by maintaining a fission competent mitochondrial shape, albeit it does not appear to constitute an essential component of the mitochondrial division machinery.

It was recently shown that ER tubules wrap around mitochondria and mediate mitochondrial constriction prior to Dnm1 assembly (Friedman et al., 2011). This is spatially and functionally linked to the ERMES that connects ER and mitochondria (Kornmann et al., 2009). The Miro GTPase Gem1 is required to disintegrate contacts between the fission machinery and the ERMES after the division event, thereby generating free mitochondrial tips (Murley et al., 2013). Intriguingly, Andrew Murley and Jodi Nunnari (UC Davis) found Mdm33 to form punctate assemblies that colocalize with the ER residing ERMES component Mmm1, Dnm1, and mitochondrial division events. Though, we found the association of ERMES with sites of assembled Dnm1 to be independent of the presence of Mdm33, suggesting that the latter is dispensable for the initial steps of mitochondrial division (Klecker et al., in preparation). It is tempting to speculate that Mdm33 assembles at mitochondrial division sites to modulate the lipid composition or membrane topology of the MIM to support Dnm1 mediated mitochondrial division (Fig. 9B, C). Taken together our results indicate that Mdm33 links mitochondrial fission and mitochondrial phospholipid metabolism. Further studies will be needed to show how this connection influences mitochondrial biogenesis.

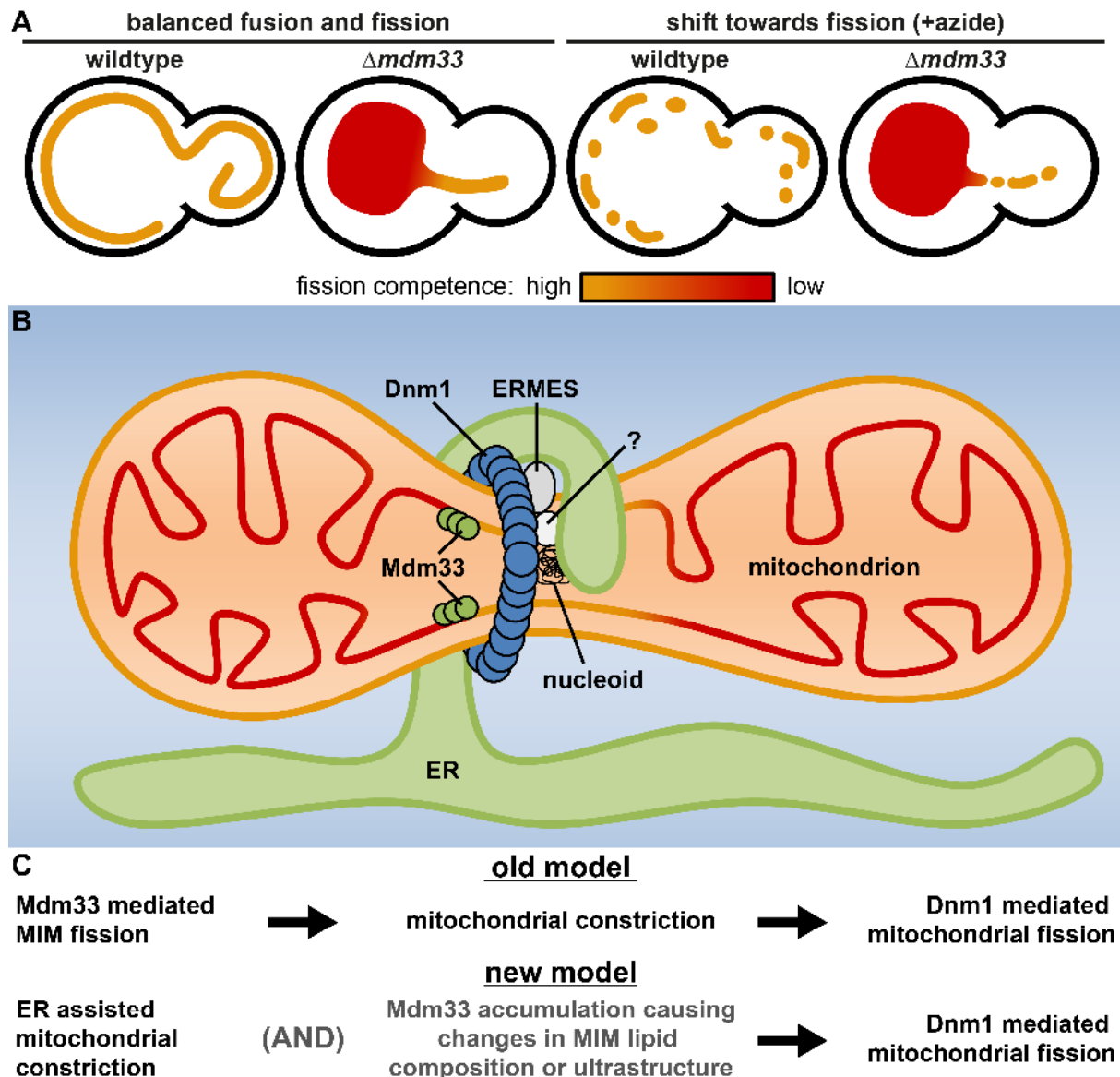


Figure 9 | Role of Mdm33 in mitochondrial division. **A.** In wildtype strains mitochondrial fusion and fission are balanced. When the cells are depleted from ATP by addition of azide, the balance is heavily shifted towards fission. The ring-like mitochondrial structures in $\Delta mdm33$ cells are likely too large to be separated by Dnm1. Thus, cells lacking Mdm33 show less mitochondrial fragmentation upon addition of azide due to the lack of fission competent mitochondria. **B.** Model for the function of Mdm33 in ER assisted mitochondrial division. Local accumulation of Mdm33 adjusts the MIM to the needs of mitochondrial division. The color of the inner membrane depicts fission competence according to **A.** ERMES = ER mitochondria encounter structure. **C.** Old and new model for the molecular function of Mdm33. Grey color indicates processes that are not essential for mitochondrial division. All images are unpublished. See text for more details.

Ups1 catalyzes intramitochondrial transport of phosphatidic acid

Ups1 acts early during CL synthesis

Cellular membranes consist of a huge variety of different lipids and membrane proteins. The synthesis of both, proteins and lipids, is tightly regulated to fit the cellular needs (Henry et al., 2012). Mitochondria play an important role in cellular membrane homeostasis and contribute significantly to the synthesis of membrane lipids. Strikingly, our study on the function of *MDM33* demonstrated that mitochondrial phospholipid biosynthesis and mitochondrial dynamics act in close cooperation. Especially mitochondrial fusion seems to heavily depend on the mitochondrial lipid composition (Furt and Moreau, 2009). We are only beginning to understand how these processes are connected. A study by Choi et al. (2006) suggested that lipids might be directly involved in the fusion process as mitochondrial fusion requires the generation of the fusogenic lipid PA in the MOM. The involvement of PA in membrane fusion is well established for SNARE mediated exocytosis (Vitale et al., 2001) and appears to be a general principle of membrane fusion. Furthermore, the biosynthesis of PE and CL are intimately linked to mitochondrial fusion in yeast (Chan and McQuibban, 2012; Joshi et al., 2012). One factor that is required for CL biosynthesis, mitochondrial fusion, and proper topogenesis of the MIM mitofusin Mgm1 is the IMS protein Ups1 (Tamura et al., 2009; Potting et al., 2010). We decided to team up with the group of Thomas Langer (University of Cologne) in order to further elucidate the molecular function of Ups1.

Previous studies had already shown that the steady-state level of CL is reduced in cells lacking Ups1 but the function of Ups1 in CL biosynthesis remained elusive (Osman et al., 2009a; Tamura et al., 2009). The group of Thomas Langer investigated the complete phospholipidome of purified mitochondria from cells lacking Ups1. Intriguingly, an accumulation of CL biosynthesis intermediates was not observable and only the level of the precursor lipid PA was significantly increased. It is a conclusive concept that the deletion of a gene encoding an enzyme will cause the substrate of the enzymatic reaction to accumulate whilst the amount of product will decline, respectively. Thus, the accumulation of PA in $\Delta ups1$ cells suggested that Ups1 acts in the initial step of the CL biosynthesis, the conversion of PA to CDP-DAG (Fig. 5). The lipid phenotype of $\Delta ups1$ cells was strikingly similar to that reported for $\Delta tam41$ mutants (Kutik et al., 2008). The molecular function of Tam41 was unknown when we performed our study. It was only known that Tam41 acts before Pgs1 (conversion of CDP-DAG to PGP) and Gep4 (dephosphorylation of PGP) and so we concluded that both, Ups1 and Tam41, act in the initial step of CL biosynthesis. We decided to investigate by electron microscopy the impact of deletion of *UPS1* and *TAM41* on the mitochondrial ultrastructure since cells lacking CL show strong defects in mitochondrial processes (Joshi et al., 2009), such as abnormal assembly of the respiratory chain complexes and supercomplexes (Zhang et al., 2005). Intriguingly, albeit depleted of CL, the deletion strains $\Delta ups1$ and $\Delta tam41$ did not show an altered mitochondrial ultrastructure (Connerth et al., 2012). This is in agreement with a previous report that reduction of CL caused by deletion of Taffazin is not necessarily associated with changes in the mitochondrial ultrastructure (Acehan et al., 2009).

The Langer group performed a genetic epistasis analysis in order to further define the function of Ups1 and Tam41 for CL metabolism (Fig. 10). Epistasis means that one mutation completely masks the phenotypic effects of other mutations. It provides a logical framework for inferring biological pathways, because here the product of one protein's action becomes the substrate for the next.

Hence, if one enzyme is missing and the pathway is completely blocked, all downstream acting enzymes can be lost without any phenotypical consequences (Roth et al., 2009). We focused on the three genes acting in the very beginning of the CL biosynthetic pathway: *UPS1*, *PGS1*, and *TAM41*. Cells lacking *TAM41* or *PGS1* suffer from very severe growth defects and this can be alleviated by additional deletion of *UPS1*. Surprisingly, we found the mitochondrial ultrastructure to be dramatically altered in cells lacking *PGS1*. The mitochondria contained extremely elongated cristae, which frequently formed MIM septa or onion-like structures. In agreement with the growth of the strains, ultrastructurally the $\Delta pgs1 \Delta ups1$ and the $\Delta tam41 \Delta ups1$ double mutants were indistinguishable from the $\Delta ups1$ single mutant (Connerth et al., 2012).

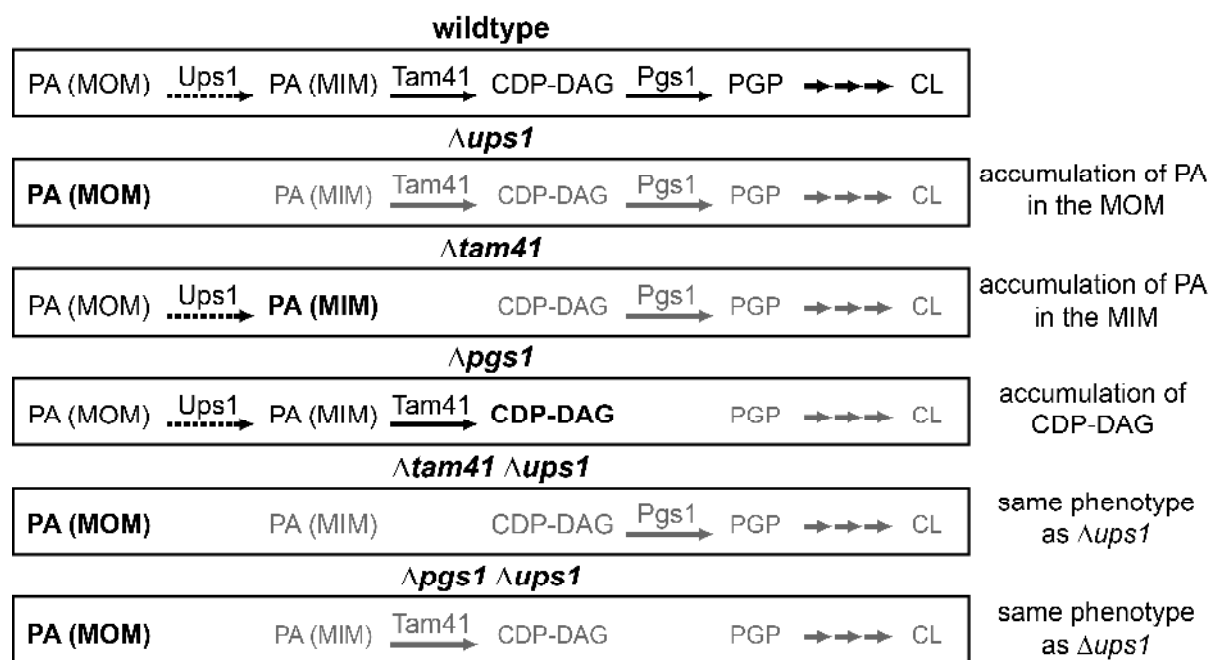


Figure 10 | Classical epistasis in the CL biosynthesis pathway. MOM = mitochondrial outer membrane. MIM = mitochondrial inner membrane. CL = cardiolipin. PGP = phosphatidylglycerol phosphate. CDP-DAG = cytidine diphosphate-diacylglycerol. PA = phosphatidic acid. Grey color indicates that this part of the pathway is hindered in the respective mutant. Bold font represents accumulation. Unpublished. See text for details.

It was puzzling that $\Delta pgs1$ mutants showed alterations in mitochondrial ultrastructure that were obviously not caused by a lack in CL. Therefore, Mathias Haag examined the phospholipidome of all analyzed single and double mutants. The only unique feature of the $\Delta pgs1$ mutant was an accumulation of CDP-DAG within the mitochondria and this was dependent on the presence of Ups1 (Fig. 10). Hence, the alterations in the mitochondrial ultrastructure caused by the deletion of *PGS1* are most likely caused by an accumulation of CDP-DAG (Connerth et al., 2012). The $\Delta pgs1 \Delta tam41$ double mutant was inviable but it was previously shown that the accumulation of CDP-DAG in $\Delta pgs1$ cells also depends on Tam41 (Osman et al., 2010). Thus, the epistasis analysis further strengthened the theory of Ups1 and Tam41 acting in the initial step of CL biosynthesis. The question remained if Tam41 acts before Ups1, or vice versa. Strains lacking *TAM41* accumulated more PA than strains lacking *UPS1* and the $\Delta ups1 \Delta tam41$ double mutant showed the same mitochondrial PA amount as the $\Delta ups1$ single mutant. Thus, in respect to the phospholipid composition, the mitochondrial ultrastructure, and the growth the $\Delta ups1$ allele was epistatic to the $\Delta tam41$ and $\Delta pgs1$ allele (Connerth et al., 2012). In biochemical pathways, the predominating mutation is always epistatic and

upstream to the masked mutation. We conclude that Ups1 acts upstream of Pgs1 and Tam41 and is required to supply Pgs1 and Tam41 with the required substrates (Fig. 10). These results are in perfect agreement with a recent study by Tamura and coworkers. They show that Tam41 catalyzes the mitochondrial conversion of PA to CDP-DAG which serves as substrate for Pgs1 (Tamura et al., 2013).

Ups1 is a novel lipid transfer protein

Mitochondria and ER cooperate in the synthesis of membrane lipids. Aside from Taz1, all mitochondrial proteins that act in the biosynthesis of CL and PE are localized in the MIM (see above). Consequently, there has to occur an extensive lipid exchange between the ER and the MOM and between both mitochondrial membranes but the molecular processes that facilitate lipid transport are only poorly understood (Tatsuta et al., 2013). Initial studies suggested that lipid exchange between MOM and MIM occurs at contact sites where both membranes encounter each other (Simbeni et al., 1991). Membrane contact sites could facilitate spontaneous transfer of phospholipids between both membranes but could not maintain different phospholipid compositions of both membranes (Tatsuta et al., 2013). The localization of Ups1 in the IMS and the requirement of Ups1 activity for early steps of CL biosynthesis suggested that Ups1 might facilitate the transport of PA from the MOM to the MIM. Consequently, the group of Thomas Langer switched to in vitro studies to address this hypothesis. For the in vitro studies they used complexes of Mdm35 and Ups1, because Ups1 assembles with Mdm35 in the IMS of yeast cells and could not be purified from *E. coli* in the absence of Mdm35 (Connerth et al., 2012). In brief, they observed that these complexes not only bind to liposomes, but that they extract lipids from liposomes and mediate the bidirectional transport of phospholipids between liposomes in vitro. Here, the Mdm35/Ups1 complexes showed a strong specificity for binding to liposomes containing negatively charged lipids and for the transport of PA, respectively. Strikingly, CL present at physiological concentrations trapped Ups1 at liposomes. Since the MIM shows high concentrations of CL this may serve to render the PA transport irreversible. Moreover, high CL concentrations inhibited PA transfer between liposomes, offering an intriguing possibility to orchestrate the biosynthesis of CL according to the cellular needs by a negative regulatory feedback mechanism. The physiological relevance of this phenomenon became clear when Ups1 was found to accumulate at the MIM in the absence of the Ups1-degrading protease Yme1 (Connerth et al., 2012).

Taken together, the following model for Ups1 activity was proposed: Ups1 is a lipid transport protein of the IMS. Upon PA-binding and PA-extraction from the donor membrane, Ups1 binds Mdm35, which stabilizes Ups1 and protects it from proteolytic degradation by Yme1 and Atp23. The Ups1/Mdm35 complex binds negatively charged phospholipids in the acceptor membrane, which is accompanied by the dissociation of Mdm35 from the complex

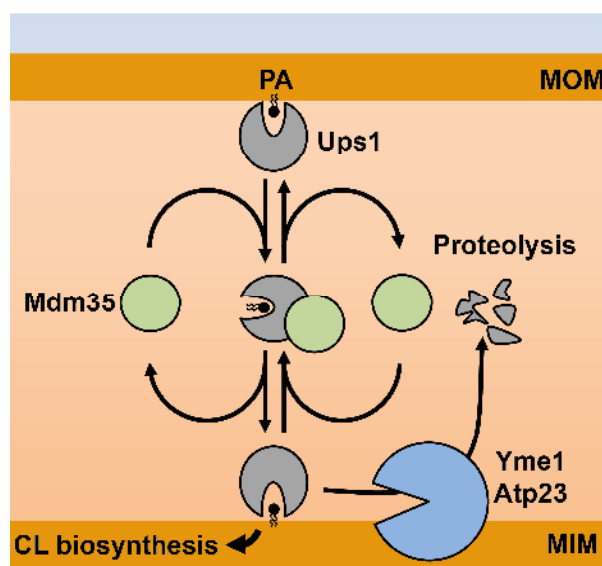


Figure 11 | Cartoon depicting the transfer of phosphatidic acid by Ups1/Mdm35 complexes. MOM = mitochondrial outer membrane. MIM = mitochondrial inner membrane. CL = cardiolipin. PA = phosphatidic acid. Adapted from: Tatsuta et al. (2013).

and the release of PA. The rapid enzymatic conversion of PA into CL in the MIM renders the transport unidirectional. Afterwards Mdm35 could extract Ups1 from the acceptor membrane and recycle it for additional transport cycles. If the CL concentration in the MIM exceeds the optimal range, Ups1 remains stably bound to the MIM and is degraded by Yme1 (Fig. 11). Therefore, the main defect in cells lacking Ups1 is impaired CL biosynthesis. It is well established that CL and PE biosynthesis mutants have defects in Mgm1 topogenesis (Joshi et al., 2012) and that both isoforms are required for fusion activity (Herlan et al., 2003). Furthermore, Mgm1 dimerization depends on CL (DeVay et al., 2009) and thus the loss of CL most likely causes mitochondrial fragmentation in $\Delta ups1$ mutants.

References

- Abutbul-Ionita, I., J. Rujiviphat, I. Nir, G.A. McQuibban, and D. Danino. 2012. Membrane tethering and nucleotide-dependent conformational changes drive mitochondrial genome maintenance (Mgm1) protein-mediated membrane fusion. *J. Biol. Chem.* 287:36634-36638.
- Acehan, D., Z. Khuchua, R.H. Houtkooper, A. Malhotra, J. Kaufman, F.M. Vaz, M. Ren, H.A. Rockman, D.L. Stokes, and M. Schlame. 2009. Distinct effects of tafazzin deletion in differentiated and undifferentiated mitochondria. *Mitochondrion.* 9:86-95.
- Achleitner, G., B. Gaigg, A. Krasser, E. Kainersdorfer, S.D. Kohlwein, A. Perktold, G. Zellnig, and G. Daum. 1999. Association between the endoplasmic reticulum and mitochondria of yeast facilitates interorganelle transport of phospholipids through membrane contact. *Eur. J. Biochem.* 264:545-553.
- Addinall, S.G., M. Downey, M. Yu, M.K. Zubko, J. Dewar, A. Leake, J. Hallinan, O. Shaw, K. James, D.J. Wilkinson, A. Wipat, D. Durocher, and D. Lydall. 2008. A genomewide suppressor and enhancer analysis of *cdc13-1* reveals varied cellular processes influencing telomere capping in *Saccharomyces cerevisiae*. *Genetics.* 180:2251-2266.
- Altmann, K., M. Durr, and B. Westermann. 2007. *Saccharomyces cerevisiae* as a model organism to study mitochondrial biology: general considerations and basic procedures. *Methods Mol. Biol.* 372:81-90.
- Altmann, K., M. Frank, D. Neumann, S. Jakobs, and B. Westermann. 2008. The class V myosin motor protein, Myo2, plays a major role in mitochondrial motility in *Saccharomyces cerevisiae*. *J. Cell Biol.* 181:119-130.
- Altmann, K., and B. Westermann. 2005. Role of essential genes in mitochondrial morphogenesis in *Saccharomyces cerevisiae*. *Mol. Biol. Cell.* 16:5410-5417.
- Amchenkova, A.A., L.E. Bakeeva, Y.S. Chentsov, V.P. Skulachev, and D.B. Zorov. 1988. Coupling membranes as energy-transmitting cables. I. Filamentous mitochondria in fibroblasts and mitochondrial clusters in cardiomyocytes. *J. Cell Biol.* 107:481-495.
- Anton, F., J.M. Fres, A. Schauss, B. Pinson, G.J. Praefcke, T. Langer, and M. Escobar-Henriques. 2011. Ugo1 and Mdm30 act sequentially during Fzo1-mediated mitochondrial outer membrane fusion. *J. Cell Sci.* 124:1126-1135.
- Atkinson, K., S. Fogel, and S.A. Henry. 1980. Yeast mutant defective in phosphatidylserine synthesis. *J. Biol. Chem.* 255:6653-6661.
- Back, J.W., M.A. Sanz, L. De Jong, L.J. De Koning, L.G. Nijtmans, C.G. De Koster, L.A. Grivell, H. Van Der Spek, and A.O. Muijsers. 2002. A structure for the yeast prohibitin complex: Structure prediction and evidence from chemical crosslinking and mass spectrometry. *Protein Sci.* 11:2471-2478.
- Baile, M.G., K. Whited, and S.M. Claypool. 2013. Deacylation on the matrix side of the mitochondrial inner membrane regulates cardiolipin remodeling. *Mol. Biol. Cell.* 24:2008-2020.
- Balla, T. 2013. Phosphoinositides: tiny lipids with giant impact on cell regulation. *Physiol. Rev.* 93:1019-1137.
- Bateson, W., E.R. Saunders, R.C. Punnett, and C.C. Hurst. 1905. Reports to the Evolution Committee of the Royal Society. Report II. *London: Harrison and Sons.*
- Beranek, A., G. Rechberger, H. Knauer, H. Wolinski, S.D. Kohlwein, and R. Leber. 2009. Identification of a cardiolipin-specific phospholipase encoded by the gene *CLD1 (YGR110W)* in yeast. *J. Biol. Chem.* 284:11572-11578.
- Bereiter-Hahn, J., and M. Voth. 1994. Dynamics of mitochondria in living cells: shape changes, dislocations, fusion, and fission of mitochondria. *Microsc. Res. Tech.* 27:198-219.

- Berger, K.H., L.F. Sogo, and M.P. Yaffe. 1997. Mdm12p, a component required for mitochondrial inheritance that is conserved between budding and fission yeast. *J. Cell Biol.* 136:545-553.
- Berger, K.H., and M.P. Yaffe. 1998. Prohibitin family members interact genetically with mitochondrial inheritance components in *Saccharomyces cerevisiae*. *Mol. Cell. Biol.* 18:4043-4052.
- Birner, R., R. Nebauer, R. Schneiter, and G. Daum. 2003. Synthetic lethal interaction of the mitochondrial phosphatidylethanolamine biosynthetic machinery with the prohibitin complex of *Saccharomyces cerevisiae*. *Mol. Biol. Cell.* 14:370-383.
- Bleazard, W., J.M. McCaffery, E.J. King, S. Bale, A. Mozdy, Q. Tieu, J. Nunnari, and J.M. Shaw. 1999. The dynamin-related GTPase Dnm1 regulates mitochondrial fission in yeast. *Nat. Cell Biol.* 1:298-304.
- Bloom, K. 2001. Nuclear migration: cortical anchors for cytoplasmic dynein. *Curr. Biol.* 11:R326-329.
- Boldogh, I.R., D.W. Nowakowski, H.C. Yang, H. Chung, S. Karmon, P. Royes, and L.A. Pon. 2003. A protein complex containing Mdm10p, Mdm12p, and Mmm1p links mitochondrial membranes and DNA to the cytoskeleton-based segregation machinery. *Mol. Biol. Cell.* 14:4618-4627.
- Boldogh, I.R., H.C. Yang, W.D. Nowakowski, S.L. Karmon, L.G. Hays, J.R. Yates, 3rd, and L.A. Pon. 2001. Arp2/3 complex and actin dynamics are required for actin-based mitochondrial motility in yeast. *Proc. Natl. Acad. Sci. USA.* 98:3162-3167.
- Boyle, G.M., X. Roucou, P. Nagley, R.J. Devenish, and M. Prescott. 1999. Identification of subunit g of yeast mitochondrial F1F0-ATP synthase, a protein required for maximal activity of cytochrome c oxidase. *Eur. J. Biochem.* 262:315-323.
- Burgess, S.M., M. Delannoy, and R.E. Jensen. 1994. *MMM1* encodes a mitochondrial outer membrane protein essential for establishing and maintaining the structure of yeast mitochondria. *J. Cell Biol.* 126:1375-1391.
- Cervený, K.L., and R.E. Jensen. 2003. The WD-repeats of Net2p interact with Dnm1p and Fis1p to regulate division of mitochondria. *Mol. Biol. Cell.* 14:4126-4139.
- Cervený, K.L., S.L. Studer, R.E. Jensen, and H. Sesaki. 2007. Yeast mitochondrial division and distribution require the cortical num1 protein. *Dev. Cell.* 12:363-375.
- Chan, E.Y., and G.A. McQuibban. 2012. Phosphatidylserine decarboxylase 1 (Psd1) promotes mitochondrial fusion by regulating the biophysical properties of the mitochondrial membrane and alternative topogenesis of mitochondrial genome maintenance protein 1 (Mgm1). *J. Biol. Chem.* 287:40131-40139.
- Chang, S.C., P.N. Heacock, C.J. Clancey, and W. Dowhan. 1998. The *PEL1* gene (renamed *PGS1*) encodes the phosphatidylglycero-phosphate synthase of *Saccharomyces cerevisiae*. *J. Biol. Chem.* 273:9829-9836.
- Chen, H., S.A. Detmer, A.J. Ewald, E.E. Griffin, S.E. Fraser, and D.C. Chan. 2003. Mitofusins Mfn1 and Mfn2 coordinately regulate mitochondrial fusion and are essential for embryonic development. *J. Cell Biol.* 160:189-200.
- Chen, S., D. Liu, R.L. Finley, Jr., and M.L. Greenberg. 2010. Loss of mitochondrial DNA in the yeast cardiolipin synthase *crd1* mutant leads to up-regulation of the protein kinase Swe1p that regulates the G2/M transition. *J. Biol. Chem.* 285:10397-10407.
- Chen, X.J., and R.A. Butow. 2005. The organization and inheritance of the mitochondrial genome. *Nat. Rev. Genet.* 6:815-825.
- Choi, S.Y., P. Huang, G.M. Jenkins, D.C. Chan, J. Schiller, and M.A. Frohman. 2006. A common lipid links Mfn-mediated mitochondrial fusion and SNARE-regulated exocytosis. *Nat. Cell Biol.* 8:1255-1262.

- Clancey, C.J., S.C. Chang, and W. Dowhan. 1993. Cloning of a gene (PSD1) encoding phosphatidylserine decarboxylase from *Saccharomyces cerevisiae* by complementation of an *Escherichia coli* mutant. *J. Biol. Chem.* 268:24580-24590.
- Claypool, S.M., P. Boontheung, J.M. McCaffery, J.A. Loo, and C.M. Koehler. 2008. The cardiolipin transacylase, tafazzin, associates with two distinct respiratory components providing insight into Barth syndrome. *Mol. Biol. Cell.* 19:5143-5155.
- Claypool, S.M., J.M. McCaffery, and C.M. Koehler. 2006. Mitochondrial mislocalization and altered assembly of a cluster of Barth syndrome mutant tafazzins. *J. Cell Biol.* 174:379-390.
- Coates, P.J., D.J. Jamieson, K. Smart, A.R. Prescott, and P.A. Hall. 1997. The prohibitin family of mitochondrial proteins regulate replicative lifespan. *Curr. Biol.* 7:607-610.
- Cohen, M.M., E.A. Amiot, A.R. Day, G.P. LeBoucher, E.N. Pryce, M.H. Glickman, J.M. McCaffery, J.M. Shaw, and A.M. Weissman. 2011. Sequential requirements for the GTPase domain of the mitofusin Fzo1 and the ubiquitin ligase SCFMdm30 in mitochondrial outer membrane fusion. *J. Cell Sci.* 124:1403-1410.
- Cohen, M.M., G.P. LeBoucher, N. Livnat-Levanon, M.H. Glickman, and A.M. Weissman. 2008. Ubiquitin-proteasome-dependent degradation of a mitofusin, a critical regulator of mitochondrial fusion. *Mol. Biol. Cell.* 19:2457-2464.
- Connerth, M., T. Tatsuta, M. Haag, T. Klecker, B. Westermann, and T. Langer. 2012. Intramitochondrial transport of phosphatidic acid in yeast by a lipid transfer protein. *Science.* 338:815-818.
- Costanzo, M., A. Baryshnikova, J. Bellay, Y. Kim, E.D. Spear, C.S. Sevier, H. Ding, J.L. Koh, K. Toufighi, S. Mostafavi, J. Prinz, R.P. St Onge, B. VanderSluis, T. Makhnevych, F.J. Vizeacoumar, S. Alizadeh, S. Bahr, R.L. Brost, Y. Chen, M. Cokol, R. Deshpande, Z. Li, Z.Y. Lin, W. Liang, M. Marback, J. Paw, B.J. San Luis, E. Shuteriqi, A.H. Tong, N. van Dyk, I.M. Wallace, J.A. Whitney, M.T. Weirauch, G. Zhong, H. Zhu, W.A. Houry, M. Brudno, S. Ragibizadeh, B. Papp, C. Pal, F.P. Roth, G. Giaever, C. Nislow, O.G. Troyanskaya, H. Bussey, G.D. Bader, A.C. Gingras, Q.D. Morris, P.M. Kim, C.A. Kaiser, C.L. Myers, B.J. Andrews, and C. Boone. 2010. The genetic landscape of a cell. *Science.* 327:425-431.
- Das, A., B.D. Slaughter, J.R. Unruh, W.D. Bradford, R. Alexander, B. Rubinstein, and R. Li. 2012. Flippase-mediated phospholipid asymmetry promotes fast Cdc42 recycling in dynamic maintenance of cell polarity. *Nat. Cell Biol.* 14:304-310.
- DeVay, R.M., L. Dominguez-Ramirez, L.L. Lackner, S. Hoppins, H. Stahlberg, and J. Nunnari. 2009. Coassembly of Mgm1 isoforms requires cardiolipin and mediates mitochondrial inner membrane fusion. *J. Cell Biol.* 186:793-803.
- Dimmer, K.S., S. Fritz, F. Fuchs, M. Messerschmitt, N. Weinbach, W. Neupert, and B. Westermann. 2002. Genetic basis of mitochondrial function and morphology in *Saccharomyces cerevisiae*. *Mol. Biol. Cell.* 13:847-853.
- Dimmer, K.S., S. Jakobs, F. Vogel, K. Altmann, and B. Westermann. 2005. Mdm31 and Mdm32 are inner membrane proteins required for maintenance of mitochondrial shape and stability of mitochondrial DNA nucleoids in yeast. *J. Cell Biol.* 168:103-115.
- Dixon, S.J., M. Costanzo, A. Baryshnikova, B. Andrews, and C. Boone. 2009. Systematic mapping of genetic interaction networks. *Annu. Rev. Genet.* 43:601-625.
- Downey, M., R. Houlsworth, L. Maringele, A. Rollie, M. Brehme, S. Galicia, S. Guillard, M. Partington, M.K. Zubko, N.J. Krogan, A. Emili, J.F. Greenblatt, L. Harrington, D. Lydall, and D. Durocher. 2006. A genome-wide screen identifies the evolutionarily conserved KEOPS complex as a telomere regulator. *Cell.* 124:1155-1168.
- Dunn, C.D., M.S. Lee, F.A. Spencer, and R.E. Jensen. 2006. A genomewide screen for petite-negative yeast strains yields a new subunit of the i-AAA protease complex. *Mol. Biol. Cell.* 17:213-226.

- Dürr, M., M. Escobar-Henriques, S. Merz, S. Geimer, T. Langer, and B. Westermann. 2006. Nonredundant roles of mitochondria-associated F-box proteins Mfb1 and Mdm30 in maintenance of mitochondrial morphology in yeast. *Mol. Biol. Cell.* 17:3745-3755.
- Egner, A., S. Jakobs, and S.W. Hell. 2002. Fast 100-nm resolution three-dimensional microscope reveals structural plasticity of mitochondria in live yeast. *Proc. Natl. Acad. Sci. USA.* 99:3370-3375.
- Elbaz, Y., and M. Schuldiner. 2011. Staying in touch: the molecular era of organelle contact sites. *Trends Biochem. Sci.* 36:616-623.
- Ephrussi, B., H. Hottinguer, and J. Tavlitzi. 1949. Action de l'acri flavine sur les levures II. Étude génétique du mutant "petite colonie". *Ann. Inst. Pasteur (Paris).* 76:419-450.
- Ephrussi, B., and P.P. Slonimski. 1955. Subcellular units involved in the synthesis of respiratory enzymes in yeast. *Nature.* 176:1207-1208.
- Espinete, C., M.A. de la Torre, M. Aldea, and E. Herrero. 1995. An efficient method to isolate yeast genes causing overexpression-mediated growth arrest. *Yeast.* 11:25-32.
- Eves, P.T., Y. Jin, M. Brunner, and L.S. Weisman. 2012. Overlap of cargo binding sites on myosin V coordinates the inheritance of diverse cargoes. *J. Cell Biol.* 198:69-85.
- Fagarasanu, A., M. Fagarasanu, G.A. Eitzen, J.D. Aitchison, and R.A. Rachubinski. 2006. The peroxisomal membrane protein Inp2p is the peroxisome-specific receptor for the myosin V motor Myo2p of *Saccharomyces cerevisiae*. *Dev. Cell.* 10:587-600.
- Fehrenbacher, K.L., H.C. Yang, A.C. Gay, T.M. Huckaba, and L.A. Pon. 2004. Live cell imaging of mitochondrial movement along actin cables in budding yeast. *Curr. Biol.* 14:1996-2004.
- Fekkes, P., K.A. Shepard, and M.P. Yaffe. 2000. Gag3p, an outer membrane protein required for fission of mitochondrial tubules. *J. Cell Biol.* 151:333-340.
- Förtsch, J., E. Hummel, M. Krist, and B. Westermann. 2011. The myosin-related motor protein Myo2 is an essential mediator of bud-directed mitochondrial movement in yeast. *J. Cell Biol.* 194:473-488.
- Frederick, R.L., K. Okamoto, and J.M. Shaw. 2008. Multiple pathways influence mitochondrial inheritance in budding yeast. *Genetics.* 178:825-837.
- Friedman, J.R., L.L. Lackner, M. West, J.R. DiBenedetto, J. Nunnari, and G.K. Voeltz. 2011. ER tubules mark sites of mitochondrial division. *Science.* 334:358-362.
- Fritz, S., D. Rapaport, E. Klanner, W. Neupert, and B. Westermann. 2001. Connection of the mitochondrial outer and inner membranes by Fzo1 is critical for organellar fusion. *J. Cell Biol.* 152:683-692.
- Fritz, S., N. Weinbach, and B. Westermann. 2003. Mdm30 is an F-box protein required for maintenance of fusion-competent mitochondria in yeast. *Mol. Biol. Cell.* 14:2303-2313.
- Frolov, V.A., A.V. Shnyrova, and J. Zimmerberg. 2011. Lipid polymorphisms and membrane shape. *Cold Spring Harb. Perspect. Biol.* 3:a004747.
- Frost, A., M.G. Elgort, O. Brandman, C. Ives, S.R. Collins, L. Miller-Vedam, J. Weibezahn, M.Y. Hein, I. Poser, M. Mann, A.A. Hyman, and J.S. Weissman. 2012. Functional repurposing revealed by comparing *S. pombe* and *S. cerevisiae* genetic interactions. *Cell.* 149:1339-1352.
- Furt, F., and P. Moreau. 2009. Importance of lipid metabolism for intracellular and mitochondrial membrane fusion/fission processes. *Int. J. Biochem. Cell Biol.* 41:1828-1836.
- Giaever, G., A.M. Chu, L. Ni, C. Connelly, L. Riles, S. Veronneau, S. Dow, A. Lucau-Danila, K. Anderson, B. Andre, A.P. Arkin, A. Astromoff, M. El-Bakkoury, R. Bangham, R. Benito, S. Brachat, S. Campanaro, M. Curtiss, K. Davis, A. Deutschbauer, K.D. Entian, P. Flaherty, F. Foury, D.J. Garfinkel, M. Gerstein, D. Gotte, U. Guldener, J.H. Hegemann, S. Hempel, Z. Herman, D.F. Jaramillo, D.E. Kelly, S.L. Kelly, P. Kotter, D. LaBonte, D.C. Lamb, N. Lan, H. Liang, H. Liao, L. Liu, C. Luo, M. Lussier,

- R. Mao, P. Menard, S.L. Ooi, J.L. Revuelta, C.J. Roberts, M. Rose, P. Ross-Macdonald, B. Scherens, G. Schimmack, B. Shafer, D.D. Shoemaker, S. Sookhai-Mahadeo, R.K. Storms, J.N. Strathern, G. Valle, M. Voet, G. Volckaert, C.Y. Wang, T.R. Ward, J. Wilhelmy, E.A. Winzeler, Y. Yang, G. Yen, E. Youngman, K. Yu, H. Bussey, J.D. Boeke, M. Snyder, P. Philippsen, R.W. Davis, and M. Johnston. 2002. Functional profiling of the *Saccharomyces cerevisiae* genome. *Nature*. 418:387-391.
- Gohil, V.M., M.N. Thompson, and M.L. Greenberg. 2005. Synthetic lethal interaction of the mitochondrial phosphatidylethanolamine and cardiolipin biosynthetic pathways in *Saccharomyces cerevisiae*. *J. Biol. Chem.* 280:35410-35416.
- Gray, M.W., G. Burger, and B.F. Lang. 1999. Mitochondrial evolution. *Science*. 283:1476-1481.
- Griffin, E.E., J. Graumann, and D.C. Chan. 2005. The WD40 protein Caf4p is a component of the mitochondrial fission machinery and recruits Dnm1p to mitochondria. *J. Cell Biol.* 170:237-248.
- Grigliatti, T.A., L. Hall, R. Rosenbluth, and D.T. Suzuki. 1973. Temperature-sensitive mutations in *Drosophila melanogaster*. XIV. A selection of immobile adults. *Mol. Gen. Genet.* 120:107-114.
- Griparic, L., and A.M. van der Bliek. 2001. The many shapes of mitochondrial membranes. *Traffic*. 2:235-244.
- Gu, Z., F. Valianpour, S. Chen, F.M. Vaz, G.A. Hakkaart, R.J. Wanders, and M.L. Greenberg. 2004. Aberrant cardiolipin metabolism in the yeast *taz1* mutant: a model for Barth syndrome. *Mol. Microbiol.* 51:149-158.
- Guan, K., L. Farh, T.K. Marshall, and R.J. Deschenes. 1993. Normal mitochondrial structure and genome maintenance in yeast requires the dynamin-like product of the *MGM1* gene. *Curr. Genet.* 24:141-148.
- Hales, K.G., and M.T. Fuller. 1997. Developmentally regulated mitochondrial fusion mediated by a conserved, novel, predicted GTPase. *Cell*. 90:121-129.
- Hammermeister, M., K. Schodel, and B. Westermann. 2010. Mdm36 is a mitochondrial fission-promoting protein in *Saccharomyces cerevisiae*. *Mol. Biol. Cell*. 21:2443-2452.
- Heil-Chapdelaine, R.A., J.R. Oberle, and J.A. Cooper. 2000. The cortical protein Num1p is essential for dynein-dependent interactions of microtubules with the cortex. *J. Cell Biol.* 151:1337-1344.
- Henry, S.A., S.D. Kohlwein, and G.M. Carman. 2012. Metabolism and regulation of glycerolipids in the yeast *Saccharomyces cerevisiae*. *Genetics*. 190:317-349.
- Herlan, M., F. Vogel, C. Bornhovd, W. Neupert, and A.S. Reichert. 2003. Processing of Mgm1 by the rhomboid-type protease Pcp1 is required for maintenance of mitochondrial morphology and of mitochondrial DNA. *J. Biol. Chem.* 278:27781-27788.
- Hermann, G.J., J.W. Thatcher, J.P. Mills, K.G. Hales, M.T. Fuller, J. Nunnari, and J.M. Shaw. 1998. Mitochondrial fusion in yeast requires the transmembrane GTPase Fzo1p. *J. Cell Biol.* 143:359-373.
- Herndon, J.D., S.M. Claypool, and C.M. Koehler. 2013. The Taz1p transacylase is imported and sorted into the outer mitochondrial membrane via a membrane anchor domain. *Eukaryot. Cell*. 12:1600-1608.
- Hoppins, S., S.R. Collins, A. Cassidy-Stone, E. Hummel, R.M. Devay, L.L. Lackner, B. Westermann, M. Schuldiner, J.S. Weissman, and J. Nunnari. 2011. A mitochondrial-focused genetic interaction map reveals a scaffold-like complex required for inner membrane organization in mitochondria. *J. Cell Biol.* 195:323-340.
- Hoppins, S., J. Horner, C. Song, J.M. McCaffery, and J. Nunnari. 2009. Mitochondrial outer and inner membrane fusion requires a modified carrier protein. *J. Cell Biol.* 184:569-581.
- Ingerman, E., E.M. Perkins, M. Marino, J.A. Mears, J.M. McCaffery, J.E. Hinshaw, and J. Nunnari. 2005. Dnm1 forms spirals that are structurally tailored to fit mitochondria. *J. Cell Biol.* 170:1021-1027.

- Ishikawa, K., N.L. Catlett, J.L. Novak, F. Tang, J.J. Nau, and L.S. Weisman. 2003. Identification of an organelle-specific myosin V receptor. *J. Cell Biol.* 160:887-897.
- Itoh, T., E.A. Toh, and Y. Matsui. 2004. Mmr1p is a mitochondrial factor for Myo2p-dependent inheritance of mitochondria in the budding yeast. *EMBO J.* 23:2520-2530.
- Itoh, T., A. Watabe, E.A. Toh, and Y. Matsui. 2002. Complex formation with Ypt11p, a rab-type small GTPase, is essential to facilitate the function of Myo2p, a class V myosin, in mitochondrial distribution in *Saccharomyces cerevisiae*. *Mol. Cell. Biol.* 22:7744-7757.
- Jakobs, S., N. Martini, A.C. Schauss, A. Egner, B. Westermann, and S.W. Hell. 2003. Spatial and temporal dynamics of budding yeast mitochondria lacking the division component Fis1p. *J. Cell Sci.* 116:2005-2014.
- Jones, B.A., and W.L. Fangman. 1992. Mitochondrial DNA maintenance in yeast requires a protein containing a region related to the GTP-binding domain of dynamin. *Genes Dev.* 6:380-389.
- Joshi, A.S., M.N. Thompson, N. Fei, M. Huttemann, and M.L. Greenberg. 2012. Cardiolipin and mitochondrial phosphatidylethanolamine have overlapping functions in mitochondrial fusion in *Saccharomyces cerevisiae*. *J. Biol. Chem.* 287:17589-17597.
- Joshi, A.S., J. Zhou, V.M. Gohil, S. Chen, and M.L. Greenberg. 2009. Cellular functions of cardiolipin in yeast. *Biochim. Biophys. Acta.* 1793:212-218.
- Jupe, E.R., X.T. Liu, J.L. Kiehlbauch, J.K. McClung, and R.T. Dell'Orco. 1996. The 3' untranslated region of prohibitin and cellular immortalization. *Exp. Cell. Res.* 224:128-135.
- Karren, M.A., E.M. Coonrod, T.K. Anderson, and J.M. Shaw. 2005. The role of Fis1p-Mdv1p interactions in mitochondrial fission complex assembly. *J. Cell Biol.* 171:291-301.
- Kelly, B.L., and M.L. Greenberg. 1990. Characterization and regulation of phosphatidylglycerolphosphate phosphatase in *Saccharomyces cerevisiae*. *Biochim. Biophys. Acta.* 1046:144-150.
- Kennedy, E.P., and S.B. Weiss. 1956. The function of cytidine coenzymes in the biosynthesis of phospholipides. *J. Biol. Chem.* 222:193-214.
- Keyhani, E. 1980. Observations on the mitochondrial reticulum in the yeast *Candida utilis* as revealed by freeze-fracture electron microscopy. *J. Cell Sci.* 46:289-297.
- Kirchman, P.A., M.V. Miceli, R.L. West, J.C. Jiang, S. Kim, and S.M. Jazwinski. 2003. Prohibitins and Ras2 protein cooperate in the maintenance of mitochondrial function during yeast aging. *Acta Biochim. Pol.* 50:1039-1056.
- Klecker, T., D. Scholz, J. Fortsch, and B. Westermann. 2013. The yeast cell cortical protein Num1 integrates mitochondrial dynamics into cellular architecture. *J. Cell Sci.* 126:2924-2930.
- Klecker, T., M. Wemmer, A. Murley, M. Haag, A. Weig, T. Langer, J. Nunnari, and B. Westermann. 2014. Mdm33 links phospholipid homeostasis to mitochondrial division. *In preparation.*
- Knoblach, B., X. Sun, N. Coquelle, A. Fagarasanu, R.L. Poirier, and R.A. Rachubinski. 2013. An ER-peroxisome tether exerts peroxisome population control in yeast. *EMBO J.* 32:2439-2453.
- Kolb-Bachofen, V., and W. Vogell. 1975. Mitochondrial proliferation in synchronized cells of *Tetrahymena pyriformis*. A morphometric study by electron microscopy on the biogenesis of mitochondria during the cell cycle. *Exp. Cell. Res.* 94:95-105.
- Kondo-Okamoto, N., J.M. Shaw, and K. Okamoto. 2003. Mmm1p spans both the outer and inner mitochondrial membranes and contains distinct domains for targeting and foci formation. *J. Biol. Chem.* 278:48997-49005.
- Koning, A.J., P.Y. Lum, J.M. Williams, and R. Wright. 1993. DiOC6 staining reveals organelle structure and dynamics in living yeast cells. *Cell Motil. Cytoskeleton.* 25:111-128.

- Kornmann, B., E. Currie, S.R. Collins, M. Schuldiner, J. Nunnari, J.S. Weissman, and P. Walter. 2009. An ER-mitochondria tethering complex revealed by a synthetic biology screen. *Science*. 325:477-481.
- Kornmann, B., C. Osman, and P. Walter. 2011. The conserved GTPase Gem1 regulates endoplasmic reticulum-mitochondria connections. *Proc. Natl. Acad. Sci. USA*. 108:14151-14156.
- Kuchler, K., G. Daum, and F. Paltauf. 1986. Subcellular and submitochondrial localization of phospholipid-synthesizing enzymes in *Saccharomyces cerevisiae*. *J. Bacteriol* 165:901-910.
- Kuroda, T., M. Tani, A. Moriguchi, S. Tokunaga, T. Higuchi, S. Kitada, and O. Kuge. 2011. *FMP30* is required for the maintenance of a normal cardiolipin level and mitochondrial morphology in the absence of mitochondrial phosphatidylethanolamine synthesis. *Mol. Microbiol.* 80:248-265.
- Kutik, S., M. Rissler, X.L. Guan, B. Guiard, G. Shui, N. Gebert, P.N. Heacock, P. Rehling, W. Dowhan, M.R. Wenk, N. Pfanner, and N. Wiedemann. 2008. The translocator maintenance protein Tam41 is required for mitochondrial cardiolipin biosynthesis. *J. Cell Biol.* 183:1213-1221.
- Labrousse, A.M., M.D. Zappaterra, D.A. Rube, and A.M. van der Bliek. 1999. *C. elegans* dynamin-related protein DRP-1 controls severing of the mitochondrial outer membrane. *Mol. Cell.* 4:815-826.
- Lackner, L.L., J.S. Horner, and J. Nunnari. 2009. Mechanistic analysis of a dynamin effector. *Science*. 325:874-877.
- Lackner, L.L., and J.M. Nunnari. 2009. The molecular mechanism and cellular functions of mitochondrial division. *Biochim. Biophys. Acta.* 1792:1138-1144.
- Lackner, L.L., H. Ping, M. Graef, A. Murley, and J. Nunnari. 2013. Endoplasmic reticulum-associated mitochondria-cortex tether functions in the distribution and inheritance of mitochondria. *Proc. Natl. Acad. Sci. USA*. 110:E458-467.
- Lazzarino, D.A., I. Boldogh, M.G. Smith, J. Rosand, and L.A. Pon. 1994. Yeast mitochondria contain ATP-sensitive, reversible actin-binding activity. *Mol. Biol. Cell.* 5:807-818.
- Legesse-Miller, A., R.H. Massol, and T. Kirchhausen. 2003. Constriction and Dnm1p recruitment are distinct processes in mitochondrial fission. *Mol. Biol. Cell.* 14:1953-1963.
- Letts, V.A., L.S. Klig, M. Bae-Lee, G.M. Carman, and S.A. Henry. 1983. Isolation of the yeast structural gene for the membrane-associated enzyme phosphatidylserine synthase. *Proc. Natl. Acad. Sci. USA*. 80:7279-7283.
- Ling, Y., C.J. Stefan, J.A. Macgurn, A. Audhya, and S.D. Emr. 2012. The dual PH domain protein Opy1 functions as a sensor and modulator of PtdIns(4,5)P(2) synthesis. *EMBO J.* 31:2882-2894.
- Lipinski, K.A., A. Kaniak-Golik, and P. Golik. 2010. Maintenance and expression of the *S. cerevisiae* mitochondrial genome--from genetics to evolution and systems biology. *Biochim. Biophys. Acta.* 1797:1086-1098.
- Macchi, M., N. El Fissi, R. Tufi, M. Bentobji, J.C. Lievens, L.M. Martins, J. Royet, and T. Rival. 2013. The *Drosophila* inner-membrane protein PMI controls crista biogenesis and mitochondrial diameter. *J. Cell Sci.* 126:814-824.
- Malinska, K., J. Malinsky, M. Opekarova, and W. Tanner. 2003. Visualization of protein compartmentation within the plasma membrane of living yeast cells. *Mol. Biol. Cell.* 14:4427-4436.
- Manford, A.G., C.J. Stefan, H.L. Yuan, J.A. Macgurn, and S.D. Emr. 2012. ER-to-plasma membrane tethering proteins regulate cell signaling and ER morphology. *Dev. Cell.* 23:1129-1140.
- Mannella, C.A. 2006. Structure and dynamics of the mitochondrial inner membrane cristae. *Biochim. Biophys. Acta.* 1763:542-548.

- Mannella, C.A., D.R. Pfeiffer, P.C. Bradshaw, Moraru, Il, B. Slepchenko, L.M. Loew, C.E. Hsieh, K. Buttle, and M. Marko. 2001. Topology of the mitochondrial inner membrane: dynamics and bioenergetic implications. *IUBMB Life*. 52:93-100.
- Mao, K., K. Wang, X. Liu, and D.J. Klionsky. 2013. The scaffold protein Atg11 recruits fission machinery to drive selective mitochondria degradation by autophagy. *Dev. Cell*. 26:9-18.
- Martens, S., and H.T. McMahon. 2008. Mechanisms of membrane fusion: disparate players and common principles. *Nat. Rev. Mol. Cell Biol.* 9:543-556.
- Mason, R.P., M. Casu, N. Butler, C. Breda, S. Campesan, J. Clapp, E.W. Green, D. Dhulkhed, C.P. Kyriacou, and F. Giorgini. 2013. Glutathione peroxidase activity is neuroprotective in models of Huntington's disease. *Nat. Genet.* 45:1249-1254.
- McClung, J.K., D.B. Danner, D.A. Stewart, J.R. Smith, E.L. Schneider, C.K. Lumpkin, R.T. Dell'Orco, and M.J. Nuell. 1989. Isolation of a cDNA that hybrid selects antiproliferative mRNA from rat liver. *Biochem. Biophys. Res. Commun.* 164:1316-1322.
- McQuibban, G.A., S. Saurya, and M. Freeman. 2003. Mitochondrial membrane remodelling regulated by a conserved rhomboid protease. *Nature*. 423:537-541.
- Mears, J.A., L.L. Lackner, S. Fang, E. Ingerman, J. Nunnari, and J.E. Hinshaw. 2011. Conformational changes in Dnm1 support a contractile mechanism for mitochondrial fission. *Nat. Struct. Mol. Biol.* 18:20-26.
- Meeusen, S., R. DeVay, J. Block, A. Cassidy-Stone, S. Wayson, J.M. McCaffery, and J. Nunnari. 2006. Mitochondrial inner-membrane fusion and crista maintenance requires the dynamin-related GTPase Mgm1. *Cell*. 127:383-395.
- Meeusen, S., J.M. McCaffery, and J. Nunnari. 2004. Mitochondrial fusion intermediates revealed in vitro. *Science*. 305:1747-1752.
- Meeusen, S., and J. Nunnari. 2003. Evidence for a two membrane-spanning autonomous mitochondrial DNA replisome. *J. Cell Biol.* 163:503-510.
- Messerschmitt, M., S. Jakobs, F. Vogel, S. Fritz, K.S. Dimmer, W. Neupert, and B. Westermann. 2003. The inner membrane protein Mdm33 controls mitochondrial morphology in yeast. *J. Cell Biol.* 160:553-564.
- Mileykovskaya, E., and W. Dowhan. 2009. Cardiolipin membrane domains in prokaryotes and eukaryotes. *Biochim. Biophys. Acta*. 1788:2084-2091.
- Miyakawa, I., H. Aoi, N. Sando, and T. Kuroiwa. 1984. Fluorescence microscopic studies of mitochondrial nucleoids during meiosis and sporulation in the yeast, *Saccharomyces cerevisiae*. *J. Cell Sci.* 66:21-38.
- Moseley, J.B., and B.L. Goode. 2006. The yeast actin cytoskeleton: from cellular function to biochemical mechanism. *Microbiol. Mol. Biol. Rev.* 70:605-645.
- Mozdy, A.D., J.M. McCaffery, and J.M. Shaw. 2000. Dnm1p GTPase-mediated mitochondrial fission is a multi-step process requiring the novel integral membrane component Fis1p. *J. Cell Biol.* 151:367-380.
- Murley, A., L.L. Lackner, C. Osman, M. West, G.K. Voeltz, P. Walter, and J. Nunnari. 2013. ER-associated mitochondrial division links the distribution of mitochondria and mitochondrial DNA in yeast. *Elife*. 2:e00422.
- Nakatsu, F., J.M. Baskin, J. Chung, L.B. Tanner, G. Shui, S.Y. Lee, M. Pirruccello, M. Hao, N.T. Ingolia, M.R. Wenk, and P. De Camilli. 2012. PtdIns4P synthesis by PI4KIIIalpha at the plasma membrane and its impact on plasma membrane identity. *J. Cell Biol.* 199:1003-1016.
- Naylor, K., E. Ingerman, V. Okreglak, M. Marino, J.E. Hinshaw, and J. Nunnari. 2006. Mdv1 interacts with assembled Dnm1 to promote mitochondrial division. *J. Biol. Chem.* 281:2177-2183.

- Nijtmans, L.G., L. de Jong, M. Artal Sanz, P.J. Coates, J.A. Berden, J.W. Back, A.O. Muijsers, H. van der Spek, and L.A. Grivell. 2000. Prohibitins act as a membrane-bound chaperone for the stabilization of mitochondrial proteins. *EMBO J.* 19:2444-2451.
- Nunnari, J., W.F. Marshall, A. Straight, A. Murray, J.W. Sedat, and P. Walter. 1997. Mitochondrial transmission during mating in *Saccharomyces cerevisiae* is determined by mitochondrial fusion and fission and the intramitochondrial segregation of mitochondrial DNA. *Mol. Biol. Cell.* 8:1233-1242.
- Opekarova, M., J. Malinsky, and W. Tanner. 2010. Plants and fungi in the era of heterogeneous plasma membranes. *Plant. Biol. (Stuttg).* 12 Suppl 1:94-98.
- Osellame, L.D., T.S. Blacker, and M.R. Duchon. 2012. Cellular and molecular mechanisms of mitochondrial function. *Best Pract. Res. Clin. Endocrinol. Metab.* 26:711-723.
- Osman, C., M. Haag, C. Potting, J. Rodenfels, P.V. Dip, F.T. Wieland, B. Brugger, B. Westermann, and T. Langer. 2009a. The genetic interactome of prohibitins: coordinated control of cardiolipin and phosphatidylethanolamine by conserved regulators in mitochondria. *J. Cell Biol.* 184:583-596.
- Osman, C., M. Haag, F.T. Wieland, B. Brugger, and T. Langer. 2010. A mitochondrial phosphatase required for cardiolipin biosynthesis: the PGP phosphatase Gep4. *EMBO J.* 29:1976-1987.
- Osman, C., C. Merkwirth, and T. Langer. 2009b. Prohibitins and the functional compartmentalization of mitochondrial membranes. *J. Cell Sci.* 122:3823-3830.
- Osman, C., C. Wilmes, T. Tatsuta, and T. Langer. 2007. Prohibitins interact genetically with Atp23, a novel processing peptidase and chaperone for the F1Fo-ATP synthase. *Mol. Biol. Cell.* 18:627-635.
- Otsuga, D., B.R. Keegan, E. Brisch, J.W. Thatcher, G.J. Hermann, W. Bleazard, and J.M. Shaw. 1998. The dynamin-related GTPase, Dnm1p, controls mitochondrial morphology in yeast. *J. Cell Biol.* 143:333-349.
- Pineau, B., M. Bourge, J. Marion, C. Mauve, F. Gilard, L. Maneta-Peyret, P. Moreau, B. Satiat-Jeunemaitre, S.C. Brown, R. De Paepe, and A. Danon. 2013. The Importance of Cardiolipin Synthase for Mitochondrial Ultrastructure, Respiratory Function, Plant Development, and Stress Responses in *Arabidopsis*. *Plant Cell.* 25:4195-4208.
- Piper, P.W., and D. Bringloe. 2002. Loss of prohibitins, though it shortens the replicative life span of yeast cells undergoing division, does not shorten the chronological life span of G0-arrested cells. *Mech. Ageing Dev.* 123:287-295.
- Piper, P.W., G.W. Jones, D. Bringloe, N. Harris, M. MacLean, and M. Mollapour. 2002. The shortened replicative life span of prohibitin mutants of yeast appears to be due to defective mitochondrial segregation in old mother cells. *Aging Cell.* 1:149-157.
- Popov-Celeketic, D., K. Mapa, W. Neupert, and D. Mokranjac. 2008. Active remodelling of the TIM23 complex during translocation of preproteins into mitochondria. *EMBO J.* 27:1469-1480.
- Potting, C., C. Wilmes, T. Engmann, C. Osman, and T. Langer. 2010. Regulation of mitochondrial phospholipids by Ups1/PRELI-like proteins depends on proteolysis and Mdm35. *EMBO J.* 29:2888-2898.
- Praefcke, G.J., and H.T. McMahon. 2004. The dynamin superfamily: universal membrane tubulation and fission molecules? *Nat. Rev. Mol. Cell Biol.* 5:133-147.
- Pruyne, D., A. Legesse-Miller, L. Gao, Y. Dong, and A. Bretscher. 2004. Mechanisms of polarized growth and organelle segregation in yeast. *Annu. Rev. Cell Dev. Biol.* 20:559-591.
- Qualmann, B., D. Koch, and M.M. Kessels. 2011. Let's go bananas: revisiting the endocytic BAR code. *EMBO J.* 30:3501-3515.

- Rapaport, D., M. Brunner, W. Neupert, and B. Westermann. 1998. Fzo1p is a mitochondrial outer membrane protein essential for the biogenesis of functional mitochondria in *Saccharomyces cerevisiae*. *J. Biol. Chem.* 273:20150-20155.
- Rival, T., M. Macchi, L. Arnaune-Pelloquin, M. Poidevin, F. Maillet, F. Richard, A. Fatmi, P. Belenguer, and J. Royet. 2011. Inner-membrane proteins PMI/TMEM11 regulate mitochondrial morphogenesis independently of the DRP1/MFN fission/fusion pathways. *EMBO Rep.* 12:223-230.
- Roth, F.P., H.D. Lipshitz, and B.J. Andrews. 2009. Q&A: epistasis. *J Biol.* 8:35.
- Rowland, A.A., and G.K. Voeltz. 2012. Endoplasmic reticulum-mitochondria contacts: function of the junction. *Nat. Rev. Mol. Cell Biol.* 13:607-625.
- Santel, A., and M.T. Fuller. 2001. Control of mitochondrial morphology by a human mitofusin. *J. Cell Sci.* 114:867-874.
- Sauvanet, C., S. Duvezin-Caubet, B. Salin, C. David, A. Massoni-Laporte, J.P. di Rago, and M. Rojo. 2012. Mitochondrial DNA mutations provoke dominant inhibition of mitochondrial inner membrane fusion. *PLoS One.* 7:e49639.
- Schauss, A.C., J. Bewersdorf, and S. Jakobs. 2006. Fis1p and Caf4p, but not Mdv1p, determine the polar localization of Dnm1p clusters on the mitochondrial surface. *J. Cell Sci.* 119:3098-3106.
- Schauss, A.C., and H.M. McBride. 2007. Mitochondrial fission: a non-nuclear role for Num1p. *Curr. Biol.* 17:R467-470.
- Scheffler, I.E. 2001. A century of mitochondrial research: achievements and perspectives. *Mitochondrion.* 1:3-31.
- Schlame, M., and D. Haldar. 1993. Cardiolipin is synthesized on the matrix side of the inner membrane in rat liver mitochondria. *J. Biol. Chem.* 268:74-79.
- Schleit, J., S.C. Johnson, C.F. Bennett, M. Simko, N. Trongtham, A. Castanza, E.J. Hsieh, R.M. Moller, B.M. Wasko, J.R. Delaney, G.L. Sutphin, D. Carr, C.J. Murakami, A. Tocchi, B. Xian, W. Chen, T. Yu, S. Goswami, S. Higgins, K.S. Jeong, J.R. Kim, S. Klum, E. Liao, M.S. Lin, W. Lo, H. Miller, B. Olsen, Z.J. Peng, T. Pollard, P. Pradeep, D. Pruett, D. Rai, V. Ros, M. Singh, B.L. Spector, H.V. Wende, E.H. An, M. Fletcher, M. Jelic, P.S. Rabinovitch, M.J. Maccoss, J.D. Han, B.K. Kennedy, and M. Kaeberlein. 2013. Molecular mechanisms underlying genotype-dependent responses to dietary restriction. *Aging Cell.* 12:1050-1061.
- Seligman, A.M., M.J. Karnovsky, H.L. Wasserkrug, and J.S. Hanker. 1968. Nondroplet ultrastructural demonstration of cytochrome oxidase activity with a polymerizing osmiophilic reagent, diaminobenzidine (DAB). *J. Cell Biol.* 38:1-14.
- Sesaki, H., C.D. Dunn, M. Iijima, K.A. Shepard, M.P. Yaffe, C.E. Machamer, and R.E. Jensen. 2006. Ups1p, a conserved intermembrane space protein, regulates mitochondrial shape and alternative topogenesis of Mgm1p. *J. Cell Biol.* 173:651-658.
- Sesaki, H., and R.E. Jensen. 1999. Division versus fusion: Dnm1p and Fzo1p antagonistically regulate mitochondrial shape. *J. Cell Biol.* 147:699-706.
- Sesaki, H., and R.E. Jensen. 2004. Ugo1p links the Fzo1p and Mgm1p GTPases for mitochondrial fusion. *J. Biol. Chem.* 279:28298-28303.
- Sesaki, H., S.M. Southard, M.P. Yaffe, and R.E. Jensen. 2003. Mgm1p, a dynamin-related GTPase, is essential for fusion of the mitochondrial outer membrane. *Mol. Biol. Cell.* 14:2342-2356.
- Shen, H., P.N. Heacock, C.J. Clancey, and W. Dowhan. 1996. The *CDS1* gene encoding CDP-diacylglycerol synthase in *Saccharomyces cerevisiae* is essential for cell growth. *J. Biol. Chem.* 271:789-795.

- Shoemaker, D.D., D.A. Lashkari, D. Morris, M. Mittmann, and R.W. Davis. 1996. Quantitative phenotypic analysis of yeast deletion mutants using a highly parallel molecular bar-coding strategy. *Nat. Genet.* 14:450-456.
- Sickmann, A., J. Reinders, Y. Wagner, C. Joppich, R. Zahedi, H.E. Meyer, B. Schonfisch, I. Perschil, A. Chacinska, B. Guiard, P. Rehling, N. Pfanner, and C. Meisinger. 2003. The proteome of *Saccharomyces cerevisiae* mitochondria. *Proc. Natl. Acad. Sci. USA.* 100:13207-13212.
- Simbeni, R., L. Pon, E. Zinser, F. Paltauf, and G. Daum. 1991. Mitochondrial membrane contact sites of yeast. Characterization of lipid components and possible involvement in intramitochondrial translocation of phospholipids. *J. Biol. Chem.* 266:10047-10049.
- Simon, V.R., S.L. Karmon, and L.A. Pon. 1997. Mitochondrial inheritance: cell cycle and actin cable dependence of polarized mitochondrial movements in *Saccharomyces cerevisiae*. *Cell Motil. Cytoskeleton.* 37:199-210.
- Simon, V.R., T.C. Swayne, and L.A. Pon. 1995. Actin-dependent mitochondrial motility in mitotic yeast and cell-free systems: identification of a motor activity on the mitochondrial surface. *J. Cell Biol.* 130:345-354.
- Skulachev, V.P. 2001. Mitochondrial filaments and clusters as intracellular power-transmitting cables. *Trends Biochem. Sci.* 26:23-29.
- Smirnova, E., L. Griparic, D.L. Shurland, and A.M. van der Bliek. 2001. Dynamin-related protein Drp1 is required for mitochondrial division in mammalian cells. *Mol. Biol. Cell.* 12:2245-2256.
- Sogo, L.F., and M.P. Yaffe. 1994. Regulation of mitochondrial morphology and inheritance by Mdm10p, a protein of the mitochondrial outer membrane. *J. Cell Biol.* 126:1361-1373.
- Steglich, G., W. Neupert, and T. Langer. 1999. Prohibitins regulate membrane protein degradation by the m-AAA protease in mitochondria. *Mol. Cell. Biol.* 19:3435-3442.
- Stradalova, V., M. Blazikova, G. Grossmann, M. Opekarova, W. Tanner, and J. Malinsky. 2012. Distribution of cortical endoplasmic reticulum determines positioning of endocytic events in yeast plasma membrane. *PLoS One.* 7:e35132.
- Stradalova, V., W. Stahlschmidt, G. Grossmann, M. Blazikova, R. Rachel, W. Tanner, and J. Malinsky. 2009. Furrow-like invaginations of the yeast plasma membrane correspond to membrane compartment of Can1. *J. Cell Sci.* 122:2887-2894.
- Stroud, D.A., S. Oeljeklaus, S. Wiese, M. Bohnert, U. Lewandrowski, A. Sickmann, B. Guiard, M. van der Laan, B. Warscheid, and N. Wiedemann. 2011. Composition and topology of the endoplasmic reticulum-mitochondria encounter structure. *J. Mol. Biol.* 413:743-750.
- Swayne, T.C., C. Zhou, I.R. Boldogh, J.K. Charalel, J.R. McFaline-Figueroa, S. Thoms, C. Yang, G. Leung, J. McInnes, R. Erdmann, and L.A. Pon. 2011. Role for cER and Mmr1p in anchorage of mitochondria at sites of polarized surface growth in budding yeast. *Curr. Biol.* 21:1994-1999.
- Tamura, Y., T. Endo, M. Iijima, and H. Sesaki. 2009. Ups1p and Ups2p antagonistically regulate cardiolipin metabolism in mitochondria. *J. Cell Biol.* 185:1029-1045.
- Tamura, Y., Y. Harada, S. Nishikawa, K. Yamano, M. Kamiya, T. Shiota, T. Kuroda, O. Kuge, H. Sesaki, K. Imai, K. Tomii, and T. Endo. 2013. Tam41 is a CDP-diacylglycerol synthase required for cardiolipin biosynthesis in mitochondria. *Cell Metab.* 17:709-718.
- Tamura, Y., O. Onguka, A.E. Hobbs, R.E. Jensen, M. Iijima, S.M. Claypool, and H. Sesaki. 2012. Role for two conserved intermembrane space proteins, Ups1p and Ups2p, [corrected] in intramitochondrial phospholipid trafficking. *J. Biol. Chem.* 287:15205-15218.
- Tan, T., C. Ozbalci, B. Brugger, D. Rapaport, and K.S. Dimmer. 2013. Mcp1 and Mcp2, two novel proteins involved in mitochondrial lipid homeostasis. *J. Cell Sci.* 126:3563-3574.

- Tang, X., B.S. Germain, and W.L. Lee. 2012. A novel patch assembly domain in Num1 mediates dynein anchoring at the cortex during spindle positioning. *J. Cell Biol.* 196:743-756.
- Tasseva, G., H.D. Bai, M. Davidescu, A. Haromy, E. Michelakis, and J.E. Vance. 2013. Phosphatidylethanolamine deficiency in Mammalian mitochondria impairs oxidative phosphorylation and alters mitochondrial morphology. *J. Biol. Chem.* 288:4158-4173.
- Tatsuta, T., K. Model, and T. Langer. 2005. Formation of membrane-bound ring complexes by prohibitins in mitochondria. *Mol. Biol. Cell.* 16:248-259.
- Tatsuta, T., M. Scharwey, and T. Langer. 2013. Mitochondrial lipid trafficking. *Trends Cell Biol.* 24:44-52.
- Tieu, Q., V. Okreglak, K. Naylor, and J. Nunnari. 2002. The WD repeat protein, Mdv1p, functions as a molecular adaptor by interacting with Dnm1p and Fis1p during mitochondrial fission. *J. Cell Biol.* 158:445-452.
- Tilney, L.G., P.S. Connelly, and D.A. Portnoy. 1990. Actin filament nucleation by the bacterial pathogen, *Listeria monocytogenes*. *J. Cell Biol.* 111:2979-2988.
- Tilney, L.G., and D.A. Portnoy. 1989. Actin filaments and the growth, movement, and spread of the intracellular bacterial parasite, *Listeria monocytogenes*. *J. Cell Biol.* 109:1597-1608.
- Tokuyasu, K.T. 1975. Dynamics of spermiogenesis in *Drosophila melanogaster*. VI. Significance of "onion" nebenkern formation. *J. Ultrastruct. Res.* 53:93-112.
- Tonachini, L., M. Monticone, C. Puri, C. Tacchetti, P. Pinton, R. Rizzuto, R. Cancedda, S. Tavella, and P. Castagnola. 2004. Chondrocyte protein with a poly-proline region (CHPPR) is a novel mitochondrial protein and promotes mitochondrial fission. *J. Cell Physiol.* 201:470-482.
- Tondera, D., F. Czauderna, K. Paulick, R. Schwarzer, J. Kaufmann, and A. Santel. 2005. The mitochondrial protein MTP18 contributes to mitochondrial fission in mammalian cells. *J. Cell Sci.* 118:3049-3059.
- Tondera, D., A. Santel, R. Schwarzer, S. Dames, K. Giese, A. Klippel, and J. Kaufmann. 2004. Knockdown of MTP18, a novel phosphatidylinositol 3-kinase-dependent protein, affects mitochondrial morphology and induces apoptosis. *J. Biol. Chem.* 279:31544-31555.
- Toulmay, A., and W.A. Prinz. 2011. Lipid transfer and signaling at organelle contact sites: the tip of the iceberg. *Curr. Opin. Cell Biol.* 23:458-463.
- Trotter, P.J., J. Pedretti, and D.R. Voelker. 1993. Phosphatidylserine decarboxylase from *Saccharomyces cerevisiae*. Isolation of mutants, cloning of the gene, and creation of a null allele. *J. Biol. Chem.* 268:21416-21424.
- Trotter, P.J., and D.R. Voelker. 1995. Identification of a non-mitochondrial phosphatidylserine decarboxylase activity (PSD2) in the yeast *Saccharomyces cerevisiae*. *J. Biol. Chem.* 270:6062-6070.
- Tuller, G., C. Hrastnik, G. Achleitner, U. Schiefthaler, F. Klein, and G. Daum. 1998. *YDL142c* encodes cardiolipin synthase (Cls1p) and is non-essential for aerobic growth of *Saccharomyces cerevisiae*. *FEBS Lett.* 421:15-18.
- van der Blik, A.M., and E.M. Meyerowitz. 1991. Dynamin-like protein encoded by the *Drosophila shibire* gene associated with vesicular traffic. *Nature.* 351:411-414.
- Vevea, J.D., T.C. Swayne, I.R. Boldogh, and L.A. Pon. 2013. Inheritance of the fittest mitochondria in yeast. *Trends Cell Biol.* 24:53-60.
- Vitale, N., A.S. Caumont, S. Chasserot-Golaz, G. Du, S. Wu, V.A. Sciorra, A.J. Morris, M.A. Frohman, and M.F. Bader. 2001. Phospholipase D1: a key factor for the exocytotic machinery in neuroendocrine cells. *EMBO J.* 20:2424-2434.

- Voeltz, G.K., W.A. Prinz, Y. Shibata, J.M. Rist, and T.A. Rapoport. 2006. A class of membrane proteins shaping the tubular endoplasmic reticulum. *Cell*. 124:573-586.
- Waizenegger, T., T. Stan, W. Neupert, and D. Rapoport. 2003. Signal-anchor domains of proteins of the outer membrane of mitochondria: structural and functional characteristics. *J. Biol. Chem.* 278:42064-42071.
- Walther, T.C., J.H. Brickner, P.S. Aguilar, S. Bernales, C. Pantoja, and P. Walter. 2006. Eisosomes mark static sites of endocytosis. *Nature*. 439:998-1003.
- Westermann, B. 2002. Merging mitochondria matters: cellular role and molecular machinery of mitochondrial fusion. *EMBO Rep.* 3:527-531.
- Westermann, B. 2008. Molecular machinery of mitochondrial fusion and fission. *J. Biol. Chem.* 283:13501-13505.
- Westermann, B. 2010. Mitochondrial fusion and fission in cell life and death. *Nat. Rev. Mol. Cell Biol.* 11:872-884.
- Wilson, D.F., J.G. Lindsay, and E.S. Brocklehurst. 1972. Heme-heme interaction in cytochrome oxidase. *Biochim. Biophys. Acta.* 256:277-286.
- Winzler, E.A., D.D. Shoemaker, A. Astromoff, H. Liang, K. Anderson, B. Andre, R. Bangham, R. Benito, J.D. Boeke, H. Bussey, A.M. Chu, C. Connelly, K. Davis, F. Dietrich, S.W. Dow, M. El Bakkoury, F. Foury, S.H. Friend, E. Gentalen, G. Giaever, J.H. Hegemann, T. Jones, M. Laub, H. Liao, N. Liebundguth, D.J. Lockhart, A. Lucau-Danila, M. Lussier, N. M'Rabet, P. Menard, M. Mittmann, C. Pai, C. Rebischung, J.L. Revuelta, L. Riles, C.J. Roberts, P. Ross-MacDonald, B. Scherens, M. Snyder, S. Sookhai-Mahadeo, R.K. Storms, S. Veronneau, M. Voet, G. Volckaert, T.R. Ward, R. Wysocki, G.S. Yen, K. Yu, K. Zimmermann, P. Philippsen, M. Johnston, and R.W. Davis. 1999. Functional characterization of the *S. cerevisiae* genome by gene deletion and parallel analysis. *Science*. 285:901-906.
- Wittschieben, B.O., G. Otero, T. de Bizemont, J. Fellows, H. Erdjument-Bromage, R. Ohba, Y. Li, C.D. Allis, P. Tempst, and J.Q. Svejstrup. 1999. A novel histone acetyltransferase is an integral subunit of elongating RNA polymerase II holoenzyme. *Mol. Cell*. 4:123-128.
- Wolf, W., A. Kilic, B. Schrul, H. Lorenz, B. Schwappach, and M. Seedorf. 2012. Yeast Ist2 recruits the endoplasmic reticulum to the plasma membrane and creates a ribosome-free membrane microcompartment. *PLoS One*. 7:e39703.
- Wong, E.D., J.A. Wagner, S.W. Gorsich, J.M. McCaffery, J.M. Shaw, and J. Nunnari. 2000. The dynamin-related GTPase, Mgm1p, is an intermembrane space protein required for maintenance of fusion competent mitochondria. *J. Cell Biol.* 151:341-352.
- Wong, E.D., J.A. Wagner, S.V. Scott, V. Okreglak, T.J. Holewinski, A. Cassidy-Stone, and J. Nunnari. 2003. The intramitochondrial dynamin-related GTPase, Mgm1p, is a component of a protein complex that mediates mitochondrial fusion. *J. Cell Biol.* 160:303-311.
- Yaffe, M.P. 2003. The cutting edge of mitochondrial fusion. *Nat. Cell Biol.* 5:497-499.
- Yang, H.C., A. Palazzo, T.C. Swayne, and L.A. Pon. 1999. A retention mechanism for distribution of mitochondria during cell division in budding yeast. *Curr. Biol.* 9:1111-1114.
- Yoshida, Y., S.Y. Miyagishima, H. Kuroiwa, and T. Kuroiwa. 2012. The plastid-dividing machinery: formation, constriction and fission. *Curr. Opin. Plant Biol.* 15:714-721.
- Youngman, M.J., A.E. Hobbs, S.M. Burgess, M. Srinivasan, and R.E. Jensen. 2004. Mmm2p, a mitochondrial outer membrane protein required for yeast mitochondrial shape and maintenance of mtDNA nucleoids. *J. Cell Biol.* 164:677-688.

- Yu, J.W., J.M. Mendrola, A. Audhya, S. Singh, D. Keleti, D.B. DeWald, D. Murray, S.D. Emr, and M.A. Lemmon. 2004. Genome-wide analysis of membrane targeting by *S. cerevisiae* pleckstrin homology domains. *Mol. Cell.* 13:677-688.
- Zhang, M., E. Mileykovskaya, and W. Dowhan. 2005. Cardiolipin is essential for organization of complexes III and IV into a supercomplex in intact yeast mitochondria. *J. Biol. Chem.* 280:29403-29408.
- Zhao, J., T. Liu, S.B. Jin, N. Tomilin, J. Castro, O. Shupliakov, U. Lendahl, and M. Nister. 2009. The novel conserved mitochondrial inner-membrane protein MTGM regulates mitochondrial morphology and cell proliferation. *J. Cell Sci.* 122:2252-2262.

The yeast cell cortical protein Num1 integrates mitochondrial dynamics into cellular architecture

Till Klecker, Dirk Scholz, Johannes Förtsch, and Benedikt Westermann*

(2013), *Journal of Cell Science* 126: 2924-2930

Zellbiologie, Universität Bayreuth, 95440 Bayreuth, Germany

* To whom correspondence should be addressed. Email: benedikt.westermann@uni-bayreuth.de

Author contributions

I generated all strains and plasmids unless stated otherwise. I performed the data acquisition or analysis for:

Figure 1B: Data analysis and statistics (data was acquired by Johannes König).

Figures 2C-D; 3A-C; 4D; 5A-D: Data acquisition and analysis.

Figure 4B: 3d reconstruction (tomography was performed by Dirk Scholz).

The article was written by Benedikt Westermann. I wrote parts of the material and methods section and of the figure legends.

The yeast cell cortical protein Num1 integrates mitochondrial dynamics into cellular architecture

Till Klecker, Dirk Scholz, Johannes Förtsch and Benedikt Westermann*

Zellbiologie, Universität Bayreuth, 95440 Bayreuth, Germany

*Author for correspondence (benedikt.westermann@uni-bayreuth.de)

Accepted 2 April 2013

Journal of Cell Science 126, 2924–2930

© 2013. Published by The Company of Biologists Ltd

doi: 10.1242/jcs.126045

Summary

During the cell cycle each organelle has to be faithfully partitioned to the daughter cells. However, the mechanisms controlling organellar inheritance remain poorly understood. We studied the contribution of the cell cortex protein, Num1, to mitochondrial partitioning in yeast. Live-cell microscopy revealed that Num1 is required for attachment of mitochondria to the cell cortex and retention in mother cells. Electron tomography of anchoring sites revealed plasma membrane invaginations directly contacting the mitochondrial outer membrane. Expression of chimeric plasma membrane tethers rescued mitochondrial fission defects in $\Delta num1$ and $\Delta mdm36$ mutants. These findings provide new insights into the coupling of mitochondrial dynamics, immobilization, and retention during inheritance.

Key words: Cell architecture, Mitochondrial fission, Organelle partitioning

Introduction

Each eukaryotic cell type has a characteristic architecture which is reflected by the size, shape, number and position of its organelles. Cellular architecture is established by the balanced assembly and disassembly of cellular structures, orchestrated organelle partitioning, directed motion of organelles on cytoskeletal tracks and activities of membrane-shaping proteins (Rafelski and Marshall, 2008; Shibata et al., 2009). As most membrane-bound organelles cannot be generated *de novo*, they have to be inherited upon cell division, and cellular architecture has to be re-established in daughter cells. In many cases, organelle partitioning and inheritance are active and ordered processes, similar to the partitioning of chromosomes during mitosis (Warren and Wickner, 1996; Ouellet and Barral, 2012). On the other hand, some cell organelles – such as mitochondria – are highly dynamic and constantly move, fuse and divide and thereby frequently change their size, shape and position in the cell (Bereiter-Hahn, 1990; Westermann, 2010). Little is known about the molecular mechanisms that integrate membrane dynamics into cellular architecture.

Saccharomyces cerevisiae is a powerful model organism for studying the cellular mechanisms of organelle segregation and inheritance (Catlett and Weisman, 2000; Pruyne et al., 2004; Fagarasanu and Rachubinski, 2007). Organelle inheritance depends on directed transport along actin cables towards the growing bud. At the same time, retention mechanisms must ensure that at least one copy of each organelle is kept in the mother cell. The mitochondrial content in buds is tightly controlled and correlates with the increase of bud size (Rafelski et al., 2012). Anterograde mitochondrial transport along actin cables into the growing bud is mediated by a myosin motor, Myo2 (Altmann et al., 2008; Förtsch et al., 2011). The mitochondrial outer membrane protein Mmr1 anchors mitochondria to bud-tip-localized ER and thereby impedes their transport back into the mother cell (Swayne et al., 2011). Mmr1 is

localized specifically to mitochondria in the bud (Itoh et al., 2004) and assembles into punctate structures connecting mitochondria and cortical ER (Swayne et al., 2011). As mitochondrial content is decreased in buds of $\Delta mmr1$ mutant cells, Mmr1 is thought to be critical for faithful inheritance of the organelle to daughter cells (Swayne et al., 2011). At the same time, a portion of the mitochondrial network is immobilized and retained in the mother during cell division (Yang et al., 1999). However, the molecular components constituting the ‘retention zone’ in the mother remained unknown.

Num1 is a large, cell-cortex-associated protein that interacts with dynein and microtubules and facilitates migration of the nucleus from the mother cell to the emerging bud (Farkasovsky and Küntzel, 2001). Surprisingly, Num1 was found to be also required for maintenance of mitochondrial distribution and morphology (Dimmer et al., 2002). It genetically and physically interacts with the mitochondrial division protein Dnm1, and mitochondria of cells lacking Num1 have a severe defect of mitochondrial division (Cervený et al., 2007). Here, we asked how the dynamic behavior of yeast mitochondria is linked to immobilization at the cell cortex and partitioning. Our results assign to Num1 a key role in the coordination of this process.

Results

Antagonistic roles of Num1 and Mmr1 in mitochondrial distribution

$\Delta dnm1 \Delta num1$ double mutant cells incubated at high temperature frequently produce mother cells devoid of mitochondria pointing to a potential role of Num1 in retention of mitochondria in mother cells (Cervený et al., 2007). However, mitochondrial partitioning defects in $\Delta num1$ single mutants were not reported, and the exact role of Num1 in mitochondrial division and inheritance remained unclear. To test whether Num1 is required for anchorage of mitochondria in the mother cell we observed yeast cells expressing mitochondria-targeted fluorescent proteins

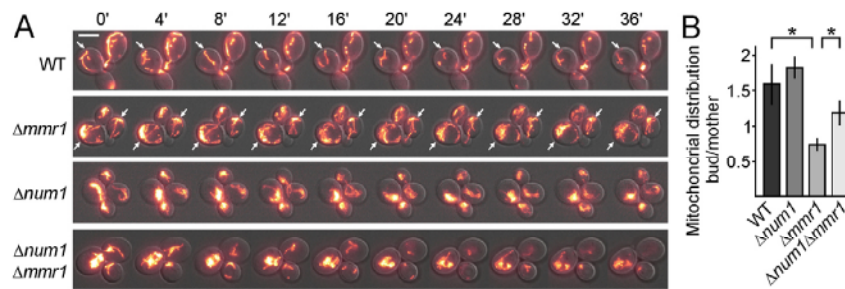


Fig. 1. Opposing effects of Num1 and Mmr1 in mitochondrial distribution. (A) Cells expressing mitochondria-targeted GFP (mtGFP) or mitochondria-targeted yeast enhanced RFP (mtERFP) were constantly supplied with fresh YPD medium in a microfluidic chamber and analyzed by time-resolved 3D fluorescence microscopy. Images are merges of DIC and maximum intensity projections of fluorescence image z stacks. Arrows indicate retention sites in mother cells. Scale bar: 5 μ m. (B) Cells were grown as in A, the fluorescence signals were related to the diameter of buds and mother cells, and the ratio of the relative mitochondrial content in buds versus mother was determined. Error bars indicate standard deviations of three independent experiments with at least 100 cells per experiment. Asterisks indicate statistically significant differences [$P=0.032$ for wild type (WT) versus $\Delta mmr1$, $P=0.027$ for $\Delta mmr1$ versus $\Delta num1\Delta mmr1$, two-tailed Student's *t*-test].

by time-resolved live-cell fluorescence microscopy. We found that some mitochondria are fixed at the cell pole opposite the bud in wild-type cells (Fig. 1A). Several of these cell cortex attachment sites persisted for the entire observation time of 1 hour (supplementary material Movie 1). Similar retention sites were observed in $\Delta mmr1$ mother cells, but not in $\Delta num1$ or $\Delta num1\Delta mmr1$ strains (Fig. 1A; supplementary material Movies 2–4). These observations suggest that Num1, but not Mmr1, is required to attach mitochondria to the mother cell cortex.

We asked whether deletion of *NUM1* results in the loss of retention sites and in consequence causes an accumulation of mitochondria in the bud. To analyze this we developed an assay to quantify mitochondrial abundance in mother cells and buds. Cells expressing mitochondria-targeted fluorescent proteins were analyzed by three-dimensional (3D) fluorescence microscopy.

The fluorescence signals in mother cells and buds were quantified in maximum intensity projections, and the cellular volumes were calculated from the cellular diameter, assuming that the cells have a spherical shape. The mitochondrial bud/mother distribution was calculated from the mitochondria/volume ratios in the bud and mother cell. We observed that the relative mitochondrial content was shifted to buds in wild-type cells (Fig. 1B). Accumulation of mitochondria in buds was slightly more pronounced in $\Delta num1$, consistent with a role of Num1 in retention in the mother cell. In contrast, $\Delta mmr1$ cells showed a deprivation of mitochondria in the bud, consistent with a role of Mmr1 in retention in the bud. Strikingly, the mitochondrial distribution defect in $\Delta mmr1$ was partially relieved by additional deletion of *NUM1* (Fig. 1B), suggesting that Num1 and Mmr1 control mitochondrial distribution in an antagonistic manner.

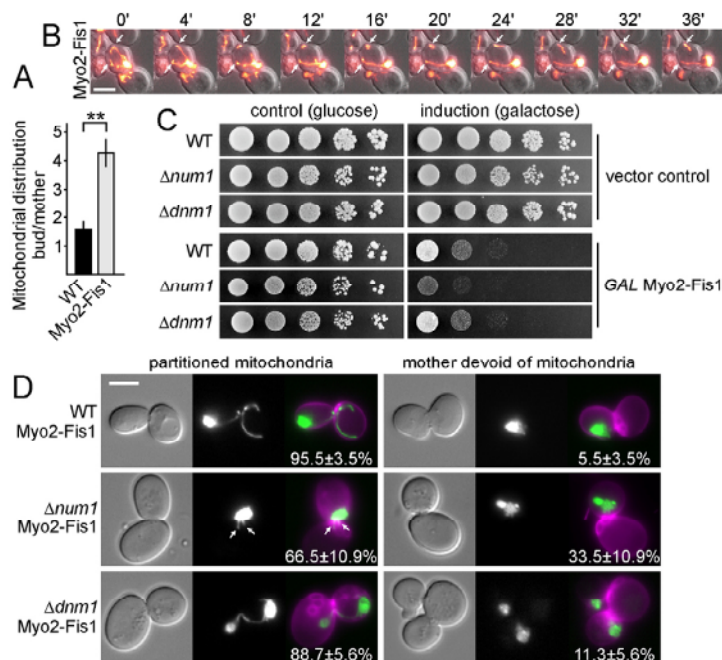


Fig. 2. Num1 is crucial for mitochondrial retention in the mother. (A) Cells expressing Myo2-Fis1 from the *MYO2* promoter and a multicopy plasmid were analyzed as in Fig. 1B. Asterisks indicate statistical significance ($P=0.0026$). (B) Cells were grown and analyzed as in Fig. 1A. Arrows indicate retention sites in mother cells. Scale bar: 5 μ m. (C) Strains were transformed with a plasmid overexpressing Myo2-Fis1 from the inducible *GAL* promoter (*GAL* Myo2-Fis1) or an empty vector. Tenfold serial dilutions were spotted on synthetic complete medium containing glucose (repression of the *GAL* promoter) or galactose (induction of the *GAL* promoter) and incubated at 30°C. (D) Cells expressing Myo2-Fis1 from the *GAL* promoter were analyzed. The cell wall was stained with calcofluor (Hammermeister et al., 2010) to visualize bud scars and thereby identify mother cells. From left to right, DIC, mtGFP fluorescence, merged image of mtGFP (green) and calcofluor fluorescence (magenta). Arrows indicate short mitochondrial tubules in a mother cell lacking Num1. Budded cells containing partitioned mitochondria or mothers devoid of mitochondria were quantified. Values are mean percentages \pm standard deviations from three independent experiments with at least 100 cells per experiment. Scale bar: 5 μ m.

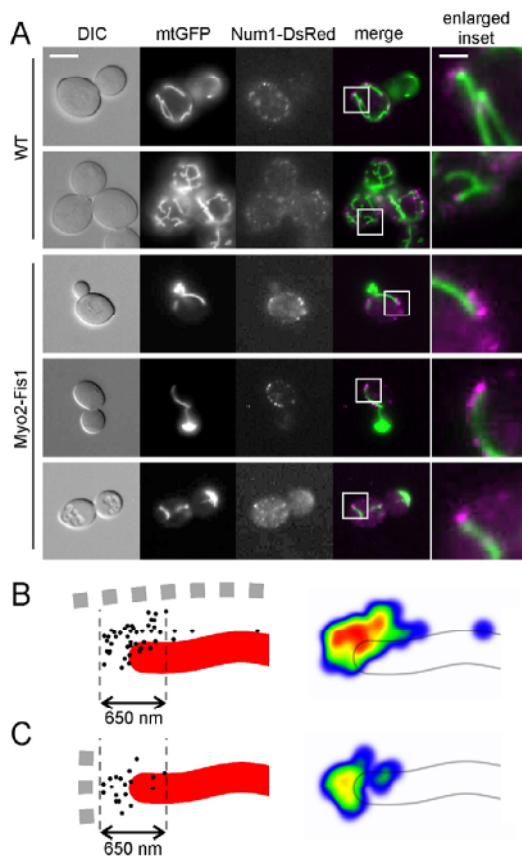


Fig. 3. Num1 colocalizes with mitochondrial tips in mother cells. (A) Cells expressing mtGFP and a chromosomal allele encoding Num1 tagged with DsRed were grown to logarithmic growth phase in YPD and analyzed by fluorescence microscopy. Myo2-Fis1 (lower three panels) was expressed from the *MYO2* promoter and a multicopy plasmid. Scale bars: 5 μ m (main images); 1,250 nm (enlarged images of the boxed regions). (B) For quantitative analysis, magnifications of 46 fluorescence micrographs showing mitochondrial ends oriented parallel to the cell cortex (row of gray squares) were aligned to a schematic mitochondrion (red). The center of the most distal Num1 patch in the field of view was assigned with a black dot (left panel); please note that the distance of the dots in the drawing is not meant to represent the optical resolution of the microscope). To generate a heat map of Num1 localization the center of each Num1 dot was assigned with a partially transparent dot. After processing the image with a Gaussian blur, the grayscale image was converted to false colors (right panel). (C) Fluorescence micrographs ($n=19$) showing mitochondrial ends oriented perpendicular to the cell cortex were analyzed as in B.

These observations suggest that Num1 is critical for retention in the mother cell and its action is antagonized by Mmr1 in the bud.

Retention of mitochondria in mother cells by Num1

Myo2-Fis1 is a chimeric mitochondria-specific motor protein with the Myo2 cargo binding domain replaced by the transmembrane anchor of the mitochondrial outer membrane protein Fis1. Overexpression of this mitochondria-specific motor results in increased anterograde transport (Förtsch et al., 2011) and an about threefold enrichment of mitochondria in the bud, compared to wild-type cells (Fig. 2A). Wild-type cells overexpressing Myo2-Fis1 typically contain a massive

accumulation of mitochondria in the bud and one or two long mitochondrial tubules extending into the mother. When such a tubule is separated from the rest of the mitochondrial network by a division event it remains fixed at the cell cortex and its free end moves randomly in the cytoplasm (Fig. 2B; supplementary material Movie 5). Apparently, cell cortex attachment sites retain mitochondria in the mother even when the balance of bidirectional transport is strongly biased to the anterograde direction.

It was not possible to overexpress Myo2-Fis1 from a constitutive promoter in Δ num1 strains, suggesting that this construct is toxic in the absence of Num1. Consistently, Myo2-Fis1 overexpression from the strong inducible *GALI* promoter produced a severe growth defect in Δ num1. This growth defect was much stronger than in wild type or mitochondrial fission-defective Δ dmf1 cells (Fig. 2C). Strikingly, one third of Δ num1 mother cells were completely devoid of mitochondria under these conditions, and most of the remaining mother cells contained only very short mitochondrial tubules close to the mother bud neck (Fig. 2D). These results suggest that retention of mitochondria by Num1 becomes essential for viability of the mother when the balance of anterograde and retrograde mitochondrial transport is shifted towards the bud.

Mitochondrial tips colocalize with Num1 in mother cells

We asked whether Num1 is attached to the tips of mitochondrial tubules extending into the mother cell. To test this, we analyzed wild-type and Myo2-Fis1-expressing cells by fluorescence microscopy in a genetic background containing a DsRed-tagged *NUM1* allele at the chromosomal locus. Num1-DsRed is functional in these strains as the tagged allele is the sole copy of this gene and produces wild-type-like mitochondria (Cervený et al., 2007). We found that cortical Num1-DsRed punctae frequently colocalized with the tips of mitochondrial tubules in mother cells (Fig. 3A). To determine whether the observed colocalization was statistically significant or simply coincidental, we quantified Num1 punctae in the vicinity of mitochondrial tips in a total number of 36 Myo2-Fis1-expressing cells. Intriguingly, most of the Num1 patches were found in a region of ± 325 nm around the mitochondrial tip; 42 of 46 Num1 punctae were found within this region when the mitochondrion was oriented parallel to the cortex (Fig. 3B), and 19 of 19 Num1 punctae were found within this region when the mitochondrion was oriented perpendicular to the cortex (Fig. 3C). We propose that Num1 punctae represent mitochondrial cortex anchors in mother cells.

Mitochondria form direct contacts with the plasma membrane in the retention zone

The tips of mitochondrial tubules extending into the mother of Myo2-Fis1-expressing cells colocalized with Num1-DsRed (Fig. 3). We reasoned that it should be possible to find these sites in electron tomograms. We observed that mitochondria in the retention zone of the mother cell were frequently located in the vicinity of electron dense material emanating from the plasma membrane (Fig. 4A–C). In some cases, it could be clearly seen that the plasma membrane formed invaginations contacting the mitochondrial outer membrane. Similar mitochondrial plasma membrane contacts could be found in wild-type cells (Fig. 4D) suggesting that Myo2-Fis1 is not involved in the formation of plasma membrane invaginations. Plasma membrane invaginations are also present in Δ num1 cells (Fig. 4E) suggesting that they are

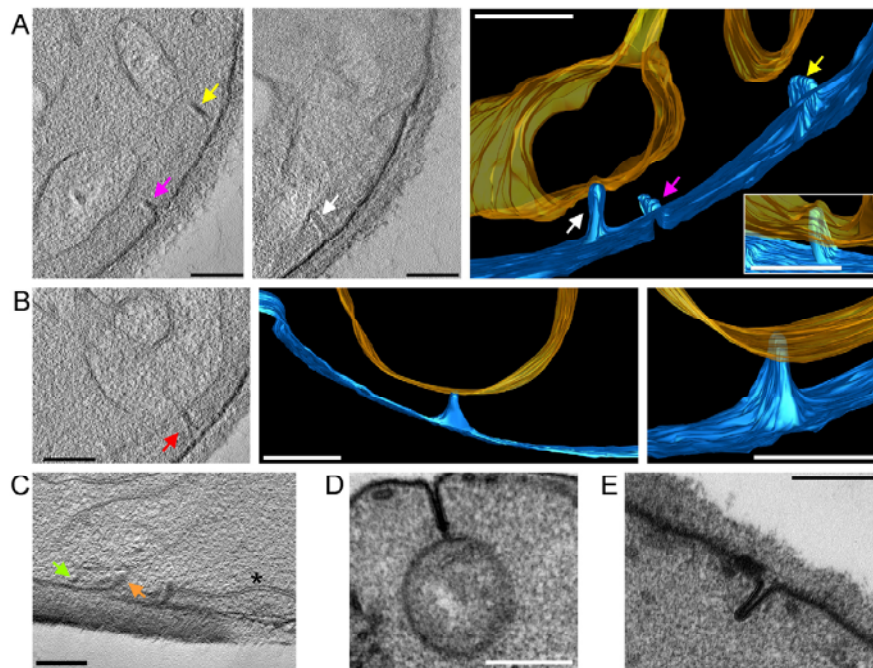


Fig. 4. Mitochondrial plasma membrane contacts. (A) A cell expressing Myo2-Fis1 from the *MYO2* promoter and a multicopy plasmid was analyzed by electron tomography. Left and middle panels show x/y planes of the same tomogram of the mother cell pole opposite the bud. Arrows indicate plasma membrane invaginations towards mitochondria. Different colors indicate different invaginations. Right panel, 3D reconstruction of the tomogram. Blue, plasma membrane; orange, mitochondrial outer membrane. Inset, the mitochondrial plasma membrane contact indicated by the white arrow, viewed from a different angle. (B,C) Tomograms of two other cells were obtained as in A. The asterisk in C marks cortical ER. (D) Electron micrograph of an ultrathin section of a wild-type cell not expressing Myo2-Fis1. (E) Electron micrograph of an ultrathin section of a $\Delta num1$ cell. Scale bars: 250 nm.

formed independently of Num1. However, we could not find mitochondria contacting these invaginations in the absence of Num1. We consider it likely that these structures represent mitochondrial cortex anchors. Thus, attachment of mitochondria in the mother appears to be established by contacts to the plasma membrane.

A chimeric plasma membrane tether rescues mitochondrial morphology defects in $\Delta num1$ and $\Delta mdm36$ mutants

Cells lacking Num1 have a severe mitochondrial division defect. Mitochondria form highly interconnected networks that are remarkably similar to aberrant mitochondria in $\Delta dnm1$ and other well characterized mitochondrial division mutants (Cerveny et al., 2007). Mutants lacking the mitochondria-associated protein Mdm36 have an indiscernible phenotype (Hammermeister et al., 2010), and Num1 and Mdm36 are thought to cooperate with Dnm1 in mitochondrial division and maintenance of mitochondrial morphology (Cerveny et al., 2007; Hammermeister et al., 2010). To test whether mitochondrial morphology defects in $\Delta num1$ and $\Delta mdm36$ mutants are caused by a defect in cell cortex attachment we generated two chimeric mitochondria–plasma membrane tethers. These consist of the N-terminal transmembrane anchor of the mitochondrial outer membrane protein Tom20, a GFP moiety, and a C-terminal pleckstrin homology (PH) domain. Tom20–GFP–PH(Num1) contains the Num1 PH domain, which is required for the cortical localization of Num1 (Tang et al., 2009). Tom20–GFP–PH(Opy1) contains the C-terminal PH domain of Opy1. Opy1 is involved in the regulation of phosphatidylinositol 4,5-bisphosphate synthesis (Ling et al., 2012), and its function is not related to Num1. Consistent with an earlier report (Yu et al., 2004) we observed that fusion proteins consisting solely of GFP and the PH domains were targeted to the plasma membrane with some background staining in the nucleus and cytosol (Fig. 5A). In

contrast, both mitochondria–plasma membrane tethers formed punctate structures that colocalized with mitochondria (Fig. 5A) and resemble Num1 foci (compare Fig. 3A). Strikingly, expression of chimeric plasma membrane tethers in $\Delta num1$ or $\Delta mdm36$ cells efficiently converted the condensed, interconnected mitochondrial nets to wild-type-like mitochondria. Importantly, the tethers were unable to rescue the mitochondrial morphology defect in $\Delta dnm1$ cells (Fig. 5A,B).

The scission of membranes by dynamin is facilitated by the generation of longitudinal tension, e.g. by molecular motors pulling the membrane along cytoskeletal tracks (Roux et al., 2006). It has been hypothesized that $\Delta num1$ cells are defective in mitochondrial division because anchorage of mitochondria by Num1 together with cytoskeleton-dependent forces is required to generate tension, which then facilitates severing of the membranes by Dnm1 (Schauss and McBride, 2007). To test this hypothesis we induced fragmentation of mitochondria with sodium azide (Fekkes et al., 2000) in the absence or presence of mitochondrial cortex tethers. Strikingly, expression of mitochondrial cortex tethers restored azide-induced mitochondrial fragmentation in about 30% of $\Delta num1$ and $\Delta mdm36$ cells, but not in $\Delta dnm1$ (Fig. 5C,D). We conclude that mitochondrial fission defects in $\Delta num1$ and $\Delta mdm36$ mutants are caused by a defect in cell cortex attachment.

Discussion

Our results assign to Num1 a key role in the attachment of mitochondria to the yeast cell cortex. In contrast to the situation in the bud, where Mmr1 anchors mitochondria to the cortical ER (Swayne et al., 2011), mitochondria establish direct contacts to the plasma membrane in the mother. Num1 appears to be critical in this process as loss of Num1 leads to growth defects and mitochondrial depletion of mother cells when anterograde mitochondrial transport is forced by overexpression of Myo2-Fis1. Thus, Num1 activity is important for mitochondrial mother/

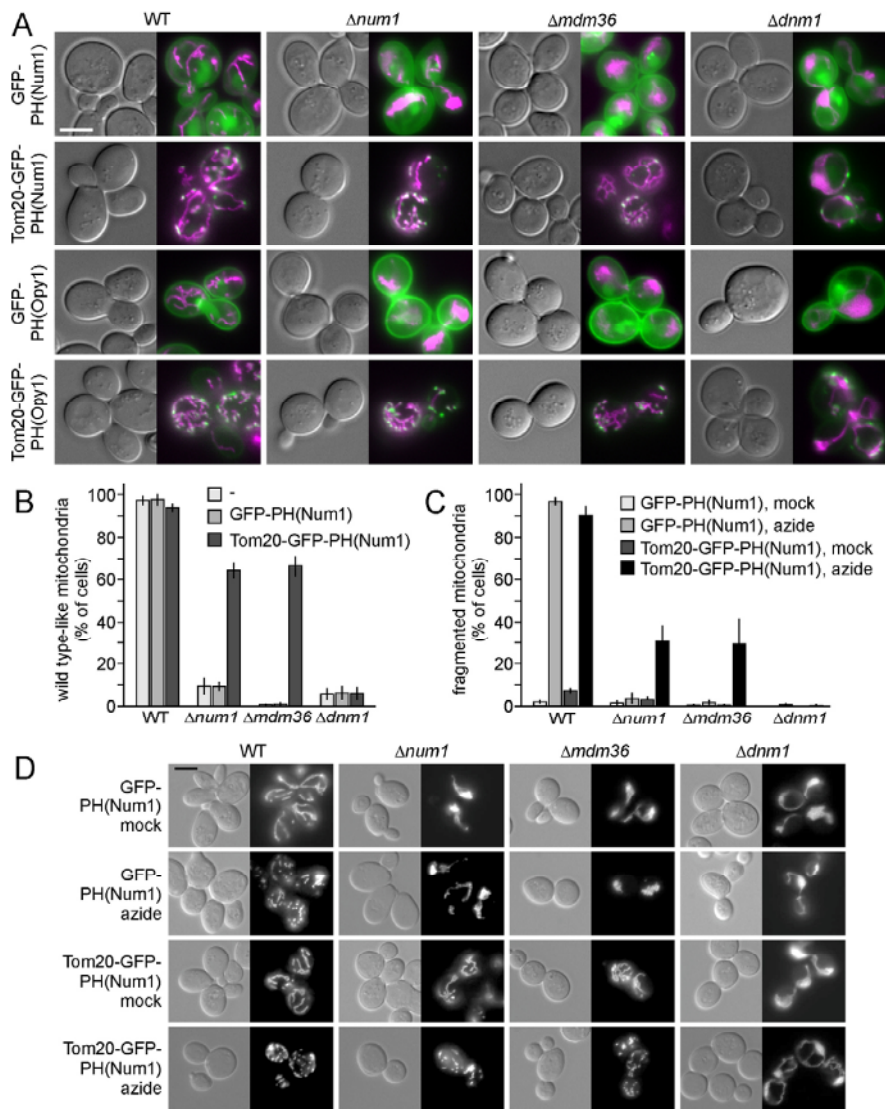


Fig. 5. Chimeric plasma membrane tethers rescue mitochondrial division defects in $\Delta num1$ and $\Delta mdm36$. (A) GFP-PH domain fusions or mitochondrial plasma membrane tethers were expressed from the *GAL* promoter in cells expressing mERFP. Each pair of images: DIC (left) and merged image of GFP fluorescence (green) and mERFP fluorescence (magenta; right). Scale bar: 5 μ m. (B) Quantification of A. For each strain, cells containing wild-type-like mitochondria were scored. Error bars indicate standard deviations of six independent experiments with at least 100 cells per experiment. (C) Cells expressing GFP-PH fusions or mitochondrial plasma membrane tethers were either mock treated or incubated for 40 minutes with 0.5 mM sodium azide, fixed in 3.7% formaldehyde, and analyzed by fluorescence microscopy. For each strain, cells containing fragmented mitochondria were scored. Error bars indicate standard deviations of four independent experiments with at least 100 cells per experiment. (D) Images of representative cells analyzed in C. Each pair of images: DIC (left) and mitochondria (right). Scale bar: 5 μ m.

bud partitioning and inheritance. A mother-cell-specific role of Num1 is in accordance with the fact that Num1 is found almost exclusively in the mother compartment of cells carrying small buds, and Num1 patches in buds are formed rather late in the cell cycle (Farkasovsky and Küntzel, 1995; Heil-Chapdelaine et al., 2000) (see also Fig. 3A). It was shown recently that mitochondrial ER contacts define the sites of fission (Friedman et al., 2011). Our results add plasma membrane contacts as an important factor of mitochondrial dynamics. We show that mitochondrial fission defects in $\Delta num1$ and $\Delta mdm36$ cells are caused by a lack of mitochondrial cell cortex attachment and can be fully rescued by expression of chimeric mitochondrial plasma membrane tethers. Hence, Num1 coordinates dynamic and static processes and thereby integrates mitochondrial dynamics into cellular architecture.

Num1 is a large, 313 kDa protein that contains an N-terminal coiled-coil domain, a possible EF-hand calcium binding site, a central repetitive part, and a C-terminal PH domain which binds

phosphoinositide PI(4,5)P₂ with high affinity (Kormanec et al., 1991; Yu et al., 2004). It was recently shown that mutants expressing truncated Num1 lacking the coiled coil region lose mitochondrial attachment to the cortex and contain abnormal mitochondria, similar to $\Delta num1$. The truncated protein was still localized to the cortex in these cells; however, it adopted an abnormal localization pattern and was present in areas not associated with mitochondria (Tang et al., 2012; Lackner et al., 2013). Mutants expressing truncated Num1 lacking the PH domain contained similarly abnormal mitochondria. In these cells the truncated protein retained its association with mitochondria, but was no longer associated with the cortex (Tang et al., 2009; Lackner et al., 2013). Intriguingly, the N-terminal domain of Num1 exhibits structural and functional similarities to Bin/Amphiphysin/Rvs (BAR) domains (Tang et al., 2012). BAR domains are known sensors of membrane curvature (Peter et al., 2004). Thus, it is tempting to speculate that the BAR-like domain of Num1 recognizes highly curved plasma membrane

invaginations to define the sites of Num1 patch assembly, as proposed by Tang et al. (Tang et al., 2012). Num1 proteins that are stably associated with the plasma membrane via their PH domains might then establish direct contacts to mitochondria at these sites by binding to yet unknown receptors on the mitochondrial surface.

It was recently suggested that the ER plays an active role in the formation of the Num1 mitochondrial tether, as ER-localized proteins co-purified with Num1, and the ER was found in the vicinity of Num1-mediated cortex attachment points observed by light microscopy (Lackner et al., 2013). We could identify cortical ER in some of our tomograms (e.g. Fig. 4C). However, we do not have evidence for direct contacts of the ER to mitochondria or the plasma membrane in the retention zone. Furthermore, Lackner et al. found that Mdm36 is involved in Num1 interaction with mitochondria, but additional factors are apparently required (Lackner et al., 2013). Thus, elucidation of the exact role of the ER and the identification of mitochondrial proteins interacting with Num1 remain challenges for the future.

Our observations suggest that the integration of mitochondrial dynamics into cellular architecture is important for mitochondrial distribution and morphology in yeast. Also in higher eukaryotic cells, such as neurons, mitochondrial distribution depends on movement, immobilization, fusion and fission (Hollenbeck and Saxton, 2005; Cai and Sheng, 2009). It will be interesting to see in the future whether similar mechanisms coordinate mitochondrial docking and division in mammalian cells and yeast.

Materials and methods

Plasmids and cloning procedures

Standard procedures were used for cloning and amplification of plasmids (Green and Sambrook, 2012). PCR was performed using *Pfu* or *phusion* polymerase (Fermentas, St. Leon-Rot, Germany) according to the manufacturer's instructions. Plasmids pYES-mtGFP (Westermann and Neupert, 2000), pYX142-mtGFP (Westermann and Neupert, 2000) and pYX142-mtERFP (Scholz et al., 2012) were used for expression of mitochondria-targeted fluorescent proteins, mtGFP and mtERFP. For the generation of an outer membrane anchored GFP, plasmid pYES-TOM20(1-36)-GFP was constructed by PCR amplification of the region of the *TOM20* gene encoding the first 36 amino acids of Tom20 by using genomic DNA as template and oligonucleotides 5'-ATTTAAAGCTTATGTCACGTCG-AACCCATATC-3' and 5'-TATATAGGATCCACCGCTATTTCTTCTTGATAGTC-3' and replacing the *HindIII* *BamHI* fragment of pYES-mtGFP. For the generation of a synthetic cortex tether, plasmid pYES-PH(Num1) was constructed by PCR amplification of the region of the *NUM1* gene encoding the C-terminal 187 amino acids of Num1 by using genomic DNA as template and oligonucleotides 5'-ATATAAAGCTTAGTGGAGAATTCAACGAACCAAGC-ATAATACCCG-3' and 5'-TTATTACTCGAGCTATCGTAAATTGCCAAATG-ATCGG-3' and cloning into the *HindIII* and *XhoI* sites of vector pYES (Invitrogen, Darmstadt, Germany). Plasmid pYES-TOM20(1-36)-GFP-PH(Num1) was created by PCR-amplification of TOM20(1-36)-GFP using pYES-TOM20(1-36)-GFP as template and oligonucleotides 5'-ATTTAAAGCTTATGTCACGTCGAAACCTATC-3' and 5'-ATATTTGAATCTTTGTATAGTTCATCCATGCC-3' and cloning into the *HindIII* and *EcoRI* sites of pYES-PH(Num1). Plasmid pYES-GFP-PH(Num1) was created by PCR amplification of GFP using pYES-mtGFP as template and oligonucleotides 5'-TTATTAAAGCTTATGAGTAAAGGAGAA-GAATTTTC-3' and 5'-ATATTTGAATCTTTGTATAGTTCATCCATGCC-3' and cloning into the *HindIII* and *EcoRI* sites of pYES-PH(Num1). Plasmids pYES-GFP-PH(Opy1) and pYES-TOM20(1-36)-GFP-PH(Opy1) were created by PCR amplification of the region of *OPY1* encoding residues 209–324 of Opy1 using genomic DNA as template and oligonucleotides 5'-AAATTTGAA-TTCGGTGGATCAGGCGATCCAAGAAATGCAGAGCACC-3' and 5'-AAATTTCTCGAGTTATATATTTTCGGCCTTAATTT-3' and cloning into the *EcoRI* and *XhoI* sites of pYES-GFP-PH(Num1) and pYES-TOM20(1-36)-GFP-PH(Num1). For generation of a plasmid allowing inducible expression of Myo2-Fis1 the whole coding sequence of Myo2-Fis1 was amplified by PCR using pRS426-Myo2-Fis1 (Förtsch et al., 2011) as template and oligonucleotides 5'-GGGGACAAGTTTGTA-CAAAAAAGCAGGCTCAAAAAAATGCTTTTGAAGTGGGTACACG-3' and 5'-GGGGACCACTTTGTACAAAGAAAGCTGGGTCTTACCTTCTTGTGTTCTTAAAGAAG-3' and cloned into pAG426-Gal-ccdB (Alberti et al., 2007) using

the Gateway cloning system (Invitrogen). The resulting plasmid was termed pAG426-Gal-Myo2-Fis1.

Yeast strain constructions

Standard procedures were used for manipulation of yeast (Sherman, 1991; Gietz et al., 1992). Yeast deletion mutants were taken from the yeast deletion collection (Giaever et al., 2002). Double deletion mutants were constructed by mating and tetrad dissection. All yeast strains were isogenic to BY4741, BY4742 and BY4743 (Brachmann et al., 1998) with the exception of strains expressing Num1-RFP (Cervený et al., 2007) that were isogenic to FY833 (Winston et al., 1995). Yeast strains used in this study are listed in supplementary material Table S1.

Microscopy

Epifluorescence microscopy was performed using an Axioplan 2 or an Axiophot microscope (Carl Zeiss Lichtmikroskopie, Göttingen, Germany) equipped with an Evolution VF Mono Cooled monochrome camera (Intas, Göttingen, Germany) with Image ProPlus 5.0 and Scope Pro4.5 software (Media Cybernetics, Silver Spring, MD) or a Leica DCF360FX Camera with Leica LAF AF Version 2.2.1 Software (Leica Microsystems, Wetzlar, Germany), respectively. Localization of Num1 punctae at mitochondrial tips (Fig. 3) was performed using a Zeiss Axiophot microscope equipped with a Zeiss Plan-Neofluar 100×/1.30 NA oil objective and a Leica DCF360FX Camera (pixel size 6.45×6.45 μm). For time-resolved live-cell microscopy, cells were trapped in a microfluidic chamber and constantly supplied with fresh medium using a CellASIC Onix Microfluidic Perfusion System (CellASIC Corp., Hayward, CA, USA) and ONIX Microfluidic Plates (Y04C Yeast Perfusion Plate, 3.5–5 μm). Cells were observed with a Leica DMI 6000 wide-field fluorescence microscope equipped with a Leica DFC360FX camera and Leica LAS AF Software Version 2.1.0. Image manipulations other than minor adjustments of brightness and contrast were not performed. Electron microscopy and tomography was performed as described (Hoppins et al., 2011). 3D tomograms were hand-segmented using the IMOD software package (Kremer et al., 1996).

Acknowledgements

We thank Stefan Geimer for help with electron microscopy.

Author contributions

T.K., J.F. and B.W. conceived and designed the experiments; T.K., D.S. and J.F. performed the experiments; T.K., D.S., J.F. and B.W. analyzed the data; T.K. and B.W. wrote the paper.

Funding

This work was supported by the Deutsche Forschungsgemeinschaft [grant number We 2174/5-1 to B.W.].

Supplementary material available online at

<http://jcs.biologists.org/lookup/suppl/doi:10.1242/jcs.126045/-DC1>

References

- Alberti, S., Gittler, A. D. and Lindquist, S. (2007). A suite of Gateway cloning vectors for high-throughput genetic analysis in *Saccharomyces cerevisiae*. *Yeast* **24**, 913–919.
- Altmann, K., Frank, M., Neumann, D., Jakobs, S. and Westermann, B. (2008). The class V myosin motor protein, Myo2, plays a major role in mitochondrial motility in *Saccharomyces cerevisiae*. *J. Cell Biol.* **181**, 119–130.
- Bereiter-Hahn, J. (1990). Behavior of mitochondria in the living cell. *Int. Rev. Cytol.* **122**, 1–63.
- Brachmann, C. B., Davies, A., Cost, G. J., Caputo, E., Li, J., Hieter, P. and Boeke, J. D. (1998). Designer deletion strains derived from *Saccharomyces cerevisiae* S288C: a useful set of strains and plasmids for PCR-mediated gene disruption and other applications. *Yeast* **14**, 115–132.
- Cai, Q. and Sheng, Z. H. (2009). Mitochondrial transport and docking in axons. *Exp. Neurol.* **218**, 257–267.
- Catlett, N. L. and Weisman, L. S. (2000). Divide and multiply: organelle partitioning in yeast. *Curr. Opin. Cell Biol.* **12**, 509–516.
- Cervený, K. L., Studer, S. L., Jensen, R. E. and Sesaki, H. (2007). Yeast mitochondrial division and distribution require the cortical num1 protein. *Dev. Cell* **12**, 363–375.
- Dimmer, K. S., Fritz, S., Fuchs, F., Messerschmitt, M., Weinbach, N., Neupert, W. and Westermann, B. (2002). Genetic basis of mitochondrial function and morphology in *Saccharomyces cerevisiae*. *Mol. Biol. Cell* **13**, 847–853.
- Fagarasanu, A. and Rachubinski, R. A. (2007). Orchestrating organelle inheritance in *Saccharomyces cerevisiae*. *Curr. Opin. Microbiol.* **10**, 528–538.
- Farkasovsky, M. and Küntzel, H. (1995). Yeast Num1p associates with the mother cell cortex during S/G2 phase and affects microtubular functions. *J. Cell Biol.* **131**, 1003–1014.

- Farkasovsky, M. and Küntzel, H. (2001). Cortical Num1p interacts with the dynein intermediate chain Pac11p and cytoplasmic microtubules in budding yeast. *J. Cell Biol.* **152**, 251-262.
- Fekkes, P., Shepard, K. A. and Yaffe, M. P. (2000). Gag3p, an outer membrane protein required for fission of mitochondrial tubules. *J. Cell Biol.* **151**, 333-340.
- Förtsch, J., Hummel, E., Krist, M. and Westermann, B. (2011). The myosin-related motor protein Myo2 is an essential mediator of bud-directed mitochondrial movement in yeast. *J. Cell Biol.* **194**, 473-488.
- Friedman, J. R., Lackner, L. L., West, M., DiBenedetto, J. R., Nunnari, J. and Voeltz, G. K. (2011). ER tubules mark sites of mitochondrial division. *Science* **334**, 358-362.
- Giaever, G., Chu, A. M., Ni, L., Connelly, C., Riles, L., Véronneau, S., Dow, S., Lucau-Danila, A., Anderson, K., André, B. et al. (2002). Functional profiling of the *Saccharomyces cerevisiae* genome. *Nature* **418**, 387-391.
- Gietz, D., St Jean, A., Woods, R. A. and Schiestl, R. H. (1992). Improved method for high efficiency transformation of intact yeast cells. *Nucleic Acids Res.* **20**, 1425.
- Green, M. R. and Sambrook, J. (2012). *Molecular Cloning*. Cold Spring Harbor, NY: Cold Spring Harbor Laboratory Press.
- Hammermeister, M., Schödel, K. and Westermann, B. (2010). Mdm36 is a mitochondrial fission-promoting protein in *Saccharomyces cerevisiae*. *Mol. Biol. Cell* **21**, 2443-2452.
- Heil-Chapdelaine, R. A., Oberle, J. R. and Cooper, J. A. (2000). The cortical protein Num1p is essential for dynein-dependent interactions of microtubules with the cortex. *J. Cell Biol.* **151**, 1337-1344.
- Hollenbeck, P. J. and Saxton, W. M. (2005). The axonal transport of mitochondria. *J. Cell Sci.* **118**, 5411-5419.
- Hoppins, S., Collins, S. R., Cassidy-Stone, A., Hummel, E., Devay, R. M., Lackner, L. L., Westermann, B., Schuldiner, M., Weissman, J. S. and Nunnari, J. (2011). A mitochondrial-focused genetic interaction map reveals a scaffold-like complex required for inner membrane organization in mitochondria. *J. Cell Biol.* **195**, 323-340.
- Itoh, T., Toh-E, A. and Matsui, Y. (2004). Mmr1p is a mitochondrial factor for Myo2p-dependent inheritance of mitochondria in the budding yeast. *EMBO J.* **23**, 2520-2530.
- Kormanec, J., Schaaff-Gerstenschläger, I., Zimmermann, F. K., Perecko, D. and Küntzel, H. (1991). Nuclear migration in *Saccharomyces cerevisiae* is controlled by the highly repetitive 313 kDa NUM1 protein. *Mol. Gen. Genet.* **230**, 277-287.
- Kremer, J. R., Mastronarde, D. N. and McIntosh, J. R. (1996). Computer visualization of three-dimensional image data using IMOD. *J. Struct. Biol.* **116**, 71-76.
- Lackner, L. L., Ping, H., Graef, M., Murley, A. and Nunnari, J. (2013). Endoplasmic reticulum-associated mitochondria-cortex tether functions in the distribution and inheritance of mitochondria. *Proc. Natl. Acad. Sci. USA* **110**, E458-E467.
- Ling, Y., Stefan, C. J., Macgurn, J. A., Audhya, A. and Emr, S. D. (2012). The dual PH domain protein Opy1 functions as a sensor and modulator of PtdIns(4,5)P₂ synthesis. *EMBO J.* **31**, 2882-2894.
- Ouellet, J. and Barral, Y. (2012). Organelle segregation during mitosis: lessons from asymmetrically dividing cells. *J. Cell Biol.* **196**, 305-313.
- Peter, B. J., Kent, H. M., Mills, I. G., Vallis, Y., Butler, P. J., Evans, P. R. and McMahon, H. T. (2004). BAR domains as sensors of membrane curvature: the amphiphysin BAR structure. *Science* **303**, 495-499.
- Pruyne, D., Legesse-Miller, A., Gao, L., Dong, Y. and Bretscher, A. (2004). Mechanisms of polarized growth and organelle segregation in yeast. *Annu. Rev. Cell Dev. Biol.* **20**, 559-591.
- Rafelski, S. M. and Marshall, W. F. (2008). Building the cell: design principles of cellular architecture. *Nat. Rev. Mol. Cell Biol.* **9**, 593-602.
- Rafelski, S. M., Viana, M. P., Zhang, Y., Chan, Y. H., Thorn, K. S., Yam, P., Fung, J. C., Li, H., Costa, L. F. and Marshall, W. F. (2012). Mitochondrial network size scaling in budding yeast. *Science* **338**, 822-824.
- Roux, A., Uyhazi, K., Frost, A. and De Camilli, P. (2006). GTP-dependent twisting of dynamin implicates constriction and tension in membrane fission. *Nature* **441**, 528-531.
- Schauss, A. C. and McBride, H. M. (2007). Mitochondrial fission: a non-nuclear role for Num1p. *Curr. Biol.* **17**, R467-R470.
- Scholz, D., Förtsch, J., Böckler, S., Kleckner, T. and Westermann, B. (2012). Analyzing membrane dynamics with live cell fluorescence microscopy - focus on yeast mitochondria. *Membrane Biogenesis: Methods and Protocols* (ed. D. Rapaport and J. M. Herrmann). *Methods Mol. Biol.* (in press).
- Sherman, F. (1991). Getting started with yeast. *Methods Enzymol.* **194**, 3-21.
- Shibata, Y., Hu, J., Kozlov, M. M. and Rapoport, T. A. (2009). Mechanisms shaping the membranes of cellular organelles. *Annu. Rev. Cell Dev. Biol.* **25**, 329-354.
- Swayne, T. C., Zhou, C., Boldogh, I. R., Charalel, J. K., McFaline-Figueroa, J. R., Thoms, S., Yang, C., Leung, G., McInnes, J., Erdmann, R. et al. (2011). Role for cER and Mmr1p in anchorage of mitochondria at sites of polarized surface growth in budding yeast. *Curr. Biol.* **21**, 1994-1999.
- Tang, X., Punch, J. J. and Lee, W. L. (2009). A CAAX motif can compensate for the PH domain of Num1 for cortical dynein attachment. *Cell Cycle* **8**, 3182-3190.
- Tang, X., Germain, B. S. and Lee, W. L. (2012). A novel patch assembly domain in Num1 mediates dynein anchoring at the cortex during spindle positioning. *J. Cell Biol.* **196**, 743-756.
- Warren, G. and Wickner, W. (1996). Organelle inheritance. *Cell* **84**, 395-400.
- Westermann, B. (2010). Mitochondrial fusion and fission in cell life and death. *Nat. Rev. Mol. Cell Biol.* **11**, 872-884.
- Westermann, B. and Neupert, W. (2000). Mitochondria-targeted green fluorescent proteins: convenient tools for the study of organelle biogenesis in *Saccharomyces cerevisiae*. *Yeast* **16**, 1421-1427.
- Winston, F., Dollard, C. and Ricupero-Hovasse, S. L. (1995). Construction of a set of convenient *Saccharomyces cerevisiae* strains that are isogenic to S288C. *Yeast* **11**, 53-55.
- Yang, H. C., Palazzo, A., Swayne, T. C. and Pon, L. A. (1999). A retention mechanism for distribution of mitochondria during cell division in budding yeast. *Curr. Biol.* **9**, 1111-1114.
- Yu, J. W., Mendrola, J. M., Audhya, A., Singh, S., Keleti, D., DeWald, D. B., Murray, D., Emr, S. D. and Lemmon, M. A. (2004). Genome-wide analysis of membrane targeting by *S. cerevisiae* pleckstrin homology domains. *Mol. Cell* **13**, 677-688.

Supplementary material

Please refer to the attached CD-ROM for Movies 1-5.



Movie 1. Mitochondrial movement in wild type cells. Wild type cells expressing mitochondria-targeted yeast enhanced RFP (mtERFP) were constantly supplied with fresh YPD medium in a microfluidic chamber and analyzed by time-resolved 3D fluorescence microscopy. Over a total time period of 1 h z stacks were obtained every 2 min. Images are merges of DIC and maximum intensity projections of fluorescence image z stacks.



Movie 2. Mitochondrial movement in *mmr1* cells. *mmr1* deletion mutants expressing mitochondria-targeted GFP (mtGFP) were analyzed as in movie 1.



Movie 3. Mitochondrial movement in *num1* cells. *num1* deletion mutants expressing mitochondria-targeted yeast enhanced RFP (mtERFP) were analyzed as in movie 1.



Movie 4. Mitochondrial movement in *mmr1 num1* cells. *mmr1 num1* double deletion mutants expressing mitochondria-targeted GFP (mtGFP) were analyzed as in movie 1.



Movie 5 Mitochondrial movement in cells overexpressing Myo2-Fis1. Cells expressing Myo2-Fis1 from the *MYO2* promoter and a multicopy plasmid and mitochondria-targeted GFP (mtGFP) were analyzed as in movie 1.

Table S1. Yeast strains used in this study

Strain	Genotype	Reference
RJ2193	MAT α NUM1-DsRed.T1-kanMX6 ura3-52 lys2 Δ 202 trp1 Δ 63 his3 Δ 200 leu2 Δ 1	Cervený et al., 2007
YJF005	MAT α his3 Δ 1 leu2 Δ 0 met15 Δ 0 ura3 Δ 0 mmr1 Δ ::kanMX4	Giaever et al., 2002
YJF043	MAT α his3 Δ 1 leu2 Δ 0 lys2 Δ 0 ura3 Δ 0 mmr1 Δ ::kanMX4	Giaever et al., 2002
YJF054	MAT α his3 Δ 1 leu2 Δ 0 lys2 Δ 0 ura3 Δ 0 myo2 Δ ::kanMX4 pRS413MYO2 pRS426-Myo2-Fis1 pYX142-mtGFP	Förtisch et al., 2011
YJF389	MAT α his3 Δ 1 leu2 Δ 0 lys2 Δ 0 ura3 Δ 0 mmr1 Δ ::kanMX4 pYX142-mtGFP	this study
YJF392	MAT α his3 Δ 1 leu2 Δ 0 lys2 Δ 0 ura3 Δ 0 num1 Δ ::kanMX4 pYX142-mtERFP	this study
YJF405	MAT α his3 Δ 1 leu2 Δ 0 lys2 Δ 0 ura3 Δ 0 met15 Δ 0 num1 Δ ::kanMX4 mmr1 Δ ::kanMX4 pYX142-mtGFP	this study
YMI009	MAT α his3 Δ 1 leu2 Δ 0 lys2 Δ 0 ura3 Δ 0 pYX142-mtERFP	this study
YMI015	MAT α ura3-52 lys2 Δ 202 trp1 Δ 63 his3 Δ 200 leu2 Δ 1 NUM1-DsRed.T1-kanMX6 pYX142-mtGFP pRS426-Myo2-Fis1	this study
YMI101	MAT α his3 Δ 1 leu2 Δ 0 lys2 Δ 0 ura3 Δ 0	Brachmann et al., 1998
YMI102	MAT α his3 Δ 1 leu2 Δ 0 lys2 Δ 0 ura3 Δ 0 num1 Δ ::kanMX4	Giaever et al., 2002
YMI103	MAT α his3 Δ 1 leu2 Δ 0 lys2 Δ 0 ura3 Δ 0 dnm1 Δ ::kanMX4	Giaever et al., 2002
YMI104	MAT α his3 Δ 1 leu2 Δ 0 lys2 Δ 0 ura3 Δ 0 mdm36 Δ ::kanMX4	Giaever et al., 2002
YMI105	MAT α his3 Δ 1 leu2 Δ 0 lys2 Δ 0 ura3 Δ 0 pYX142-mtERFP pYES-mtGFP	this study
YMI106	MAT α his3 Δ 1 leu2 Δ 0 lys2 Δ 0 ura3 Δ 0 num1 Δ ::kanMX4 pYX142-mtERFP pYES-mtGFP	this study
YMI107	MAT α his3 Δ 1 leu2 Δ 0 lys2 Δ 0 ura3 Δ 0 dnm1 Δ ::kanMX4 pYX142-mtERFP pYES-mtGFP	this study
YMI108	MAT α his3 Δ 1 leu2 Δ 0 lys2 Δ 0 ura3 Δ 0 pYX142-mtERFP pYES-GFP-PH(Num1)	this study
YMI109	MAT α his3 Δ 1 leu2 Δ 0 lys2 Δ 0 ura3 Δ 0 num1 Δ ::kanMX4 pYX142-mtERFP pYES-GFP-PH(Num1)	this study
YMI110	MAT α his3 Δ 1 leu2 Δ 0 lys2 Δ 0 ura3 Δ 0 dnm1 Δ ::kanMX4 pYX142-mtERFP pYES-GFP-PH(Num1)	this study
YMI111	MAT α his3 Δ 1 leu2 Δ 0 lys2 Δ 0 ura3 Δ 0 mdm36 Δ ::kanMX4 pYX142-mtERFP pYES-GFP-PH(Num1)	this study
YMI112	MAT α his3 Δ 1 leu2 Δ 0 lys2 Δ 0 ura3 Δ 0 pYX142-mtERFP pYES-TOM20(1-36)-GFP-PH(Num1)	this study
YMI113	MAT α his3 Δ 1 leu2 Δ 0 lys2 Δ 0 ura3 Δ 0 num1 Δ ::kanMX4 pYX142-mtERFP pYES-TOM20(1-36)-GFP-PH(Num1)	this study
YMI114	MAT α his3 Δ 1 leu2 Δ 0 lys2 Δ 0 ura3 Δ 0 dnm1 Δ ::kanMX4 pYX142-mtERFP pYES-TOM20(1-36)-GFP-PH(Num1)	this study
YMI115	MAT α his3 Δ 1 leu2 Δ 0 lys2 Δ 0 ura3 Δ 0 mdm36 Δ ::kanMX4 pYX142-mtERFP pYES-TOM20(1-36)-GFP-PH(Num1)	this study
YMI116	MAT α his3 Δ 1 leu2 Δ 0 lys2 Δ 0 ura3 Δ 0 pYX142-mtERFP pYES-GFP-PH(Opy1)	this study
YMI117	MAT α his3 Δ 1 leu2 Δ 0 lys2 Δ 0 ura3 Δ 0 num1 Δ ::kanMX4 pYX142-mtERFP pYES-GFP-PH(Opy1)	this study
YMI118	MAT α his3 Δ 1 leu2 Δ 0 lys2 Δ 0 ura3 Δ 0 dnm1 Δ ::kanMX4 pYX142-mtERFP pYES-GFP-PH(Opy1)	this study
YMI119	MAT α his3 Δ 1 leu2 Δ 0 lys2 Δ 0 ura3 Δ 0 pYX142-mtERFP pYES-TOM20(1-36)-GFP-PH(Opy1)	this study
YMI120	MAT α his3 Δ 1 leu2 Δ 0 lys2 Δ 0 ura3 Δ 0 num1 Δ ::kanMX4 pYX142-mtERFP pYES-TOM20(1-36)-GFP-PH(Opy1)	this study
YMI121	MAT α his3 Δ 1 leu2 Δ 0 lys2 Δ 0 ura3 Δ 0 dnm1 Δ ::kanMX4 pYX142-mtERFP pYES-TOM20(1-36)-GFP-PH(Opy1)	this study
YMI122	MAT α his3 Δ 1 leu2 Δ 0 lys2 Δ 0 ura3 Δ 0 pYX142-mtGFP pRS426	this study
YMI123	MAT α his3 Δ 1 leu2 Δ 0 lys2 Δ 0 ura3 Δ 0 num1 Δ ::kanMX4 pYX142-mtGFP pRS426	this study
YMI124	MAT α his3 Δ 1 leu2 Δ 0 lys2 Δ 0 ura3 Δ 0 dnm1 Δ ::kanMX4 pYX142-mtGFP pRS426	this study
YMI125	MAT α his3 Δ 1 leu2 Δ 0 lys2 Δ 0 ura3 Δ 0 pYX142-mtGFP pAG426-Gal-Myo2-Fis1	this study
YMI126	MAT α his3 Δ 1 leu2 Δ 0 lys2 Δ 0 ura3 Δ 0 num1 Δ ::kanMX4 pYX142-mtGFP	this study

	pAG426-Gal-Myo2-Fis1	
YMI127	MAT α his3 Δ 1 leu2 Δ 0 lys2 Δ 0 ura3 Δ 0 dnm1 Δ ::kanMX4 pYX142-mtGFP	this study
	pAG426-Gal-Myo2-Fis1	
YMI128	MAT α ura3-52 lys2 Δ 202 trp1 Δ 63 his3 Δ 200 leu2 Δ 1 NUM1-DsRed.T1-kanMX6 pYX142-mtGFP pRS426	this study
YMI146	MAT α his3 Δ 1 leu2 Δ 0 lys2 Δ 0 ura3 Δ 0 mdm36 Δ ::kanMX4 pYX142-mtERFP pYES-GFP-PH(Opy1)	this study
YMI147	MAT α his3 Δ 1 leu2 Δ 0 lys2 Δ 0 ura3 Δ 0 mdm36 Δ ::kanMX4 pYX142-mtERFP pYES-TOM20(1-36)-GFP-PH(Opy1)	this study
YMI148	MAT α his3 Δ 1 leu2 Δ 0 lys2 Δ 0 ura3 Δ 0 mdm36 Δ ::kanMX4 pYX142-mtERFP pYES-mtGFP	this study
YMI149	MAT α his3 Δ 1 leu2 Δ 0 lys2 Δ 0 ura3 Δ 0 pRS426-Myo2-Fis1	this study

Mdm33 links phospholipid homeostasis to mitochondrial division

Till Klecker^{1,*}, Megan Wemmer^{2,*}, Andrew Murley², Matthias Haag³, Alfons Weig⁴, Thomas Langer³, Jodi Nunnari^{2,†}, and Benedikt Westermann^{1,†}

(2014) in preparation

¹ Zellbiologie, Universität Bayreuth, 95440 Bayreuth, Germany

² Department of Molecular and Cellular Biology, University of California, Davis, Davis, CA 95616, USA

³ Institut für Genetik, Universität zu Köln, 50674 Köln, Germany

⁴ DNA Analytik, Universität Bayreuth, 95440 Bayreuth, Germany

[†] To whom correspondence should be addressed.

Email: benedikt.westermann@uni-bayreuth.de or Email: jmnunnari@ucdavis.edu

* These authors contributed equally to this work.

Author contributions

I generated all strains and plasmids that are mentioned in the materials and methods section, unless stated otherwise. I performed the data acquisition or analysis for:

Figures 2A; 2C-E; 3; 4B-E; 5; S1; S2: Data acquisition and analysis.

Figure 2B: The cells were transformed, grown, and harvested by me. Alfons Weig performed all subsequent steps. I analyzed the data.

Figure 4A: I isolated the mitochondria that were subsequently analyzed by Mathias Haag.

The article was written by me and Benedikt Westermann.

Abstract

Mitochondrial dynamics and membrane lipid homeostasis both affect mitochondrial morphology and function, but the molecular basis and functional interconnections of these processes are not completely understood. Here we show that in yeast the mitochondrial inner membrane protein Mdm33 links phospholipid homeostasis to mitochondrial fission. Genetic and proteomic data reveal multiple interactions of Mdm33 with components of phospholipid metabolism and mitochondrial membrane homeostasis. Lipid profiling by mass spectrometry of mitochondria isolated from Mdm33-overexpressing cells reveals a role in modulating the levels of phosphatidylethanolamine and cardiolipin. Furthermore, we show that mutants lacking Mdm33 show strongly decreased mitochondrial fission activity. Strikingly, GFP-Mdm33 is localized to discrete foci that spatially and temporally coincide with punctate structures formed by the major mitochondrial fission factor, Dnm1. Our results support a model suggesting that Mdm33 locally modulates the phospholipid composition and physical properties of the inner membrane to support mitochondrial division by Dnm1.

Introduction

Mitochondria play key roles in cellular energy metabolism, various biochemical pathways, developmental processes, apoptosis, and aging (Nunnari and Suomalainen, 2012). This multitude of functions is reflected by the shape of the mitochondrial compartment. Mitochondria are highly dynamic organelles that constantly adapt their morphology to the requirements of cellular physiology by frequent fusion and fission (Westermann, 2010; Friedman and Nunnari, 2014) and remodeling of their ultrastructure (Zick et al., 2009). As many of the molecular components and cellular pathways have been conserved during evolution, mitochondrial structure and dynamics can be studied in baker's yeast *Saccharomyces cerevisiae* as a model organism (Okamoto and Shaw, 2005; Merz et al., 2007). Fusion and fission of the mitochondrial outer membrane are mediated by dynamin-related GTPases. Fzo1 in yeast and mitofusins Mfn1 and Mfn2 in mammals are large, membrane-bound proteins that constitute the key components of the outer membrane fusion machinery. Dnm1 in yeast and Drp1 in mammals are soluble dynamin-related proteins that are recruited to the mitochondrial surface by membrane-bound receptors and adaptor proteins to assemble oligomeric rings that sever the mitochondrial outer membranes. Mgm1 in yeast and Opa1 in mammals are dynamin-related GTPases that are associated with the inner membrane and are thought to constitute the mediators of inner membrane fusion (Hoppins et al., 2007; Westermann, 2010; Chan, 2012). It is currently unknown whether a separate machinery for division of the inner membrane exists, or whether both mitochondrial membranes are severed simultaneously by dynamin rings on the outer membrane (Chan, 2012; Elgass et al., 2013).

Mitochondria display a complex organization also at the ultrastructural level. The mitochondrial inner membrane consists of two subcompartments: Cristae are membrane invaginations that accommodate the respiratory chain complexes, and the inner boundary membrane constitutes an inner envelope closely apposed to the outer membrane. Both are connected by narrow, tubular cristae junctions (Mannella, 2006; Zick et al., 2009; van der Laan et al., 2012). The molecular mechanisms and components that shape the mitochondrial inner membrane are only poorly understood. At least three different protein complexes are thought to contribute to this process. First, loss of Mgm1/Opa1 leads to perturbation of inner membrane structure, both in yeast and

mammals (Olichon et al., 2003; Amutha et al., 2004; Griparic et al., 2004). Intriguingly, the function of Mgm1/Opa1 in mitochondrial fusion can be uncoupled from its role in maintenance of mitochondrial ultrastructure, suggesting that it plays a specific role in this process (Frezza et al., 2006; Meeusen et al., 2006). Second, dimerization and higher order assembly of ATP synthase, which is an abundant complex in the inner membrane, is an important determinant of cristae structure (Paumard et al., 2002; Strauss et al., 2008). And third, Mic60 (formerly named Fcj1 or mitofilin) was proposed to play an important role in the formation of cristae junctions in yeast and metazoans (John et al., 2005; Rabl et al., 2009). Recently it was shown that Mic60 is part of a larger complex, termed MICOS (Pfanner et al., 2014), that serves as an organizer of inner membrane structure (Harner et al., 2011; Hoppins et al., 2011; von der Malsburg et al., 2011; Alkhaja et al., 2012).

Mounting evidence suggests that not only membrane shaping protein complexes but also the lipid composition of the inner membrane is a major factor determining mitochondrial ultrastructure. Mitochondria of yeast cells lacking enzymes involved in cardiolipin (CL) biogenesis contain extremely elongated cristae sheets that sometimes form inner membrane septae or onion-like structures (Claypool et al., 2008; Mileykovskaya and Dowhan, 2009; Connerth et al., 2012). Similarly, mitochondrial cristae defects were observed in *Arabidopsis* leaf cells, human lymphoblasts, and mouse cardiomyocytes defective in cardiolipin biogenesis (Acehan et al., 2009; Gonzalez et al., 2013; Pineau et al., 2013). Furthermore, ultrastructural defects of mitochondria were revealed by electron microscopy of yeast and mammalian cells with reduced phosphatidylserine (PS) or phosphatidylethanolamine (PE) levels (Chan and McQuibban, 2012; Tasseva et al., 2013).

Deletion or overexpression of the yeast *MDM33* gene induces severe defects both in mitochondrial dynamics and mitochondrial ultrastructure. The *MDM33* gene was isolated in a screen for yeast mutants with aberrant mitochondrial distribution and morphology (Dimmer et al., 2002). The Mdm33 protein is located in the mitochondrial inner membrane with the major part of the protein facing the matrix. Mutants lacking Mdm33 contain large, extended mitochondria frequently forming hollow spheres that enclose portions of the cytoplasm. Aberrant $\Delta m d m 3 3$ mitochondria contain swollen parts filled with cristae and extended parts that are devoid of cristae (Messerschmitt et al., 2003). For unknown reasons overexpression of *MDM33* leads to a growth arrest (Espinet et al., 1995; Messerschmitt et al., 2003). Mitochondria of *MDM33*-overexpressing cells are highly fragmented and contain septated or vesiculated inner membranes (Messerschmitt et al., 2003). However, it remained unclear whether the primary function of Mdm33 is the structural organization of the inner membrane, or inner membrane division, and whether these functions are interconnected. To reveal the role of Mdm33 in mitochondrial biogenesis we systematically analyzed and functionally characterized its genetic and proteomic interactions. Our results suggest that Mdm33 modulates the phospholipid composition of the inner membrane to facilitate Dnm1-dependent division.

Results

***MDM33* interacts with genes involved in phospholipid metabolism and mitochondrial membrane homeostasis**

The MITO-MAP (Hoppins et al., 2011) is based on 616,270 distinct pairwise genetic interactions of 1,482 genes and provides a comprehensive view of the connections between cellular pathways related to mitochondrial functions. We took advantage of this resource to look for genes that

positively or negatively interact with *MDM33* in double deletions (Fig. 1A). Positive genetic interactions frequently occur between genes acting in a common pathway, whereas negative interactions point to compensatory pathways (Dixon et al., 2009). Strikingly, *MDM33* shows strong positive interactions with the genes encoding enzymes required for synthesis of the major phospholipids, PS, PE, and phosphatidylcholine (PC), and negative interactions with genes required for CL biosynthesis (Fig. 1B). Furthermore, *MDM33* positively interacts with the prohibitin genes, *PHB1* and *PHB2*, encoding an inner membrane complex modulating mitochondrial phospholipid homeostasis (Osman et al., 2009b) and with genes encoding subunits of the ER mitochondria encounter structure (ERMES) that is required for exchange of lipids between mitochondria and the ER (Kornmann et al., 2009). Two clusters of negative genetic interactors comprise components of mitochondrial distribution and ATP synthase subunits (Fig. 1A). These data point to a role of Mdm33 in phospholipid metabolism and mitochondrial membrane homeostasis, processes that also might be critical for mitochondrial distribution and function.

Suppression of *MDM33* overexpression-dependent growth arrest

Overexpression of *MDM33* is associated with a growth arrest (Espinet et al., 1995; Messerschmitt et al., 2003). This allowed us to screen for genes rescuing *MDM33* overexpression. We reasoned that Mdm33 presumably requires interaction partners to exert its function, and that these interaction partners will also be required to induce the growth arrest. Thus, deletion of a gene encoding an interaction partner required for Mdm33 function should relieve the overexpression-induced growth defect. A similar strategy was recently successfully employed to isolate factors involved in recycling of the Cdc42 GTPase, a key regulator of cell polarity (Das et al., 2012). In contrast to the study by Das et al., who screened for suppressors in an array of deletion mutants on agar plates, we decided to identify putative suppressors by quantifying the abundance of deletion mutants in cell pools by a microarray-based approach (Fig. S1A, B).

To induce *MDM33* overexpression-dependent growth arrest we transformed a multicopy plasmid expressing *MDM33* from the strong, inducible *GAL1/10* promoter into a pool containing the 4,987 strains of the *MAT α* haploid non-essential yeast deletion library (Giaever et al., 2002). We expected that only deletion mutants that are unable to express *MDM33* properly or lack interaction partners of Mdm33 should be able to grow under inducing conditions. In a proof-of-principle experiment we plated a similar number of transformants of the isogenic wild type and the deletion mutant pool on repressing and inducing media. As expected, transformants of the wild type and pooled deletion mutants could grow well on glucose-containing medium (SD) when *MDM33* overexpression was repressed. Importantly, wild type transformants ceased to grow on galactose-containing medium (SGal) when *MDM33* overexpression was induced. In contrast, some transformants of the deletion pool produced colonies under inducing conditions (Fig. 2A) suggesting that yeast cells are able to cope with high Mdm33 levels when critical interacting genes are lacking.

To screen for genes interacting with *MDM33* we grew the transformed yeast deletion pool under repressing and inducing conditions on agar plates. As each strain of the yeast deletion library is labeled with a unique molecular barcode sequence (Fig. S1A) (Giaever et al., 2002) microarray hybridization can be used to quantify deletion mutants in pools. We isolated genomic DNA from the pooled transformants and determined the abundance of the deletion mutants under inducing vs. repressing conditions in two independent experiments. After high-density oligonucleotide array hybridization, approximately 80% of the deletion mutants produced a good signal after growth on

glucose-containing medium, but were not detectable after growth on galactose-containing medium (Fig. 2B). As expected, $\Delta gal3$ and $\Delta gal4$, which lack factors important for induction of the *GAL1/10* promoter, grew well under inducing conditions (Fig. S1C). Several 100 mutants lacking proteins of various cellular functions produced a significant signal under inducing conditions and thus represent putative interaction partners of *MDM33* (Table S1). Consistent with the results described above, deletion of genes encoding mitochondrial fusion or fission factors did not suppress lethality upon *MDM33* overexpression.

To identify candidates that genetically interact with *MDM33* upon both overexpression and deletion we merged the results from the suppressor screen with the MITO-MAP (interaction score less than -3 or more than 3). Six genes showed high scores in both screens (Fig. 2C). *ELP3* encodes a subunit of the RNA polymerase II holoenzyme and is responsible for transcriptional elongation (Wittschieben et al., 1999). This gene shows a very high number of genetic interactions and was excluded from further analysis as it likely interacts with *MDM33* in an indirect manner. The remaining five genes encode mitochondrial proteins, namely the two subunits of the prohibitin complex, Phb1 and Phb2 (Osman et al., 2009b); the subunit g of the ATP synthase, Atp20 (Boyle et al., 1999); a regulatory subunit of the mitochondrial protein import motor complex, Pam17 (Popov-Celeketic et al., 2008); and a CL biosynthesis factor, Fmp30 (Kuroda et al., 2011).

After transformation of the *MDM33*-overexpressing plasmid into deletion mutants we confirmed that deletion of either of these genes suppresses the growth defect (Fig. 2D). Next, we chose the prohibitin mutants to confirm in double deletion mutants that both $\Delta phb1$ and $\Delta phb2$ show a positive genetic interaction with $\Delta mdm33$ (Fig. S2A). Notably, $\Delta phb1$ strains did not suppress the growth defect when *PHB1* was substituted from a plasmid, indicating that the suppression is directly caused by the absence of *PHB1* (Fig. S2B). It has been observed that overexpression of several genes encoding mitochondrial inner membrane proteins is toxic in yeast (Sopko et al., 2006). To test whether our screen yielded specific suppressors for *MDM33* we took $\Delta phb1$ and $\Delta phb2$ mutants and overexpressed two non-related genes encoding mitochondrial inner membrane proteins, *SCO2* and *YHM2*, that have been reported to cause a growth arrest when expressed from the *GAL1/10* promoter (Sopko et al., 2006). *Sco2* acts in the delivery of copper to the cytochrome c oxidase (Nittis et al., 2001), whereas *Yhm2* catalyzes mitochondrial citrate/oxoglutarate antiport (Castegna et al., 2010). Deletion of the prohibitin genes did not affect the growth of *SCO2* or *YHM2* overexpressing strains (Fig. 2E). We conclude that the suppression of overexpression induced growth defects in our suppressor mutant strains is specific for *MDM33*. Taken together, our genetic analysis suggests that Phb1, Phb2, Pam17, Fmp30, Atp20, and Mdm33 act in closely related cellular pathways.

***MDM33* is part of a genetic network regulating mitochondrial phospholipid biosynthesis**

Our genetic analysis based on the MITO-MAP (Fig. 1) and the *MDM33* overexpression suppressor screen (Fig. 2) revealed that *PHB1/2*, *PAM17*, *FMP30*, *ATP20*, and *MDM33* can be integrated into a highly interconnected genetic interaction network. This network includes ERMES, the ERMES regulatory subunit Gem1, and genes of the mitochondrial phospholipid biosynthesis pathways, namely *PSD1* and *CRD1* (Fig. 3A). *Psd1* catalyzes the conversion of PS to PE within mitochondria while *Crd1* catalyzes an irreversible condensation reaction to couple phosphatidylglycerol and cytidine

diphosphate-diacylglycerol (CDP-DAG) to form CL (Clancey et al., 1993; Trotter et al., 1993). Thus, genetic data indicate a role of Mdm33 in mitochondrial phospholipid metabolism.

Next, we asked whether the genetic interactions have an impact on mitochondrial morphology. We systematically examined mitochondrial morphology in 79 mutants with combined deletions of the *MDM33* gene and genes interacting with *MDM33* or encoding proteins involved in mitochondrial structure or dynamics (Table S2). Δ *mdm33* was found to be epistatic to most of the other deletion alleles, substantiating its central role in mitochondrial morphogenesis. However, deletion of *FMP30*, *GEM1*, *MDM10*, *MDM12*, *MDM31*, *MDM34*, *MMM1*, *PHB1*, or *PHB2* resulted in a mitochondrial morphology phenotype that was epistatic to Δ *mdm33* (Fig. 3B). Intriguingly, all of these genes are implicated in mitochondrial lipid metabolism: (i) Lipid production in mitochondria requires import of precursor lipids from the ER at contact sites that are formed by the ERMES complex that consists of Mdm10, Mdm12, Mdm34, and Mmm1 (Kornmann et al., 2009). These contacts are regulated by Gem1 (Kornmann and Walter, 2010; Stroud et al., 2011). (ii) Both Fmp30 and prohibitins are known to show strong genetic interactions with genes involved in mitochondrial CL and PE biosynthesis, and Fmp30 is required for the maintenance of a sufficient CL level in the absence of mitochondrial PE synthesis (Birner et al., 2003; Osman et al., 2009a; Kuroda et al., 2011). (iii) Mdm31 is known to play an important role in CL biosynthesis in mitochondria, and overexpression of *MDM31* can partially compensate for the loss of ERMES (Tamura et al., 2012a). The requirement of mitochondrial phospholipid biosynthesis factors for the formation of the Δ *mdm33* mitochondrial phenotypes further supports a potential role of Mdm33 in mitochondrial phospholipid metabolism.

In contrast, lariat-shaped mitochondria characteristic for Δ *mdm33* could be found in double mutants lacking the inner membrane fusion factor Mgm1 and in triple mutants lacking the outer membrane fusion and fission factors Fzo1 and Dnm1 (Fig. 3B). This suggests that Mdm33 acts upstream of mitochondrial fusion and fission.

Mdm33 physically interacts with Phb1, Phb2, and Atp20

In a parallel approach to identify Mdm33 interaction partners, we cross-linked lysates of cells expressing functional GFP-Mdm33 fusions and subjected them to immunoprecipitation using anti-GFP antibodies. Interacting proteins were identified by mass spectrometry (LC-MS/MS). The most robust interacting proteins were the prohibitins, which were detected with high scores in three different strains expressing GFP-Mdm33 either from an allele integrated into the genome, a low copy, or a multi-copy plasmid. In addition, Atp1 and Atp2, the alpha and beta subunits of the F1 sector of the ATP synthase, were found to interact with GFP-Mdm33 (Table 1). Thus, the proteomic analysis suggests proximity between the Mdm33 complex, prohibitins, and the ATP synthase. These results are in good agreement with the genetic interactions of *MDM33* with *PHB1*, *PHB2*, and *ATP20*.

Mdm33 controls phospholipid homeostasis in mitochondria

Our genetic and proteomic analyses suggested that *MDM33* might participate in mitochondrial lipid metabolism. To test this, we analyzed the phospholipid composition of mitochondria isolated from wild type or Mdm33 overexpressing cells by mass spectrometry. Strikingly, phospholipids that are synthesized in mitochondria, PE and CL, were strongly reduced in mitochondria of strains overexpressing *MDM33* (Fig. 4A), suggesting that Mdm33 affects mitochondrial phospholipid homeostasis. The combined deletion of genes required for production of CL and PE is synthetic lethal

in yeast, indicating that CL and PE are partially redundant and that a sufficient level of either of them is required for cell survival (Gohil et al., 2005). Thus, the disturbance of mitochondrial phospholipid biosynthesis upon overexpression of *MDM33* might cause the observed growth defect. Furthermore, it is known that changes in mitochondrial lipid composition can cause septation of the mitochondrial inner membrane (Connerth et al., 2012). Therefore, we consider it likely that changes of mitochondrial ultrastructure observed upon overexpression of *MDM33* are a consequence of alterations of the PE and CL content in mitochondrial membranes.

PE biosynthesis occurs via multiple pathways (Fig. S3). In yeast the main pathway starts in the ER where PS is synthesized. PS is then transported to the mitochondrial inner membrane where the PS decarboxylase, Psd1, converts it to PE. It was recently suggested that ERMES is critical for establishing mitochondrial ER contacts that are required for phospholipid exchange between both organelles (Kornmann et al., 2009). Therefore, we checked whether the formation of ERMES is impaired by overexpression of *MDM33*. Impairment of ERMES is expected to change the localization of Mmm1, an ER-resident ERMES subunit, from patch-like assemblies to a diffuse ER signal (Kornmann et al., 2009). Analysis of Mmm1-ERFP expressing strains by fluorescence microscopy revealed that ERMES localization is not affected by *MDM33* overexpression (Fig. 4B).

It was recently shown that Psd1 is required for processing of Mgm1 (Chan and McQuibban, 2012), a dynamin-related protein that exists in two alternatively processed forms that are both required for mitochondrial inner membrane fusion (Herlan et al., 2003). As mitochondria are similarly fragmented in cells lacking Mgm1 (Wong et al., 2000) and in cells overexpressing *MDM33* (Messerschmitt et al., 2003), we considered the possibility that altered lipid composition of mitochondria containing excess Mdm33 results in a defect in processing of Mgm1. However, Western blot analysis of total cell extracts revealed that this is not the case (Fig. 4C).

Next, we examined the conversion of PS to PE by addition of liposomes containing fluorescently labeled PS (NBD-PS) to isolated mitochondria and subsequent thin layer chromatography of mitochondrial lipids (Tamura et al., 2012b). A Western blot analysis revealed that the protein level of Psd1 was not changed in mitochondria isolated from *MDM33* overexpressing strains (Fig. 4D). However, mitochondria containing high Mdm33 levels showed only about 50-70% PS to PE conversion activity compared to the wild type (Fig. 4D, E). Taken together, our results suggest that Mdm33 has a direct impact on PE synthesis in mitochondria.

Mdm33 contributes to mitochondrial division

Δ *mdm33* cells harbor large mitochondria that are often interconnected, and overexpression of *MDM33* results in mitochondrial fragmentation. These observations are suggestive of a role of Mdm33 in mitochondrial division (Messerschmitt et al., 2003). To test a function of Mdm33 in this process more directly, we induced mitochondrial fragmentation in wild type, Δ *dnm1*, and Δ *mdm33* cells by treatment with sodium azide (Fekkes et al., 2000) and observed mitochondrial morphology by fluorescence microscopy (Fig. 5A). Treatment of wild type cells led to rapid mitochondrial fragmentation, while Δ *dnm1* mitochondria remained interconnected, confirming that fragmentation is dependent on the mitochondrial fission machinery. In contrast, Δ *mdm33* mutants retained considerable fission activity. However, the number of cells with fragmented mitochondria was strongly reduced compared to the wild type suggesting that Mdm33 promotes mitochondrial fission (Fig. 5A). Next, we analyzed cells expressing Dnm1-GFP by time-resolved live cell fluorescence

microscopy. We could observe Dnm1-GFP-dependent matrix constriction and mitochondrial division in $\Delta mdm33$ cells (Fig. 5B). However, these events were restricted to a rather small tubular portion of the mitochondria and never occurred in the large ring-like structures. We conclude that Mdm33 contributes to efficient mitochondrial division, albeit it does not appear to constitute an essential component of the mitochondrial division machinery.

It was recently shown that ER tubules wrap around mitochondria and mediate mitochondrial constriction prior to Dnm1 assembly (Friedman et al., 2011). This is spatially and functionally linked to the ERMES complex that tethers the ER and mitochondria (Kornmann et al., 2009). The Miro GTPase Gem1 is required to disintegrate these contacts after the division event, thereby generating free mitochondrial tips (Murley et al., 2013). We asked whether the association of ERMES with sites of mitochondrial division might be disturbed in cells lacking Mdm33. We observed that the ER-resident ERMES subunit Mmm1 colocalizes with Dnm1-GFP in wild type and $\Delta mdm33$ cells, suggesting that this step of mitochondrial division does not require Mdm33 (Fig. 5C).

To test whether mitochondrial fragmentation and growth arrest upon *MDM33* overexpression depend on the outer membrane fission machinery we overexpressed *MDM33* in $\Delta dnm1$ strains. We observed a strong growth defect in cells lacking Dnm1, although we did not observe mitochondrial fragmentation (Fig. 5D, E). Instead we found parts of the mitochondrial network to be swollen. Electron microscopy revealed that overexpression of *MDM33* in the absence of Dnm1 causes swelling of the mitochondria and inner membrane septa formation (Fig. 5F). This indicates that mitochondrial fragmentation upon *MDM33* overexpression is Dnm1-dependent, whereas growth arrest and inner membrane remodeling are independent of Dnm1. Taken together, our results are consistent with the idea that Mdm33 is important to keep mitochondria in a fission-competent shape.

Mdm33 foci are present at sites of mitochondrial division

Next, we asked whether Mdm33 is present at sites of mitochondrial division. To test this, we co-expressed functional fusion proteins GFP-Mdm33 and Dnm1-mCherry and labelled mitochondria with mito-BFP. Intriguingly, GFP-Mdm33 was found to accumulate in fluorescent foci in many cells. The majority of these foci co-localized with Dnm1-mCherry. Time-resolved fluorescence microscopy showed that these foci are formed transiently and coincide with the formation of Dnm1-mCherry foci and mitochondrial constriction or division (Fig. 6). These results suggest that Mdm33 cooperates with Dnm1 in mitochondrial division. Similarly, GFP-Mdm33 foci were found to also co-localize with Mmm1-mCherry (Fig. S4) suggesting that Mdm33 is required already at an early step of fission when the division sites are selected.

Discussion

Mitochondrial fission and phospholipid metabolism both affect mitochondrial structure and morphology. However, only little is known about the functional relationship of these processes. Here, we show that Mdm33 interacts in many ways with molecular components and pathways of mitochondrial phospholipid homeostasis. At the same time, Mdm33 is present at sites of mitochondrial fission, and mutants show severe fission defects. We propose that Mdm33 links mitochondrial inner membrane lipid homeostasis to mitochondrial division.

Division of the mitochondrial double membrane is a complex process that conceivably requires machineries acting inside and outside the organelle (Westermann, 2010; Friedman and Nunnari, 2014). Recent evidence suggests that the ER marks the sites of mitochondrial division. It wraps around the outer membrane and thereby constricts the diameter of the mitochondrial tubule to a size that allows the Dnm1 division ring to assemble on the cytosolic side of the organelle (Friedman et al., 2011). However, it remained unclear whether the process of ER-associated mitochondrial division (ERMD) also requires fission proteins acting on the mitochondrial inner membrane. While some primitive algal mitochondria have retained FtsZ-related fission proteins from their bacterial ancestors (Beech et al., 2000), animals, fungi, and most plants lack mitochondrial FtsZ homologs. Thus, it is possible that FtsZ in mitochondria has been replaced by other factors during the evolution of most eukaryotic lineages. Our previous characterization of the $\Delta mdm33$ mutant provided evidence for a role of Mdm33 in mitochondrial inner membrane division (Messerschmitt et al., 2003). Mutant cells have a unique phenotype with extremely extended and often ring-shaped giant mitochondria. It is conceivable that these aberrant organelles can form only in the absence of frequent division events. Here, we show that deletion of the *MDM33* gene impedes azide-induced mitochondrial fragmentation, and we observed a striking co-localization of Mdm33 and Dnm1 during fission. Taken together, these observations show that Mdm33 is a fission-promoting factor.

We found that Mdm33 genetically and physically interacts with prohibitins, which are known modulators of mitochondrial inner membrane homeostasis (Osman et al., 2009b). Strikingly, Mdm33 overexpression lowers the rate of mitochondrial PE biosynthesis and CL levels. It is well established that also prohibitins have an intimate functional relationship with the lipid composition of mitochondrial membranes, especially with the levels of PE and CL. We previously proposed that ring-like prohibitin complexes might serve as membrane organizers modulating the distribution of CL and PE within the membrane (Osman et al., 2009a). Our genetic and proteomic data suggest that Mdm33 and prohibitins cooperate in this process. It is therefore conceivable that, similar to prohibitins, Mdm33 acts as a membrane scaffold ensuring proper organization of the inner membrane and regulating lipid biosynthesis.

Accumulating evidence suggests that modulation of lipid composition is an important aspect of mitochondrial membrane fusion and fission (Furt and Moreau, 2009). For example, fusion requires the local generation of the fusogenic lipid phosphatidic acid (PA) in the mitochondrial outer membrane (Choi et al., 2006), the biosynthesis of PE and CL are intimately linked to mitochondrial fusion in yeast (Chan and McQuibban, 2012; Joshi et al., 2012), and CL plays a major role mitochondrial division in *Arabidopsis thaliana* (Pan et al., 2014). We show here that Mdm33 has an impact on the abundance of CL and PE. These are both non-bilayer forming lipids with small headgroups and therefore confer negative curvature to mitochondrial membranes, a feature that is particularly important during fusion or fission (Huttner and Zimmerberg, 2001; Chernomordik and Kozlov, 2003; van den Brink-van der Laan et al., 2004; McMahan and Gallop, 2005). Thus, it is conceivable that Mdm33 activity affects the capacity of the inner membrane to undergo fission.

Our cytological and genetic interaction data support an auxiliary role of Mdm33 in mitochondrial fission. Time-resolved fluorescence microscopy revealed that mitochondrial fission events do occur in the absence of Mdm33, albeit at strongly reduced frequency. This indicates that Mdm33 is not an essential part of the division machinery. Ring-shaped mitochondria characteristic for mutants lacking *MDM33* are prevalent in double and triple mutants lacking fusion and fission factors. Thus, the $\Delta mdm33$ deletion is epistatic to the deletion of genes encoding core components of the fusion and

fission machineries. Furthermore, Mdm33 overexpression-induced inner membrane septae form independently of Dnm1. These observations suggest that Mdm33 acts upstream of fusion and fission.

We consider it likely that Mdm33 prepares the inner membrane for division by local modulation of its phospholipid composition and biophysical properties. Although they are antagonistic activities, fusion and fission of membranes are related processes. In both cases membranes fuse and mix the lipids of their bilayers followed by separation of a hemi-fused intermediate. In case of fusion the membranes belong to two different organelles, while fission can be regarded as the fusion of organellar membranes from the inner side of the same organelle (Chernomordik and Kozlov, 2003; Kozlov et al., 2010). Thus, fusion and fission of mitochondria could both require local adjustments of the membrane lipid composition to lower the energy barrier of lipid bilayer mixing. In this scenario Mdm33 might contribute to the formation of microdomains that are particularly enriched in PE and CL to generate curvature. Formation of these microdomains then renders the membrane competent for fission (i.e. fusion of the inner membrane from the matrix side). It is conceivable that this activity facilitates mitochondrial constriction at division sites by mitochondrial ER interactions and helps in severing the mitochondrial double membranes by the Dnm1 division ring that is assembled on the outer membrane.

Materials and Methods

Plasmids and cloning procedures

Standard procedures were used for cloning and amplification of plasmids (Green and Sambrook, 2012). PCR was performed using *Pfu* polymerase (Fermentas, St. Leon-Rot, Germany) or the *GoTaq* polymerase (Promega, Madison, WI) according to the manufacturer's instructions. Plasmids pYX142-mtGFP (Westermann and Neupert, 2000), pVT100U-mtGFP (Westermann and Neupert, 2000), pYX142-mtERFP (Scholz et al., 2012), pYX223-*MDM33* (Messerschmitt et al., 2003), pHS20 (Sesaki and Jensen, 1999), pTT46(Phb1) (Tatsuta et al., 2005), pESC-*SCO2* (Zhu et al., 2001), and pESC-*YHM2* (Zhu et al., 2001) were described previously. The pRS316-*MMM1*-ERFP plasmid containing the promoter and coding region of *MMM1* fused to the yeast-enhanced mRFP (Keppler-Ross et al., 2008) coding sequence was provided by Stefan Böckler (Universität Bayreuth, Germany). To obtain pYX223-mtBFP, the BFP fused to the Su9 mitochondrial presequence was subcloned from pYES-mtBFP (Westermann and Neupert, 2000) into the *HindIII* and *XhoI* sites of pYX223. The FLAG-tagged version of *MDM33* was constructed by PCR-amplification-based fusion of the FLAG tag to the fragment encoding the mature part of *MDM33* using the oligonucleotides 5'-ATA TAT GGA TCC GAT TAT AAA GAT GAT GAC GAT AAG CTA CAG AAC GGT GAT ACT CC-3' and 5'-AAT TTT CTC GAG TTT TAA CGA TAT TCT TGC GC-3' and genomic DNA as template. This fragment was then cloned into the *BamHI* and *XhoI* sites of pMM112 (Messerschmitt et al., 2003), yielding pRS316-FLAG-*MDM33*. Plasmid pYX223-FLAG-*MDM33* was created by PCR-amplification of the fragment containing the import sequence, the FLAG tag and the mature part of *MDM33* using pRS316-FLAG-*MDM33* as template and oligonucleotides 5'-TAT AAA GCT TAT GTT GAG ATA CTA TGG GGC GAC-3' and 5'-AAT TTT CTC GAG TTT TAA CGA TAT TCT TGC GC-3' and cloning into the *HindIII* and *XhoI* sites of pYX223.

Yeast strain constructions

Standard procedures were used for manipulation of yeast (Sherman, 1991; Gietz et al., 1992). Yeast deletion mutants were taken from the yeast deletion collection (Giaever et al., 2002). Double

deletion mutants were constructed by mating and tetrad dissection. All yeast strains were isogenic to BY4741, BY4742, and BY4743 (Brachmann et al., 1998). For rapid generation of double mutants the synthetic genetic array (SGA) technology was used (Baryshnikova et al., 2010). ORF replacement of *MDM33* was achieved by homologous recombination. The *URA3* marker used for this purpose was amplified using the plasmid pYES-*mtGFP* (Westermann and Neupert, 2000) as template and oligonucleotides 5'-GAT CAT TGG GGT CTT TTT CGT TGT GAA ATT GTA ACG GGT GAA CTC AGT GAT TGA ATC TTA GAT CAC ACT GCC TTT G and 5'-TGT ATT TAT GAT TTT ATT ATG TAC AAG GAT AAA GGA TGA AAA AAA TGC ATG CGT GTT ACC GCT GTT GAG ATC CAG TTC.

Microscopy

Epifluorescence microscopy in Figs. 3-5 was performed using an Axiophot or an Axioplan 2 microscope (Carl Zeiss Lichtmikroskopie, Göttingen, Germany) equipped with a Leica DCF360FX Camera with Leica LAF AF Version 2.2.1 Software (Leica Microsystems, Wetzlar, Germany) or an Evolution VF Mono Cooled monochrome camera (Intas, Göttingen, Germany) with Image ProPlus 5.0 and Scope Pro4.5 software (Media Cybernetics, Silver Spring, MD), respectively. For time-resolved live cell microscopy in Fig. 5B cells were observed with a Leica DMI 6000 wide field fluorescence microscope equipped with a Leica DFC360FX camera and Leica LAS AF Software Version 2.1.0. Image manipulations other than minor adjustments of brightness and contrast were not performed. For time-resolved live cell microscopy in Figs. 6 and S4 cells were grown to midlog phase, sonicated in brief, concentrated, and immobilized on microscope slides on a 3% lowmelt agarose bed in growth medium. Cells were viewed with a microscope (IX70 DeltaVision; Olympus) using a 60× 1.4 NA objective lens (Olympus) and a 100 W mercury lamp (Applied Precision). Light microscopy images composed of a z stack with 0.4 μm increments of the whole cell were collected using an integrated, cooled charge-coupled device (CCD) based camera (CoolSNAP HQ; Photometrics) equipped with a Sony Interline Chip. Datasets were processed using DeltaVision's iterative, constrained three-dimensional deconvolution method to remove out of focus light. Projection of the z stack was generated with Applied Precision software and images were manipulated in Photoshop (Adobe), making linear adjustments to brightness or contrast.

For electron microscopy, cells were grown to log phase and prepared essentially as described previously (Bauer et al., 2001). Ultra-thin 50 nm sections were post-stained for 20 min 2% uranyl acetate and for 3 min in lead citrate. Samples were examined in a CEM 902 (Carl Zeiss, Oberkochen, Germany) transmission electron microscope operated at 80 kV. Micrographs were taken using a 1350 × 1050 pixel Erlangshen ES500W CCD camera (Gatan, Peasanton, CA) and Digital Micrograph software (version 1.70.16).

Microarray design and hybridization

The *S. cerevisiae* TAG microarray design is based on the Saccharomyces Genome Deletion Project (Giaever et al., 2002). The 20mer UpTAG and DownTAG sequences were taken from the *MATα* mating type strains. Reinvestigations of the yeast knockout strain collection by deep sequence analysis of the TAG sequences revealed yeast deletion strains that contained mutated TAG barcodes in comparison to the originally designed barcodes (Eason et al., 2004; Smith et al., 2009). We included the originally designed barcodes as well as the combined mutated barcodes of the two re-sequencing projects in our microarray design. If the mutated sequence contained deletions of one or more nucleotides, the mutated sequence was filled up with T's to a 20mer sequence. In addition, a

limited set of 500 mismatches of UpTAG sequences were designed by exchange of the eleventh nucleotide (A \leftrightarrow T, G \leftrightarrow C). Furthermore, the primer sequences used for labeling the TAG barcodes were also included in the microarray design. All TAG sequences were uploaded to the Agilent eArray website and extended to a final length of 60 nucleotides with Agilent's linker sequences. Probes were randomly distributed across the array using the 8x15k format and printed slides were ordered directly from Agilent Technologies (Waldbronn, Germany).

Genomic DNA from yeast samples was extracted using the NucleoMag 96 Plant DNA extraction kit (Machery-Nagel, Dueren, Germany) on a KingFisher magnetic particle processor (Thermo Scientific, Langenselbold, Germany). Genomic DNA was precipitated with ethanol and suspended in TE buffer. TAG barcode sequences were labeled by asymmetric PCR (20 μ l) using 200 ng genomic DNA as described (Pan et al., 2007). After PCR labeling, 3.6 μ l blocking oligonucleotides U1c and U2c (50 μ M each) were added to 1.5 μ l of the upTAG PCR labeling reaction, heated to 100°C for 1 min, and kept at room temperature for at least 20 min; downTAG samples were treated in the same way with downTAG blocking oligonucleotides D1c and D2c. A hybridization solution was prepared by combining Cy3- and a Cy5-blocked TAG samples (each 4.5 μ l), 9 μ l nuclease-free water, 4.5 μ l 10X Blocking Agent and 22.5 μ l 2X Hi-RPM Buffer (Agilent Technologies). The hybridization mix was added to the Agilent 8x15k arrays and hybridized at 50°C for ca. 16 h. Microarrays were washed using Oligo aCGH Wash Buffer 1 and 2 (Agilent Technologies) as recommended by the manufacturer; decomposition of cyanine dyes was protected by incubating the slides in a Stabilization and Drying Solution (Agilent Technologies).

Dry microarray slides were scanned in a FLA8000 slide scanner (Fujifilm) at 5 μ m pixel resolution in confocal mode. Microarray images were analyzed using the ArrayVision software v8.0, rev4.0 (GE Life Sciences); spot intensities were calculated as background-corrected median-based trimmed mean densities. Spot values of each microarray experiment were scaled to a total array intensity of 147,680,000 units to facilitate comparison of independent experiments (total intensity normalization) (Quackenbush, 2002).

Genetic interaction network

The genetic interaction network was visualized using the Cytoscape software (Shannon et al., 2003).

Immunoprecipitation and LC MS/MS analysis

Immunoprecipitation was performed basically as described in Hoppins et al. (2011) with the following adjustments. 500 ODUs of GFP-tagged strains or an untagged W303 control were lysed in IPLB (20 mM HEPES, pH 7.4, 150 mM KOAc, 2 mM Mg(Ac)₂, 1 mM EGTA, and 0.6 M Sorbitol) with 1X protease inhibitor cocktail set I (CalBiochem) on ice for 10 min and cleared. Lysates were crosslinked by addition of 1 mM DSP (Thermo Scientific) and allowed to incubate on ice for 30 min. Crosslinking was quenched with the addition of 100 mM Tris pH 7.4. Membranes were then solubilized with 1% digitonin on ice for 30 minutes, and subsequently cleared at 12,000x g for 10 min at 4°C. The supernatant was incubated with 50 μ l antiGFP microbeads (Miltenyi Biotec Inc.) on ice for 30 min. The beads were isolated using Miltenyi μ columns and a μ MACS separator (Miltenyi Biotec Inc.), washed three times with IPLB with 0.1% digitonin and protease inhibitors, and washed twice with IPLB containing no digitonin or protease inhibitors. Onbead trypsin digestion was performed, beads were incubated for 30 min at room temperature in 25 μ l elution buffer I (2 M urea; 50 mM Tris, pH

7.5, 1 mM DTT, and 5 µg/ml trypsin). This was followed by two 50 µl applications of elution buffer II (2 M urea; 50 mM Tris, pH 7.5, and 5 mM chloroacetamide). Elutions were collected and digestion was allowed to continue at room temperature overnight. Reactions were stopped with 1 µl trifluoroacetic acid (TFA). Peptide samples were submitted to the Genome Center Proteomics Core at the University of California, Davis, for mass spectrometry (LC MS/MS) based protein identification. Urea from the peptide samples was removed using desalting tips (Aspire RP30; Thermo Fisher Scientific). The tips were prepared by pipetting 60% acetonitrile up and down 20 times and then equilibrated with 0.1% TFA by pipetting up and down 15 times. The peptide sample was pulled through the tip 15 times before being washed with 0.1% TFA. The peptides were eluted from the tips using 100 µl of 60% acetonitrile and dried via vacuum centrifugation. Protein identification was performed using a Paradigm HPLC and CTC Pal autosampler (both from Bruker) paired to either a LTQ ion trap mass spectrometer (Thermo Fisher Scientific) or Thermo-Finnigan LTQFT ultra ion trap mass spectrometer (Thermo Fisher Scientific) through an ADVANCE Plug and Play Nano Spray Source (Bruker). Peptides were desalted onto a nanotrap (Zorbax 300SBC18; Agilent Technologies), then eluted from the trap and separated by a 200 mm × 15 cm Magic C18 AQ column (Bruker) at a flow rate of 2 µl/min. Peptides were eluted using a 60 min gradient of 2-80% buffer B (buffer A, 0.1% formic acid; buffer B, 95% aceto nitrile/0.1% formic acid). The elution gradient was set at 2-35% buffer B for 30 min, increased from 35-80% buffer B for 2 min, and held at 80% buffer B for 1 min. The gradient then decreased from 80-2% buffer B over 2 min and equilibrated for 25 min. The top 10 ions in each survey scan were subjected to automatic low energy collision induced dissociation. Tandem mass spectra were extracted by BioWorks version 3.3. Mass charge state deconvolution and deisotoping were not performed. All MS/MS samples were analyzed using X! Tandem. The raw data was analyzed with X! Tandem using the UniProt *Saccharomyces cerevisiae* database appended with the cRAP database, which includes a compilation of common laboratory contaminants, and both forward and reverse sequences were utilized in the data analysis. Trypsin was set as the cleaving enzyme in the X! Tandem search parameters. X! Tandem was searched with a fragment ion mass tolerance of 0.4 D and a parent ion tolerance of 1.8 D. Iodoacetamide derivative of cysteine was specified in X! Tandem as a fixed modification. Deamidation of asparagine and glutamine, oxidation of methionine and tryptophan, sulfone of methionine, tryptophan oxidation to formylkyn urenine of tryptophan, and acetylation of the N terminus were specified in X! Tandem as variable modifications. Scaffold (version Scaffold_2_02_033_00_07; Proteome Software Inc.) was used to validate MS/MS based peptide and protein identifications. Proteins with a t test P value ≤ 0.05 comparing unique peptides obtained from mass spec of tagged strain to untagged control were further investigated.

Lipid profiling by mass spectrometry and in vitro Psd1 activity assay

Mitochondria for lipid profiling and measurement of Psd1 activity were isolated from yeast cells by differential centrifugation (Daum et al., 1982) and further purified by sucrose gradient centrifugation (Hammermeister et al., 2010). Lipid content of isolated mitochondria was determined as described (Osman et al., 2009a). The preparation of liposomes and the in vitro assay for Psd1 activity were performed essentially as described previously (Tamura et al., 2012b). Lipids in stock solutions in chloroform were mixed at the desired molar ratio, and the solvent was evaporated under a flow of dry nitrogen. The dried lipids were hydrated in 800 µl of reaction buffer (300 mM sucrose, 150 mM KCl, 10 mM Tris-HCl, pH 7.5, 1 mM DTT) by repeated cycles of incubation at 30°C, vortexing, and freeze-thawing. After 1 h hydration the liposomes were prepared by extruding 30 times at 30°C using

an Avanti Mini-Extruder with 0.2 μm polycarbonate membranes according to the manufacturer's instructions. Liposomes were stored at 4°C and used within 5 days.

For thin layer chromatography, phospholipids were extracted from mitochondria by vortexing in 500 μl of 2:1 chloroform/methanol for 15 min at room temperature using a Disruptor Genie (Scientific Industries, Bohemia, NY). 100 μl of water was added and the samples were vortexed for additional 5 min. The organic phase was separated by centrifugation at 400 x g for 5 min and dried under a constant flow of nitrogen. The samples were resuspended in 60 μl of chloroform and 20 μl of each sample was subjected to TLC analysis. Silica gel plates (Fluka Analytical, Sigma-Aldrich, St. Louis, MO) were developed with chloroform / methanol / acetone / water / acetic acid (50:10:20:5:15, vol/vol/vol/vol/vol). NBD fluorescence was imaged with an ImageQuant LAS 4000 gel documentation system (GE Healthcare Europe GmbH, Freiburg, Germany) using excitation and detection wavelengths for GFP.

Online supplemental material

Fig. S1 shows an outline of the suppressor screen and growth of $\Delta gal3$ and $\Delta gal4$ suppressors. Fig. S2 shows negative genetic interactions of $\Delta mdm33$ and prohibitin mutants and complementation of prohibitin mutants by *PHB1*. Fig. S3 shows a sketch of phosphatidylethanolamine biosynthesis pathways. Fig. S4 shows co-localization of GFP-Mdm33 and Mmm1-mCherry. Table S1 shows microarray results from the *MDM33* overexpression suppressor screen. Table S2 summarizes mitochondrial phenotypes of double deletion mutants.

Acknowledgments

We are grateful to Stefan Böckler, Brigitte Neumann, and Takashi Tatsuta for providing strains or plasmids. We thank the Westermann lab for comments on the manuscript and discussions. This work was supported by the Deutsche Forschungsgemeinschaft.

Abbreviations list

CDP-DAG, cytidine diphosphate-diacylglycerol
CL, cardiolipin
ERMD, ER-associated mitochondrial division
ERMES, ER mitochondria encounter structure
LC-MS/MS, liquid chromatography tandem mass spectrometry
NBD, Nitro-2-1,3-Benzoxa-Diazol-4-yl
PA, phosphatidic acid
PC, phosphatidylcholine
PE, phosphatidylethanolamine
PS, phosphatidylserine
SGA, synthetic genetic array

References

- Acehan, D., Z. Khuchua, R.H. Houtkooper, A. Malhotra, J. Kaufman, F.M. Vaz, M. Ren, H.A. Rockman, D.L. Stokes, and M. Schlame. 2009. Distinct effects of *tafazzin* deletion in differentiated and undifferentiated mitochondria. *Mitochondrion*. 9:86-95.
- Alkhaja, A.K., D.C. Jans, M. Nikolov, M. Vukotic, O. Lytovchenko, F. Ludewig, W. Schliebs, D. Riedel, H. Urlaub, S. Jakobs, and M. Deckers. 2012. MINOS1 is a conserved component of mitofilin complexes and required for mitochondrial function and cristae organization. *Mol. Biol. Cell*. 23:247-257.
- Amutha, B., D.M. Gordon, Y. Gu, and D. Pain. 2004. A novel role of Mgm1p, a dynamin-related GTPase, in ATP synthase assembly and cristae formation/maintenance. *Biochem. J*. 381:19-23.
- Baryshnikova, A., M. Costanzo, S. Dixon, F.J. Vizeacoumar, C.L. Myers, B. Andrews, and C. Boone. 2010. Synthetic genetic array (SGA) analysis in *Saccharomyces cerevisiae* and *Schizosaccharomyces pombe*. *Methods Enzymol*. 470:145-179.
- Bauer, C., V. Herzog, and M.F. Bauer. 2001. Improved technique for electron microscope visualization of yeast membrane structure. *Microsc. Microanal.* 7:530-534.
- Beech, P.L., T. Nheu, T. Schultz, S. Herbert, T. Lithgow, P.R. Gilson, and G.I. McFadden. 2000. Mitochondrial FtsZ in a chromophyte alga. *Science*. 287:1276-1279.
- Birner, R., R. Nebauer, R. Schneiter, and G. Daum. 2003. Synthetic lethal interaction of the mitochondrial phosphatidylethanolamine biosynthetic machinery with the prohibitin complex of *Saccharomyces cerevisiae*. *Mol. Biol. Cell*. 14:370-383.
- Boyle, G.M., X. Roucou, P. Nagley, R.J. Devenish, and M. Prescott. 1999. Identification of subunit g of yeast mitochondrial F1F0-ATP synthase, a protein required for maximal activity of cytochrome c oxidase. *Eur. J. Biochem*. 262:315-323.
- Castegna, A., P. Scarcia, G. Agrimi, L. Palmieri, H. Rottensteiner, I. Spera, L. Germinario, and F. Palmieri. 2010. Identification and functional characterization of a novel mitochondrial carrier for citrate and oxoglutarate in *Saccharomyces cerevisiae*. *J. Biol. Chem*. 285:17359-17370.
- Chan, D.C. 2012. Fusion and fission: interlinked processes critical for mitochondrial health. *Annu. Rev. Genet*. 46:265-287.
- Chan, E.Y.L., and G.A. McQuibban. 2012. Phosphatidylserine decarboxylase 1 (Psd1) promotes mitochondrial fusion by regulating the biophysical properties of the mitochondrial membrane and alternative topogenesis of mitochondrial genome maintenance protein 1 (Mgm1). *J. Biol. Chem*. 287:40131-40139.
- Chernomordik, L.V., and M.M. Kozlov. 2003. Protein-lipid interplay in fusion and fission of biological membranes. *Annu. Rev. Biochem*. 72:175-207.
- Choi, S.Y., P. Huang, G.M. Jenkins, D.C. Chan, J. Schiller, and M.A. Frohman. 2006. A common lipid links Mfn-mediated mitochondrial fusion and SNARE-regulated exocytosis. *Nat. Cell Biol*. 8:1255-1262.
- Clancey, C.J., S.C. Chang, and W. Dowhan. 1993. Cloning of a gene (*PSD1*) encoding phosphatidylserine decarboxylase from *Saccharomyces cerevisiae* by complementation of an *Escherichia coli* mutant. *J. Biol. Chem*. 268:24580-24590.
- Claypool, S.M., P. Boontheung, J.M. McCaffery, J.A. Loo, and C.M. Koehler. 2008. The cardiolipin transacylase, tafazzin, associates with two distinct respiratory components providing insight into Barth syndrome. *Mol. Biol. Cell*. 19:5143-5155.

- Connerth, M., T. Tatsuta, M. Haag, T. Klecker, B. Westermann, and T. Langer. 2012. Intramitochondrial transport of phosphatidic acid in yeast by a lipid transfer protein. *Science*. 338:815-818.
- Das, A., B.D. Slaughter, J.R. Unruh, W.D. Bradford, R. Alexander, B. Rubinstein, and R. Li. 2012. Flippase-mediated phospholipid asymmetry promotes fast Cdc42 recycling in dynamic maintenance of cell polarity. *Nat. Cell Biol.* 14:304-310.
- Daum, G., P.C. Böhni, and G. Schatz. 1982. Import of proteins into mitochondria. *J. Biol. Chem.* 257:13028-13033.
- Dimmer, K.S., S. Fritz, F. Fuchs, M. Messerschmitt, N. Weinbach, W. Neupert, and B. Westermann. 2002. Genetic basis of mitochondrial function and morphology in *Saccharomyces cerevisiae*. *Mol. Biol. Cell.* 13:847-853.
- Dixon, S.J., M. Costanzo, A. Baryshnikova, B. Andrews, and C. Boone. 2009. Systematic mapping of genetic interaction networks. *Annu. Rev. Genet.* 43:601-625.
- Eason, R.G., N. Pourmand, W. Tongprasit, Z.S. Herman, K. Anthony, O. Jejelowo, R.W. Davis, and V. Stolc. 2004. Characterization of synthetic DNA bar codes in *Saccharomyces cerevisiae* gene-deletion strains. *Proc. Natl. Acad. Sci. USA.* 101:11046-11051.
- Elgass, K., J. Pakay, M.T. Ryan, and C.S. Palmer. 2013. Recent advances into the understanding of mitochondrial fission. *Biochim. Biophys. Acta.* 1833:150-161.
- Espinet, C., M.A. de la Torre, M. Aldea, and E. Herrero. 1995. An efficient method to isolate yeast genes causing overexpression-mediated growth arrest. *Yeast.* 11:25-32.
- Fekkes, P., K.A. Shepard, and M.P. Yaffe. 2000. Gag3p, an outer membrane protein required for fission of mitochondrial tubules. *J. Cell Biol.* 151:333-340.
- Frezza, C., S. Cipolat, O. Martins de Brito, M. Micaroni, G.V. Beznoussenko, T. Rudka, D. Bartoli, R.S. Polishuck, N.N. Danial, B. De Strooper, and L. Scorrano. 2006. OPA1 controls apoptotic cristae remodeling independently from mitochondrial fusion. *Cell.* 126:177-189.
- Friedman, J.R., L.L. Lackner, M. West, J.R. DiBenedetto, J. Nunnari, and G.K. Voeltz. 2011. ER tubules mark sites of mitochondrial division. *Science.* 334:358-362.
- Friedman, J.R., and J. Nunnari. 2014. Mitochondrial form and function. *Nature.* 505:335-343.
- Furt, F., and P. Moreau. 2009. Importance of lipid metabolism for intracellular and mitochondrial membrane fusion/fission processes. *Int. J. Biochem. Cell Biol.* 41:1828-1836.
- Giaever, G., A.M. Chu, L. Ni, C. Connelly, L. Riles, S. Veronneau, S. Dow, A. Lucau-Danila, K. Anderson, B. Andre, A.P. Arkin, A. Astromoff, M. El-Bakkoury, R. Bangham, R. Benito, S. Brachat, S. Campanaro, M. Curtiss, K. Davis, A. Deutschbauer, K.D. Entian, P. Flaherty, F. Foury, D.J. Garfinkel, M. Gerstein, D. Gotte, U. Guldener, J.H. Hegemann, S. Hempel, Z. Herman, D.F. Jaramillo, D.E. Kelly, S.L. Kelly, P. Kotter, D. LaBonte, D.C. Lamb, N. Lan, H. Liang, H. Liao, L. Liu, C. Luo, M. Lussier, R. Mao, P. Menard, S.L. Ooi, J.L. Revuelta, C.J. Roberts, M. Rose, P. Ross-Macdonald, B. Scherens, G. Schimmack, B. Shafer, D.D. Shoemaker, S. Sookhai-Mahadeo, R.K. Storms, J.N. Strathern, G. Valle, M. Voet, G. Volckaert, C.Y. Wang, T.R. Ward, J. Wilhelmy, E.A. Winzeler, Y. Yang, G. Yen, E. Youngman, K. Yu, H. Bussey, J.D. Boeke, M. Snyder, P. Philippsen, R.W. Davis, and M. Johnston. 2002. Functional profiling of the *Saccharomyces cerevisiae* genome. *Nature.* 418:387-391.
- Gohil, V.M., M.N. Thompson, and M.L. Greenberg. 2005. Synthetic lethal interaction of the mitochondrial phosphatidylethanolamine and cardiolipin biosynthetic pathways in *Saccharomyces cerevisiae*. *J. Biol. Chem.* 280:35410-35416.
- Gonzalvez, F., M. D'Aurelio, M. Boutant, A. Moustapha, J.P. Puech, T. Landes, L. Arnaune-Pelloquin, G. Vial, N. Taleux, C. Slomianny, R.J. Wanders, R.H. Houtkooper, P. Bellenger, I.M. Moller, E. Gottlieb, F.M. Vaz, G. Manfredi, and P.X. Petit. 2013. Barth syndrome: cellular compensation of

- mitochondrial dysfunction and apoptosis inhibition due to changes in cardiolipin remodeling linked to *tafazzin* (*TAZ*) gene mutation. *Biochim. Biophys. Acta.* 1832:1194-1206.
- Green, M.R., and J. Sambrook. 2012. *Molecular Cloning*. Cold Spring Harbor Laboratory Press, Cold Spring Harbor, New York. 1890 pp.
- Griparic, L., N.N. van der Wel, I.J. Orozco, P.J. Peters, and A.M. van der Bliek. 2004. Loss of the intermembrane space protein Mgm1/OPA1 induces swelling and localized constrictions along the lengths of mitochondria. *J. Biol. Chem.* 279:18792-18798.
- Hammermeister, M., K. Schödel, and B. Westermann. 2010. Mdm36 is a mitochondrial fission-promoting protein in *Saccharomyces cerevisiae*. *Mol. Biol. Cell.* 21:2443-2452.
- Harner, M., C. Körner, D. Walther, D. Mokranjac, J. Kaesmacher, U. Welsch, J. Griffith, M. Mann, F. Reggiori, and W. Neupert. 2011. The mitochondrial contact site complex, a determinant of mitochondrial architecture. *EMBO J.* 30:4356-4370.
- Herlan, M., F. Vogel, C. Bornhövd, W. Neupert, and A.S. Reichert. 2003. Processing of Mgm1 by the rhomboid-type protease Pcp1 is required for maintenance of mitochondrial morphology and of mitochondrial DNA. *J. Biol. Chem.* 278:27781-27788.
- Hoppins, S., S.R. Collins, A. Cassidy-Stone, E. Hummel, R.M. Devay, L.L. Lackner, B. Westermann, M. Schuldiner, J.S. Weissman, and J. Nunnari. 2011. A mitochondrial-focused genetic interaction map reveals a scaffold-like complex required for inner membrane organization in mitochondria. *J. Cell Biol.* 195:323-340.
- Hoppins, S., L. Lackner, and J. Nunnari. 2007. The machines that divide and fuse mitochondria. *Annu. Rev. Biochem.* 76:751-780.
- Huttner, W.B., and J. Zimmerberg. 2001. Implications of lipid microdomains for membrane curvature, budding and fission. *Curr. Opin. Cell Biol.* 13:478-484.
- John, G.B., Y. Shang, L. Li, C. Renken, C.A. Mannella, J.M. Selker, L. Rangell, M.J. Bennett, and J. Zha. 2005. The mitochondrial inner membrane protein mitofilin controls cristae morphology. *Mol. Biol. Cell.* 16:1543-1554.
- Joshi, A.S., M.N. Thompson, N. Fei, M. Huttemann, and M.L. Greenberg. 2012. Cardiolipin and mitochondrial phosphatidylethanolamine have overlapping functions in mitochondrial fusion in *Saccharomyces cerevisiae*. *J. Biol. Chem.* 287:17589-17597.
- Keppler-Ross, S., C. Noffz, and N. Dean. 2008. A new purple fluorescent color marker for genetic studies in *Saccharomyces cerevisiae* and *Candida albicans*. *Genetics.* 179:705-710.
- Kornmann, B., E. Currie, S.R. Collins, M. Schuldiner, J. Nunnari, J.S. Weissman, and P. Walter. 2009. An ER-mitochondria tethering complex revealed by a synthetic biology screen. *Science.* 325:477-481.
- Kornmann, B., and P. Walter. 2010. ERMES-mediated ER-mitochondria contacts: molecular hubs for the regulation of mitochondrial biology. *J. Cell Sci.* 123:1389-1393.
- Kozlov, M.M., H.T. McMahon, and L.V. Chernomordik. 2010. Protein-driven membrane stresses in fusion and fission. *Trends Biochem. Sci.* 35:699-706.
- Kuroda, T., M. Tani, A. Moriguchi, S. Tokunaga, T. Higuchi, S. Kitada, and O. Kuge. 2011. FMP30 is required for the maintenance of a normal cardiolipin level and mitochondrial morphology in the absence of mitochondrial phosphatidylethanolamine synthesis. *Mol. Microbiol.* 80:248-265.
- Mannella, C.A. 2006. Structure and dynamics of the mitochondrial inner membrane cristae. *Biochim. Biophys. Acta.* 1763:542-548.
- McMahon, H.T., and J.L. Gallop. 2005. Membrane curvature and mechanisms of dynamic cell membrane remodelling. *Nature.* 438:590-596.

- Meeusen, S., R. DeVay, J. Block, A. Cassidy-Stone, S. Wayson, J.M. McCaffery, and J. Nunnari. 2006. Mitochondrial inner-membrane fusion and crista maintenance requires the dynamin-related GTPase Mgm1. *Cell*. 127:383-395.
- Merz, S., M. Hammermeister, K. Altmann, M. Dürr, and B. Westermann. 2007. Molecular machinery of mitochondrial dynamics in yeast. *Biol. Chem.* 388:917-926.
- Messerschmitt, M., S. Jakobs, F. Vogel, S. Fritz, K.S. Dimmer, W. Neupert, and B. Westermann. 2003. The inner membrane protein Mdm33 controls mitochondrial morphology in yeast. *J. Cell Biol.* 160:553-564.
- Mileykovskaya, E., and W. Dowhan. 2009. Cardiolipin membrane domains in prokaryotes and eukaryotes. *Biochim. Biophys. Acta.* 1788:2084-2091.
- Murley, A., L.L. Lackner, C. Osman, M. West, G.K. Voeltz, P. Walter, and J. Nunnari. 2013. ER-associated mitochondrial division links the distribution of mitochondria and mitochondrial DNA in yeast. *eLife*. 2:e00422.
- Nittis, T., G.N. George, and D.R. Winge. 2001. Yeast Sco1, a protein essential for cytochrome c oxidase function is a Cu(I)-binding protein. *J. Biol. Chem.* 276:42520-42526.
- Nunnari, J., and A. Suomalainen. 2012. Mitochondria: in sickness and in health. *Cell*. 148:1145-1159.
- Okamoto, K., and J.M. Shaw. 2005. Mitochondrial morphology and dynamics in yeast and multicellular eukaryotes. *Annu. Rev. Genet.* 39:503-536.
- Olichon, A., L. Baricault, N. Gas, E. Guillou, A. Valette, P. Belenguer, and G. Lenaers. 2003. Loss of OPA1 perturbs the mitochondrial inner membrane structure and integrity, leading to cytochrome c release and apoptosis. *J. Biol. Chem.* 278:7743-7746.
- Osman, C., M. Haag, C. Potting, J. Rodenfels, P.V. Dip, F.T. Wieland, B. Brügger, B. Westermann, and T. Langer. 2009a. The genetic interactome of prohibitins links their function to cardiolipin and phosphatidylethanolamine in mitochondria. *J. Cell Biol.* 184:583-596.
- Osman, C., C. Merkwirth, and T. Langer. 2009b. Prohibitins and the functional compartmentalization of mitochondrial membranes. *J. Cell Sci.* 122:3823-3830.
- Pan, R., A.D. Jones, and J. Hu. 2014. Cardiolipin-mediated mitochondrial dynamics and stress response in *Arabidopsis*. *Plant Cell*. in press.
- Pan, X., D.S. Yuan, S.L. Ooi, X. Wang, S. Sookhai-Mahadeo, P. Meluh, and J.D. Boeke. 2007. dSLAM analysis of genome-wide genetic interactions in *Saccharomyces cerevisiae*. *Methods*. 41:206-221.
- Paumard, P., J. Vaillier, B. Couлары, J. Schaeffer, V. Soubannier, D.M. Mueller, D. Brethes, J.P. di Rago, and J. Velours. 2002. The ATP synthase is involved in generating mitochondrial cristae morphology. *EMBO J.* 21:221-230.
- Pfanner, N., M. van der Laan, P. Amati, R.A. Capaldi, A.A. Caudy, A. Chacinska, M. Darshi, M. Deckers, S. Hoppins, T. Icho, S. Jakobs, J. Ji, V. Kozjak-Pavlovic, C. Meisinger, P.R. Odgren, S.K. Park, P. Rehling, A.S. Reichert, M.S. Sheikh, S.S. Taylor, N. Tsuchida, A.M. van der Bliet, I.J. van der Klei, J.S. Weissman, B. Westermann, J. Zha, W. Neupert, and J. Nunnari. 2014. Uniform nomenclature for the mitochondrial contact site and cristae organizing system. *J. Cell Biol.* in press.
- Pineau, B., M. Bourge, J. Marion, C. Mauve, F. Gilard, L. Maneta-Peyret, P. Moreau, B. Satiat-Jeunemaitre, S.C. Brown, R. De Paepe, and A. Danon. 2013. The importance of cardiolipin synthase for mitochondrial ultrastructure, respiratory function, plant development, and stress responses in *Arabidopsis*. *Plant Cell*.
- Popov-Celeketic, D., K. Mapa, W. Neupert, and D. Mokranjac. 2008. Active remodelling of the TIM23 complex during translocation of preproteins into mitochondria. *EMBO J.* 27:1469-1480.
- Quackenbush, J. 2002. Microarray data normalization and transformation. *Nat. Genet.* 32 Suppl:496-501.

- Rabl, R., V. Soubannier, R. Scholz, F. Vogel, N. Mendl, A. Vasiljev-Neumeyer, C. Körner, R. Jagasia, T. Keil, W. Baumeister, M. Cyrklaff, W. Neupert, and A.S. Reichert. 2009. Formation of cristae and crista junctions in mitochondria depends on antagonism between Fcj1 and Su e/g. *J. Cell Biol.* 185:1047-1063.
- Scholz, D., J. Förtsch, S. Böckler, T. Klecker, and B. Westermann. 2012. Analyzing membrane dynamics with live cell fluorescence microscopy with a focus on yeast mitochondria. *Meth. Mol. Biol.* 1033:275-283.
- Sesaki, H., and R.E. Jensen. 1999. Division versus fusion: Dnm1p and Fzo1p antagonistically regulate mitochondrial shape. *J. Cell Biol.* 147:699-706.
- Shannon, P., A. Markiel, O. Ozier, N.S. Baliga, J.T. Wang, D. Ramage, N. Amin, B. Schwikowski, and T. Ideker. 2003. Cytoscape: a software environment for integrated models of biomolecular interaction networks. *Genome Res.* 13:2498-2504.
- Smith, A.M., L.E. Heisler, J. Mellor, F. Kaper, M.J. Thompson, M. Chee, F.P. Roth, G. Giaever, and C. Nislow. 2009. Quantitative phenotyping via deep barcode sequencing. *Genome Res.* 19:1836-1842.
- Sopko, R., D. Huang, N. Preston, G. Chua, B. Papp, K. Kafadar, M. Snyder, S.G. Oliver, M. Cyert, T.R. Hughes, C. Boone, and B. Andrews. 2006. Mapping pathways and phenotypes by systematic gene overexpression. *Mol. Cell.* 21:319-330.
- Strauss, M., G. Hofhaus, R.R. Schröder, and W. Kühlbrandt. 2008. Dimer ribbons of ATP synthase shape the inner mitochondrial membrane. *EMBO J.* 27:1154-1160.
- Stroud, D.A., S. Oeljeklaus, S. Wiese, M. Bohnert, U. Lewandowski, A. Sickmann, B. Guiard, M. van der Laan, B. Warscheid, and N. Wiedemann. 2011. Composition and topology of the endoplasmic reticulum-mitochondria encounter structure. *J. Mol. Biol.* 413:743-750.
- Tamura, Y., O. Onguka, A.E. Hobbs, R.E. Jensen, M. Iijima, S.M. Claypool, and H. Sesaki. 2012a. Role for two conserved intermembrane space proteins, Ups1p and Ups2p, [corrected] in intra-mitochondrial phospholipid trafficking. *J. Biol. Chem.* 287:15205-15218.
- Tamura, Y., O. Onguka, K. Itoh, T. Endo, M. Iijima, S.M. Claypool, and H. Sesaki. 2012b. Phosphatidylethanolamine biosynthesis in mitochondria: phosphatidylserine (PS) trafficking is independent of a PS decarboxylase and intermembrane space proteins UPS1P and UPS2P. *J. Biol. Chem.* 287:43961-43971.
- Tasseva, G., H.D. Bai, M. Davidescu, A. Haromy, E. Michelakis, and J.E. Vance. 2013. Phosphatidylethanolamine deficiency in Mammalian mitochondria impairs oxidative phosphorylation and alters mitochondrial morphology. *J. Biol. Chem.* 288:4158-4173.
- Tatsuta, T., K. Model, and T. Langer. 2005. Formation of membrane-bound ring complexes by prohibitins in mitochondria. *Mol. Biol. Cell.* 16:248-259.
- Trotter, P.J., J. Pedretti, and D.R. Voelker. 1993. Phosphatidylserine decarboxylase from *Saccharomyces cerevisiae*. Isolation of mutants, cloning of the gene, and creation of a null allele. *J. Biol. Chem.* 268:21416-21424.
- van den Brink-van der Laan, E., J.A. Killian, and B. de Kruijff. 2004. Nonbilayer lipids affect peripheral and integral membrane proteins via changes in the lateral pressure profile. *Biochim. Biophys. Acta.* 1666:275-288.
- van der Laan, M., M. Bohnert, N. Wiedemann, and N. Pfanner. 2012. Role of MINOS in mitochondrial membrane architecture and biogenesis. *Trends Cell Biol.* 22:185-192.
- von der Malsburg, K., J.M. Müller, M. Bohnert, S. Oeljeklaus, P. Kwiatkowska, T. Becker, A. Loniewska-Lwowska, S. Wiese, S. Rao, D. Milenkovic, D.P. Hutu, R.M. Zerbes, A. Schulze-Specking, H.E. Meyer, J.C. Martinou, S. Rospert, P. Rehling, C. Meisinger, M. Veenhuis, B. Warscheid, I.J. van

- der Klei, N. Pfanner, A. Chacinska, and M. van der Laan. 2011. Dual role of mitofilin in mitochondrial membrane organization and protein biogenesis. *Dev. Cell.* 21:694-707.
- Westermann, B. 2010. Mitochondrial fusion and fission in cell life and death. *Nat. Rev. Mol. Cell Biol.* 11:872-884.
- Westermann, B., and W. Neupert. 2000. Mitochondria-targeted green fluorescent proteins: convenient tools for the study of organelle biogenesis in *Saccharomyces cerevisiae*. *Yeast.* 16:1421-1427.
- Wittschieben, B.O., G. Otero, T. de Bizemont, J. Fellows, H. Erdjument-Bromage, R. Ohba, Y. Li, C.D. Allis, P. Tempst, and J.Q. Svejstrup. 1999. A novel histone acetyltransferase is an integral subunit of elongating RNA polymerase II holoenzyme. *Mol. Cell.* 4:123-128.
- Wong, E.D., J.A. Wagner, S.W. Gorsich, J.M. McCaffery, J.M. Shaw, and J. Nunnari. 2000. The dynamin-related GTPase, Mgm1p, is an intermembrane space protein required for maintenance of fusion competent mitochondria. *J. Cell Biol.* 151:341-352.
- Zhu, H., M. Bilgin, R. Bangham, D. Hall, A. Casamayor, P. Bertone, N. Lan, R. Jansen, S. Bidlingmaier, T. Houfek, T. Mitchell, P. Miller, R.A. Dean, M. Gerstein, and M. Snyder. 2001. Global analysis of protein activities using proteome chips. *Science.* 293:2101-2105.
- Zick, M., R. Rabl, and A.S. Reichert. 2009. Cristae formation-linking ultrastructure and function of mitochondria. *Biochim. Biophys. Acta.* 1793:5-19.

Figure Legends

Figure 1. *MDM33* interacts with genes encoding components of phospholipid biosynthesis. (A) Genetic connection scatter plot of *MDM33*. The plot was generated using data from the MITO-MAP (Hoppins et al., 2011). Each point in the scatter plot represents one gene. The x-axis represents the cosine correlation between the $\Delta mdm33$ interaction scores and the interaction scores obtained for the represented gene. The y-axis indicates interaction score between $\Delta mdm33$ and the represented gene. Several genes acting in phospholipid metabolism, mitochondrial inner membrane homeostasis (prohibitins), mitochondrial ER contacts (ER mitochondria encounter structure, ERMES), mitochondrial distribution, and ATP synthase are highlighted. (B) Pathways of phospholipids biosynthesis. Positive (green), neutral (black), and negative (red) genetic interaction scores are indicated. CDP-DAG, cytidine diphosphate-diacylglycerol; CL, cardiolipin; MLCL, monolyso-cardiolipin; PA, phosphatidic acid; PC, phosphatidylcholine; PDME, phosphatidyl-dimethyl-ethanolamine; PE, phosphatidyl-ethanolamine; PG, phosphatidylglycerol; PGP, phosphatidyl-glycerolphosphate; PI, phosphatidylinositol; PMME, phosphatidylmonomethyl-ethanolamine; PS, phosphatidylserine.

Figure 2. Genome-wide screen for suppressors of *MDM33*-overexpression induced growth arrest. (A) Wild type cells or pooled deletion strains were transformed with pYX223-*MDM33* or the empty vector and plated on synthetic complete medium containing glucose or galactose as carbon source. Growth was observed after 3 days of incubation at 30°C. (B) A pool containing the 4987 strains of the *MAT α* haploid non-essential yeast deletion library was transformed with pYX223-*MDM33*, plated on synthetic complete medium containing glucose or galactose as carbon source and strain abundance was quantified by microarray hybridization. Shown are normalized and background corrected microarray fluorescence signal values for the barcodes of each deletion strain. (C) Each point in the scatter plot represents one gene. The x-axis shows the genetic interaction score between *MDM33* and the represented gene according to the MITO-MAP (Hoppins et al., 2011; compare Fig. 1). The y-axis indicates the normalized and background corrected microarray fluorescence signal taken from (B). (D) Strains were transformed with a multicopy plasmid overexpressing *MDM33* from the inducible *GAL1/10* promoter or the respective empty vector. 10-fold serial dilutions were spotted on synthetic complete medium containing glucose or galactose as carbon source and incubated at 30°C

for 2 (glucose) or 8 (galactose) days. (E) Strains were transformed with an empty vector or a multicopy plasmid overexpressing *SCO2* or *YHM2* from the inducible *GAL1/10* promoter. 10-fold serial dilutions were spotted on synthetic complete medium containing glucose or galactose as carbon source. Growth was scored after incubation at 30°C for 3 days.

Figure 3. *MDM33* is part of a genetic network regulating mitochondrial phospholipid biosynthesis. (A) Genetic interaction network of *MDM33*. Nodes represent deleted or overexpressed genes; edges represent genetic interactions. The network is based on the scores obtained in the suppressor screen (blue) and in the MITO-MAP (blue and grey). (B) Cells expressing mitochondrial matrix targeted GFP (mtGFP) were grown to logarithmic growth phase in YPD and analyzed by fluorescence microscopy. Cell outlines are indicated by a white line. The arrow indicates smaller spherical mitochondria in the $\Delta mgm1 \Delta mdm33$ double mutant. Bar, 5 μ m.

Figure 4. *Mdm33* acts in mitochondrial phospholipid homeostasis. (A) Phospholipidome of mitochondria isolated from cells harboring the indicated plasmids and grown in synthetic complete medium containing galactose as carbon source. Phospholipid analysis was done by quantitative mass spectrometry. Data represent mean values + SD. (B) Cells expressing mitochondrial matrix targeted GFP (mtGFP), and ERFP-tagged Mmm1 (pRS316-*MMM1*-ERFP) were transformed with a multicopy plasmid overexpressing *MDM33* from the inducible *GAL1/10* promoter or the empty vector, grown to the logarithmic growth phase in synthetic complete media containing galactose as carbon source, and analyzed by fluorescence microscopy. Bar, 5 μ m. (C) Western blot analysis of whole cell extracts carrying an empty vector or overexpressing *Mdm33* under control of the *GAL1/10* promoter from a multicopy plasmid (pYX223-*MDM33*). Cells were grown overnight in synthetic complete media containing galactose as carbon source and diluted to logarithmic growth phase. Protein was extracted from the cells by boiling in sample buffer after alkaline treatment. (D) In vitro Psd1 activity assay. Isolated mitochondria of the indicated strains were incubated with liposomes containing NBD-PS for 30 minutes at 30°C, the reaction was stopped, and the total lipids were isolated and separated by TLC. Shown is the NBD-fluorescence. The same samples were analyzed by Western blotting. (E) Quantifications are the ratio of the NBD-PE and NBD-PS signals normalized to the wild type-ratio. Shown are mean values and standard deviation obtained from three independent experiments.

Figure 5. *Mdm33* is required for mitochondrial fission. (A) Cells expressing mitochondrial matrix targeted GFP (mtGFP) were grown to logarithmic growth phase in YPD, either mock-treated or incubated for 40 min with 0.5 mM sodium azide, fixed in 3.7% formaldehyde, and analyzed by fluorescence microscopy. For each strain cells containing fragmented mitochondria were scored. Error bars indicate standard deviations of 3 independent experiments with 150 cells per experiment. Images are merges of DIC and GFP fluorescence (green). Bar: 5 μ m. (B) Time lapse series of cells grown to logarithmic growth phase in synthetic complete medium and expressing mitochondrial matrix targeted ERFP (mtERFP) and *DNM1*-GFP. Images represent maximum intensity projections of fluorescence image z stacks. Arrows highlight mitochondrial division events. Bar, 5 μ m. (C) Cells expressing *DNM1*-GFP, *MMM1*-ERFP, and mitochondria targeted BFP (mtBFP) were grown to logarithmic growth phase in synthetic complete medium and analyzed by fluorescence microscopy. For both strains cells were scored for association of Mmm1-ERFP with Dnm1-GFP patches. Bar, 5 μ m. (D) Strains were transformed with a multicopy plasmid overexpressing *MDM33* from the inducible *GAL1/10* promoter (pYX223-*MDM33*) or an empty vector. 10-fold serial dilutions were spotted on synthetic complete medium containing glucose (repression of the *GAL* promoter) or galactose (induction of the *GAL* promoter) as carbon source and incubated at 30°C for 2-4 days. (E) Cells expressing *MDM33* from the *GAL* promoter and mtGFP were grown overnight in synthetic complete medium containing galactose as carbon source, diluted to logarithmic growth phase and analyzed by fluorescence microscopy. Bar, 5 μ m. (F) Electron micrographs of ultrathin sections of cells grown as in (E). Bars, 200 nm.

Figure 6. GFP-*Mdm33* forms foci co-localizing with Dnm1-mCherry. (A) GFP-*Mdm33* foci and Dnm1-mCherry punctae coincide spatially. The mitochondrial matrix was labelled with BFP.

Arrowheads highlight co-localization of GFP-Mdm33 and Dnm1-mCherry. Images are projections of z-stacks. Bar, 2 μ m. (B) GFP-Mdm33 foci and Dnm1-mCherry punctae coincide temporally. Cells were analyzed as above for 210 sec taking a z-stack every 10 sec. Bars, 2 μ m.

Tables

Table 1. Mdm33 is in vicinity of prohibitins and ATP synthase. Immunoprecipitates of cross-linked GFP-Mdm33 were analyzed by mass spectrometry. The number of peptides and percent coverage is shown for each identified protein.

protein identified	total spectrum count (% coverage)		
	integrated GFP-Mdm33	low copy GFP-Mdm33	high copy GFP-Mdm33
Mdm33	203 (64%)	450 (76%)	512 (77%)
Phb1	8 (20%)	35 (56%)	45 (56%)
Phb2	13 (22%)	48 (49%)	65 (51%)
Atp1	9 (12%)	42 (24%)	54 (28%)
Atp2	9 (15%)	120 (60%)	74 (43%)

Supplemental materials

Figure S1. Screen for genetic interaction partners of *MDM33*. (A) Schematic representation of a bar-coded deletion allele in strains of the yeast deletion collection (Giaever et al., 2002). (B) Outline of the microarray-based genome wide suppressor screen. (C) Strains were transformed with a multicopy plasmid overexpressing *MDM33* from the inducible *GAL1/10* promoter or the respective empty vector. 10-fold serial dilutions were spotted on synthetic complete medium containing glucose or galactose as carbon source and incubated at 30°C for 2 (glucose) or 4 days (galactose).

Figure S2. *PHB1* and *PHB2* genetically interact with *MDM33*. (A) Double mutants of $\Delta phb1/2$ and $\Delta mdm33$ were generated by tetrad dissection. The growth of more than 150 spores was scored for each cross and set in relation to the mean growth of the wild type spores. Shown are representative tetrads and the mean colony size in % of wild type. Error bars indicate standard error. Green bars indicate the difference of the observed colony size and the size that would be expected if the genes would not interact. (B) Strains harboring a multicopy plasmid overexpressing *MDM33* from the inducible *GAL1/10* promoter (pYX223-*MDM33*) or the respective empty vector were transformed with a low copy plasmid expressing *PHB1*. 10-fold serial dilutions were spotted on synthetic complete medium containing glucose (repression of the *GAL* promoter) or galactose (induction of the *GAL* promoter) as carbon source and incubated at 30°C for 2-4 days.

Figure S3. Phosphatidylethanolamine biosynthesis pathways in yeast. Dashed lines indicate transport while solid lines indicate enzymatic reactions. OM: Mitochondrial outer membrane. IM: mitochondrial inner membrane. G/E/V: Golgi / endosome / vacuole. ERMES: ER-mitochondria encounter structure. PS: Phosphatidylserine. PE: Phosphatidylethanolamine. Etn: Ethanolamine. Etn-P: Phosphorylethanolamine. CDP-Etn: CDP-ethanolamine. CDP-DAG: CDP-diacylglycerol.

Figure S4. GFP-Mdm33 forms foci co-localizing with Mmm1-mCherry. Images are projections of z-stacks. Bar, 2 μ m.

Table S1. Scores from the microarray-based genome-wide screen for suppressors of *MDM33* overexpression induced toxicity. A pool containing the 4987 strains of the *MAT α* haploid non-essential yeast deletion library was transformed with pYX223-*MDM33*, plated on synthetic complete medium containing glucose or galactose as carbon source and strain abundance was quantified by microarray hybridization. Given are normalized and background corrected microarray fluorescence signal values for the barcodes of each deletion strain under both conditions. The table also includes scores for the genetic interaction between the indicated gene and *MDM33* and their respective interactome similarity. Latter scores were taken from the MITO-MAP. Red color indicates negative genetic interaction whilst green color indicates positive genetic interaction with a threshold of -3 and +3, respectively.

Table S2. Screen for genes that are required for the formation of aberrant mitochondrial structures in the Δ *mdm33* mutant. Cells expressing mitochondrial matrix targeted GFP (mtGFP) were grown to logarithmic growth phase in YPD and mitochondrial morphology was analyzed by fluorescence microscopy. The table provides information about the mitochondrial phenotype of 79 double mutants that were generated using the SGA technology. It also includes scores for the genetic interaction between both deleted genes and the interactome similarity. These scores were taken from the MITO-MAP. Yellow color indicates that the strains did not exhibit Δ *mdm33* mitochondrial morphology.

Please refer to the attached CD-ROM for Tab. S1 and S2.

Figures

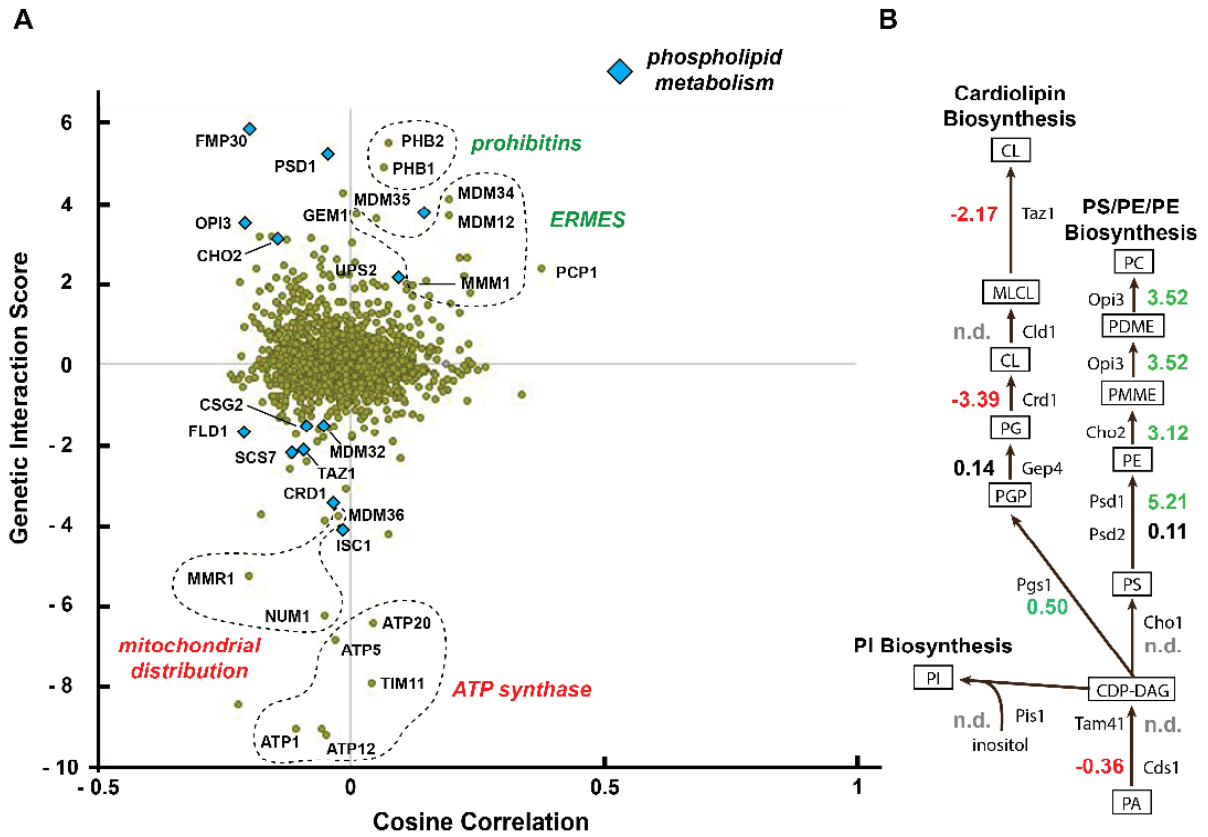


Figure 1

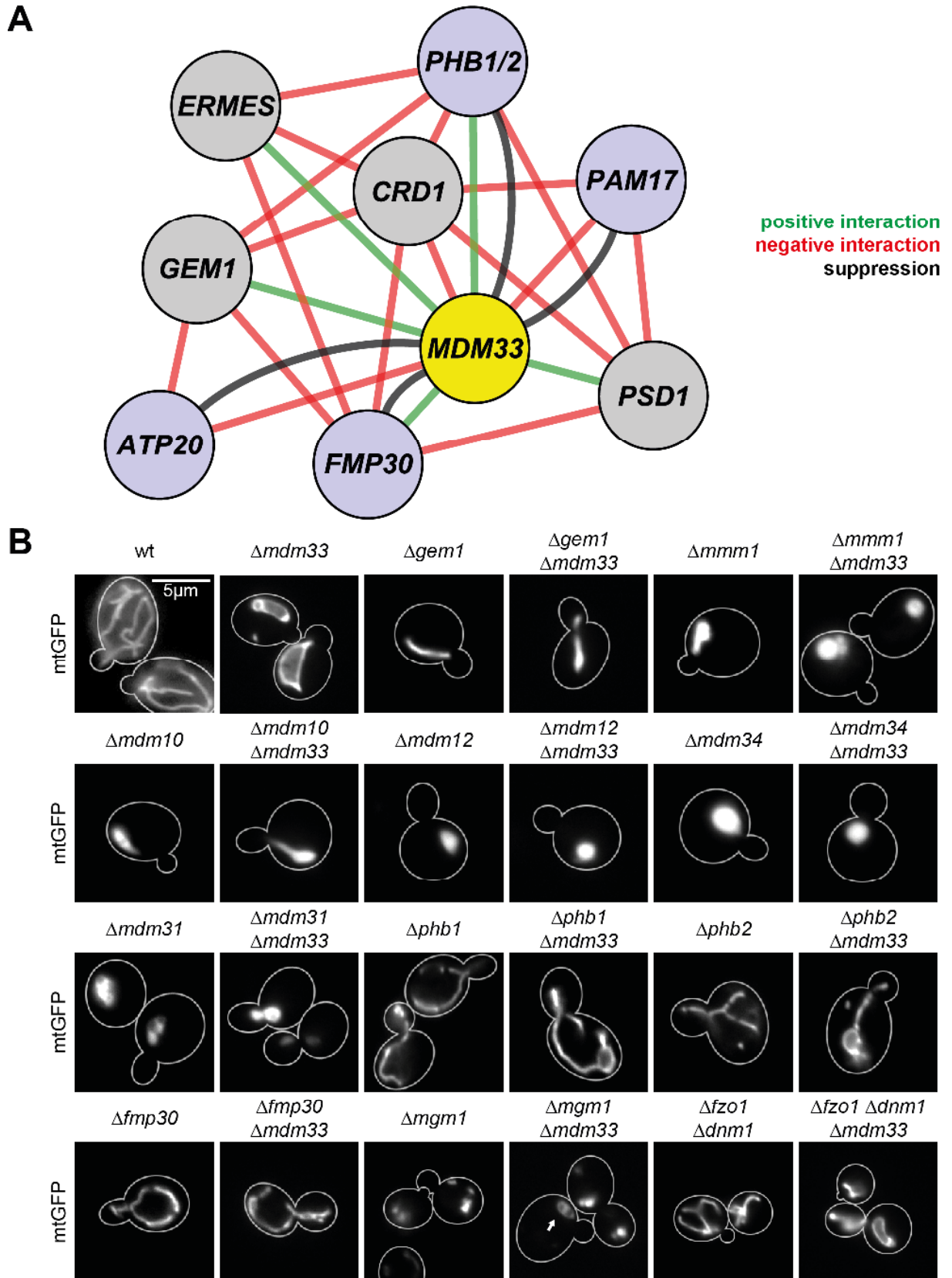


Figure 3

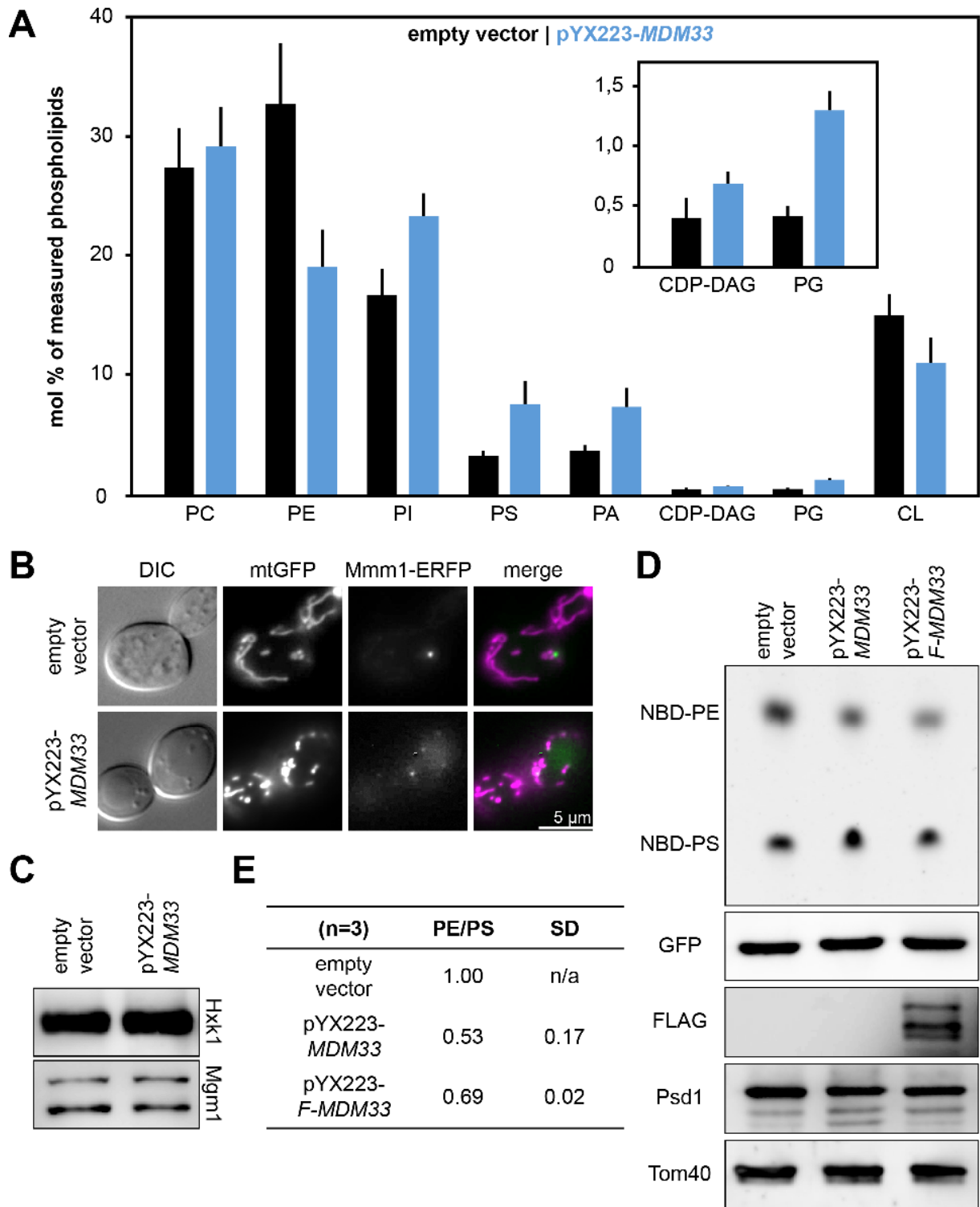


Figure 4

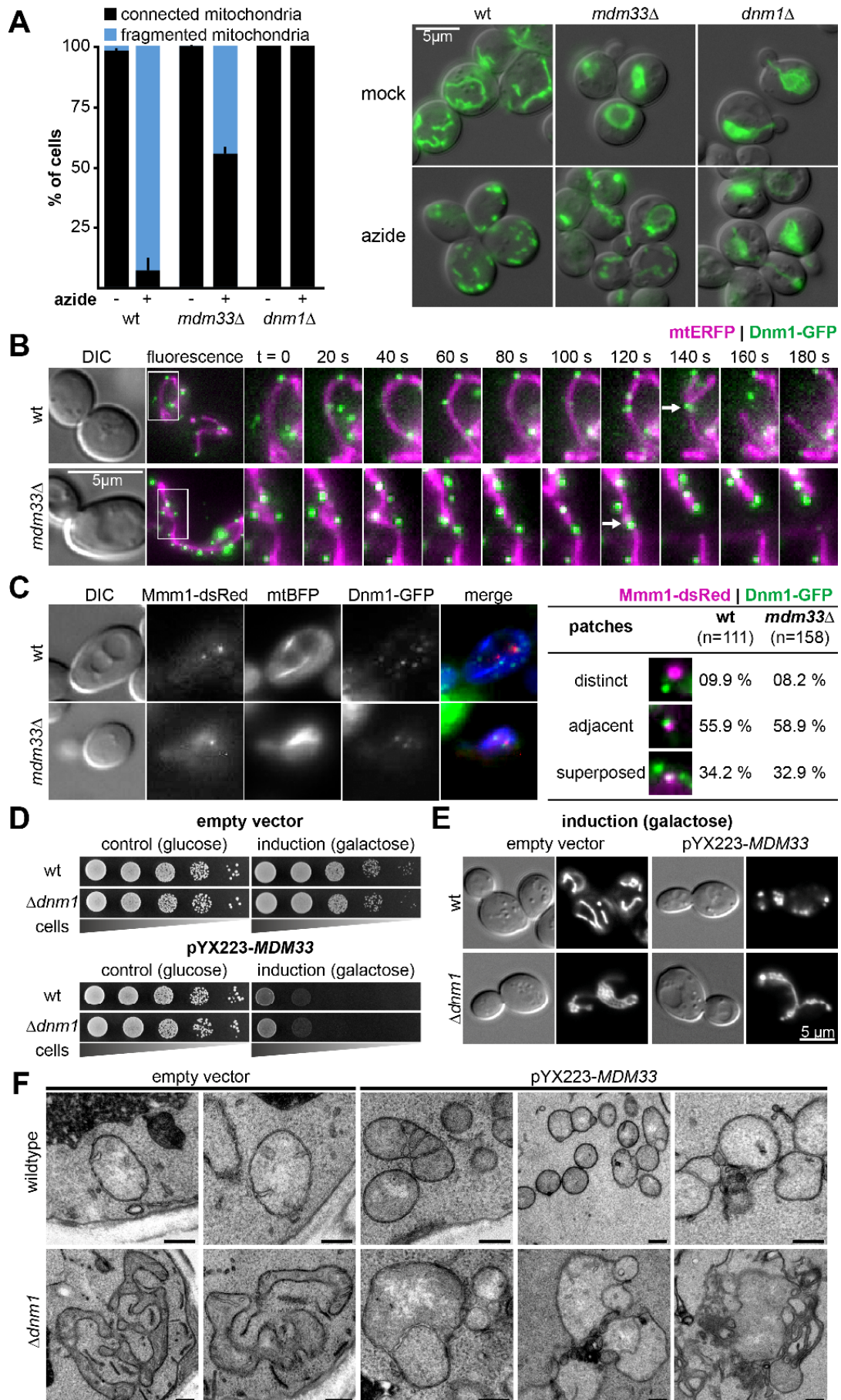


Figure 5

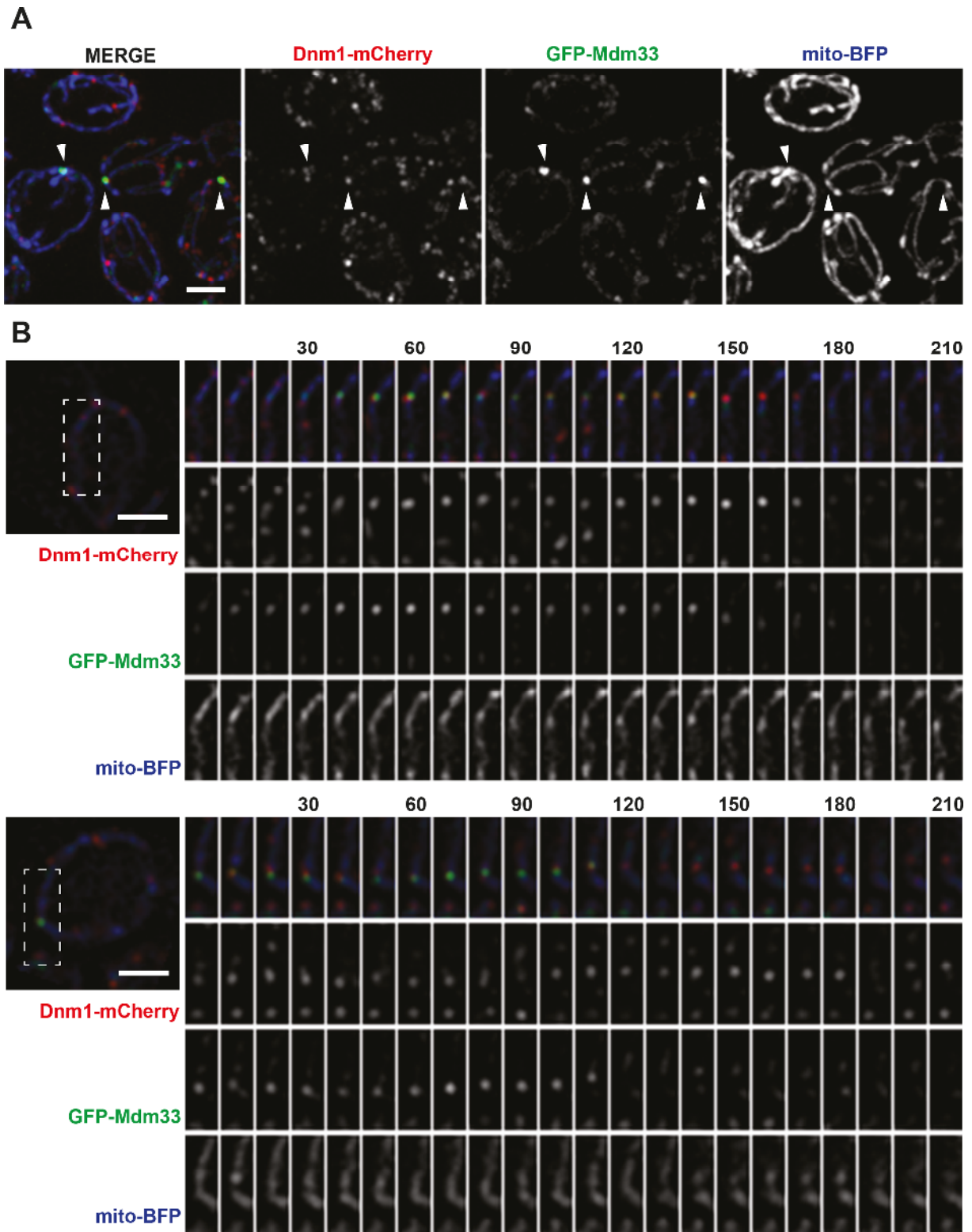


Figure 6

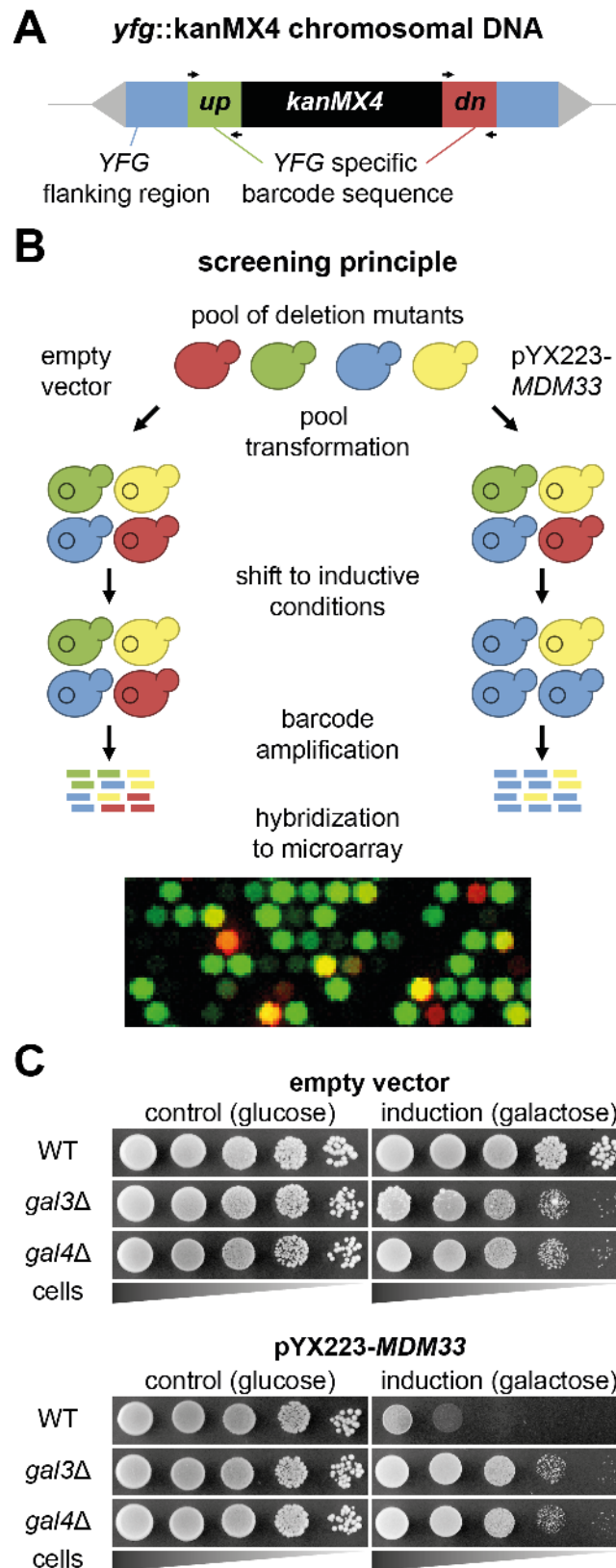


Figure S1

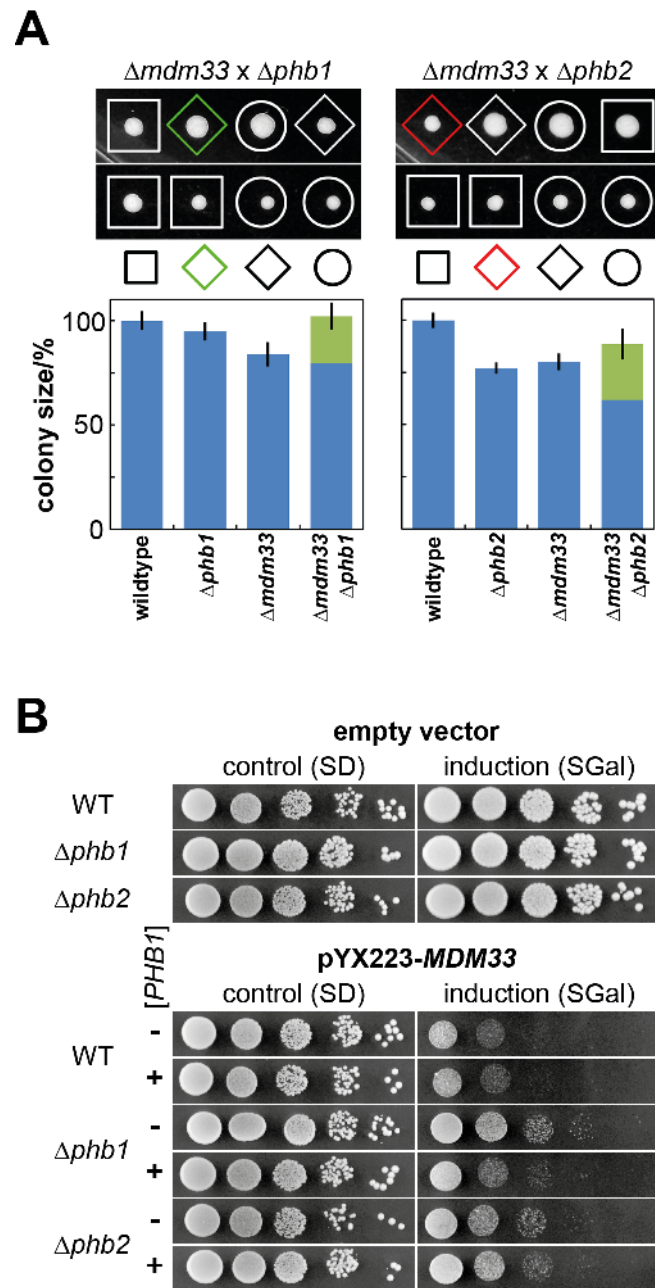


Figure S2

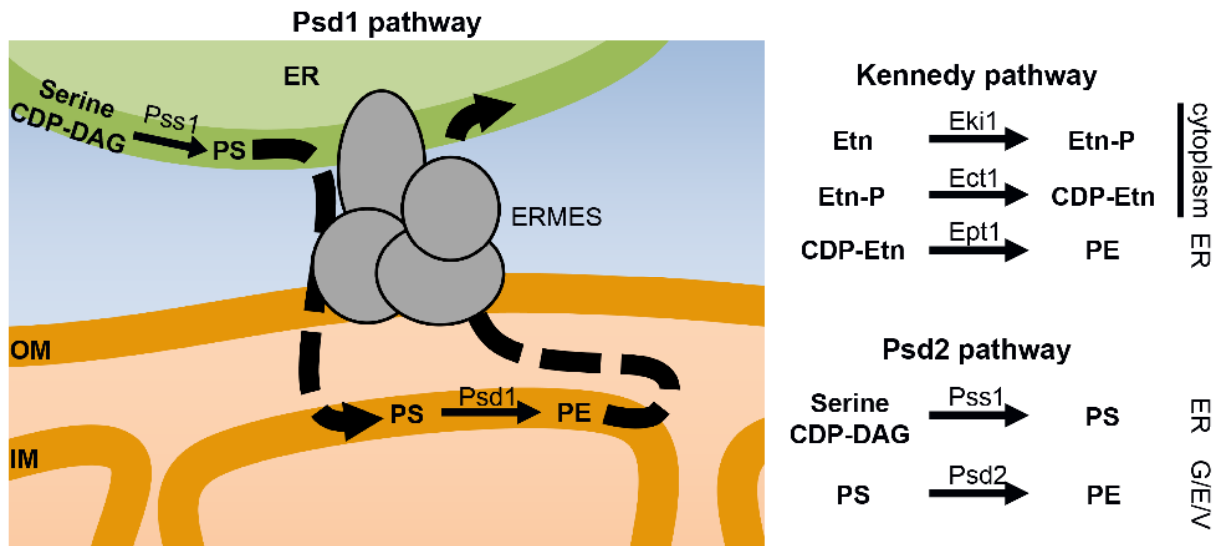


Figure S3

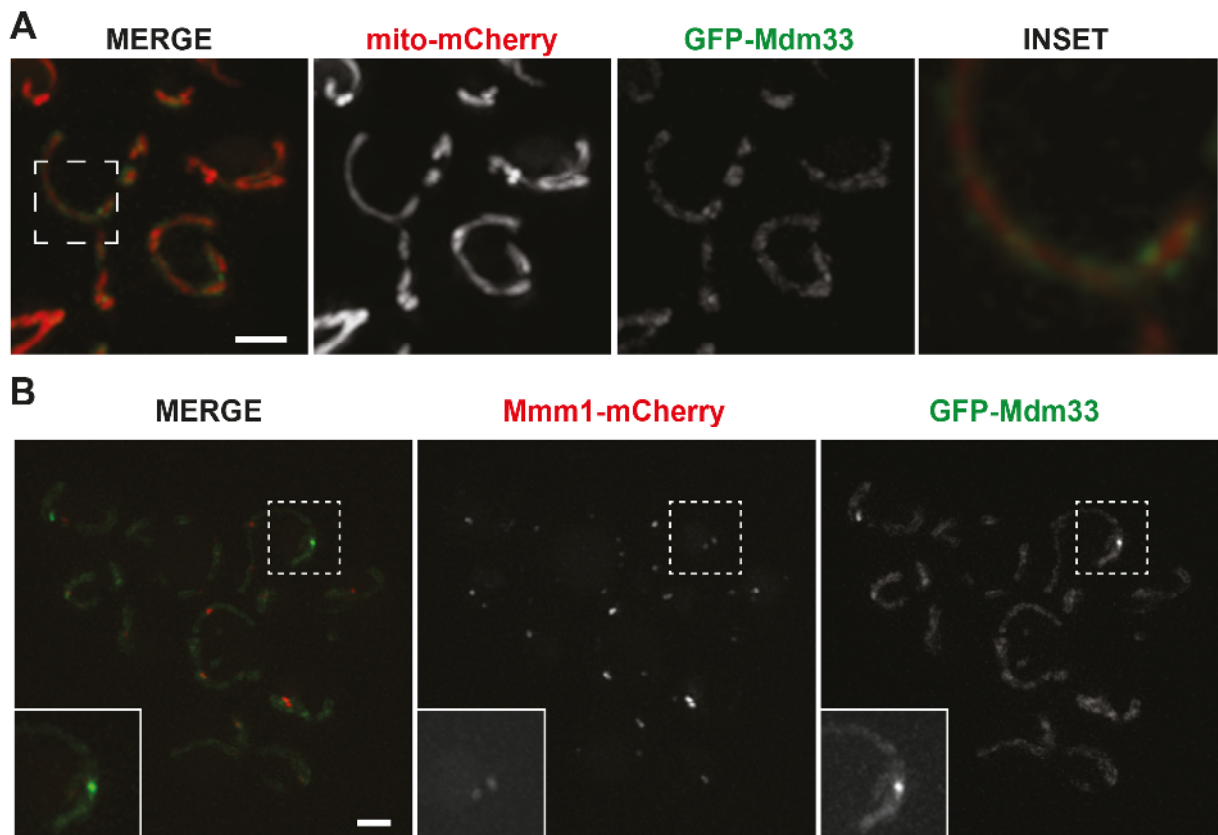


Figure S4

Intramitochondrial Transport of Phosphatidic Acid in Yeast by a Lipid Transfer Protein

Melanie Connerth^{1,*}, Takashi Tatsuta^{1,*}, Mathias Haag^{1,*}, Till Klecker², Benedikt Westermann², and Thomas Langer^{1,3,†}

(2012) *Science* 338: 815-818

¹ Institute for Genetics, Cologne Excellence Cluster on Cellular Stress Responses in Aging-Associated Diseases (CECAD), Center for Molecular Medicine (CMMC), University of Cologne, 50674 Cologne, Germany.

² Institute for Cell Biology and Electron Microscopy Laboratory, University of Bayreuth, 95440 Bayreuth, Germany.

³ Max-Planck-Institute for Biology of Aging, 50931 Cologne, Germany.

[†] To whom correspondence should be addressed. Email: thomas.langer@uni-koeln.de

* These authors contributed equally to this work.

Author contributions

I performed the electron microscopy, was involved in the interpretation of the acquired data, and drafted figure 2B.

Intramitochondrial Transport of Phosphatidic Acid in Yeast by a Lipid Transfer Protein

Melanie Connerth,^{1*} Takashi Tatsuta,^{1*} Mathias Haag,^{1*} Till Klecker,² Benedikt Westermann,² Thomas Langer^{1,3†}

Mitochondria are dynamic organelles whose function depends on intramitochondrial phospholipid synthesis and the supply of membrane lipids from the endoplasmic reticulum. How phospholipids are transported to and in-between mitochondrial membranes remained unclear. We identified Ups1, a yeast member of a conserved family of intermembrane space proteins, as a lipid transfer protein that can shuttle phosphatidic acid between mitochondrial membranes. Lipid transfer required the dynamic assembly of Ups1 with Mdm35 and allowed conversion of phosphatidic acid to cardiolipin in the inner membrane. High cardiolipin concentrations prevented membrane dissociation of Ups1, leading to its proteolysis and inhibiting transport of phosphatidic acid and cardiolipin synthesis. Thus, intramitochondrial lipid trafficking may involve a regulatory feedback mechanism that limits the accumulation of cardiolipin in mitochondria.

Each cellular membrane has a characteristic lipid composition that is required for its function (1, 2). Phospholipids are synthesized predominantly in the endoplasmic reticulum (ER) and must be redistributed to all cellular membranes (3). Extensive exchange of phospho-

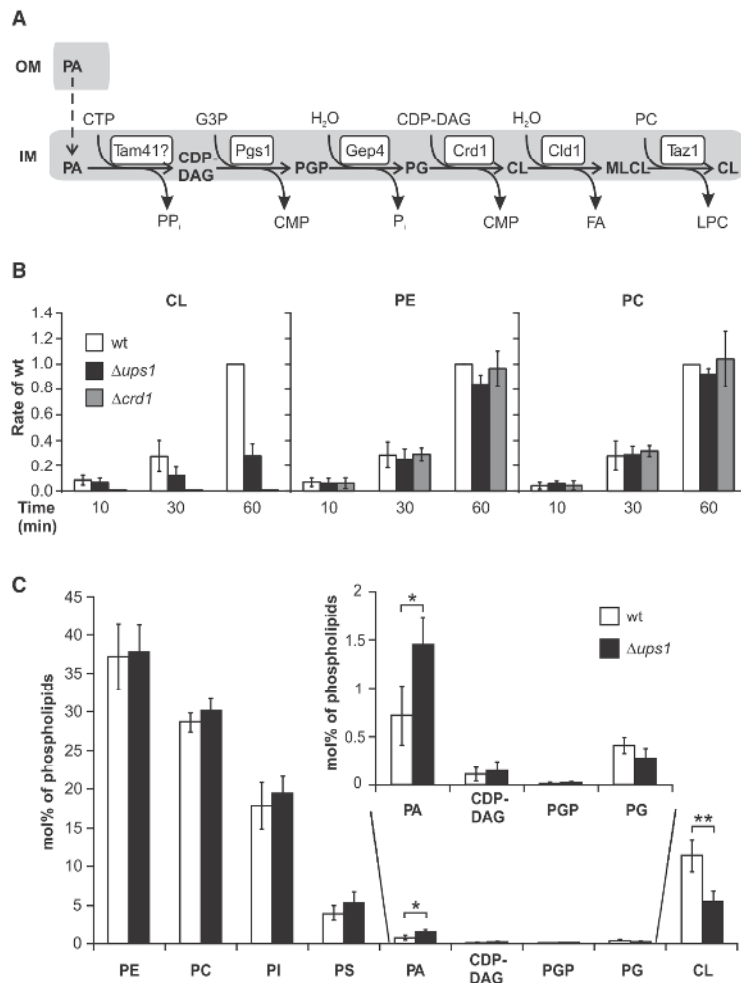
lipids between the ER and mitochondria is important in the synthesis of specific lipids (4, 5). These include cardiolipin (CL), a signature phospholipid of mitochondrial membranes, which is required for mitochondrial function and morphogenesis (5). CL is synthesized along an enzymatic cascade in the mitochondrial inner membrane (IM) from phosphatidic acid (PA) that is imported from the ER (Fig. 1A). However, how phospholipids shuttle from the ER to mitochondria, across the outer membrane (OM) to the IM and back, is not understood.

In yeast, Ups1 and Ups2, members of the conserved MSF1/PRELI protein family localized in the mitochondrial intermembrane space (IMS),

¹Institute for Genetics, Cologne Excellence Cluster on Cellular Stress Responses in Aging-Associated Diseases (CECAD), Center for Molecular Medicine (CMMC), University of Cologne, 50674 Cologne, Germany. ²Institute for Cell Biology and Electron Microscopy Laboratory, University of Bayreuth, 95440 Bayreuth, Germany. ³Max-Planck-Institute for Biology of Aging, 50931 Cologne, Germany.

*These authors contributed equally to this work. †To whom correspondence should be addressed. E-mail: thomas.langer@uni-koeln.de

Fig. 1. CL synthesis in $\Delta ups1$ mitochondria. **(A)** Enzymatic cascade mediating CL synthesis. The function of Tam41 at early stages of CL synthesis is unclear. MLCL, monolysocardiolipin; LPC, lysophosphatidylcholine; G3P, glycerol-3-phosphate; FA, fatty acid; CMP, cytidine 5'-monophosphate; CTP, cytidine 5'-triphosphate; P_i, inorganic phosphate; PP_i, inorganic pyrophosphate. Other abbreviations are used as in the text. **(B)** Impaired CL synthesis in $\Delta ups1$ mitochondria. Incorporation of ³²P into CL, PE, or PC was monitored at the indicated times in wild-type (wt), $\Delta ups1$, and $\Delta crd1$ cells. ³²P incorporation in wt was set to 1. **(C)** Phospholipidome of sucrose gradient-purified wt and $\Delta ups1$ mitochondria determined by MS. Data represent mean values \pm SD, $n = 4$; * $P < 0.05$, ** $P < 0.005$ (unpaired t test, two-tailed).



REPORTS

are required for the mitochondrial accumulation of CL and phosphatidylethanolamine (PE), respectively (6, 7). Incorporation of ³²P into CL was impaired in $\Delta ups1$ mitochondria and completely inhibited in the absence of the cardiolipin synthase *Crd1* (Fig. 1B). To define the role of *Ups1* in CL synthesis, we determined the phospholipidome of $\Delta ups1$ mitochondria by quantitative mass spectrometry (MS) (Fig. 1C). CL was reduced in $\Delta ups1$ mitochondria, whereas other main phospholipids remained unaffected (Fig. 1C and fig. S1) (6, 8). The low-abundance precursor phospholipid PA accumulated in these mitochondria (Fig. 1C), suggesting that *Ups1* acts early during CL synthesis.

To substantiate this conclusion, we performed a genetic epistasis analysis of *UPS1* with genes affecting early steps of CL synthesis such as *PGS1* and *TAM41*. *Pgs1* catalyzes the formation of phosphatidylglycerolphosphate (PGP) (9, 10), whereas *Tam41* acts before *Pgs1*, exerting an unknown function (11–13). Cell growth was severely impaired upon deletion of *PGS1*, *TAM41*, or both, but restored upon deletion of *UPS1* (Fig. 2A and fig. S2). Ultrastructurally, mitochondria lacking *Pgs1* contained extremely elongated cristae sheets, which remained connected to the

inner boundary membrane and frequently formed IM septae or onionlike structures (Fig. 2B). Deletion of *UPS1* did not affect the mitochondrial ultrastructure but restored mitochondrial cristae morphology in $\Delta pgs1$ cells (Fig. 2B).

We further determined by MS the mitochondrial phospholipidome of cells lacking *Ups1* in combination with *Pgs1* or *Tam41* (Fig. 2C and fig. S3). CL was reduced or absent in mitochondria lacking either protein, but PA, phosphatidylinositol (PI), and cytidine 5'-diphosphate-diaclyglycerol (CDP-DAG) accumulated in mitochondria lacking *Pgs1* (Fig. 2C and fig. S3). Thus, the different membrane lipid composition rather than merely the absence of CL affects cristae morphology in $\Delta pgs1$ mitochondria. Deletion of *TAM41* resulted in accumulation of PA but not CDP-DAG, suggesting that *Tam41* affects CDP-DAG synthesis (Fig. 2C). The phospholipid composition of *Pgs1*- and *Tam41*-deficient mitochondria lacking *Ups1* was similar to that of $\Delta ups1$ mitochondria. Thus, *Ups1* is epistatic to *Pgs1* and *Tam41*.

The requirement of *Ups1* in the IM for early steps of CL synthesis suggests that *Ups1* may facilitate the transport of PA to the IM (Fig. 1A). To define the molecular function of *Ups1*, we carried out in vitro experiments with purified *Ups1*.

Ups1 assembles with *Mdm35*, which ensures its accumulation in the IMS and protects *Ups1* against degradation by *Yme1* (14). Consistently, *Ups1* was prone to aggregation upon expression in *Escherichia coli* and recovered in the soluble fraction only when coexpressed with *Mdm35* (fig. S4). This allowed purification of heterodimeric *Ups1*-*Mdm35* complexes to homogeneity (fig. S5).

To examine whether *Ups1*-*Mdm35* binds phospholipids, we performed flotation experiments using liposomes composed of phosphatidylcholine (PC) (80%) and another phospholipid (20%) (Fig. 3A). *Ups1* exclusively bound to liposomes containing negatively charged phospholipids such as CL, PA, phosphatidylglycerol (PG), phosphatidylserine (PS), PI, or CDP-DAG but did not interact with PE or PC (Fig. 3, A and B). Purified *Mdm35* did not bind any phospholipid tested (fig. S6), suggesting liposome binding via *Ups1*. The low amount of *Mdm35* recovered with floated membranes in the presence of *Ups1* indicated that liposome binding destabilizes *Ups1*-*Mdm35* complexes (Fig. 3B).

Next, we investigated whether the *Ups1*-*Mdm35* complex transfers phospholipids between liposomes in vitro. Donor liposomes, whose lipid composition resembles that of the OM, were

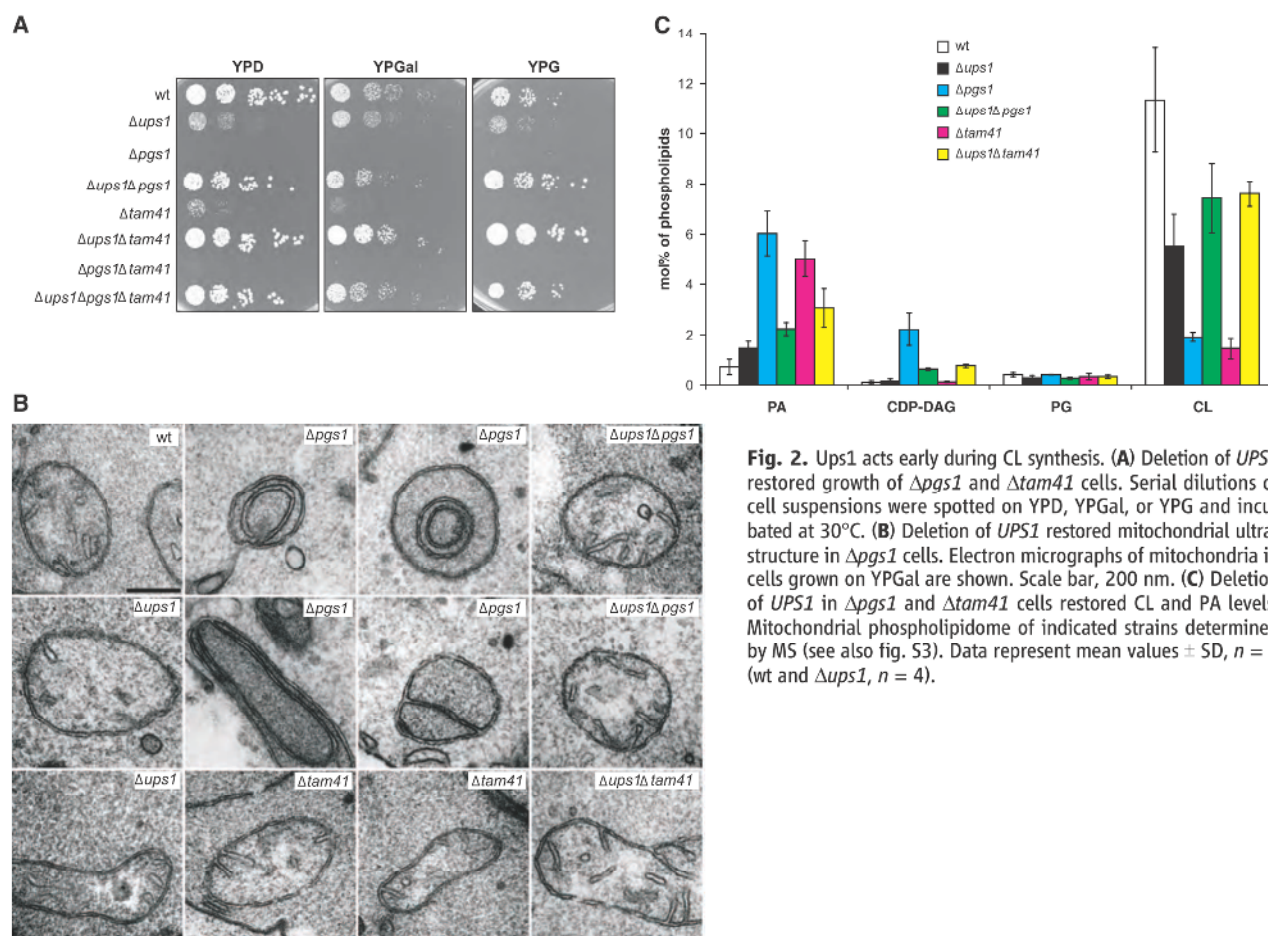


Fig. 2. *Ups1* acts early during CL synthesis. (A) Deletion of *UPS1* restored growth of $\Delta pgs1$ and $\Delta tam41$ cells. Serial dilutions of cell suspensions were spotted on YPD, YPGal, or YPG and incubated at 30°C. (B) Deletion of *UPS1* restored mitochondrial ultrastructure in $\Delta pgs1$ cells. Electron micrographs of mitochondria in cells grown on YPGal are shown. Scale bar, 200 nm. (C) Deletion of *UPS1* in $\Delta pgs1$ and $\Delta tam41$ cells restored CL and PA levels. Mitochondrial phospholipidome of indicated strains determined by MS (see also fig. S3). Data represent mean values \pm SD, $n = 3$ (wt and $\Delta ups1$, $n = 4$).

incubated with Ups1-Mdm35 complexes and acceptor liposomes resembling the IM but lacking PA, PS, PG, or CDP-DAG. We isolated acceptor membranes after flotation and determined their phospholipid composition by MS (Fig. 3C and fig. S7).

Ups1-Mdm35 complexes, but not Mdm35, facilitated PA transfer (Fig. 3C). To further define the transport specificity, we used PC-PE donor liposomes containing one negatively charged phospholipid only (Fig. 3D). Transfer of PA but not of

PI, CDP-DAG, CL, PS, or PG occurred, substantiating the high selectivity of Ups1. Lipid transfer assays using ¹⁴C-PA and ¹⁴C-PC confirmed the protein-dependent and lipid-specific transport of PA by Ups1-Mdm35 complexes (Fig. 3E).

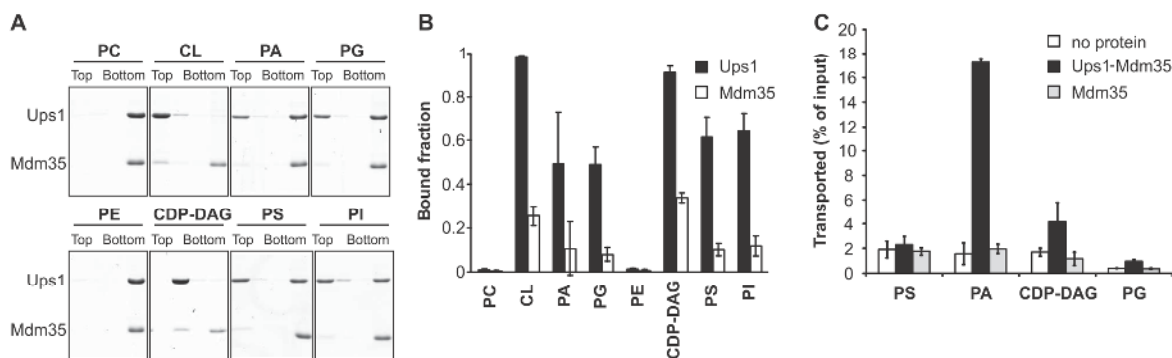


Fig. 3. Lipid transfer by Ups1-Mdm35 complexes in vitro. (A) Phospholipid binding. Purified Ups1-Mdm35 complexes were incubated with liposomes composed of PC (80%) and the indicated phospholipid (20%), and binding was assessed by flotation of liposomes in a sucrose gradient. (B) Quantification of (A). (C) Lipid transport. Donor liposomes (50 μM; PC/PE/PI/CL/PA/PG/PS/CDP-DAG/NBD-PE = 40/24.6/10/5/5/5/5/0.4%) and acceptor liposomes (200 μM; PC/PE/PI/CL/Rhod-PE = 42.2/25.4/16.2/16.1/0.1%) were incubated with Ups1-Mdm35 complexes for 10 min. Acceptor liposomes were analyzed by MS. (D) Lipid specificity. Donor liposomes composed of PC (50%), PE (40%), and 10% of the indicated lipid were incubated with acceptor liposomes (PC/PE = 50/50%) and Ups1-Mdm35 complexes (66.7 nM). Acceptor liposomes were analyzed by MS. (E) PA transport. Donor liposomes (50 μM; PC/PE/PI/lactosyl-PE/PS/CL/PA/NBD-PE = 40/17.1/15/10/5/5/0.4%) containing ¹⁴C-PA or ¹⁴C-PC and acceptor liposomes (200 μM; PC/PE/PI/CL/Rhod-PE = 42.2/25.4/16.2/16.1/0.1%) were incubated for 10 min with the indicated proteins. Data represent mean values ± SD, n = 3.

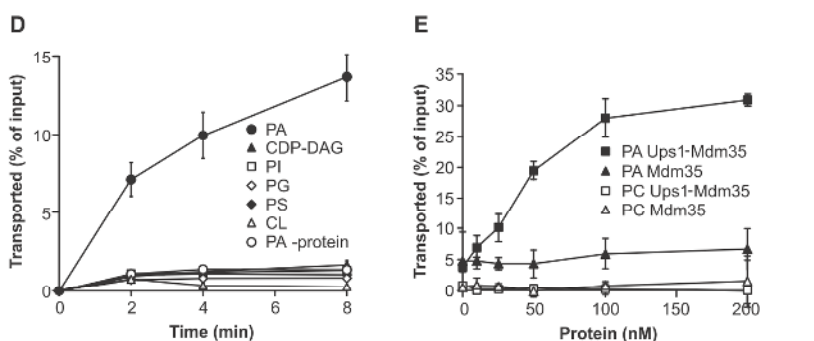
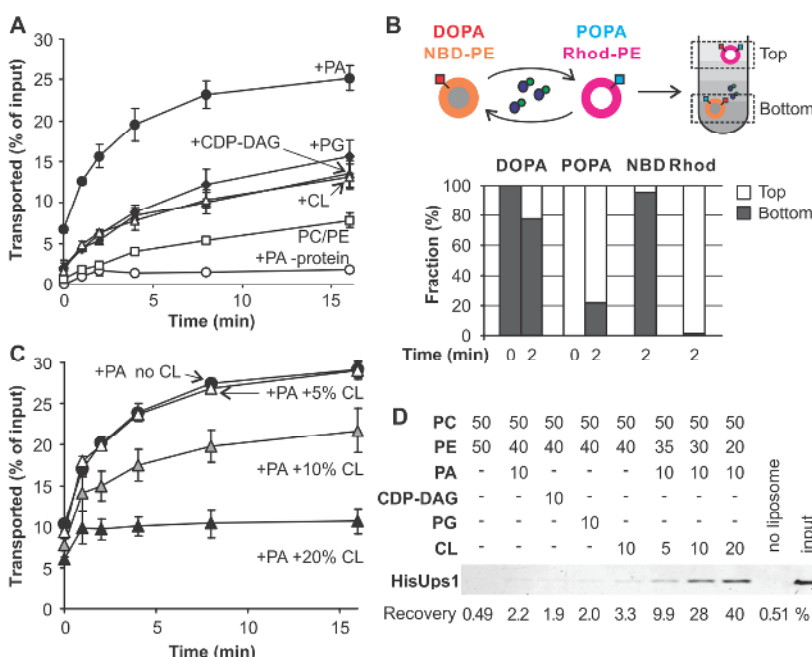


Fig. 4. Characteristics of PA transfer by Ups1-Mdm35 complexes. (A) Negatively charged phospholipids in the acceptor membrane facilitated PA transport. Ups1-Mdm35 complexes (20 nM) were incubated with donor liposomes (25 μM; PC/PE/PA/lactosyl-PE/NBD-PE = 50/29.6/10/10/0.4%) containing ¹⁴C-PA and acceptor liposomes (100 μM) composed of PC and PE (50/40%) and the indicated phospholipid (10%). Data represent mean values ± SEM, n = 3. (B) Bidirectional transport of PA. Ups1-Mdm35 complexes (20 nM) were incubated with heavy liposomes [(50 μM; PC/PE/DOPA(*di*-18:1PA)/NBD-PE = 50/39.9/10/0.1%)] and light liposomes [(50 μM; PC/PE/POPA(16:1/18:1PA)/Rhod-PE = 50/39.9/10/0.1%)]. Liposomes were separated by flotation and lipids analyzed by MS. (C) CL in the acceptor membrane inhibits PA transport. Donor liposomes (25 μM; PC/PE/PA/lactosyl-PE/NBD-PE = 50/29.6/10/10/0.4%) containing ¹⁴C-PA and acceptor liposomes (100 μM; PC/PE/PA/Rhod-PE = 50/39.9/10/0.1%) containing increasing concentrations of CL (replacing PE) were incubated with Ups1-Mdm35 complexes (20 nM). Data represent mean values ± SEM, n = 3. (D) Ups1 remains bound to CL-rich liposomes. Ups1-Mdm35 complexes (20 nM) were incubated with liposomes (100 μM) of the indicated composition. Liposome-associated proteins were analyzed by SDS-polyacrylamide gel electrophoresis and immunoblotting.



	PC	PE	PA	CDP-DAG	PG	CL	no liposome	input
PC	50	50	50	50	50	50	50	50
PE	50	40	40	40	40	35	30	20
PA	-	10	-	-	-	10	10	10
CDP-DAG	-	-	10	-	-	-	-	-
PG	-	-	-	10	-	-	-	-
CL	-	-	-	-	10	5	10	20

Recovery 0.49 2.2 1.9 2.0 3.3 9.9 28 40 0.51 %

REPORTS

Because negatively charged phospholipids like CL, PG, or CDP-DAG were bound by Ups1 but not efficiently transported, we tested whether they influence PA transport when present in acceptor membranes (Fig. 4A). We observed slow PA transport in the absence of any negatively charged phospholipid. However, transport was accelerated when CL, PG, or CDP-DAG was present in the acceptor membrane (10%) (Fig. 4A), indicating that Ups1 binding is rate-limiting for transport under these conditions. Although binding to Ups1 with similar efficiency (Fig. 3A), the presence of PA in acceptor membranes stimulated the transport more than other negatively charged phospholipids (Fig. 4A).

We reasoned that Ups1-Mdm35 complexes mediated PA transport in a bidirectional manner, similar to that of other lipid transfer proteins (15, 16). Accordingly, PA in acceptor liposomes could facilitate membrane dissociation of Ups1 after PA delivery. To obtain evidence for bidirectional transport, we included PA with different acyl chains in donor 1,2-dioleoyl-*sn*-glycero-3-phosphate (DOPA) and acceptor 1-palmitoyl-2-oleoyl-*sn*-glycero-3-phosphate (POPA) liposomes and monitored the redistribution of PA in the presence of Ups1-Mdm35 complexes by MS (Fig. 4B). DOPA accumulated in acceptor membranes at levels similar to those of POPA in donor membranes, suggesting that PA transport can occur bidirectionally and independent of its acyl chain composition (Fig. 4B).

The IM contains higher concentrations of CL than the OM (17). We thus performed lipid transfer assays at optimal PA and increasing CL concentrations in acceptor membranes (Fig. 4C). CL inhibited PA transfer when present in acceptor membranes at concentrations that mimic the IM (10 to 20%). Similarly, PG exerted an inhibitory effect on PA transport (fig. S8). At high CL concentrations, Ups1 remained associated with liposomes (Fig. 4D), indicating that CL impairs the dissociation of Ups1 from the membrane. Similarly, Ups1 accumulated at the IM in mitochondria that contain similar concentrations of CL but lack Yme1, which is responsible for its rapid turnover (14) (fig. S9). Thus, CL present at physiological concentrations traps Ups1 irreversibly at membranes, where it is degraded by Yme1, rendering PA transport irreversible.

Here, we identify Ups1 as a lipid transfer protein in the IMS that acts early during CL biosynthesis. Our *in vitro* results suggest that Ups1 mediates PA transport between mitochondrial membranes in distinct steps (fig. S10): Upon PA binding to Ups1 and PA extraction from the membrane, Ups1 assembles with Mdm35, which stabilizes Ups1 in a transfer-competent conformation. Negatively charged phospholipids facilitate the interaction of Ups1-Mdm35 complexes with the acceptor membrane, which is accompanied by the dissociation of Mdm35 and the release of PA. The enzymatic conversion of PA into CL in the IM provides directionality to the transport reaction.

Ups1 binds but does not transfer negatively charged phospholipids like CL, which is en-

riched at contact sites between the IM and OM (18). PA accumulates at these sites in Δ ups1 mitochondria (fig. S11). CL binding may thus recruit Ups1 to contact sites and facilitate PA transfer at sites of close membrane apposition *in vivo*, although direct membrane contacts are not required for Ups1-mediated PA transport *in vitro* (figs. S12 and S13). Moreover, high CL concentrations impair the dissociation of Ups1 from the IM and inhibit PA transfer, offering an intriguing possibility to limit CL accumulation in the IM.

Our epistasis analysis revealed an alternative route for CL synthesis that is activated in the absence of Ups1 and does not depend on PGP synthesis by Pgs1. These observations indicate that CL precursor lipids other than PA can reach the IM by other means. Although this pathway remains to be defined, the positive genetic interaction of Ups1 with Pgs1 and Tam41 suggests deleterious effects of PA accumulating in the IM in Δ pgs1 and Δ tam41 mitochondria.

The mechanism of PA transport by Ups1 is reminiscent of other known lipid transfer proteins that shuttle lipids between cellular membranes (2, 19). Although not related at the sequence level, structural modeling using template-based comparative modeling [i-TASSER (20)] suggests a fold for Ups1 similar to that of phosphatidylinositol transfer proteins (fig. S14). Ups1 is functionally conserved from yeast to human and a member of a conserved family of mitochondrial proteins (21). Other family members may serve as lipid transfer proteins with different lipid specificity within mitochondria.

References and Notes

1. G. van Meer, D. R. Voelker, G. W. Feigenson, *Nat. Rev. Mol. Cell Biol.* **9**, 112 (2008).
2. W. A. Prinz, *Cell* **143**, 870 (2010).
3. G. Daum, N. D. Lees, M. Bard, R. Dickson, *Yeast* **14**, 1471 (1998).
4. B. Kornmann, P. Walter, *J. Cell Sci.* **123**, 1389 (2010).
5. C. Osman, D. R. Voelker, T. Langer, *J. Cell Biol.* **192**, 7 (2011).
6. C. Osman *et al.*, *J. Cell Biol.* **184**, 583 (2009).
7. Y. Tamura, T. Endo, M. Iijima, H. Sesaki, *J. Cell Biol.* **105**, 1029 (2009).
8. Y. Tamura *et al.*, *J. Biol. Chem.* **287**, 15205 (2012).
9. S. C. Chang, P. N. Heacock, C. J. Clancey, W. Dowhan, *J. Biol. Chem.* **273**, 9829 (1998).
10. M. Janitor, M. Obernauerová, S. D. Kohlwein, J. Subik, *FEMS Microbiol. Lett.* **140**, 43 (1996).
11. S. Kutik *et al.*, *J. Cell Biol.* **183**, 1213 (2008).
12. C. Osman, M. Haag, F. T. Wieland, B. Brügger, T. Langer, *EMBO J.* **29**, 1976 (2010).
13. Y. Harada, Y. Tamura, T. Endo, *Biochem. Biophys. Res. Commun.* **392**, 228 (2010).
14. C. Potting, C. Wilmes, T. Engmann, C. Osman, T. Langer, *EMBO J.* **29**, 2888 (2010).
15. M. de Saint-Jean *et al.*, *J. Cell Biol.* **195**, 965 (2011).
16. A. M. Kasper, G. M. Helmkamp Jr., *Biochim. Biophys. Acta* **664**, 22 (1981).
17. E. Zinser *et al.*, *J. Bacteriol.* **173**, 2026 (1991).
18. R. Simbeni, L. Pon, E. Zinser, F. Paltauf, G. Daum, *J. Biol. Chem.* **266**, 10047 (1991).
19. K. Hanada, K. Kumagai, N. Tomishige, T. Yamaji, *Biochim. Biophys. Acta* **1791**, 684 (2009).
20. A. Roy, A. Kucukural, Y. Zhang, *Nat. Protoc.* **5**, 725 (2010).
21. H. Sesaki *et al.*, *J. Cell Biol.* **173**, 651 (2006).

Acknowledgments: We thank G. Zimmer for technical assistance, S. Geimer for advice on electron microscopy, T. Endo for sharing unpublished results, and J. Nunnari for yeast strains. This work was supported by grants from the Deutsche Forschungsgemeinschaft (SFB635, FOR885) and the European Research Council (AdG No. 233078) to T.L.

Supplementary Materials

www.sciencemag.org/cgi/content/full/science.1225625/DC1
Materials and Methods
Figs. S1 to S16
Table S1
References (22–31)

4 June 2012; accepted 17 September 2012
Published online 4 October 2012;
10.1126/science.1225625



www.sciencemag.org/cgi/content/full/science.1225625/DC1

Supplementary Materials for

Intramitochondrial Transport of Phosphatidic Acid in Yeast by a Lipid Transfer Protein

Melanie Connerth, Takashi Tatsuta, Mathias Haag, Till Klecker, Benedikt Westermann,
Thomas Langer*

*To whom correspondence should be addressed. E-mail: thomas.langer@uni-koeln.de

Published 4 October 2012 on *Science Express*
DOI: 10.1126/science.1225625

This PDF file includes:

Materials and Methods
Figs. S1 to S16
Table S1
References (22–31)

Materials and Methods

Yeast strains and growth conditions

S. cerevisiae strains used in this study are derivatives of S288c (22) and are listed in Table S1. Yeast transformation was performed using standard methods and ORF replacement was achieved by homologous recombination (23). Yeast strains were cultivated in YPD (2% peptone, 1% yeast extract, 2% glucose), YPG (3% glycerol, 1% yeast extract, 2% glucose) or YPGal (2% peptone, 1% yeast extract, 0.5% lactate, 2% galactose) as indicated.

Cell fractionation and isolation of mitochondrial membranes

Cell fractionation and isolation of mitochondria from yeast cells grown in YPGal was performed according to standard procedures (24, 25). For further purification, crude mitochondria were washed, resuspended in buffer A (0.6 M sorbitol, 5 mM MES pH 6.0) and loaded on a continuous sucrose gradient [20-50% (w/v) in buffer A]. Sucrose gradient purified-mitochondria were collected from the lower third of the gradient after centrifugation at 100,000 $\times g$ for 1 h and washed in cold SEM buffer (10 mM MOPS/KOH pH 7.2, 1 mM EDTA, 0.25 M sucrose). Isolation of outer and inner membrane fractions was performed as described by Harner et al. (26). Since membrane vesicles derived from wt and $\Delta ups1$ mitochondria exhibit different buoyant densities, wt vesicles were separated on a 27-42% (w/v), $\Delta ups1$ vesicles on a 27-35% (w/v) sucrose gradient to obtain a similar distribution of marker proteins. Intermediate density fractions containing contact sites were identified by immunoblotting using Fcj1 and Aim13 as marker proteins (26, 27). Fractions containing OM or IM vesicles were identified by immunoblotting with respective marker proteins. Protein concentration was determined by the Bradford assay. Fractionation of cell organelles and the purity of mitochondria were assessed by SDS-PAGE and Western blotting according to standard procedures (see Fig. S15).

Monitoring cardiolipin synthesis in vivo

Logarithmically growing cells (10 OD) were resuspended in YPGal medium (1.7 ml) containing ^{32}P -phosphoric acid (10 μ Ci) and incubated at 30°C. At time points indicated, cells were collected and snap frozen in liquid nitrogen. After thawing, cells were resuspended in 300 μ l ice cold SHKCl buffer (50 mM HEPES/KOH pH 7.4, 0.6 M sucrose, 80 mM KCl, 1 mM PMSF) and glass beads (200 μ l) were added. Samples were vortexed 4 x 30 s and cooled on ice for 30 s in between. After addition of ice cold SHKCl buffer (400 μ l) cell debris was removed by centrifugation at 1,200 $\times g$ for 3 min. Mitochondria were isolated from the supernatant fraction by centrifugation at 17,500 $\times g$ for 10 min. The mitochondrial pellet fraction was washed in SHKCl buffer (400 μ l) and lipids were extracted using chloroform/methanol [2:1 (v/v); 1.5 ml] for 1 h. Lipids were separated by thin layer chromatography using chloroform/methanol/ammonia [50:50:3 (v/v/v)]. The incorporation of ^{32}P into different phospholipid classes was quantified using the ImageQuant TL software (GE Healthcare).

Electron microscopy

Cells were grown to mid log phase in liquid YPGal medium and prepared as previously described (28). Ultrathin 50-60 nm sections were post-stained in 2% uranyl acetate for 15 min and in lead citrate for 4 min. Samples were examined using a ZEISS CEM 902 (Carl Zeiss, Oberkochen, Germany) transmission electron microscope operated at 80 kV. For taking micrographs a 1350 x 1050 pixel Erlangshen ES500W CCD camera (Gatan, Peasanton CA) and Gatan Digital Micrograph software (Version 1.70.16) were used.

Purification of Ups1/Mdm35 complexes

A *UPS1* variant, which encodes Ups1 harboring an amino terminal hexahistidine peptide, and *MDM35* were cloned into pETDuet-1 vector (Merck) and expressed in *E. coli* Origami B (DE3) cells. After incubation at 37°C for 2 h, the culture was shifted to 30°C for 1 h and Ups1 and Mdm35 were expressed after adding 0.1 mM IPTG for 5 h. Cells were collected, washed and resuspended in lysis buffer B [50 mM Tris/HCl, pH 8, 250 mM NaCl, 1x complete EDTA-free protease inhibitor cocktail (Roche), 1 mM PMSF, 40 mM imidazole]. Cells were treated by Emulsi-Flex C5 cell disruptor (Avestin) two times at 20,000 psi and the lysate was centrifuged at 30,000 xg for 20 min. The supernatant was passed through a 0.45 µm filter and applied on a HisTrap column (GE healthcare). Bound proteins were eluted with a linear gradient of imidazole and the peak fractions were collected and concentrated in a spin concentrator (Amicon Ultra, Millipore). The concentrate was applied on a HiLoad 16/60 superdex-75 pg column (GE healthcare) and the peak fractions were collected and concentrated. The concentrate was dialyzed in buffer C (10 mM Tris/HCl, pH 7.4, 150 mM NaCl) and stored at -80°C. The protein concentration was determined by absorbance at 280 nm and calculated using the extinction coefficient of the protein complex.

Mass spectrometric lipid analysis

Lipids were extracted from sucrose gradient-purified mitochondria (100 µg) or when indicated from total cell homogenate (100 µg), endoplasmic reticulum (100 µg), crude mitochondria (100 µg), outer and inner mitochondrial membrane fractions or liposomes in the presence of internal standards that were obtained from Avanti Polar Lipids: PC 17:0-14:1, PE 17:0-14:1, PI 17:0-14:1, PS 17:0-14:1, PG 17:0-14:1, PA 17:0-14:1, CDP-DAG 17:0-18:1 and CL 14:0-14:0-14:0-14:0. Lipid extraction was performed according to Bligh and Dyer (29). Briefly, 1.875 ml chloroform/methanol/25% HCl [40:80:0.6, (v/v/v)] and x µl sample was added to the lipid standards. After vortexing for 30 s, H₂O (0.5 ml – x µl sample) was added followed by vortexing. After the addition of 0.5 ml chloroform and 0.5 ml H₂O, the sample was mixed again and phase separation was induced by centrifugation (800 xg, 2 min). The lower chloroform phase was transferred to a second vial and the remaining phases were washed with chloroform and H₂O. The chloroform phase of the second vial was transferred to a third vial and the chloroform phase of the initial vial was combined with the aqueous phase of the second vial followed by re-extraction. After phase separation, the chloroform phases were combined and evaporated by a gentle stream of argon at 37°C. Lipids were dissolved in 10 mM ammonium acetate in methanol (positive mode analysis) or 5 mM ammonium acetate and 0.05% piperidine in methanol (negative mode analysis) and analyzed by flow injection using an Agilent 1200 HPLC system (Waldbronn, Germany) with a solvent mixture of 10 mM ammonium acetate in methanol. A flow gradient was performed starting with 30 µl/min for 1 min followed by 11 min of 20 µl/min and 150 µl/min for 8 min. Mass spectrometric analysis was done on a 4000 QTrap triple quadrupole mass spectrometer (Applied Biosystems, Darmstadt, Germany) equipped with a Turbo V electrospray ion source under following settings: curtain gas, 10; collision gas, medium; capillary voltage, ± 4500 V; source temperature, 200 °C; ion source gas 1, 25; ion source gas 2, 20; interface heating, enabled. Nitrogen was used as collision gas at 3.8 x 10⁻⁵ torr. The quadrupoles Q1 and Q3 were operated at unit resolution. PC analysis was carried out in positive ion mode by scanning for precursors of m/z 184 at a collision energy (CE) of 45 eV. PE, PI, PS, PG, PA and CDP-DAG measurements were performed in positive ion mode by scanning for neutral losses of 141 Da, 277 Da, 185 Da, 189 Da, 115 Da and 403 Da at CEs of 30 eV, 35 eV, 30 eV, 35 eV, 25 eV and 40 eV, respectively. PGP species were identified in positive ion mode by scanning for neutral losses of 269 Da at a CE of 35 eV. Quantification was done by multiple reaction monitoring (MRM) with 20 ms dwell time. As a PGP standard is commercially not available, we performed quantification of PGP using the PG standard, assuming that both lipid classes show the same mass spectrometric response behavior. CL species were identified in negative

ion mode by scanning for precursors of m/z 152.9 and quantified by MRM as singly charged ions $[M-H]^-$ at a CE of -90 eV with 100 ms dwell time. Mass spectra were processed by the LipidView Software Version 1.1 (AB Sciex, Darmstadt, Germany) for identification and quantification of lipids. Lipid amounts (pmol) were corrected for response differences between internal standards and endogenous lipids.

Liposomes

Phospholipids including 18:1 Lactosyl PE (1,2-dioleoyl-sn-glycero-3-phosphoethanolamine-N-lactosyl), NBD-PE [1,2-dioleoyl-sn-glycero-3-phosphoethanolamine-N-(7-nitro-2-1,3-benzoxadiazol-4-yl)], and Rhod-PE [1,2-dipalmitoyl-sn-glycero-3-phosphoethanolamine-N-(lissamine rhodamine B sulfonyl)] were obtained from Avanti Polar Lipids. Lipids in stock solutions in chloroform were mixed at the desired molar ratio, and the solvent was evaporated under a flow of argon. The lipid film was hydrated in buffer BLT (5 mM Tris/HCl pH 7.4, 150 mM NaCl) or buffer BLTS (10% sucrose in buffer BLT). The suspension was incubated at room temperature for 1 h and extruded through polycarbonate filters of the desired pore size using a mini-extruder (Avanti Polar Lipids). Liposomes were stored on ice and used within 2 days.

Assessment of liposome binding by flotation

Ups1/Mdm35 complexes (5 μ M) were incubated with liposomes (2 mM total lipids, extruded on 1 μ m filter) in 50 μ l buffer FB (MES/NaOH, pH 5.5, 100 mM NaCl, 2 mM EDTA) at 20°C for 10 min. After incubation, the sample was mixed with 100 μ l of 60% sucrose in buffer FB, put into an ultracentrifuge tube and overlaid with 1.35 ml of FB30 (30% sucrose in FB), 1 ml of FB10 (10% sucrose in FB) and 250 μ l of FB. Tubes were centrifuged at 200,000 $\times g$ for 1.5 h. Four fractions of 700 μ l were collected from the top and proteins in the fractions were precipitated by TCA and analyzed by Tris-Tricine SDS-PAGE and stained with colloidal coomassie brilliant blue. The assay was performed at low pH since lowering pH drastically stabilizes the liposome-protein complexes (see Fig. S16). On the other hand, the size of liposomes did not significantly affect the binding properties.

Lipid transfer assays

The assay was established based on previously described procedures for CERT or Osh proteins (15, 30) (Fig. S7). In a standard reaction, Ups1/Mdm35 complexes (20 nM) were incubated with donor liposomes (25 μ M total lipids, 0.1 μ m, containing 0.4% NBD-PE, reconstituted in BLTS) and an acceptor liposome (100 μ M total lipids, 0.1 μ m, containing 0.1% of Rhod-PE, reconstituted in BLT) in 300 μ l buffer TA (20 mM Tris/HCl pH 7.4, 150 mM NaCl, 1 mM EDTA) at 25°C. After incubation the mixture was placed on ice, mixed with 100 μ l buffer TA30 (30% sucrose in TA) and incubated for 10 min. The mix was placed on an ultracentrifuge tube and overlaid with 600 μ l buffer TA5 (5% sucrose in TA), 400 μ l of TA2.5 (2.5% sucrose in TA) and 75 μ l buffer TA. Tubes were centrifuged at 217,000 $\times g$ for 2.5 h. A fraction of 750 μ l was collected from the top and isolated lipids were analysed by MS. Recovery of donor and acceptor liposomes was assessed by fluorescence of NBD-PE and Rhod-PE (NBD-PE, 535 nm, excitation at 485 nm; Rhod-PE, 595 nm, excitation at 535 nm) before and after flotation.

The assay using radioactive lipids was performed essentially as described above with following modifications. The donor liposome contained 21 nCi 14 C-PA [L- α -dioleoyl (oleoyl-1- 14 C)] or 14 C-PC [L- α -dioleoyl, (dioleoyl-1- 14 C); American Radiolabeled Chemicals] per assay and 10 mol% lactosyl-PE. After incubation for the indicated times, the sample (150 μ l) was mixed with 30 μ l of 2.5 mg/ml of *R. communis* agglutinin RCA120 (Sigma) and incubated for 15 min at 4°C. Tubes were centrifuged for 5 min at 16,100 $\times g$. The radioactivity transferred to acceptor liposomes was determined in the supernatant.

To monitor lipid exchange between two liposomes, one liposome (heavy liposome) containing 10% DOPA (18:1/18:1 PA) was reconstituted in BLT containing 12.5% sucrose, while the other liposome (light liposome) containing 10% POPA (16:0/18:1 PA) was reconstituted in BLT. After the reaction, the liposome mixture was placed on the top of a sucrose cushion composed of 300 μ l TA20 and 300 μ l TA10 in an ultracentrifuge tube and then overlaid with TA5, TA2.5 and TA and subjected to centrifugation as described above. After centrifugation, three fractions of 600 μ l were taken from the top. Recovery of liposomes was assessed by fluorescence of NBD-PE and Rhod-PE. Lipids were extracted from liposomes and analyzed by MS.

Assessment of liposome binding using filter assays

Ups1/Mdm35 complexes (20 nM) were incubated with liposomes (100 μ M total lipids, 0.1 μ m) in 400 μ l buffer TA at 16°C for 4 min. After incubation, samples were concentrated using Microcon YM-100 by centrifugation at 5,000 \times g until the solution on the filter cup was reduced to \sim 20 μ l. 380 μ l of buffer TA was added to the filter cup and the solution was transferred to a new tube with 400 μ l of 0.1% sodium deoxycholate. Proteins were precipitated by TCA and analyzed by Tris-Tricine SDS-PAGE and immunoblotting using polyclonal antisera directed against Ups1.

Structural modeling of Ups1

The amino acid sequence of Ups1 was analyzed using the 3D protein structure prediction tool i-TASSER (20). The best scored model [C-score=-1.29, TM-score=0.55 \pm 0.15, 7.8 \pm 4.4Å (RSMD)] was chosen and used for further molecular modeling and structural alignment against the crystal structure of PITP α [PDB:1T27 (31)].

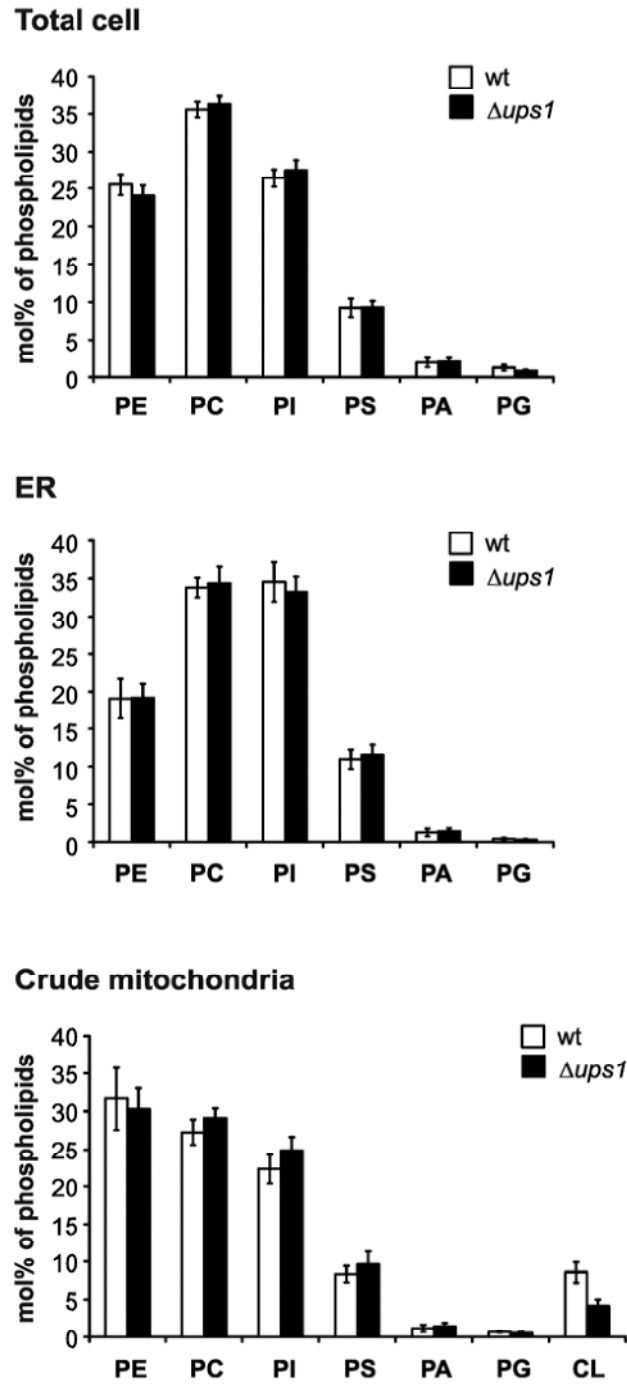
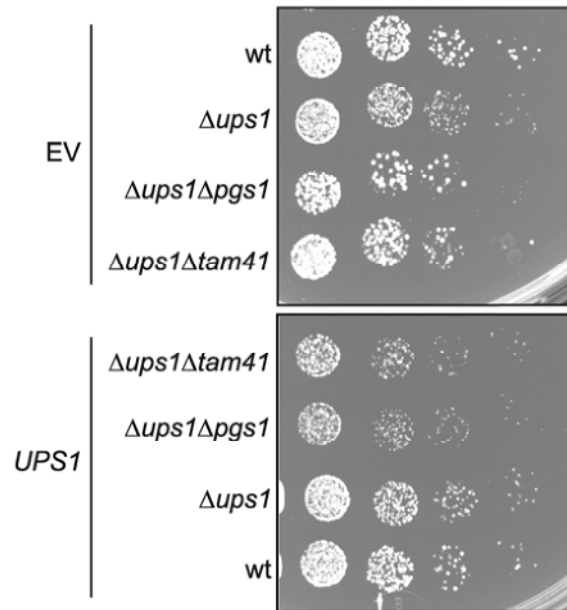


Fig. S1

Phospholipidome of total cell, endoplasmic reticulum (ER) and crude mitochondria derived from wt and $\Delta ups1$ cells. Phospholipid analysis was done by MS. Data represent mean values \pm SD, $N=4$.

**Fig. S2**

Expression of *UPS1* reduced cellular growth of the double mutant cells $\Delta ups1\Delta pgs1$ and $\Delta ups1\Delta tam41$. Serial dilutions of cell suspensions were spotted on YPD and incubated at 30°C. EV, empty vector; *UPS1*, pRS316-*UPS1*.

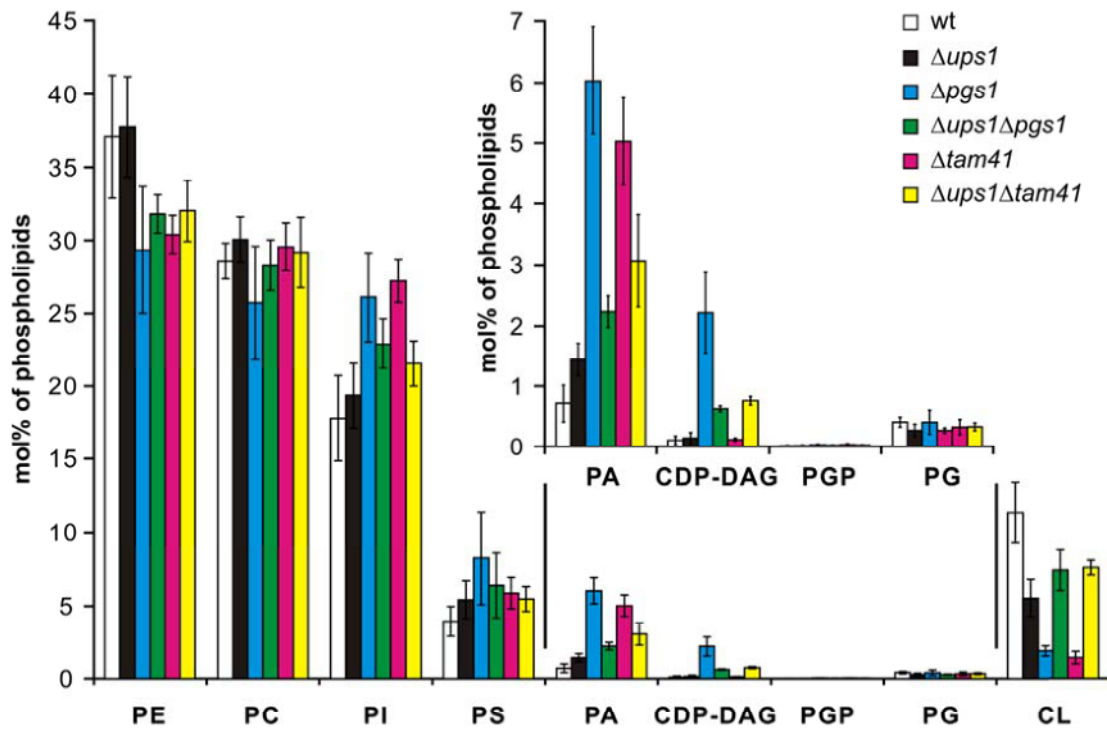


Fig. S3

Deletion of *UPS1* restored CL and PA levels in $\Delta pgs1$ and $\Delta tam41$ mitochondria. Quantitative lipid analysis of sucrose gradient-purified mitochondria isolated from the indicated strains was done by MS. Data represent mean values \pm SD, $N=3$ ($N=4$ for wt and $\Delta ups1$).

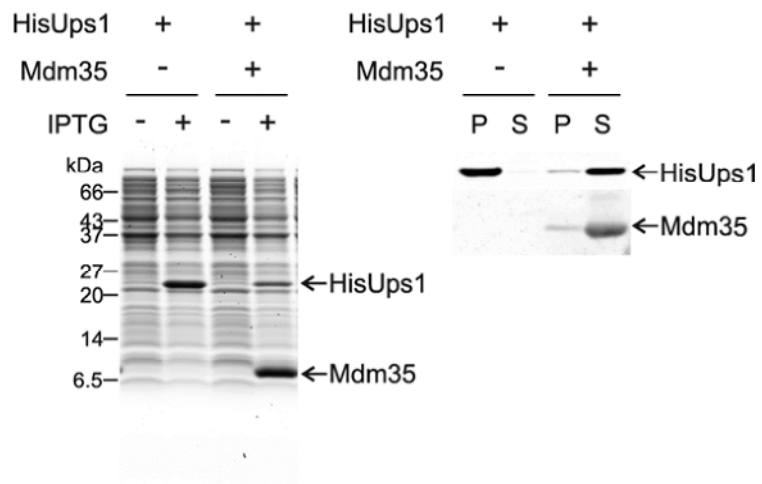
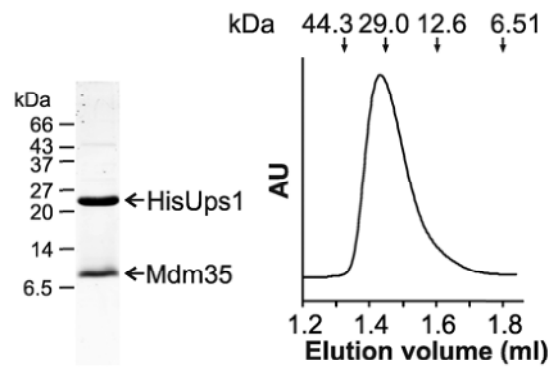
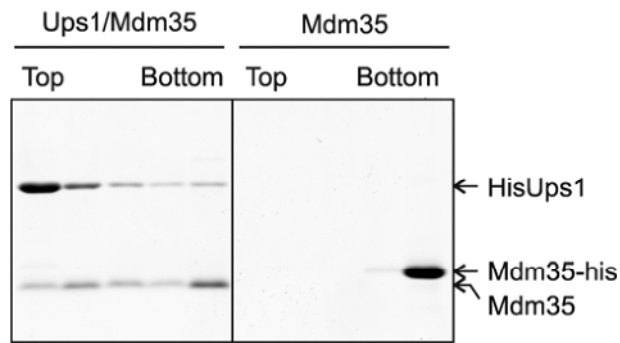


Fig. S4

Ups1 accumulated in *E. coli* in a soluble form in the presence of Mdm35 only. Left panel: expression of HisUps1 and Mdm35 in Origami-B (DE3) 5 hrs after addition of 0.1 mM IPTG. Right panel: Cells were lysed in buffer B and proteins were recovered in the supernatant (S) or pellet (P) fraction after centrifugation.

**Fig. S5**

Ups1 formed a heterodimer with Mdm35. Left panel: Purified protein (10 μ g) was analyzed by Tricine-SDS-PAGE followed by colloidal coomassie staining. Right panel: Size exclusion chromatography of purified Ups1/Mdm35 complexes using a Superdex 75 PC3.2/30 column. AU, arbitrary units.

**Fig. S6**

Mdm35 did not bind to phospholipids. Ups1/Mdm35 complexes or C-terminally his-tagged Mdm35 were incubated with liposomes composed of PC (80%) and CL (20%). Liposomes were floated in a sucrose gradient to assess binding of proteins.

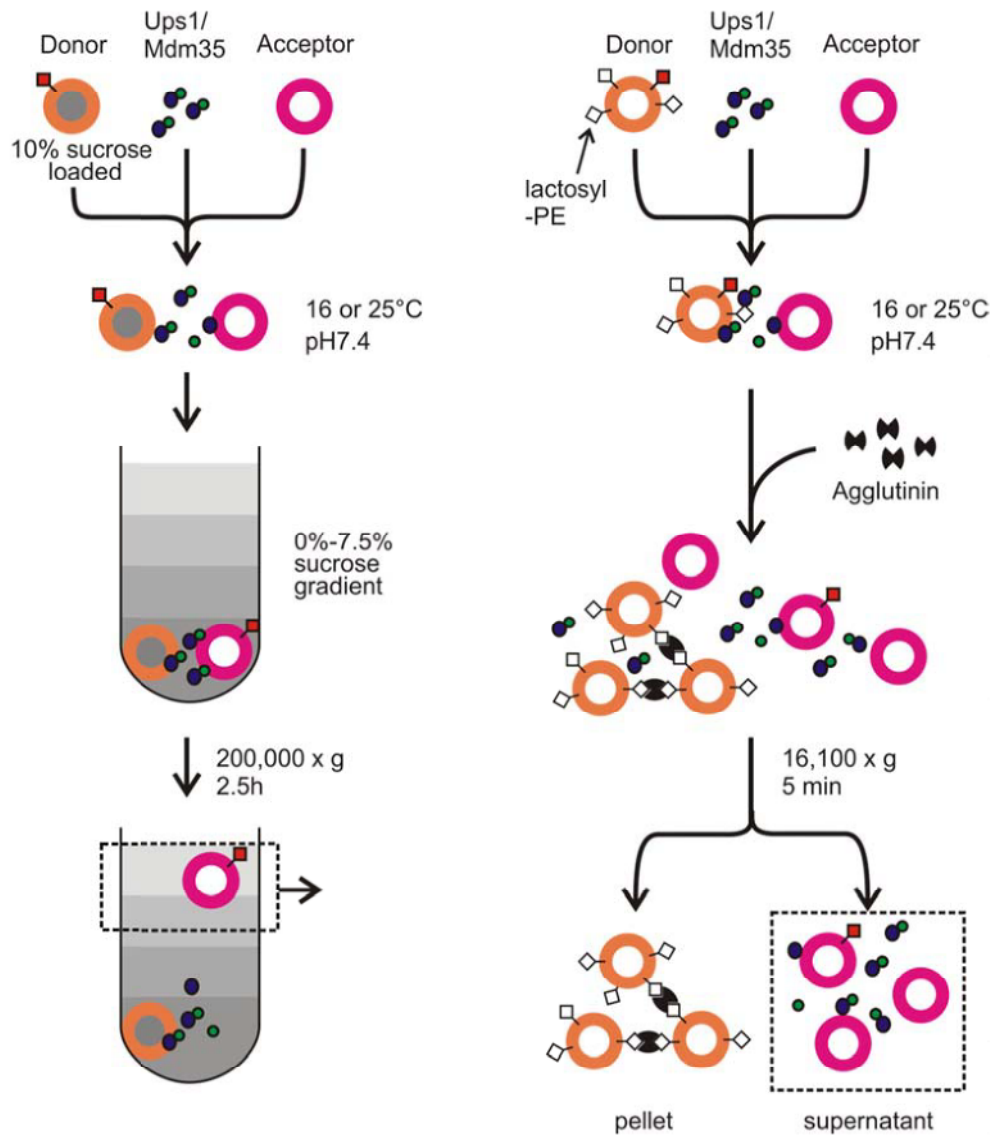
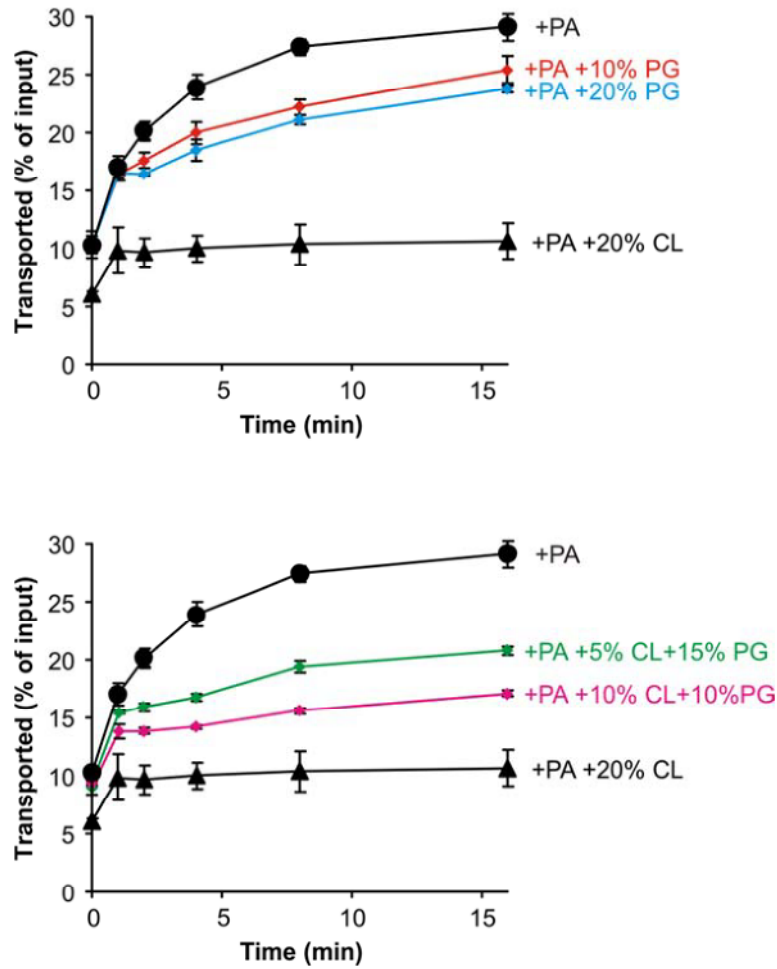
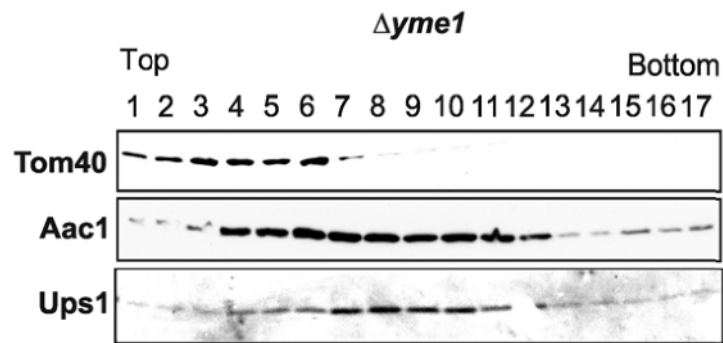


Fig. S7

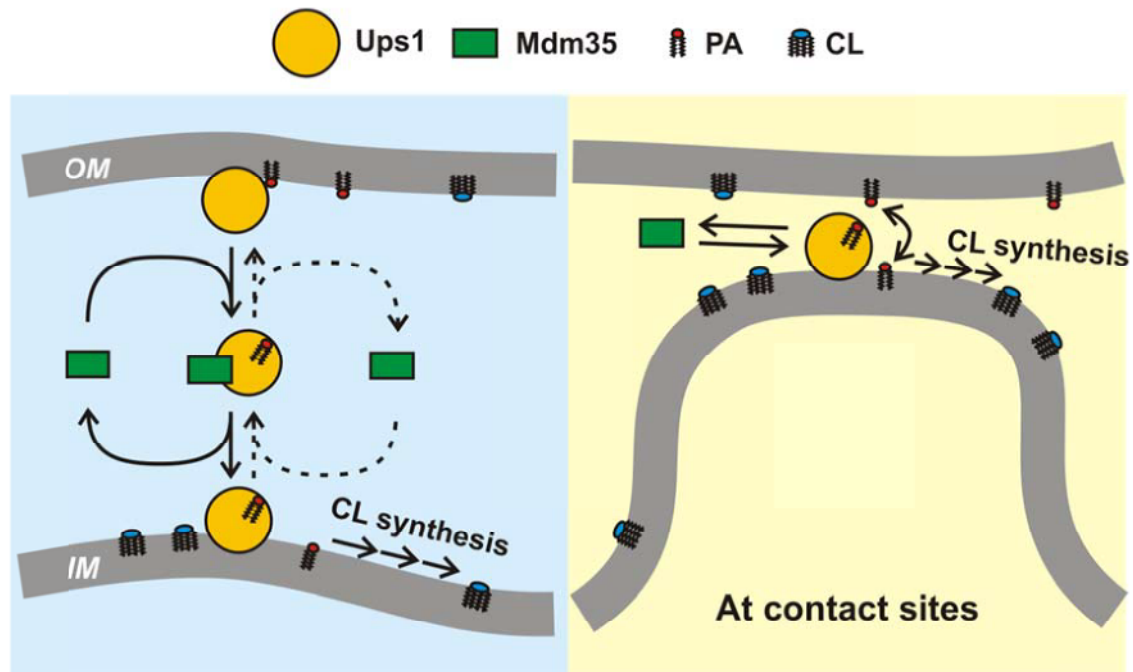
Schematic representations of phospholipid transport assays. Left panel: Separation of donor and acceptor liposomes by sucrose gradient flotation. Donor liposomes contain sucrose (10%). Right panel: Separation of liposomes using agglutinin. Agglutinin allows separation of donor liposomes containing lactosyl-PE (10%) by centrifugation. In each case recovery of liposomes was monitored by fluorescence from NBD-PE (donor) or rhodamine-PE (acceptor).

**Fig. S8**

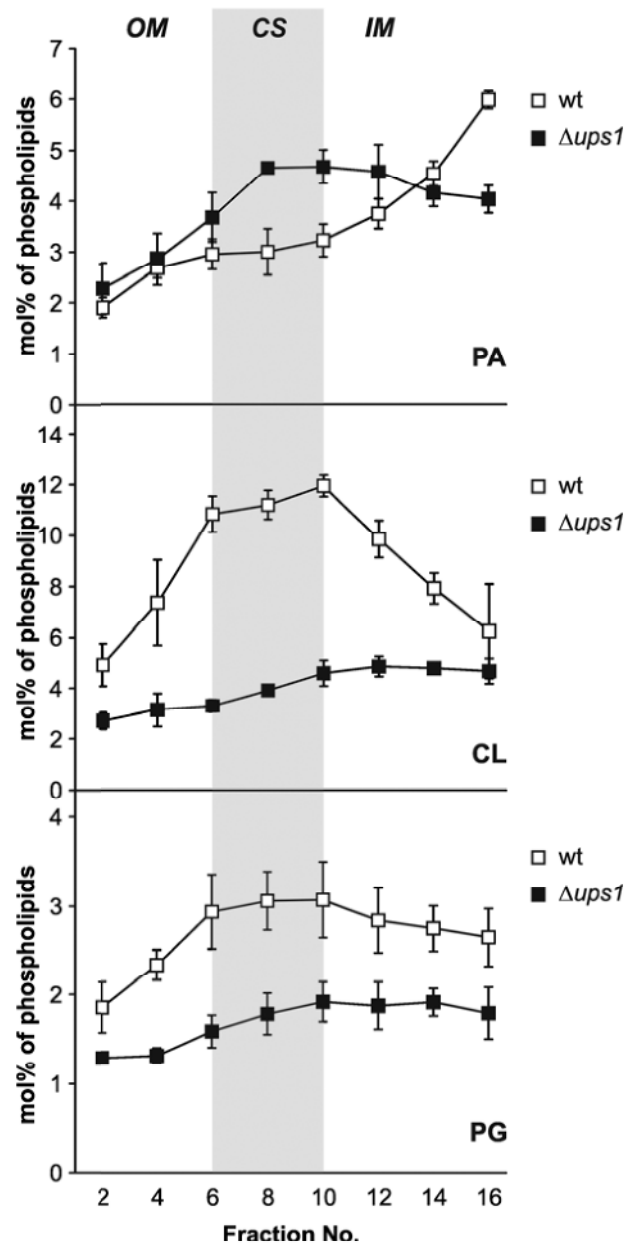
PG in the acceptor membrane inhibited PA transport. Donor liposomes (25 μ M; PC/PE/PA/lactosyl-PE/NBD-PE=50/29.6/10/10/0.4%) containing 14 C-PA and acceptor liposomes (100 μ M; PC/PE/PA/Rhod-PE=50/39.9/10/0.1%) containing increasing concentrations of PG or CL as indicated (replacing PE) were incubated with Usp1/Mdm35 complexes (20 nM). Data represent mean values \pm SEM, $N=3$.

**Fig. S9**

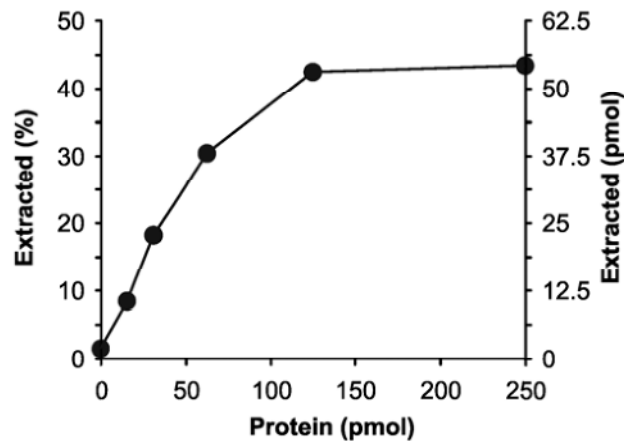
Ups1 was bound to the IM in $\Delta yme1$ mitochondria. Mitochondrial membrane vesicles generated by sonication were fractionated by density gradient centrifugation. Gradient fractions were analyzed by SDS-PAGE and immunoblotting using Tom40 and Aac1 as marker proteins for OM and IM, respectively.

**Fig. S10**

Model for intramitochondrial PA transfer by Ups1/Mdm35 complexes. Left panel: Ups1-mediated PA transport between mitochondrial membranes. Mdm35 forms a heterodimer with Ups1 and stabilizes a transport-competent conformation. Conversion of PA into CL in the IM provides directionality of the transport. Right panel: Ups1-mediated PA transport may occur at contact sites. CL binding by Ups1 may ensure recruitment of Ups1/Mdm35 complexes to contact sites that are enriched in CL.

**Fig. S11**

Distribution of PA, CL and PG in outer (OM), inner membrane (IM) and contact site (CS) fractions derived from wt and $\Delta ups1$ cells. Mitochondrial membranes were sonicated and fractionated by sucrose gradient centrifugation as described in Materials and Methods. Fractions marked in grey contain Fcj1 and Aim13 as marker for contact sites. Phospholipid analysis was done by MS. The amount of PA, CL and PG was normalized to the total phospholipid amount in each fraction. Data represent mean values \pm SD, $N=3$.

**Fig. S12**

Extraction of PA from liposomes by Ups1/Mdm35. Indicated amounts of Ups1/Mdm35 complexes were incubated with donor liposomes (25 μ M; PC/PE/PA/lactosyl-PE/NBD-PE=50/34.6/5/10/0.4%) containing 14 C-PA without acceptor liposomes. The total amount of PA in the reaction is 125 pmol. Liposomes were collected by ultracentrifugation (200,000 \times g, 1 h) and the radioactivity in the resulting supernatant was determined by scintillation counting and used to calculate the amount of extracted PA (right Y-axis).

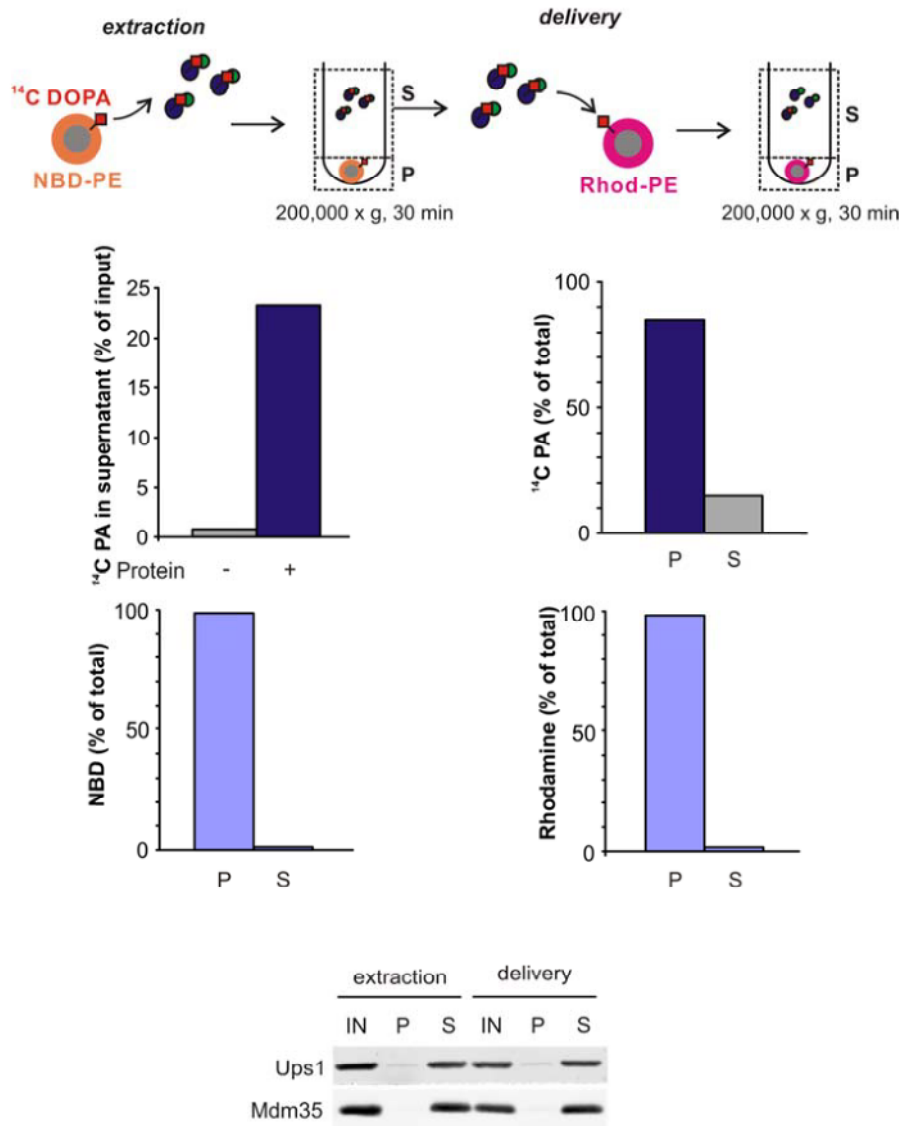


Fig. S13

Staging of lipid transfer reaction. A schematic representation of the assay is shown in the top panel. Ups1/Mdm35 complexes (2 μM) were incubated with donor liposomes (200 μM ; PC/PE/PA/lactosyl-PE/NBD-PE=50/34.6/5/10/0.4%, filled with 12.5% sucrose) containing ^{14}C -PA for 10 min at 25°C. After removal of liposomes by centrifugation, supernatant fractions containing the protein complex and PA were incubated with acceptor liposomes (100 μM , PC/PE/PA/Rhod-PE=50/39.9/10/0.1%, filled with 12.5% sucrose). After incubation for 10 min at 25°C, liposomes were separated by centrifugation and radioactivity in the liposome pellet and the soluble fraction was measured by scintillation counting (second panel). Separation of liposomes or proteins was assessed by fluorescence spectroscopy (third panel) or by SDS-PAGE (lower panel), respectively. Proteins were detected by immunoblotting using antibodies directed against Ups1 or Mdm35 (lower panel).

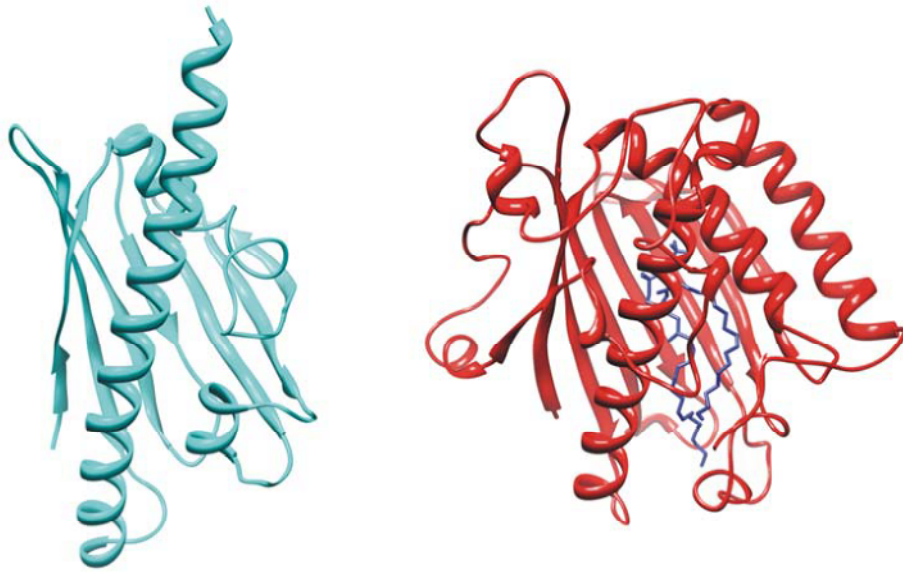
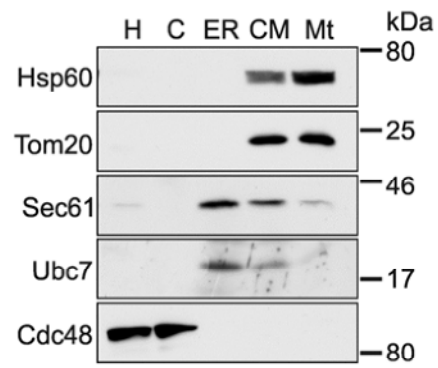
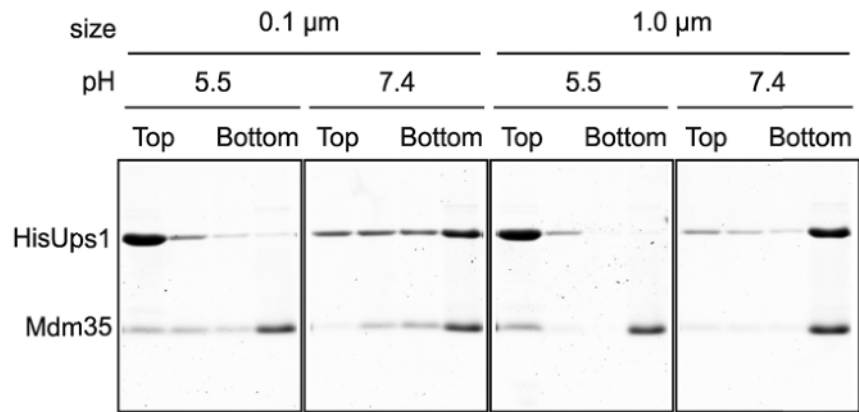


Fig. S14

Structural modeling of Ups1 using template-based comparative modeling and iterative refinements (i-TASSER). A structural model for Ups1 (left) and the crystal structure of PITP complexed with PC [PDB:1T27, (31)] are shown.

**Fig. S15**

Purity of isolated membrane fractions. 40 μ g of protein were separated by SDS-PAGE and analyzed by Western blotting for the presence of marker proteins for mitochondria (Hsp60, Tom20), ER (Sec61, Ubc7) and cytosol (Cdc48). H, homogenate; C, cytosol; ER, endoplasmic reticulum; CM, crude mitochondria; Mt, sucrose gradient-purified mitochondria.

**Fig. S16**

Binding of Ups1/Mdm35 complexes to liposomes was pH-dependent but is not dependent on liposome size. Ups1/Mdm35 complexes were incubated with liposomes composed of PC (80%) and CL (20%) at indicated conditions. Liposomes were floated in a sucrose gradient to assess binding of Ups1/Mdm35 complexes.

Table S1
Yeast strains used in this study

Strain	Alternative name	Background	Genotype	Source
CG214	wildtype (wt)	S288c	<i>MATa his3Δ1 leu2Δ0 met15Δ0 lys2Δ0 ura3Δ0</i>	(6)
PD49	<i>Δups1</i>	S288c	<i>MATa his3Δ1 leu2Δ0 ura3Δ0 Δups1::hphNT1</i>	(6)
MC19	<i>Δups1Δtam41</i>	S288c	<i>MATa his3Δ1 leu2Δ0 met15Δ0 lys2Δ0 ura3Δ0 Δups1::hphNT1 Δtam41::kanMX6</i>	This study
MC20	<i>Δups1Δpgs1</i>	S288c	<i>MATa his3Δ1 leu2Δ0 met15Δ0 lys2Δ0 ura3Δ0 Δups1::hphNT1 Δpgs1::kanMX6</i>	This study
CG772	<i>Δpgs1Δtam41</i>	S288c	<i>MATa his3Δ1 leu2Δ0 met15Δ0 lys2Δ0 ura3Δ0 Δtam41::kanMX6 Δpgs1::NatNT2</i>	(12)
MC52	<i>Δups1Δpgs1Δtam41</i>	S288c	<i>MATa his3Δ1 leu2Δ0 met15Δ0 lys2Δ0 ura3Δ0 Δups1::NatNT1 Δpgs1::hghNT2 Δtam41::kanMX6</i>	This study
CG577	<i>Δpgs1</i>	S288c	<i>MATa his3Δ1 leu2Δ0 met15Δ0 lys2Δ0 ura3Δ0 Δpgs1::hphNT1</i>	(12)
CG760	<i>Δtam41</i>	S288c	<i>MATa his3Δ1 leu2Δ0 met15Δ0 lys2Δ0 ura3Δ0 Δtam41::kanMX6</i>	(12)
VIA5	<i>Δyme1</i>	W303	<i>MATa can1Δ100 his3Δ11,15 leu2Δ3,112 ura3Δ1 ade2Δ1 trp1Δ1 Δyme1::ADE2</i>	(14)
CG637	<i>Δcrd1</i>	S288c	<i>MATa his3Δ1 leu2Δ0 met15Δ0 ura3Δ0 Δcrd1::KanMX4</i>	Euroscarf collection
MC32	<i>FCJ1-HA AIM13-FLAG</i>	W303	<i>MATa can1Δ100 his3Δ11,15 leu2Δ3,112 ura3Δ1 ade2Δ1 trp1Δ1 FCJ1-HA::kanMX6 AIM13-FLAG::HIS3</i>	(27)
MC64	<i>FCJ1-HA AIM13-FLAG Δups1</i>	W303	<i>MATa can1Δ100 his3Δ11,15 leu2Δ3,112 ura3Δ1 ade2Δ1 trp1Δ1 FCJ1-HA::kanMX6 AIM13-FLAG::HIS3 Δups1::NatNT2</i>	This study
MC135	wt + pRS316	S288c	<i>MATa his3Δ1 leu2Δ0 met15Δ0 lys2Δ0 ura3Δ0 pRS316</i>	This study
MC136	wt + pRS316- <i>UPS1</i>	S288c	<i>MATa his3Δ1 leu2Δ0 met15Δ0 lys2Δ0 ura3Δ0 pRS316-UPS1</i>	This study
MC137	<i>Δups1</i> + pRS316	S288c	<i>MATa his3Δ1 leu2Δ0 met15Δ0 lys2Δ0 ura3Δ0 Δups1::hphNT1 pRS316</i>	This study

MC138	$\Delta ups1$ + pRS316- <i>UPS1</i>	S288c	<i>MATα his3Δ1 leu2Δ0 met15Δ0 lys2Δ0 ura3Δ0 $\Delta ups1::hphNT1$ pRS316-<i>UPS1</i></i>	This study
MC130	$\Delta ups1\Delta pgs1$ + pRS316	S288c	<i>MATα his3Δ1 leu2Δ0 met15Δ0 lys2Δ0 ura3Δ0 $\Delta ups1::hphNT1$ $\Delta pgs1::kanMX6$ pRS316</i>	This study
MC131	$\Delta ups1\Delta pgs1$ + pRS316- <i>UPS1</i>	S288c	<i>MATα his3Δ1 leu2Δ0 met15Δ0 lys2Δ0 ura3Δ0 $\Delta ups1::hphNT1$ $\Delta pgs1::kanMX6$ pRS316-<i>UPS1</i></i>	This study
MC132	$\Delta ups1\Delta tam41$ + pRS316	S288c	<i>MATα his3Δ1 leu2Δ0 met15Δ0 lys2Δ0 ura3Δ0 $\Delta ups1::hphNT1$ $\Delta tam41::kanMX6$ pRS316</i>	This study
MC133	$\Delta ups1\Delta tam41$ + pRS316- <i>UPS1</i>	S288c	<i>MATα his3Δ1 leu2Δ0 met15Δ0 lys2Δ0 ura3Δ0 $\Delta ups1::hphNT1$ $\Delta tam41::kanMX6$ pRS316-<i>UPS1</i></i>	This study

References and Notes

1. G. van Meer, D. R. Voelker, G. W. Feigenson, Membrane lipids: Where they are and how they behave. *Nat. Rev. Mol. Cell Biol.* **9**, 112 (2008). [doi:10.1038/nrm2330](https://doi.org/10.1038/nrm2330) [Medline](#)
2. W. A. Prinz, Lipid trafficking sans vesicles: Where, why, how? *Cell* **143**, 870 (2010). [doi:10.1016/j.cell.2010.11.031](https://doi.org/10.1016/j.cell.2010.11.031) [Medline](#)
3. G. Daum, N. D. Lees, M. Bard, R. Dickson, Biochemistry, cell biology and molecular biology of lipids of *Saccharomyces cerevisiae*. *Yeast* **14**, 1471 (1998). [doi:10.1002/\(SICI\)1097-0061\(199812\)14:16<1471::AID-YEA353>3.0.CO;2-Y](https://doi.org/10.1002/(SICI)1097-0061(199812)14:16<1471::AID-YEA353>3.0.CO;2-Y) [Medline](#)
4. B. Kornmann, P. Walter, ERMES-mediated ER-mitochondria contacts: Molecular hubs for the regulation of mitochondrial biology. *J. Cell Sci.* **123**, 1389 (2010). [doi:10.1242/jcs.058636](https://doi.org/10.1242/jcs.058636) [Medline](#)
5. C. Osman, D. R. Voelker, T. Langer, Making heads or tails of phospholipids in mitochondria. *J. Cell Biol.* **192**, 7 (2011). [doi:10.1083/jcb.201006159](https://doi.org/10.1083/jcb.201006159) [Medline](#)
6. C. Osman *et al.*, The genetic interactome of prohibitins: Coordinated control of cardiolipin and phosphatidylethanolamine by conserved regulators in mitochondria. *J. Cell Biol.* **184**, 583 (2009). [doi:10.1083/jcb.200810189](https://doi.org/10.1083/jcb.200810189) [Medline](#)
7. Y. Tamura, T. Endo, M. Iijima, H. Sesaki, Ups1p and Ups2p antagonistically regulate cardiolipin metabolism in mitochondria. *J. Cell Biol.* **185**, 1029 (2009). [doi:10.1083/jcb.200812018](https://doi.org/10.1083/jcb.200812018) [Medline](#)
8. Y. Tamura *et al.*, Role for two conserved intermembrane space proteins, Ups1p and Up2p, in intra-mitochondrial phospholipid trafficking. *J. Biol. Chem.* **287**, 15205 (2012). [doi:10.1074/jbc.M111.338665](https://doi.org/10.1074/jbc.M111.338665) [Medline](#)
9. S. C. Chang, P. N. Heacock, C. J. Clancey, W. Dowhan, The PEL1 gene (renamed PGS1) encodes the phosphatidylglycero-phosphate synthase of *Saccharomyces cerevisiae*. *J. Biol. Chem.* **273**, 9829 (1998). [doi:10.1074/jbc.273.16.9829](https://doi.org/10.1074/jbc.273.16.9829) [Medline](#)
10. M. Janitor, M. Obernauerová, S. D. Kohlwein, J. Subík, The pel1 mutant of *Saccharomyces cerevisiae* is deficient in cardiolipin and does not survive the disruption of the CHO1 gene encoding phosphatidylserine synthase. *FEMS Microbiol. Lett.* **140**, 43 (1996). [Medline](#)
11. S. Kutik *et al.*, The translocator maintenance protein Tam41 is required for mitochondrial cardiolipin biosynthesis. *J. Cell Biol.* **183**, 1213 (2008). [doi:10.1083/jcb.200806048](https://doi.org/10.1083/jcb.200806048) [Medline](#)
12. C. Osman, M. Haag, F. T. Wieland, B. Brügger, T. Langer, A mitochondrial phosphatase required for cardiolipin biosynthesis: The PGP phosphatase Gep4. *EMBO J.* **29**, 1976 (2010). [doi:10.1038/emboj.2010.98](https://doi.org/10.1038/emboj.2010.98) [Medline](#)
13. Y. Harada, Y. Tamura, T. Endo, Identification of yeast Art5 as a multicopy suppressor for the mitochondrial translocator maintenance protein Tam41. *Biochem. Biophys. Res. Commun.* **392**, 228 (2010). [doi:10.1016/j.bbrc.2010.01.024](https://doi.org/10.1016/j.bbrc.2010.01.024) [Medline](#)
14. C. Potting, C. Wilmes, T. Engmann, C. Osman, T. Langer, Regulation of mitochondrial phospholipids by Ups1/PRELI-like proteins depends on proteolysis and Mdm35. *EMBO J.* **29**, 2888 (2010). [doi:10.1038/emboj.2010.169](https://doi.org/10.1038/emboj.2010.169) [Medline](#)

15. M. de Saint-Jean *et al.*, Osh4p exchanges sterols for phosphatidylinositol 4-phosphate between lipid bilayers. *J. Cell Biol.* **195**, 965 (2011). [doi:10.1083/jcb.201104062](https://doi.org/10.1083/jcb.201104062) [Medline](#)
16. A. M. Kasper, G. M. Helmkamp Jr., Intermembrane phospholipid fluxes catalyzed by bovine brain phospholipid exchange protein. *Biochim. Biophys. Acta* **664**, 22 (1981). [doi:10.1016/0005-2760\(81\)90025-4](https://doi.org/10.1016/0005-2760(81)90025-4) [Medline](#)
17. E. Zinser *et al.*, Phospholipid synthesis and lipid composition of subcellular membranes in the unicellular eukaryote *Saccharomyces cerevisiae*. *J. Bacteriol.* **173**, 2026 (1991). [Medline](#)
18. R. Simbeni, L. Pon, E. Zinser, F. Paltauf, G. Daum, Mitochondrial membrane contact sites of yeast. Characterization of lipid components and possible involvement in intramitochondrial translocation of phospholipids. *J. Biol. Chem.* **266**, 10047 (1991). [Medline](#)
19. K. Hanada, K. Kumagai, N. Tomishige, T. Yamaji, CERT-mediated trafficking of ceramide. *Biochim. Biophys. Acta* **1791**, 684 (2009). [doi:10.1016/j.bbalip.2009.01.006](https://doi.org/10.1016/j.bbalip.2009.01.006) [Medline](#)
20. A. Roy, A. Kucukural, Y. Zhang, I-TASSER: A unified platform for automated protein structure and function prediction. *Nat. Protoc.* **5**, 725 (2010). [doi:10.1038/nprot.2010.5](https://doi.org/10.1038/nprot.2010.5) [Medline](#)
21. H. Sesaki *et al.*, Ups1p, a conserved intermembrane space protein, regulates mitochondrial shape and alternative topogenesis of Mgm1p. *J. Cell Biol.* **173**, 651 (2006). [doi:10.1083/jcb.200603092](https://doi.org/10.1083/jcb.200603092) [Medline](#)
22. C. B. Brachmann *et al.*, Designer deletion strains derived from *Saccharomyces cerevisiae* S288C: A useful set of strains and plasmids for PCR-mediated gene disruption and other applications. *Yeast* **14**, 115 (1998). [doi:10.1002/\(SICI\)1097-0061\(19980130\)14:2<115::AID-YEA204>3.0.CO;2-2](https://doi.org/10.1002/(SICI)1097-0061(19980130)14:2<115::AID-YEA204>3.0.CO;2-2) [Medline](#)
23. C. Janke *et al.*, A versatile toolbox for PCR-based tagging of yeast genes: New fluorescent proteins, more markers and promoter substitution cassettes. *Yeast* **21**, 947 (2004). [doi:10.1002/yea.1142](https://doi.org/10.1002/yea.1142) [Medline](#)
24. T. Tatsuta, T. Langer, Studying proteolysis within mitochondria. *Methods Mol. Biol.* **372**, 343 (2007). [doi:10.1007/978-1-59745-365-3_25](https://doi.org/10.1007/978-1-59745-365-3_25) [Medline](#)
25. B. Gaigg, R. Simbeni, C. Hrastnik, F. Paltauf, G. Daum, Characterization of a microsomal subfraction associated with mitochondria of the yeast, *Saccharomyces cerevisiae*. Involvement in synthesis and import of phospholipids into mitochondria. *Biochim. Biophys. Acta* **1234**, 214 (1995). [doi:10.1016/0005-2736\(94\)00287-Y](https://doi.org/10.1016/0005-2736(94)00287-Y) [Medline](#)
26. M. Harner *et al.*, The mitochondrial contact site complex, a determinant of mitochondrial architecture. *EMBO J.* **30**, 4356 (2011). [doi:10.1038/emboj.2011.379](https://doi.org/10.1038/emboj.2011.379) [Medline](#)
27. S. Hoppins *et al.*, A mitochondrial-focused genetic interaction map reveals a scaffold-like complex required for inner membrane organization in mitochondria. *J. Cell Biol.* **195**, 323 (2011). [doi:10.1083/jcb.201107053](https://doi.org/10.1083/jcb.201107053) [Medline](#)
28. C. Bauer, V. Herzog, M. F. Bauer, Improved technique for electron microscope visualization of yeast membrane structure. *Microsc. Microanal.* **7**, 530 (2001). [Medline](#)
29. E. G. Bligh, W. J. Dyer, A rapid method of total lipid extraction and purification. *Can. J. Biochem. Physiol.* **37**, 911 (1959). [doi:10.1139/o59-099](https://doi.org/10.1139/o59-099) [Medline](#)

30. K. Kumagai *et al.*, CERT mediates intermembrane transfer of various molecular species of ceramides. *J. Biol. Chem.* **280**, 6488 (2005). [doi:10.1074/jbc.M409290200](https://doi.org/10.1074/jbc.M409290200) [Medline](#)
31. M. D. Yoder *et al.*, Structure of a multifunctional protein. Mammalian phosphatidylinositol transfer protein complexed with phosphatidylcholine. *J. Biol. Chem.* **276**, 9246 (2001). [doi:10.1074/jbc.M010131200](https://doi.org/10.1074/jbc.M010131200) [Medline](#)

Acknowledgments

I am grateful to:

- ... My principal investigator Benedikt Westermann for his continuous support.
- ... My wife and my family.
- ... The whole Westermann group.
- ... Prof. Dr. Stephan Clemens and Prof. Dr. Olaf Stemmann for fruitful discussions.
- ... Rita Grotjahn and Dr. Stefan Geimer for help with electron microscopy.
- ... Stefan Böckler, Johannes König, Nadine Hock, Takashi Tatsuta, Brigitte Neumann, Matthias Drobny, and Joschka Bauer for providing plasmids and strains.
- ... Stefan Böckler and Maria Klecker for comments on the manuscript.
- ... The DFG for funding.
- ... The *Studienstiftung des deutschen Volkes* and to the *Max-Weber Programm Bayern* for financial support at the beginning of my thesis.

Appendix

List of publications

Connerth, M.*, T. Tatsuta*, M. Haag*, T. Klecker, B. Westermann, and T. Langer. 2012. Intramitochondrial transport of phosphatidic acid in yeast by a lipid transfer protein. *Science*. 338:815-818. doi: 10.1126/science.1225625.

Klecker, T., D. Scholz, J. Förtsch, and B. Westermann. 2013. The yeast cell cortical protein Num1 integrates mitochondrial dynamics into cellular architecture. *J. Cell Sci.* 126:2924-2930. doi: 10.1242/jcs.126045.

Scholz, D., J. Förtsch, S. Böckler, T. Klecker, and B. Westermann. 2013. Analyzing membrane dynamics with live cell fluorescence microscopy with a focus on yeast mitochondria. *Methods Mol. Biol.* 1033:275-283. doi: 10.1007/978-1-62703-487-6_17.

Klecker, T.*, M. Wemmer*, A. Murley, M. Haag, A. Weig, T. Langer, J. Nunnari, and B. Westermann. 2014. Mdm33 links phospholipid homeostasis to mitochondrial division. *Manuscript in preparation*.

The asterisk marks equally contributing authors.

CD-ROM

The print-version of this thesis contains an additional CD-ROM. The enclosed CD-ROM is divided into three directories:

.../Movies: contains the supplementary movies for Klecker et al., 2013, *J. Cell Sci.*

.../Tables: contains the two supplementary tables for Klecker et al., 2014, *in preparation*.

.../Thesis: contains a high-resolution PDF-version of this thesis.

Copyright and Permissions

This work includes two articles that have already been published in the *Journal of Cell Science* and in *Science*. Both Journals allow the reproduction of the article in a thesis.

Journal of Cell Science

Author rights

“Authors remain the owners of the copyright to the article and retain the following non-exclusive rights (for further details, please refer to the license agreement that accompanies article proofs):

(1) authors may reproduce the article, in whole or in part, in any printed book (including a thesis) of which they are author, provided the original article is properly and fully attributed; (...)”

Taken from: http://jcs.biologists.org/site/journal/rights_permissions.xhtml, 2014 – 02 – 16.

Science

Permission for Authors

“3. Authors can immediately use final work for non-profit purposes — no permission needed.

The author retains the non-exclusive right to use the final, published version of the work, immediately after it is made public by AAAS and without further permission, for educational and other non-commercial purposes. Such purposes include, for example, print collections of the author’s own writings; completion of the author’s thesis or dissertation; oral presentations by the author; educational courses taught by the author or offered by the author’s institution; and distribution of photocopies by the author to colleagues for non-commercial purposes (not for further re-distribution). (...)”

Taken from: http://www.sciencemag.org/site/feature/contribinfo/prep/lic_info.pdf, 2014 – 02 – 16.

Erklärung

Ich versichere, dass ich diese Arbeit selbständig verfasst und keine anderen als die angegebenen Quellen und Hilfsmittel benutzt habe. Wörtlich wiedergegebene Textstellen, auch Einzelsätze und Teile davon, sind als Zitate kenntlich gemacht. Alle Abbildungen wurden von mir eigenständig erstellt und bearbeitet. Bei übernommenen oder nachempfundenen Abbildungen ist die Quelle genannt.

Ferner erkläre ich, dass ich nicht versucht habe, diese Arbeit anderweitig einzureichen. Ich habe keine gleichartige Promotionsprüfung an einer anderen Hochschule abgelegt oder endgültig nicht bestanden.

Bayreuth, 16.07.2014

Till Klecker